DEVELOPING THIN FILM COMPOSITE MEMBRANES FOR ENGINEERED OSMOSIS PROCESSES

by

Soleyman Sahebi

A Thesis submitted in fulfilment for the degree of

Doctoral of Philosophy

School of civil and Environmental Engineering
Faculty of Engineering and Information Technology
University of Technology, Sydney (UTS),
New South Wales, Australia

Jun 2015

Certificate of Authorship

I certify that the work in this thesis has not previously been submitted for a degree nor has it been submitted as part of requirements for a degree except as fully acknowledged within the text.

I also certify that the thesis has been written by me. Any help that I have received in my research work and the preparation of the thesis itself has been acknowledged. In addition, I certify that all information sources and literature used are indicated in the thesis.

Soleyman Sahebi

Signature of Student: Production Note: Signature removed prior to publication.

Date: 28-06-2015

ACKNOWLEDGEMENTS

I wish to express my heartfelt gratitude for my mother Mrs Sara for whom my success and progress matter the most. Her encouragement and inspiration gave me strength throughout my entire life. She was mother and father for me and my siblings from the very moment of our childhood since my father passed away early. Nothing is enough to appreciate her young life she spent for me, my brother and sister. Then I would like to dedicate this thesis that I achieved through a great challenge to my dear mom. Without her sacrifices, I never could have reached this stage. I also dedicate my thesis to my father who passed away very early but through his hard work and wise planning, our family managed to overcome all challenges and financial hardship years after his passing.

This dissertation would not have been possible without the support and encouragement of my principal supervisor Dr. Ho Kyong Shon. I would like to express my deepest gratitude and appreciation to him. I would like also to thank my co-supervisor Dr. Sherub Phuntsho for his kind support and his wisdom during my study at UTS. I also would like to express my sincere appreciation to Prof. Chung Tai-Shung (Neal) who give me a training opportunity into his fascinating membrane research group and Dr Han Gang who worked with me during the time in the National University of Singapore (NUS). I have learned and benefited a lot from the training workshop and without this opportunity this thesis would not be possible.

I also would like to thank my friends and research group members at UTS who made this journey memorable. I want to thank Lura Chekli, Fouze Lotfi, Ibrahim El Saliby, Tahir Majeed, Jung Eun Kim, Yun Chul Woo, Myoung Jun Park and I also appreciate Dr.Leonard D. Tijing for his kind help during my study. I also thank my

elder brother Mr Saeed Sahebi and dear friend Dr. Diako Ebrahimi for their support and encouragement during my thesis when I faced very hard, stressful and challenging moments. Their advice gave me the light and encouragement to maintain the momentum.

Finally, I thank my beloved fiancé Nasim for the pain she has had to endure during my absence and cope with this condition in order to support my study while she had an internship and was passing through a difficult period of her study. I would like also to thank Nasim's family, especially her mother Mrs. Ziba Hesami who has been like a loving mother and Mr Salimiaghdam, who been as a precious father to me. I also want to thank my brother in-law Dr. Chia Salimiaghdam for his support during the time I was away and busy with this study.

Last but not least, I would like to thank the University of Technology, Sydney for offering me APA scholarships for my PhD studies at UTS and later on NCEDA scholarship by the National Centre of Excellence in Desalination Australia.

TABLE OF CONTENTS

Journal Articles Published

1. ***Sahebi, S**., Phuntsho, S., Eun Kim, J., Hong, S., & Kyong Shon, H. (2015). Pressure assisted fertiliser drawn osmosis process to enhance final dilution of the fertiliser draw solution beyond osmotic equilibrium. Journal of Membrane Science, 481(0), 63-72.

2. *Phuntsho, S., **Sahebi, S**., Majeed, T., Lotfi, F., Kim, J. E., & Shon, H. K. (2013). Assessing the major factors affecting the performances of forward osmosis and its implications on the desalination process. Chemical Engineering Journal, 231, 484-496.

3. *Majeed, T., **Sahebi, S**., Lotfi, F., Kim, J. E., Phuntsho, S., Tijing, L. D., & Shon, H. K. (2014). Fertilizer-drawn forward osmosis for irrigation of tomatoes. Desalination and Water Treatment, 53(10), 2746-2759.

4. **Chae, S.-R., Noeiaghaei, T., Jang, H.-C., Sahebi, S., Jassby, D., Shon, H.-K., Park, J.-S. (2015). Effects of natural organic matter on separation of the hydroxylated fullerene nanoparticles by cross-flow ultrafiltration membranes from water. Separation and Purification Technology, 140(0), 61-68.

5. *Majeed, T., Phuntsho, S., **Sahebi, S**., Kim, J. E., Yoon, J. K., Kim, K., & Shon, H. K. (2014). Influence of the process parameters on hollow fiber-forward osmosis membrane performances. Desalination and Water Treatment, 54(4-5), 817-828.

6. **Ahmadi, M., Ramavandi, B., & **Sahebi, S**. (2014). Efficient Degradation of a Biorecalcitrant Pollutant from Wastewater Using a Fluidized Catalyst-Bed Reactor. Chemical Engineering Communications, 202(8), 1118-1129.

7. **Ramavandi, B., Asgari, G., Faradmal, J., **Sahebi, S**., & Roshani, B. (2014). Abatement of Cr (VI) from wastewater using a new adsorbent, cantaloupe peel: Taguchi L16 orthogonal array optimization. Korean Journal of Chemical Engineering, 31(12), 2207-2214.

8. **Asgari, G., Ramavandi, B., & **Sahebi, S**. (2013). Removal of a cationic dye from wastewater during purification by Phoenix dactylifera. Desalination and Water Treatment, 52(37-39), 7354-7365.

9. **Ramavandi, B., Jafarzadeh, M., & **Sahebi, S**. (2014). Removal of phenol from hyper-saline wastewater using Cu/Mg/Al–chitosan–H2O2 in a fluidized catalytic bed reactor. *Reaction Kinetics, Mechanisms and Catalysis, 111*(2), 605-620.

Conference papers and presentations

1. *Soleyman Sahebi, Ho Kyong Shon , **Sherub Phuntsho**, Fezeh Lotfi, Jung Eun Kim. Factors Affecting the Performances of Forward Osmosis Desalination Process.
   Euro-membrane conference. Sep 23 – 27, 2012, London, UK.

2. **Chae, So-Ryong; Jang, Hee-Chan; Lee, Jieun; Noeiaghaei, Tahereh; **Sahebi, Soleyman**; Shon, Ho-Kyong; Kim, Jong-Oh and Wiesner, Mark R. Recovery of engineered nanomaterials by dead-end and cross-flow ultrafiltration membranes from water : Chemeca 2012: Quality of life through chemical engineering: 23-26 September 2012, Wellington, New Zealand

3. *Sherub Phuntsho, **Soleyman Sahebi**, Amit Chanan, Ho Kyong Shon.," Pressure assisted osmosis: overcoming limitations of osmotic equilibrium in forward osmosis process", IWA-WWC&E 2014 Portugal.

4. ***Soleyman Sahebi**, Ho Kyong Shon , Sherub Phuntsho, Major factors affecting performances of forward osmosis desalination, FEIT Showcase June 12, 2012, Faculty of Engineering & Information Technology, University of Technology Sydney (UTS), Sydney, Australia.

**Publications made during the PhD candidature including articles not entirely related to the Thesis. *Articles related to the Thesis.

ABSTRACT

The high demand for clean water resources has generated substantial research interest in terms of sustainable and low energy water purification technologies such as forward osmosis (FO). Compared to other membrane based technologies, the FO process is less energy intensive. However, there are challenges that need solutions to enable the FO to compete with other technologies for desalination. Suitable draw solution and a proper membrane are required to overcome the FO process challenges. Enormous effort has been expended to find a new material and better membrane design in order to develop a novel FO membrane that can meet high performance demands in relation to water flux, salt rejection and mechanical strength. This is of particular importance for the newly introduced concept of pressure assisted osmosis (PAO). The objectives of this dissertation are to understand the fundamentals of the FO and PAO as a basis for fabricating a suitable membrane for the FO and PAO process.

In the first part of the work, PAO and its potential application to overcome the limitations of osmotic equilibrium in the FO process is investigated. One of the practical applications of the FO process is desalination for irrigation purposes through the means of hybrid desalination units such as fertiliser drawn forward osmosis (FDFO). The utilisation of PAO in FDFO desalination is assessed .By integrating the PAO process into the FDFO desalination unit, water flux can be generated beyond the point of osmotic equilibrium. As a result, diluted fertilizer as DS in the FDFO unit can be applied for direct fertigation without the need for an additional post-treatment process such as nanofiltration to recover the fertiliser draw solution (DS). Integration of the PAO process has proved to be very effective in

generating extra water flux. This can serve to reduce the capital costs since no separate post-treatment process such as the NF is necessary.

In the second part of the work, a thin film composite membrane for the FO and PAO process is fabricated through Polyethersulfone as a polymer materials base. Phase inversion in the precipitation bath and membrane formation mechanism of these polymers, both with and without backing fabric support, is investigated. The membrane chemical properties and hydrophilicity have been found to play a key role in the mass transfer of water flux during the FO process. Therefore, attention has been directed at increasing the hydrophilicity of the membrane through blending sulphonated materials. It has been found that sulphonation not only affects the membrane performance but also the membrane structure and morphology. Through sulphonation, porosity and hydrophilicity of the substrate increases while the finger like structure disappears. This leads one to suppose that the high water flux does not have a direct relationship with the finger like membrane structure. Regardless of membrane morphology, substrate hydrophilicity is the key to achieving a high performance membrane. Sulphonation has been found to have a tremendous effect on the physical and chemical properties of the membrane. While sulphonation dramatically increases the hydrophilicity of the substrate, it decreases the membrane mechanical strength. Due to higher hydrophilicity and lower ICP as a result of blending the sulphonation polymer, a membrane with better performance in terms of water flux and selectivity has been developed for the FO process.

In the last part of the work, a special thin film composite (TFC) flat sheet membrane on a backing fabric is developed for the PAO application. The newly developed concept of PAO has introduced a hydraulic pressure to the feed side to overcome

osmotic equilibrium and the extraction of more water. Accordingly, under the PAO process, a membrane with considerable mechanical strength is required. A thin film composite membrane supported on woven mesh fabric is designed to specifically solve the problem by embedding a woven mesh fabric support. An earlier part of this study reveals that the mechanical stability and special physical properties of the support layer are critical for the PAO process.

LIST OF ABBREVIATIONS

AL-DS	:	Active layer – draw solution
AL-FS	:	Active layer - feed solution
AL	:	Active layer
BW	:	Brackish water
CA	:	Cellulose acetate
CTA	:	Cellulose triacetate
CP	:	Concentration polarization
DI	:	Deionized water
DS	:	Draw solution
ECP	:	External concentration polarization
FDFO	:	Fertilizer drawn forward osmosis
FO	:	Forward osmosis
FS	:	Feed solution
ICP	:	Internal concentration polarization
IP	:	Interfacial polymerization
LMH	:	$L/m^2/h$
MW	:	Molecular weight
NF	:	Nanofiltration
PA	:	Polyamide
PAI	:	Poly (amide-imide)
PAO	:	Pressure assisted osmosis
PBI	:	Polybenzimidazole
PES	:	Polyethersulfone
PRO	:	Pressure-retarded osmosis
PSf	:	Polysulfone
PWP	:	Pure water permeability
RO	:	Reverse osmosis
RSF	:	Reverse solute flux
SEM	:	Scanning electron microscope
SL	:	Support layer
SRSF	:	Specific reverse solute flux
SW	:	Sea water
TFC	:	Thin film composite
TFN	:	Thin film nanocomposite

LIST OF SYMBOLS

A	:	Water permeability coefficient (L .m^{-2} .h^{-1}.bar^{-1})
B	:	Salt permeability coefficient (m.s^{-1})
D/Ds	:	Diffusion coefficient (m^2 s^{-1})
J_s	:	Solute flux (g.m^{-2}.h^{-1})
J_w	:	Water flux (L m^{-2} h^{-1})
k	:	Mass transfer coefficient
K	:	Solute diffusion resistance (s.m^{-1})
M	:	Molar concentration of the solution
Mw	:	Molecular weight (mol.g^{-1})
n	:	Van't Hoff factor
P	:	Applied hydraulic pressure (bar)
Re	:	Reynolds number
Sc	:	Schmidt number
Sh	:	Sherwood number
T	:	Absolute temperature (in K)
t	:	Thickness of the membrane (m)
Δt	:	Time interval (h)
ΔV	:	Volume change (L)
ΔP	:	Pressure change (bar)
π	:	Osmotic pressure (bar)
φ	:	Osmotic pressure coefficient
σ	:	Reflection coefficient,
ε	:	Porosity
β	:	van't Hoff coefficient
τ	:	Tortuosity

LIST OF FIGURES

LIST OF TABLES

Chapter 1

INTRODUCTION

1.1 **Background**

Water is essential for all life on Earth; there is no substitute for it. However while water resources are abundant on Earth, water supplies are not meeting human demands. Water resources are not scarce but the supply of usable water is limited. With the industrial revolution after the eighteenth century in addition to residential and agricultural sectors, the commercial, industrial and power generation sectors increase rapidly. Furthermore, population growth and the global consumption of water has increased exponentially.

Seawater consists of 97% of the world‘s water resources. Removing the dissolved salt and mineral concentration through a desalination process is regarded as a solution to solve the water shortage. However, in the desalination industry major interests focus on developing cost-effective processes to provide suitable water quality for different sectors to meet their quality standard. Water used in different sectors requires a specific water quality. Various desalination technologies have been developed and improved. However, developing new cost effective technologies have yet to be found especially for the agricultural sector where very large volumes of low-cost water are required.

Membrane based technologies are gaining popularity over other desalination processes. In the membrane based processes semi permeable membranes are utilised to separate water molecules from dissolved salts and other impurities. Reverse osmosis (RO), Nanofiltration (NF), Microfiltration (MF) and Ultrafiltration (UF) are common technologies in water treatment application. RO is the most popular technology used for the desalination industry today to produce high quality water; however, this process requires massive energy. Most of the energy requirements for

desalination by the RO process are consumed by the feed pressurisation step. Depending on the water total dissolved solids (TDS) quality energy requirements vary which, means for brackish water carrying less TDS than seawater the process is less energy intensive and less energy is required for pressurisation. However, still energy consumption is far too high by economical standards.

Recently forward osmosis (FO) has been introduced as a low cost water desalination process. It does not require pressure and driving force generated by osmotic pressure of the draw solution. Then, energy requirements for FO are limited to the pumps consumption used for the crossflow arrangement of the FS and DS on both sides of the membranes. As the FO does not require the kind of additional energy to pressurise feed water streams as the RO required, it can be considered as an environmentally friendly desalination technology having a low carbon footprint. These advantages attract considerable research attention and in a short period of time its potential has been evaluated in a wide range of applications such as sea and brackish water desalination, wastewater treatment, power generation, food processing and fertigation for farming.

For example, fertiliser drawn forward osmosis (FDFO) is a similar unique concept which uses commercially available fertilisers as draw solution to desalinate brackish/sea water for agricultural use (Phuntsho et al. 2011). Unlike many other FO processes, in FDFO, the resultant low concentration fertilizer DS does not require any necessary regeneration and thus can easily be used with some concentration adjustments to irrigate any suitable agricultural crops. In this FO process, as the final step of draw solute recovery is eliminated, it helps the FDFO process to take a real advantage from the low cost FO desalination. However, water production is limited

as the feed solution and draw solution reach an osmotic equilibrium. This reduces the available driving force (net osmotic pressure difference) across the semipermeable membrane which results in continuous flux decreases. Thus, to overcome the osmotic equilibrium an applied hydraulic pressure during the FO process is introduced with the aim of enhancing the water flux. This approach exploits the synergies of the two driving forces (osmotic pressure and the hydraulic pressure) in a single stage. The pressure assisted osmosis (PAO) could be more advantageous particularly for the FDFO desalination process where the maximum dilution of the fertiliser DS is preferred for meeting the nutrient concentrations acceptable for direct fertigation. At the end, to get advantages of FO process, suitable semi permeable membranes are required. FO membrane for various FO applications needs different properties and characterisation. Therefore, a high performance membrane that could function sustainably can extend the scope of FO water desalination to large-scale applications.

1.2 **Research Motivation**

Since FO study gained momentum decades ago, extensive effort has been made to fabricate a suitable membrane for the process. Considering FO is not a pressure based desalination technology and the driving force is generated by draw solutes, a specific membrane is required for the process. Polymeric asymmetric membranes are commercialised for the FO process; however, to achieve high water flux the concentration polarization phenomena, especially the internal concentration polarization (ICP) need to be considered as major factors affecting the water transport across the semi permeable membrane.

Considering different types of FO applications, FO membranes with different characteristics are required. For example, a high permeable membrane with low

structural parameter can perform well under the FO process while for the pressure retarded osmosis (PRO) and PAO also a high permeable membrane is required; however, it should be able to withstand the applied pressure. Each particular FO application needs a FO membrane with specific properties which are closely related to the feed and draw solution and types of application. For example, in the recently studied PAO process, Reverse solute flux (RSF) which is a serious operational issue in the FO, seems to be better controlled despite higher water flux produced by the PAO process. This particular phenomenon gives an edge for the design of a high permeable membrane for the PAO process by producing a thinner and controlled polyamide (PA) layer to achieve higher water flux. Thus, this study first focus on evaluating new PAO application and this is fundamental to designing a suitable membrane for the FO and PAO process. Finding and developing a suitable membrane remain as major challenges for further development of FO application. This becomes a primary motive for this current research work.

1.3 **Objectives and Scope of the Study**

Cellulose triacetate (CTA) membrane has been used for the FO and PAO process. TFC membrane comprising Psf and PES in their support polymeric structure is commonly used for the RO application. However, the TFC-FO membrane has recently become of research interest. Even though TFC-FO has been fabricated commercially in recent years, the fundamental studies on the mechanism of water and salt transport of the polymers are insufficient. Furthermore, fabrication procedure to embed the woven or nonwoven backing fabric support in the membrane structure has not been investigated thoroughly. Lack of clear guidelines and methodology to successfully make a stable embedded membrane with high

performance has pushed the research on FO membrane to ignore developing the membrane on fabric support. Membrane that has been synthesized without a backing fabric support is not mechanically stable. Furthermore, the membrane formation and chemical properties in relation to increased porosity, hydrophilicity and decreased ICP for forward osmosis is also an interesting topic for researchers. Due to applied hydraulic pressure required in the process, the PAO membrane needs to be reinforced for a sustainable performance.

The main objective of this research is to develop a high performance membrane for FO and PAO process. This fundamentals and factors affecting the FO and PAO processes and their relationship with the membrane design and property will be investigated.

Looking into the above research insufficiencies, the main objectives of this study are:

- Assessing the fundamentals of membrane fabrication on top of backing fabric support through phase inversion and interfacial polymerization.
- Developing high performance FO membrane by increasing membrane substrate hydrophlicity.
- Developing a stable membrane that can endure the applied hydraulic pressure in the PAO process with high water permeability.
- Further investigating the new concept of PAO and their potential on FDFO desalination unit.

1.4 Structure Outline of the Thesis

The study looks into three main aspects: FO and PAO fundamentals through potential integration of PAO in the FDFO desalination process, developing a high performance membrane for the FO and a suitable membrane for the PAO processes. The outline of the thesis which is consists of seven chapters is as follows:

Chapter 1 as an introduction chapter included background, research motivation, objectives and scope of the study.

Chapter 2 provides information and literature about membrane based desalination techniques and their alternatives, FO and PAO process, FO applications, FO challenges, membranes for engineered osmosis, engineering principles for the design of polymeric membranes, phase inversion membranes, composite membranes, custom designs of flat sheet FO membranes and finally important factors in fabricating TFC FO membranes.

Chapter 3 presents materials and methods used in this study. Chapter 4 gives an osmotic processes classification, modelling and investigates the pressure assisted fertiliser drawn osmosis process to enhance final dilution of the fertiliser draw solution beyond osmotic equilibrium.

Chapter 5 a high performance TFC FO membrane is developed on a hydrophilic substrate through a sulphonated polyethersulfone (PES).

Chapter 6 a sustainable TFC membrane supported on a compacted woven fabric mesh support is developed for the PAO.

Chapter 7 summarises the outcomes, general conclusions, recommendations and future work.

Chapter 2

LITERATURE REVIEW

2.1 Introduction

The chapter provides a brief introduction to forward osmosis (FO), classifications of the osmotic processes and recent developments and latest findings on the FO process, application, membrane materials and fabrication methods with a particular focus on pressure assisted osmosis (PAO). This chapter first discusses the water-related issues as a threat to global welfare and security, followed by available desalination technologies for seawater and brackish water desalination. The review also identifies the major challenges for the FO process to be able to replace or compete with current desalination technologies. The challenges include suitable draw solution (DS) and fluid management with the main focus on a possible new membrane material and the fabrication method to provide a robust and high performance membrane for FO application including PAO. Application of FO on hybrid systems as an opportunity to expand engineered osmosis is also covered. Although DS and fluid management are not limiting factors in PAO and in hybrid systems as much as a single standalone FO. However, finding a suitable membrane remains as a most important issue. Any successful FO application particularly in PAO and hybrid FO units such as FO-PAO, FO-RO, etc. depends on a customized enhanced FO membrane with good mechanical strength.

2.2 Current and emerging technologies for global water crises

Fresh water is vital for mankind and therefore, water scarcity can greatly endanger the world's welfare and security. Reclamation of wastewater and treatment of brackish and saline water has the potential to fulfil the future demand (Qadir et al. 2007; Vörösmarty et al. 2010). Feasibility of these projects is currently limited by technical and financial obstacles, particularly, in undeveloped countries. Initial

investment in equipment required for water purification and cost of energy is still high even for developed countries (Ghaffour et al. 2013). Engineered osmosis or FO is an emerging process in membrane based technologies for desalination or water purification (McGinnis & Elimelech 2008). In FO, a higher concentrated solution draws water through a membrane from a feed solution with lower concentration. The process is spontaneous and based on osmosis that occurs by different solution concentrations in feed and DS (Logan & Elimelech 2012). The process can be done with very little energy required for the pumps to keep constant flow of the solution. Based on the osmosis principal, FO can be used for a wide variety of solution treatments in different industries such as wastewater treatment, food processing and energy production, etc. (Garcia-Castello et al. 2009; Logan & Elimelech 2012; Rahardianto et al. 2007). In FO, different kinds of organic and inorganic materials as a DS can be used. They may include natural salt, fertilizers, soluble polymers, volatile gases and magnetic nanomaterial (Achilli. et al. 2010). Utilizing FO to produce potable water from brackish or sea water is still a challenge. That is due to a further process required to recover the DS to be able to obtain fresh drinking water (Cath et al. 2006). However, in some FO applications rather than drinking water applications, DS recovery may not require or be necessary for the process. For example, the separation of the DS is not required when FO is used to desalinate brackish water through fertilizer for fertigation purposes or applying FO in food processing or energy production, through pressure retarded osmosis (PRO) (Logan & Elimelech 2012; Phuntsho et al. 2011) .

Reverse osmosis (RO) is a more familiar process than engineered osmosis in the field of desalination. Thus, the RO process will be explained briefly before further

discussion of FO. The concept of "osmosis" has been discovered and studied for several centuries. One of the earliest studies on osmosis goes back to 1748 by the French scientist Nollet. Over the next two centuries many researchers evaluated these phenomena (Williams 2003). By the mid-1950s, researchers have succeeded in producing fresh water from seawater. However, low flux was the main challenge for commercialization until the discovery by Sidney Loeb and Srinivasa Sourirajan for making asymmetric membranes for seawater desalination (Glater 1998). In the late-1970s, John Cadotte discovered that a composite membrane could be made through interfacial polymerization of m-phenylene diamine (MPD) and trimesoyl chloride (TMC) (Cadotte 1981). This new composite membrane had higher flux and low salt passage compared to previous membranes. Almost all commercial RO membranes are now made by the John Cadotte fabrication method. The thin film composite (TFC) FO membrane fabrication method is a modified design of this method as well.

In pressure based membranes such as RO, most of the consumed energy is in regard to the applied hydraulic pressure. Required pressure for treating brackish water ranges from 15–25 bar while for higher saline feeds such as seawater systems it varies from 54 to 80 bar (Ng et al. 2006). In general, however, it is difficult to calculate the cost of water treatment and desalination by RO systems. It means that the cost can vary greatly over different regions geographically, sea water quality and other costs related to work force and maintenance (Greenlee et al. 2009). Figure 2.1 illustrates major desalination technologies by capacities. RO accounts for 59.85 % of total water production (Global Water Intelligence (GWI/IDA DesalData)).

In general, energy cost related to the RO operation, fouling and maintenance are the major challenges of RO plants. Finding indicate that pre-treatment of water can

reduce the cost by up to 30% for sea water desalination in the RO process (Pearce 2008). FO has successfully been deployed for pre-treatment of sea water with high solids content. Thus, there is a potential cost savings in RO using FO as a pre-treatment unit. FO as an emerging technology may be added to the list of technologies in stand-alone or hybrid systems for comparison in terms of their contribution for desalination in the near future.

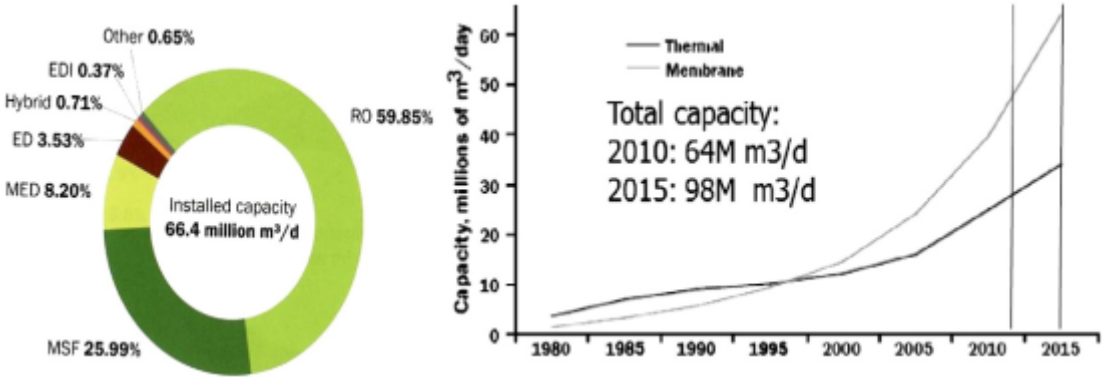

Figure 2.1: Illustration of major desalination technologies with their relative contributions to worldwide capacity for desalination. Data obtained from (Global Water Intelligence (GWI/IDA DesalData)).

2.3 **Forward osmosis (FO)**

FO utilizes the osmotic pressure differences between the draw solution (DS) and the feed solution (FS) as a driving force to transfer water across the membrane without external hydraulic pressure (Tijing et al. 2014). Unlike RO, FO operates at no applied hydraulic pressures or just requires a very low pressure (in the case of pressure assisted osmosis). Therefore, it requires a much lower energy and compared to the other pressure-driven membrane processes, it has a lower membrane fouling tendency, (Cath et al. 2006). Extensive work has been undertaken to investigate the concept of FO for many applications, such as treatment of wastewater, membrane bio-reactor, food industries and farm fertigation. As discussed, FO has gained

popularity in numerous fields, however, newly introduced PAO has gained research momentum for practical FO application in hybrid systems including a recovery tool in fertilizer drawn forward osmosis (FDFO) or for enhancing performance in oil and gas wastewater treatment (Coday et al. 2013; Hickenbottom et al. 2013a).

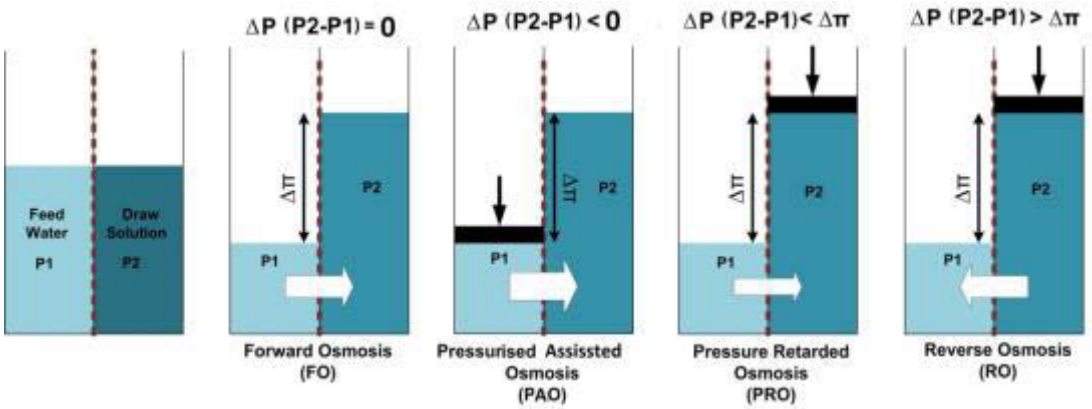

Figure 2.2: Water flow and relationship between RO, PRO, FO and PAO for an ideal semi-permeable membrane. In FO, water diffuses to the more saline side of the membrane and ΔP is approximately zero. PAO is similar to FO but additional pressure is applied on the feed side. In PRO, positive pressure ($\Delta\pi > \Delta P$) occurs and as a result of water diffuses to the more saline liquid side. In RO, due to hydraulic pressure ($\Delta P > \Delta\pi$), water diffuses to the less saline side.

Figure 2.2 illustrates the difference between the RO and different engineered osmosis. Regardless of different FO application, the flow of water naturally is from low concentrated solution (P1) to higher concentrated solution (P2) while in RO water flux flow requires applied hydraulic pressure to overcome osmotic pressure ($\Delta\pi$). Thus water flow is from (P2) to (P1). It also shows the relationship between RO, PRO, FO and PAO for an ideal semi-permeable membrane.

The general equation for the water transport through the salt rejecting membranes is given by the following equation.

$$Jw = A\ [\Delta P - \sigma\ \Delta\pi]$$

Where J_w is the water flux, A is the pure water permeability coefficient, $\Delta\pi$ is the net osmotic pressure between the feed and the permeate solution, ΔP is the applied pressure and σ is the reflection coefficient. Generally, reflection coefficient is assumed unity for salt rejecting membranes. The net osmotic pressure ($\Delta\pi$) can be written as follows:

$$\Delta\pi = \pi_F - \pi_p$$

Where π_F is the osmotic pressure on the FS and π_p is the osmotic pressure of the permeate. Then based on hydraulic pressure applied at the feed solution side, osmotic processes can be classified into four categories which are depicted in Figure 2.2.

Figure 2.2 illustrates jars containing dissolved solutes in water. For the first jar on the left side if this state is allowed to continue, the spontaneous flow of the water through a semi-permeable membrane from a low concentrated solution (P1) to a higher concentrated solution (P2) occurs; this refers to natural osmosis, or FO. This is the principle behind the use of concentrated DS as a driving force for desalination. Unlike the FO process, in the RO process water diffuses through the semipermeable membrane by applied hydraulic pressure while the salt ions are rejected by thin rejection layer.

PRO and FO processes are similar in principal but in the PRO process, the applied pressure is on the DS side [ΔP (P2-P1) < $\Delta\pi$] opposite to the osmotic gradient that partially retards the water crossing the FO membrane generated by the osmotic driving force. The schematic of Figure 2.2 further shows the definition and principles of PRO. As can be seen, generated hydraulic pressure within the DS chamber can be

used to drive a hydraulic turbine for energy production. Lastly, the PAO process can be described as an in-situ combination of RO and FO processes. The total osmotic pressure on the permeate side is therefore a combination of both the osmotic pressure of the permeate (π_F) and the DS (π_D) that is already present on the permeate side of the membrane. Applied hydraulic pressure on the feed side (P1) is bigger than on the permeate side (DS side) then ΔP (P2-P1) < 0, where the driving force is $= \Delta P - (\pi_F - \pi_p + \pi_D)$ for the PAO process (Sahebi et al. 2015).

Despite the great advantages of FO over other pressurised membrane based technologies, still this technology is more and less limited to the research field. There are a few challenges that limit the commercialization of FO for the practical field especially in the desalination sector. However, a description of the PAO and PRO process is given prior to further clarification of challenges that limit the FO process.

2.3.1 **Pressure Assisted Osmosis (PAO)**

Given that the FO process is concentration-based, it can be hindered by operational process limitations. Limited water can be induced through the semi-permeable FO membrane because of a number of factors that have been extensively studied (Phuntsho et al. 2013). Firstly, besides the Internal Concentration Polarisation (ICP), which is a major limiting factor in the FO system, other factors such as External Concentration Polarisation (ECP), membrane fouling and reverse solute can substantially impact the net osmotic pressure (Δπ) values across the semi-permeable membrane which is the main driving force in the FO (McCutcheon & Elimelech 2006a; Mi & Elimelech 2008). Secondly, the transfer of water across the membrane continues until the osmotic pressure of the DS reaches an equilibrium state with the feed solution (FS) (Coday et al. 2013; Phuntsho. et al. 2014). Extensive efforts have

been made to optimize the operating factor, the membrane materials while modifying the design in order to reduce those limiting factors, particularly, the ICP. However, the ICP remains a major issue in the FO membrane (McCutcheon & Elimelech 2006a; McCutcheon. & Elimelech. 2007). Recently, a few studies on the combined processes of hydraulic pressure and the osmotic process known as PAO have reported attempts to exploit the synergies of the two processes in a single stage to overcome low flux in the FO process (Coday et al. 2013; Yun et al. 2013b). Use of external pressure to induce water flux beyond the point of osmotic equilibrium seems to be very useful especially for water production using fertilizer for fertigation by FO application or treating oil and gas wastewater products.

In PAO, water flux through the semi-permeable membrane will be induced due to combined action of osmotic ($\Delta\pi$) and hydraulic applied pressures (ΔP). The newly developed PAO concept is of particle interest in a hybrid FO system. An external hydraulic pressure (ΔP) is applied on the feed side of the membrane; further water flux can be induced from the FS towards the DS side. The advantage with this concept is that, the applied pressure does not have to overcome feed osmotic pressure ($\Delta\pi$) (as in RO or NF) due to the state of osmotic equilibrium created within the membrane by the presence of the DS on the opposite side of the FS. Figure 2.2 presents the water flux diagram for PAO processes as a function of hydraulic pressure.

Applying PAO may be particularly interesting in a hybrid FO-PAO system in the fertilizer drawn forward osmosis (FDFO) unit. In a current FDFO system which is a hybrid FO-NF system, energy consumption is observed to be less energy-intensive in this system compared to other pressure-based membranes, like RO; however, the

final diluted DS (fertilizer) still requires a post-treatment process to meet the acceptable nutrient levels for fertigation (Phuntsho, Shon , et al. 2012). Based on recent studies, the primary objective of providing this hydraulic pressure in the FO process was to enhance water flux (Blandin et al. 2013; Coday et al. 2013; Yun et al. 2013b). Then new concepts of applying hydraulic pressure seem to be a right step to expand FO application especially in hybrid FO systems for saving energy and lowering the foot print.

2.3.2 PAO for energy savings in desalination units, oil and gas wastewater treatment.

The concept of PAO can be combined with other desalination units for performance enhancement or energy savings and as a result can reduce the footprint. For example, it can be utilized as a pre-treatment step for RO desalination. That can result in a significant dilution of the feed resources and fouling problem. A slight hydraulic applied pressure to the feed side can result in a greater dilution of the RO feed; this can contribute a significant saving in the energy cost in the RO plant. This can be regarded as an anti-fouling strategy in RO desalination plants that decreases operational costs. Furthermore, it can be applied in the hybrid desalination units such as FDFO. Using the PAO process could dilute the fertiliser DS beyond the osmotic equilibrium concentrations so that the final fertiliser concentration can meet the fertigation standard. Hence, no separate post-treatment process such as NF is necessary for recovery of fertiliser. Figure 2.3 shows FDFO desalination unit for fertigation using fertilizer as DS and NF for recovery of fertilizer. In this hybrid system NF can be replaced entirely with PAO. When DS reaches equilibrium state with the feed solution, replacing the NF unit with PAO can further dilute the obtained water in the DS side to reach standard nutrients limits for fertigation.

Replacing the NF unit with PAO in the FDFO can fulfil two objectives: less energy requirement because DS recovery will not be necessary through NF and desalinated water can be applied directly for fertigation without dilution with fresh water which can ease the operation.

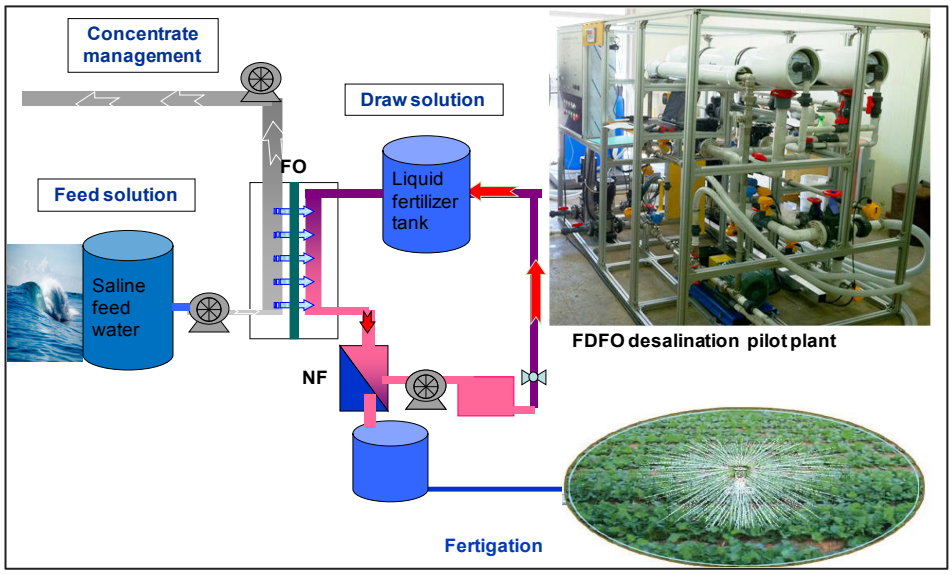

Figure 2.3: Schematic of FDFO desalination unit for fertigation using NF for DS recovery.

PAO seems to be another promising application for treating industrial wastewater as well. There are industries that utilize RO or other treatment plant for reducing their industrial wastewater problems to eliminate heavy metals and hazardous materials. The main objective will be removing hazardous elements from the wastewater to a standard level before discharging the product water to the sea/river or stream.

Treatment and reuse of oil and gas (O&G) production wastewater from shale gas or oil production from hydraulic fracturing in an environmental friendly manner is critical to sustainability and meeting stringent regulations (Shaffer et al. 2013). High salinity, free and emulsified hydrocarbons, silts and clays released from producing

formations, and process additives common in O&G drilling wastewater render many conventional treatment technologies ineffective. FO has been established as a promising solution for treatment and desalination of complex industrial streams and especially O&G exploration and production wastewaters (Coday et al. 2014). The FO or PAO process can operate as a stand-alone technology with minimal pre-treatment or be coupled with other advanced processes such as RO or membrane distillation (MD).

During well hydraulic fracturing in oil and gas exploration, a large volume of fresh water is consumed. It generates larger volumes of contaminated wastewater. A novel concept of FO can be utilized for treatment of drilling waste. FO has two major benefits: the volume of the waste stream can be greatly reduced thus lessening the need for a fresh water source. Hickenbottom et al. indicate that by using FO more than 80% of the water from the drilling waste could be recovered (Hickenbottom et al. 2013b). Backwashing was presented to be an effective cleaning technique to restore water flux.

Figure 2.4 (a) shows the schematic of oil and gas waste water treatment applying the FO and PAO process. Salt has been used as DS for treating drilling waste water while Figure 2.4 (b) shows Oasays' membrane brine concentrator (MBC). Oasays accepted to set up a full-scale MBC system in a shale gas fracturing application. MBC can outperform RO especially for the feed with a high TDS (5000 mg/l). The cost is also 50 % lower than brine concentrator evaporators that are operating in the shale markets today.

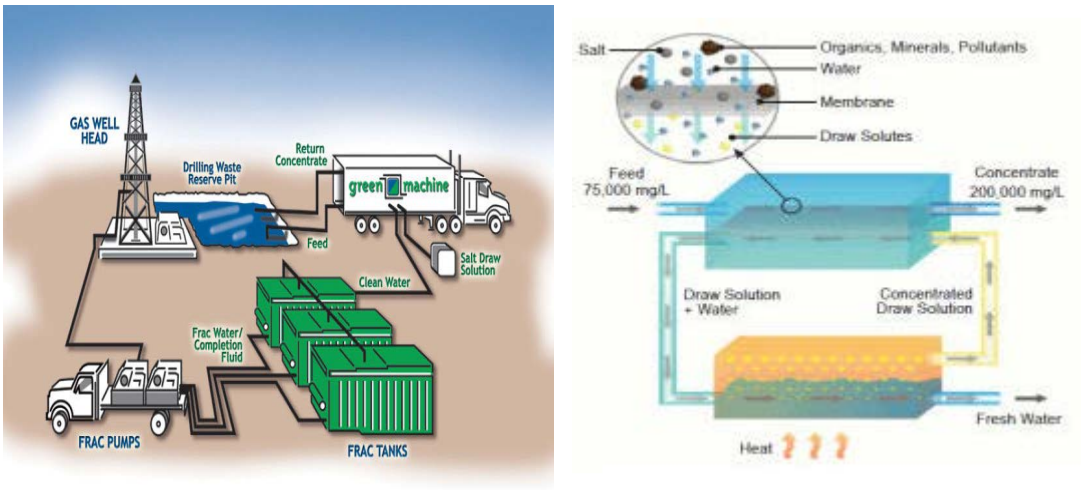

(a) (b)

Figure 2.4: (a) Schematic of oil and gas waste water treatment applying FO and PAO process, adapted with permission from (Coday et al. 2014) , and (b) Illustration of Oasays' membrane brine concentrator (MBC).

2.3.3 **Pressure Retarded Osmosis (PRO)**

Salinity or salty aquifer has the potential to produce energies if they exposed to the stream with no or less salinity via a semi permeable membrane. Equilibrium occurs between these two streams if a proper FO membrane is placed between two streams (Lee et al. 1981a). This power generation method is called pressure retarded osmosis (PRO). Sidney Loeb the pioneer of RO membrane and osmotic process considered PRO potential for power generation and made presentations (for example Euro membrane 1995) on the Dead Sea to Mediterranean PRO scheme (Loeb et al. 1978; Loeb et al. 1976). Figure 2.5 illustrates the simplified schematic diagram of a PRO system with relevant dimension where PRO can utilize and extract the power of salt and equilibrium with the help of a semi-permeable membrane. In principle, a PRO system based on engineered osmosis would take in seawater and river water on either side of a membrane. The flow of water to the DS creates a flow that can be delivered through a turbine to generate power. The world's first PRO plant with a capacity of

4 kW was started by Statkraft on 2009 in Norway (Helfer et al. 2014). Through this research and further studies by several groups finding a suitable membrane has been identified as a major limiting factor (Kim & Elimelech 2012; Yip & Elimelech 2011).

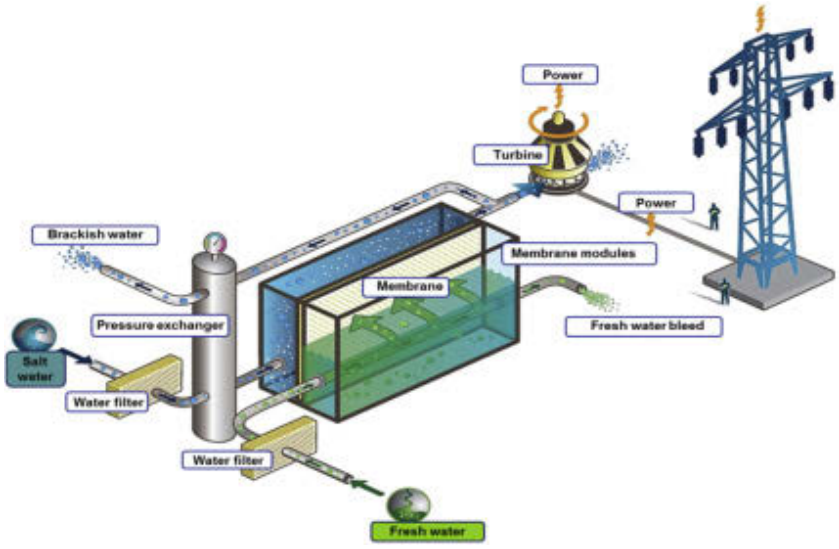

Figure 2.5: Illustration of a PRO system with relevant dimension (Banchik. et al. 2014b).

Through recent studies it has been concluded that the optimal dimensions of large PRO systems, 95 % of a system's maximum output can be produced using only half or less of the membrane area (Banchik et al. 2014; Banchik. 2013; Banchik. et al. 2014a). This can decrease the size of the membrane which can lower much of PRO plant cost. Then a nonlinear relationship between membrane area and power output exists for large systems. When the number of membrane increases, the generated power can increases to a certain point, after which it levels off gradually. Furthermore, they found that a mix of treated wastewater and RO plant brine can produce twice as much power as a combination of river stream and seawater (Banchik. 2013; Banchik. et al. 2014b). Based on this fact, a PRO system could even

power a wastewater treatment plant in coastal regions by taking in seawater as DS and treated wastewater as a feed to generate renewable energy to cover the power required for the treatment plant. So in parts of the world especially in a coastal city a large volume of required water can be generated through a desalination plant now or will be in near future. Thus produced brine from desalination plants can be used to generate power and cover large amount of power required for a desalination plant. Further research is required to see whether it can be economically viable or not (Zhang et al. 2013).

2.4 **Hybrid FO applications**

FO systems can be divided into two categories: stand-alone FO units and hybrid FO units. The most important hybrid FO units are discussed below in more detail.

As illustrated schematically in Figure 2.6, the concentrated feed solution is the output of the FO system while permeate consisting of reusable water (potable or non-potable depending on the design of the system).

In hybrid FO systems, the FO part still functions as an energy-efficient water extractor, extracting water from a feed stream, which is difficult (expensive) to treat with traditional membrane technologies.

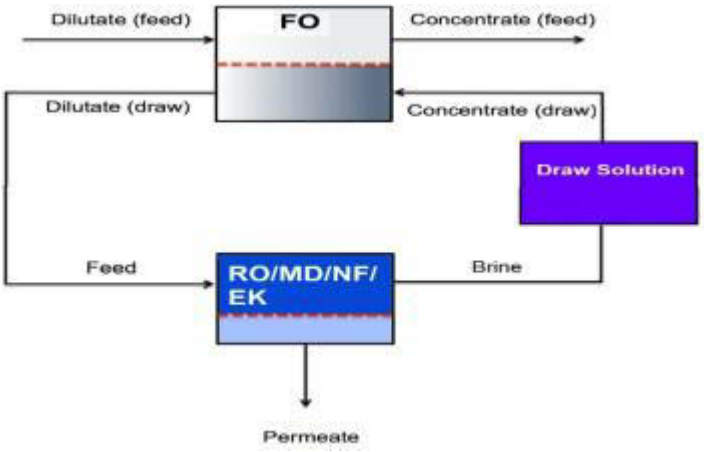

Figure 2.6: Schematic of hybrid forward osmosis systems for desalination of seawater, wastewater treatment and energy production.

Hybrid FO systems can be divided into 2 categories as well: (1) hybrid FO systems for water treatment (NF-FO, RO-FO, MD-FO, etc.) and (2) hybrid FO systems for energy production (PRO-MD). The RO-FO will be explained; this seems to be more promising for water treatment and desalination in addition to PRO-MD for energy production.

2.4.1 **Hybrid RO-FO system**

Hybrid FO with RO (low-pressure reverse osmosis) systems is a versatile hybrid system for several applications including low cost seawater desalination, and to reduce fouling propensity of producing fresh water from impaired-quality water sources, compared to conventional high pressure RO systems. This hybrid system can be divided into two categories: open and closed RO-FO hybrid systems.

Open RO-FO hybrid systems can be the most suitable option for desalination when urban run-off water or municipal waste water can be used as feed and DS can be seawater. The seawater as a DS, draws fresh water from the waste water stream. The DS will be diluted which can be desalinated by low pressure brackish water RO while reducing the wastewater volume. Hence, the economical benefits include:

- Less energy requirements to desalinate the diluted seawater
- Reduced volume of wastewater means saving cost of transporting or treatment

However, closed RO-FO hybrid systems can be useful for the wastewater with higher total suspended solids (TSS) which is difficult to treat. In this hybrid system a specific osmotic agent can be used as DS. Due to the high fouling tendency of this kind of feed solution, stand-alone RO application will be difficult and expensive. Thus pre-treatments are absolutely necessary. FO can be placed as a pre-treatment which is far less prone to fouling. During FO operation, first water permeates from the feed side (wastewater with high TSS) to the DS side with specific osmotic agents to the draw fresh water from the waste water stream and reduces its volume. In the first RO hybrid system which used seawater as a DS, then diluted seawater desalinated by low pressure RO then brine can be disposed as in a common RO desalination plant. However, with a specific osmotic agent used as DS in the second system, diluted product will be treated with low pressure RO but re-concentrated DS will return back to the FO cycle. Hence, the economical benefits include:

- Less energy and maintenance requirements due to low-fouling FO membranes
- Reduced volume of wastewater means saving cost of transporting or treatment
- The product water can be re-used for industrial processes

2.4.2 Hybrid PRO-MD system

Heat engines are well known for their efficiency in the heating and cooling and converting of low grade heat to mechanical work and electricity. An osmotic heat engine can be used for converting unproductive low temperature biomass heat (non-combustion), low-concentration solar thermal energy, geothermal heat sources or ocean thermal energy conversion. An ammonia–carbon dioxide osmotic heat engine was first reported by Yale university in 2007 (Robert L. McGinnis, McCutcheon, & Elimelech, 2007). This is a closed cycle PRO process. It is well known as an osmotic heat engine (OHE) that uses a combination of a highly concentrated NH3/CO2 DS and a deionized working fluid. This is power generation from osmotic pressure gradients and allows for a probable operating efficiency of 5–10%. A relatively more completed system suggested by Yale University contains a hybrid PRO−MD, utilizing low-grade heat for power generation. This system can operate as an osmotic heat engine and work in a closed-loop system. Initial assessment shows that the hybrid PRO-MD system can achieve an energy efficiency of 9.8% theoretically with a temperature difference of 40 °C with 1 M NaCl as DS. Furthermore, since the heat source can be powered by virtually any kind of energy, osmotic heat engines (OHE) are very versatile with a wide range of applicability. OHE can be a promising technology to generate electricity from any low-grade heat sources. Figure 2.7 shows a schematic of a hybrid PRO−MD system for power generation. To advance OHE beyond conceptualization, several factors need to be considered carefully. Currently there is a technology gap for bringing this

system to be able to compare with the same conventional energy generator system. For example, the hydraulic pressures on the PRO membrane are nearly 46, 100, and 220 bar for the 1, 2, and 4 mol/kg NaCl as DS, respectively.

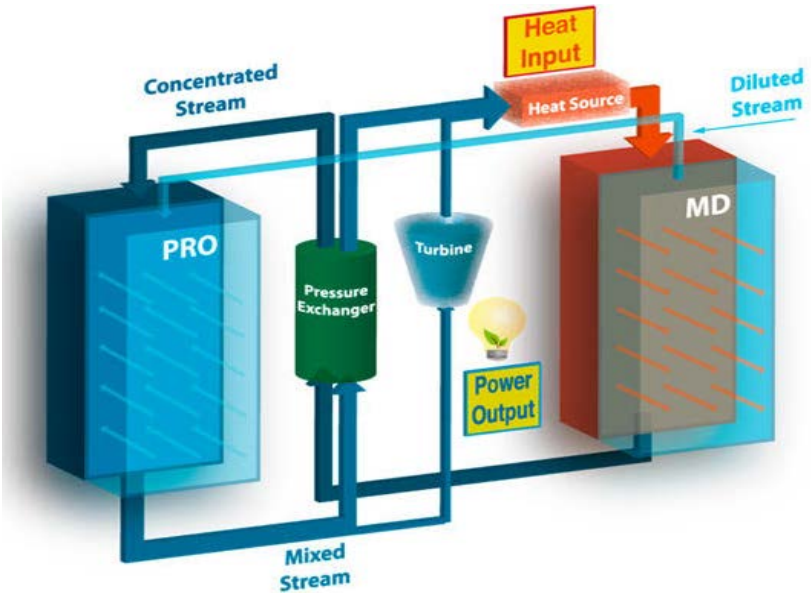

Figure 2.7: Schematic of hybrid pressure retarded osmosis−membrane distillation system for power generation from low-grade heat (Lin et al. 2014).

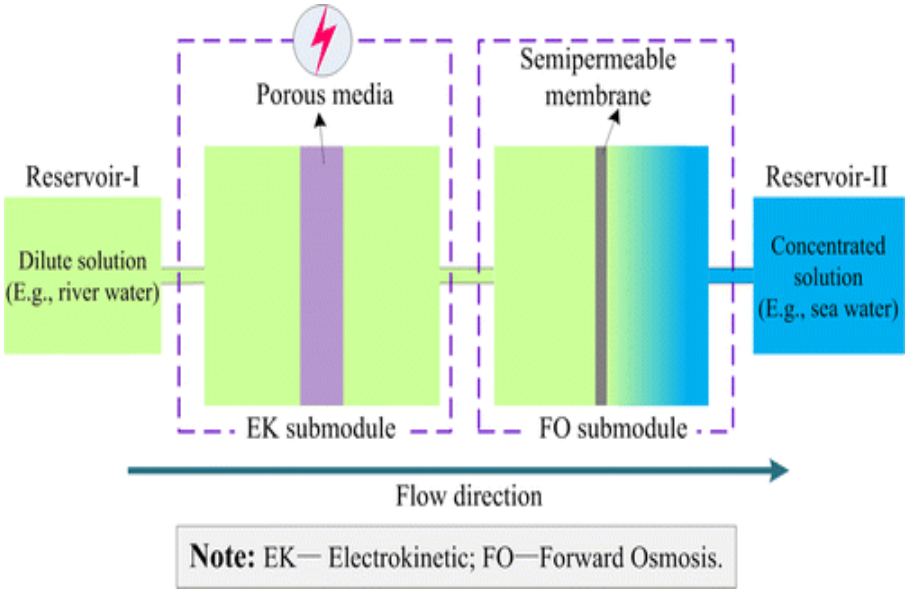

Figure 2.8: Energy conversion from salinity gradients by forward osmosis–electrokinetics (Jiao et al. 2014).

Therefore, a mechanically robust PRO membrane is needed to be capable of withstanding the intense pressure. This is absolutely necessary to take advantage of the energy efficiency achieved by a high DS concentration in the hybrid PRO-MD system.

There is another novel hybrid FO system for energy production that can convert a salinity gradient to electricity through Forward Osmosis–Electrokinetics hybrid system (EK-FO). Figure 2.8 illustrates the schematic of the EK-FO process. However, energy efficiency from this system seems to be lower than hybrid PRO-MD system (Jiao et al. 2014; Lin et al. 2014). Although hybrid systems have been developed to ignore FO limitation in desalination sector for production of potable water but still those limitation factors exist to some extent. Challenges that limit the FO process will be discussed in more details in the following sections.

2.5 **FO challenges**

FO has few challenges before full commercialisation. These include finding a suitable DS, a better membrane and recently added, and better fluid management when applying the FO in the practical large scale field.

2.5.1 **Draw solution**

2.5.1.1 **Osmotic agents**

There are several elements and chemicals that can be used as DS in FO. Ionic salts, regular fertilizer and other osmotic agents. For instance, calcium salts are of interest because of retrograde solubility. Surfactants exhibit great changes in solubility at a distinct temperature (Gadelha et al. 2014). Poly-electrolytes and water soluble polymers are potential non-volatile and non-toxic alternatives as well. However, the osmotic potential of polymers are unexpectedly low due to the length of the polymer chain (Picorel et al. 1998). Interestingly, Li.D et al. introduced stimuli-responsive hydrogels as the draw solutes for the FO process (Li et al. 2011). As mentioned in the previous section, a few novel studies have tried to use FO in hybrid desalination systems setup with DS as medium. For instance, Ge et al. used hydrogels as the draw solute in a hybrid MD-FO unit (Ge et al. 2013). In the MD-FO hybrid, DS will be thermally recovered. MD runs at a higher temperature compared to FO. Therefore, higher water flux is obtained due to substantial reduction of hydrogel viscosity. Also many researches have been done to select a suitable osmotic agent as a DS and it is not clear which DS to introduce that would meet all the criteria that have been pointed out for suitable osmotic agents.

2.5.1.2 **Screening osmotic agents for FO application**

DS for FO needs to generate relatively high osmotic pressure, to be easily recoverable, to have low cost and low leakage (reverse salt flux) and zero toxicity. A variety of DS have been investigated for the FO process in recent years. Unfortunately most of the potential agents can be ignored for FO desalination due to toxicity or reactivity concerns (Ge et al. 2013). The conventional ionic salt has the least difficulty in handling and toxicity, given that the recovery of DS is crucial for obtaining the product water as potable drinking water. Firstly, an alternative osmotic agent such as magnetoferritin seems to be interesting. Magnetoferritin has potential as an osmotic agent. It can be recovered with a magnetic field. However, low osmotic pressure generated by magnetoferritin makes it non feasible for any practical application despite the easy recovery (Kim et al. 2011). Furthermore smart DS for FO have seen significant advances in which smart draw agents with responsive properties can be recovered under different stimuli from water. Also there are few limited operational factors in addition to low water flux for this proposed DS as well.

Therefore in conclusion DS screening focus will be on salt base ionic elements which can meet most of the criteria for suitable DS for FO process. First of all, after the initial screening mentioned at the beginning of this section, the best DS for the FO process can be categorized in diffident terms. Achilli et al. studied wide varieties of potential osmotic agents as a DS for FO and concluded that the best DS ranked in terms of performance were $KHCO_3$, $CaCl_2$, $MgCl_2$, $MgSO_4$, plus $NaHCO_3$. However, in terms of replenishment cost analysis the best DS were $KHCO_3$, $MgSO_4$, NaCl, $NaHCO_3$, and Na_2SO_4. Considering performance and cost effectiveness ($KHCO_3$, $MgSO_4$, and $NaHCO_3$) have been ranked the most suitable (Achilli. et al. 2010).

Adding fouling factor (chemical fouling) which is common in the FO application, chemical fouling can screen it further and determine the most suitable DS in the FO process. When either feed or DS containing ions with scale precursor potential (for example Ca^{2+}, Ba^{2+}, SO_4^{2-}, Mg^{2+} and CO_3^{2-}) the chance of scaling will increase on the membrane surface. This is particularly true when the feed solution concentration is above the solubility limits of water-soluble minerals such as $CaCO_3$ (calcite), $CaSO_4$ (gypsum), $BaSO_4$ (barite), and Mg $(OH)_2$ (Achilli. et al. 2010; Fritzmann et al. 2007; Rahardianto et al. 2007) .

$Mg(OH)_2$ can be formed only at pH greater than 9 (Rahardianto et al. 2007). Thus, there will be a low risk of scaling in use of $MgCl_2$ in most FO applications. Other DS's with higher risk of scaling that is ($CaCl_2$, $MgSO_4$, $KHCO_3$, $NaHCO_3$, and Na_2SO_4) limited to specific FO applications with pure feed solutions. For food concentration $NaHCO_3$ or $KHCO_3$ may be most desirable due to high FO water flux with low reverse salt diffusion. Due to various ion matrix of the feed solutions in the case of FO application in brackish or seawater treatment, DS which contain scale precursors are not recommended. Therefore, $MgCl_2$ may be the most suitable DS for various water and wastewater applications. However, considering the different characteristics of those DS, specific FO application and types of membrane being used are essential prior to selecting appropriate DS (Achilli. et al. 2010). Table 2.1 shows the history of draw solutes used in FO with different regeneration method.

In conclusion, organic, inorganic compounds and polymers have the potential to be used as a DS. Draw agents with responsive properties are attractive for FO application. The stimuli-responsive polymer hydrogel draw agent has also been investigated in the FO process. The stimuli-responsive property of hydrogels can be enhanced by further optimization. However, most of the stimuli such as solar

irradiation, direct heating and magnetic nano particles have been studied in the non-continuous FO processes. More work is required to develop continuous stimuli FO processes for practical applications.

Table 2.1 History of draw solutes used in FO with different regeneration methods. Modified from (Ge et al. 2013) .

Year	Osmotic agent	Regenerating method	References
1965	So_2	Heating or air	(Batchelder 1965)
1972	Al_2So_4	stripping	(Frank 1972)
1975	Glucose	Precipitation by	(Kravath & Davis 1975)
1976	Nutrient solution	doping $Ca(OH)_2$	(Kessler & Moody 1976)
1989	Fructose	None	(Stache 1989)
1997	MgCl2	None	(Loeb et al. 1997)
2002	KNO_3, SO_2	None	(McGinnis 2002)
2005	NH_4HCO_3	None	(McCutcheon. et al. 2005)
2008	Salt, ethanol	SO_2 removed	(McCormick. et al. 2008)
2010	Magnetic nanoparticles	through standard	(Ling et al. 2010)
2011	Fertilizer	means	(Phuntsho et al. 2011)
2011	Stimuli-responsive	Heating	(Li et al. 2011)
	polymer hydrogels	Pervaporation	(Kim et al. 2014)
2014	Thermo-responsive	Magnetic field	
	copolymers with ionic	Direct application	
	group	Pressure- heating	
		Heating to 70 °C	

2.5.2 **Membrane**

The second limitation that challenges the FO process is a lack of a suitable membrane. The FO process can run without hydraulic pressure as a driving force. As

it is a unique process, it needs a unique membrane to fulfil the osmotic requirement. The process for making a suitable and durable FO membrane has yet to be discovered. Fabricating a suitable membrane for FO is another major challenge. A review of the literature and history of research on the FO process presents that there are mainly three pathways to membranes that can be used in FO process. The most common approach and the earliest one was using a RO membrane for FO application. The main obstacle is low water flux across the membrane due to a thick backing fabric support and a dense hydrophobic support polymer that hinders the water transport. Although there is limited published data on this approach, in recent studies, fluxes of up to 3.1 $Lm^{-2}h^{-1}$ were reported (Arena. et al. 2011). The low fluxes can be mainly related to the fact that RO membranes possess a relatively thick polymer support and the support of a non-woven fabric to withstand the high applied hydraulic pressure.

The second approach is to modify the RO membrane for FO application. Also it is almost impossible to replace the thick backing fabric but further modification on the membrane polymer support structure is possible by increasing the hydrophilicity nature of the support. There are few works that mainly focus on increasing membrane hydrophilicity. It has been done through direct and indirect sulphonation, dopamine and polyethylene glycol coating treatment to increase the membrane wettability. Using dopamine for RO membrane modification proves to be interesting. Also results have not been promising for the FO process however a very large improvement is found for pressure retarded osmosis (PRO) for energy production (Arena et al. 2011).

The third and final approach is to design and fabricate a membrane that is customised for the FO process. Understanding the fundamentals of the FO process, and its dependency on osmotic pressure and the role of osmotic agent, make it possible to design a membrane that can suit the process. So far a membrane that is robust, hydrophilic, thin with porous backing fabric support has been recommended based on fundamental findings (Gray et al. 2006). Although the FO already has been exploited in several applications, designing a suitable membrane remains as a major challenge (Yip & Elimelech 2011). FO desalination technologies can be viable in the coming years, if a proper high performance membrane is carefully considered. There are a few considerations that need to be overseen regarding a suitable membrane for FO which are concentration polarization (CP) and fouling. Concentration polarization is an existing problem in most of the membrane separation technologies. CP, however, is the main reason for low water flux in FO membranes; the CP will be explained in more detail and fabrication of suitable membrane will be discussed in section 2.5.

2.5.2.1 **Concentration polarization in an osmotic driven membrane**

The flux in an osmotic driven membrane such as FO depends on osmotic pressure difference ($\Delta\pi$) across the membrane thin active layer. However, the osmotic pressure is lower across the active layer compared to bulk osmotic pressure in the feed and DS. This results in lower water flux which is often attributed to several phenomena (Cath et al. 2006). Two types of CP phenomena, (1) external CP and, (2) internal CP in osmotic driven membrane processes can take place as discussed in more details below:

2.5.2.1.1 **External concentration polarization**

In the RO process, CP mostly occurs on the exterior surface of the membrane which is known as external concentration polarization (ECP) (McCutcheon & Elimelech 2006c). Due to constant pressure and rejection of solute by the rejection layer of the membrane, bulk osmotic pressure near the membrane surface increasingly builds up. This causes a reduction in water flux through the membrane (Hoek & Elimelech 2003). The actual osmotic pressure is higher than that in the bulk and water flux is therefore reduced. ECP is a well-known phenomenon in the RO membranes. Also ECP exists in the FO process but it is not a major problem compared to the RO process or existence of ICP that is much more common with FO (Mccutcheon & Elimelech 2007). In membranes with a dense symmetric structure used as a FO membrane, the ECP can causes a dilutive effect on the DS near the membrane surface, causing osmotic pressure decrease resulting in water flux decline. Unlike the RO membrane, ECP effects depend on operational mode as well (Tan & Ng 2008).

FO process divides into two operational modes known as FO and PRO modes shown in Figure 2.9. In the PRO mode DS faces the selective layer while in the FO mode the DS faces the support layer. Effects of ECP have been observed to be opposite in the two modes. However, in the both modes it can reduce the water flux through dilutive ECP in PRO mode on DS side and concentrative ECP in FO mode on feed solution side. Furthermore, regardless of the operational modes, it is well known that the ECP can be limited by increasing the water flow rate (McCutcheon & Elimelech 2006a).

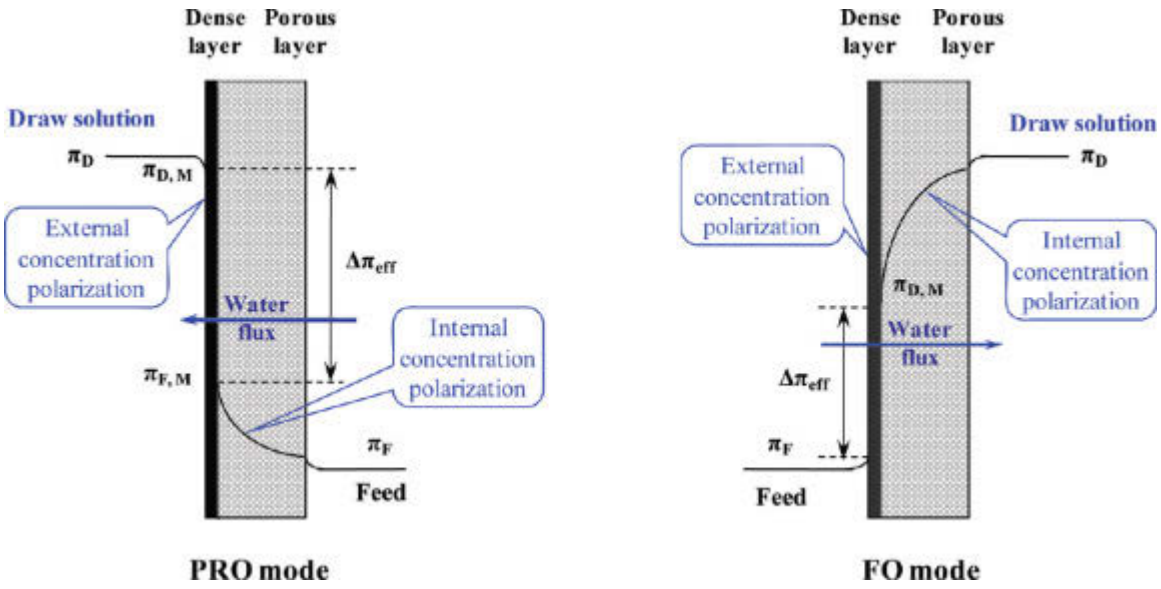

Figure 2.9: Water flux transport in the PRO and FO mode in FO process (Wang et al. 2010).

2.5.2.2 **Internal concentration polarization**

Internal concentration polarization (ICP) is a more severe problem in the FO process which is related to the membrane structure (Hoek & Elimelech). This phenomenon occurs within the semi permeable membrane. Solute characteristics may play a role in the ICP effect as well. Solute with different diffusivity and molecular size can affect the ICP (Zhao & Zou 2011). Thus the ICP can be related to the membrane substrate morphology directly or solute characteristics indirectly. It means the ICP depends on both morphology and solute diffusivity in the FO membrane. Solute diffusivity is an element chemical property but it can be hindered by membrane tortuosity (Mitragotri et al. 2011). Similar to ECP, there are different ICP effects depending on operational modes. In the PRO mode, mostly concentrative ICP exists. Solute accumulates in the membrane support structure through feed solution as well as reverse solute flux from DS. As a result, this increases the osmotic pressure within the membrane structure in the feed side, resulting in water flux decline (Yip &

Elimelech 2011). Furthermore, dilutive ICP occurs in the FO mode resulting in DS osmotic pressure decrease and water flux decline. In conclusion, it has been revealed that, firstly ICP can causes more flux decline compared to the ECP, secondly ICP is more obvious in the PRO mode and finally ICP is more severe at the higher DS concentration (Tang et al. 2010). Unlike ECP, the ICP effects cannot be limited by hydrodynamic flow conditions such as increasing turbulence through applying a spacer or water flow rate (Xu et al. 2010). Through this fundamental, a considerable effort has been made to design a suitable membrane for the FO process to minimize the ICP effect in recent years. Thus the desirable membrane structure needs to be a thin substrate which is highly porous and possesses a low structural parameter.

2.5.2.3 **Reverse solute flux (RSF)**

Another major problem in the FO process which is directly related to the membrane properties is reverse solute flux (RSF). Also this phenomenon can be related to the types of different DS based on their molecular size and monovalent or divalent ions as well (Zhao & Zou 2011). However, the membrane is the main barrier that can limit RSF regardless of DS properties. Permeated salt from the DS side can accumulate in the membrane structure and reduce the effective driving force required for the FO process. Furthermore, the mechanism of fouling in FO is relatively different with RO and is reversible (Mi & Elimelech 2010). Recent studies revealed that RSF is correlated with membrane fouling. The reverse diffusion of draw solutes can enhance the osmotic pressure within the cake layer and accelerate the FO fouling (Tang et al. 2010). Specific reverse solute flux (SRSF) which is the amount of RSF per obtained water flux can represent membrane selectivity regardless of DS concentration (Phillip et al. 2010). In addition to water flux and membrane rejection,

SRSF can be the third measurement for membrane performance. RSF can be controlled based on two strategies in FO: the first is a membrane with desired morphologies that has been discussed previously and, the second is the selection of a suitable osmotic agent as a DS. For example, multivalent ions (Mg^{2+} and Ca^{2+}) can encounter higher salt rejection compared to monovalent ions (Na^{+}). Higher rejection can lower salt reverse flux in the FO process. Also monovalent ions have lower diffusivity which can enhance greater ICP (Zhao & Zou 2011). Generally, RSF is an undesirable phenomenon in the FO process which can be minimized by design of a suitable membrane. However, RSF is a much lower problem in other FO application like the PAO process. In the PAO process applied hydraulic pressure can increase the water flux that likely limits the diffusivity of the draw solutes through the membrane. This occurs due to enhanced convective water flux that drives the draw solutes away from the membrane (Phuntsho, Shon , et al. 2012).

Fouling is a common problem with the different kinds of membranes but it is rarely with the FO membranes if suitable membrane and proper DS are chosen based on feed solution properties (Tang et al. 2010). Thus, fouling can be related to RSF indirectly. Improved membrane resistance to fouling can be achieved through a modified selective layer or special support structure designed for limiting the fouling on both sides of the membrane. Wang et al. (Wang et al. 2010) designed a double-skinned FO which limits the solutes in the DS from entering into the membrane porous substrate. This can decrease the ICP within the membrane structure and potential fouling across the membrane surface. Water flux was 48.2 L $m^{-2}h^{-1}$ while reverse salt flux was 6.5 g $m^{-2}h^{-1}$ using 5.0 M $MgCl_2$ as the DS (Tang et al. 2010). In addition, as mentioned before, properties and diffusivities of the osmotic agent are

related to RSF and as a consequence in the fouling formation (Tang et al. 2010; Zhao & Zou 2011).

2.5.3 **Fluid management**

Researchers on FO have raised two major challenges which are to identify a suitable DS and to develop an appropriate membrane to decrease the effect of CP, reverse solute diffusion and fouling (Cath et al. 2006; Chung 2012).

Yale University has recently presented a standard methodology for assessing performance in osmotically driven membrane processes (Cath et al. 2013). The first pilot plant on FO was developed by Yale University 8 years ago (Elimelech 2007). They have concluded that the most important factor to advance the field of FO is the development of new membranes. Another study has a further investigation and conclusion for FO capability performance in a large pilot scale. Robert W. Field and Jun Jie Wu suggested a third area which is as important as the other two challenges especially for the practical large scale application (Field & Wu 2013). Even if the ICP is reduced within membranes and a suitable DS is found but there is other factor that can limit the FO application. Unlike RO with only one influential film mass transfer coefficient, there will be three in FO for desalination. As module size increases, mass transfer limitation is more vigorous in FO than in other membranes. Developing a module with superb film mass transfer coefficients may not be feasible for large scale application. Thus, the FO future may lie with the wastewater niche applications or PRO for energy production. Then regarding FO application, PRO might be more important for energy production than FO for potable water desalination.

2.6 **Membrane for engineered osmosis**

Any dense permeable material with selective properties can be used as a membrane for FO (Lacey & Loeb 1972). By 1960, the Loeb–Sourirajan process for developing high-flux RO membranes revolutionized membrane separation technology for desalination (Bui et al. 2011; Cath et al. 2006). They evaluated the use of asymmetric polyamide membranes for the FO process. RO membranes used for all studies involving osmosis in the 1970s; however, lower flux than expected was common with those RO membranes (Cath et al. 2006). Later on, during the 1990s, Osmotek Inc. developed a special membrane for FO. This membrane has been evaluated successfully in a wide variety of applications (Cath et al. 2006; Cath et al. 2005; Mallevialle et al. 1996).

HTI membrane is made of cellulose triacetate (CTA). CTA FO membrane is different from RO membranes in regards to thickness and backing fabric support. RO membranes are comprised of a thin active layer and a thick porous polymeric substrate with a thick backing fabric support. Instead of the CTA FO membrane embedded polyester mesh provides mechanical support. Based on the results, the CTA FO membrane is superior to RO membranes for FO application (Cath et al. 2006). Thinner membrane substrate and the lack of a thick nonwoven fabric support are the major contributing factors for HTI FO high performance compared to the RO membranes.

In summary, an excellent membrane for FO would be a thin membrane, porous and hydrophilic membrane. Higher hydrophilicity is required for enhanced flux and reduced membrane fouling. Furthermore, the membrane needs reasonable mechanical strength to withstand hydraulic pressure especially when used for PRO or PAO (Cath et al. 2006). Designing a robust membrane for FO is critical for further

advance in FO application. Membranes that can achieve high flux and salt rejection with high mechanical strength to support high hydraulic pressures especially for PAO and PRO application will result in higher efficiency in current applications.

2.6.1 **Polymeric membranes**

In terms of applications, membrane can be divided into two main groups: Industrial applications including desalination (FO, RO, UF, MF, ED, MD, gas separation, per-evaporation and medical application (artificial kidneys, controlled release pharmaceuticals and blood oxygenators) (Baker 2000). Polymeric membranes can be categorized in terms of substrate structure and fabrication methods, regardless of their application. Membrane differences in terms of substrate structure and configuration are briefly discussed before explaining the fabrication methods.

2.6.1.1 **Substrate structure**

In terms of substrate structure, membranes can be divided into two categories, (1) membranes with symmetrical structure, and (2) membranes with asymmetric structure. The following sections will briefly define the two structure differences.

2.6.1.1.1 **Symmetrical membranes**

Symmetrical membranes have a uniform structure and morphology. These substrates can be either microporous or dense films. They are be used in packaging applications and industrial use. However, making a symmetrical membrane thinner than 20 μm, mechanically strong and defect-free, is difficult. Therefore, due to their dense structure with high thickness, water flux is limited (Hughes 1996). Figure 2.10 shows the symmetrical and asymmetrical membrane differences.

2.6.1.1.2 **Asymmetric membranes**

In the 1960s, the development of asymmetric cellulose acetate membranes consisting of a thin surface layer on a microporous support was a breakthrough in membrane fabrication technology. There was a limit to manufacturing mechanically strong symmetrical membranes. The development of novel membrane fabrication techniques was considered a revolution in membrane technology (Baker 2000). Figure 2.10 shows the diagrams of the principal types of symmetrical and asymmetrical membranes. Asymmetric membranes can be fabricated thorough several different casting method. For example asymmetric composite membranes are in general an improvement over phase inversion membranes, since the composite technique allows fabricating and modifying the support and active (skin) layer independently (Baker 2000; Nunes & Peinemann 2001). Therefore, asymmetric membranes have a much improved performance and are widely used for pressure based membrane processes, such as RO for seawater desalination.

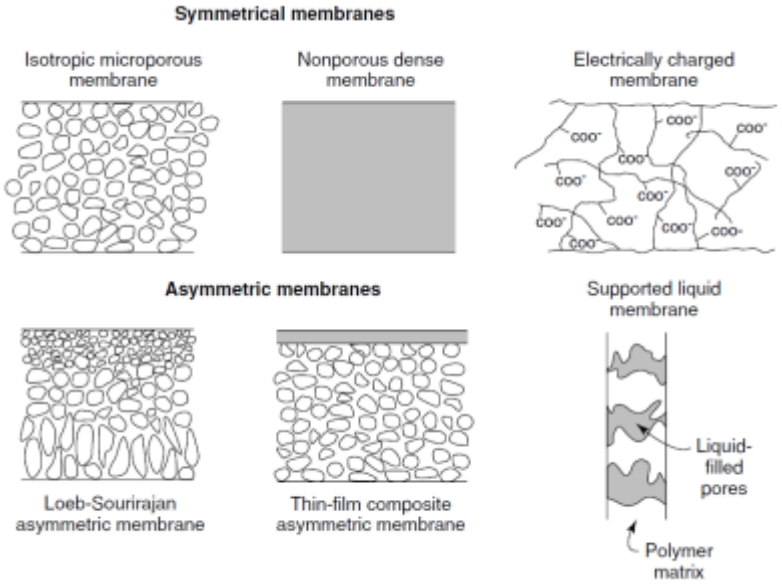

Figure 2.10: Illustration of the principal types of membrane in terms of their structure (Baker 2000).

2.6.1.2 **Membrane modules**

FO membrane modules are divided into 4 generic design and configuration, (1) the plate & frame module, (2) the spiral wound module, (3) the tubular module, and (4) the hollow fibre module (Stephenson et al. 2000). As it can be seen from Figure 2.11, the tubular and the hollow fiber modules are very similar but the difference is the inner dimensions of their tubular/hollow fiber membrane components.

Each design potentially caters to different application areas and thus they are treated separately. There are two criteria for characterization of those modules, (1) achievable packing density and, (2) industrial application. However, packing density is a more important characterization criterion because it contributes remarkably to the overall footprint of an FO system. This means the smaller the packing density the larger the FO system footprint and vice versa. Figure 2.11 illustrates the schematic of 4 types of membrane modules.

2.6.1.2.1 **Spiral wound module**

Spiral wound module is the most common membrane configuration. They are based on flat sheet membranes with high packing density. For example, they can reach packing densities as high as 1200 m^2/m^3 with the distance between membrane layers less than 1mm. Therefore, the spiral wound modules tend to foul very easily especially for wastewater streams (Schwinge et al. 2004). However, packing density cannot reach the same values for FO as it is in the case for spiral wound RO modules, because the FO must be a cross flow on either side of each individual membrane layer. Thus the total thickness of spacers between membrane layers increases the total thickness of spacers between membrane layers which resulted in

packing efficiency decreases. Packing densities of the spiral wound modules for FO are half of RO and close to 600 m^2/m^3 (Cath et al. 2006).

Similar to RO, the spiral wound FO modules for industrial water treatment are limited to applications where the feed contains low concentrations of fouling agents (Xu et al. 2010). In conclusion, this module due to high packing density is suitable for large-volume applications; however, membrane fouling is a main issue if the feed is not pre-treated to remove the majority of fouling agents.

2.6.1.2.2 **The plate and frame module**

Plate & and frame module that are also known as stacked membrane modules are for the feed such as wastewater that contains high amounts of fouling. Most of commercial membrane bioreactor (MBR) modules belong to the plate & frame configuration (Lutchmiah et al. 2014). This module typically consists of flat sheet membranes sealed to frames. The frame provides the overall flow distribution and mechanical integrity of the module. It has the lowest packing density and largest footprint among the four module designs. Therefore, it has been excluded from being used in high volume applications such as municipal waste water treatment and desalination of seawater. However, in many lower volume applications, where the waste streams to be treated contain high amounts of fouling agents and/or have high viscosities, the low packing density of plate & frame modules represents an operational advantage.

The larger distance between membrane sheets in this module results in a lower pressure drop across the module therefore lower energy required for pumping solutions through the module as well as a lower propensity towards clogging of flow channels due to accumulation of fouling agents. In conclusion, the biggest advantage

for this module is ease of operation when the feed contains high amounts of fouling agents or for feed with high viscosities. However, the large footprint increases space requirements which make it unsuitable for high volume applications (Beaudry & Herron 1997).

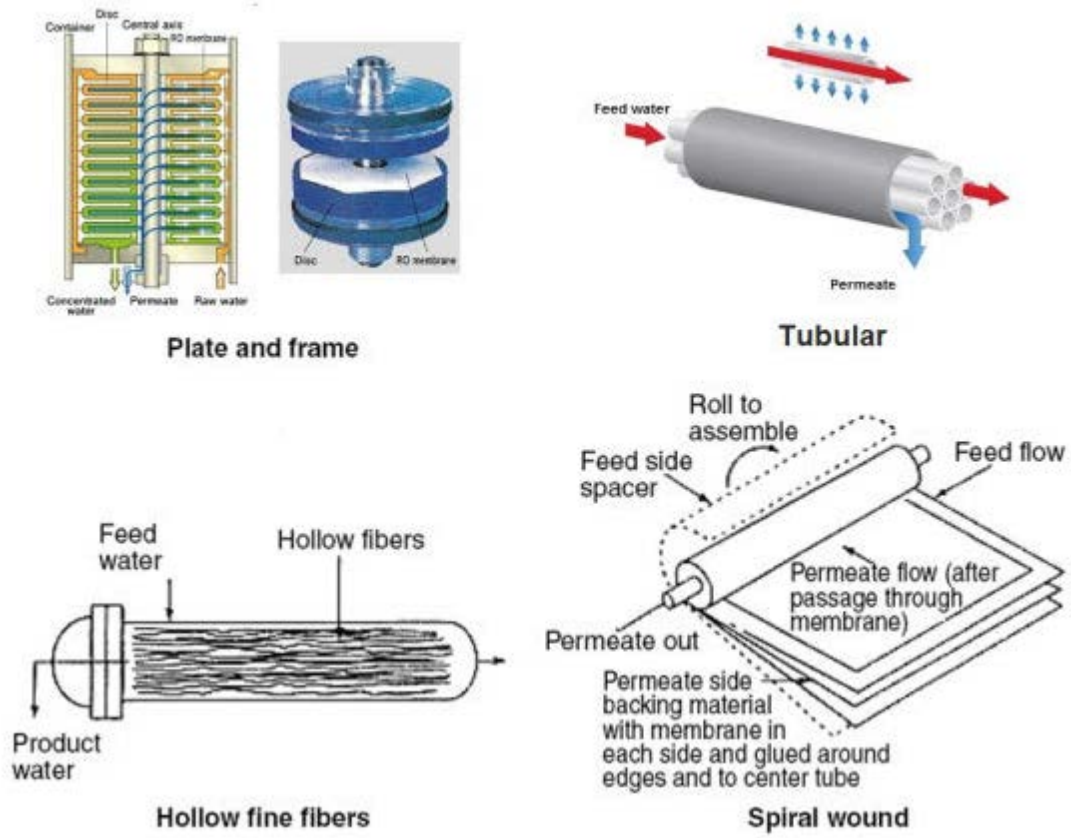

Figure 2.11: Schematic for membrane modules. Modified from (Sincero & Sincero 2002).

2.6.1.2.3 **Hollow fibre module**

The hollow fibre modules are similar to tubular modules with much higher packing densities. Due to their small internal diameters these modules are prone to fouling and clogging. Therefore, their usage is limited to applications where the feed solution contains low concentrations of fouling agents such as in desalination. They have a small footprint due to high packing density but significantly are prone to fouling and membrane clogging (Bui et al. 2011).

2.6.1.2.4 **Tubular module**

This module is well-known in the water treatment industry for ultra-filtration applications. Due to the nature of the modules, lower packing density, feed with high fouling agents and high viscosity they will have less effect on. They have Inner diameters of the modules ranging from 5 mm to 15 mm that are coated with micro-porous polymeric layers on either the inside or outside walls. Regarding FO industrial application, the tubular modules may be a suitable option for feed with high fouling / high viscosity wastewater streams. Then they are similar to plate and frame modules for FO application of high foulant feed. The main advantage is that they have up to 4-5 times higher packing densities compared to plate and frame modules which significantly reduce the overall footprint of the tubular FO modules. However, the overall thickness of the porous tube wall might render the tubular configuration unfit for FO processes due to severe build-up of ICP (Kimura & Nakao 1975).

2.7 **Engineering principles for the design of polymeric membranes**

There are several different techniques to prepare synthetic membranes, including sintering, stretching, track-etching, solvent evaporation, water vapor imbibition and phase inversion. Among these technologies, phase inversion is the most widely used method for preparing polymeric membranes. It is a very convenient and versatile technique that potentially allows various kinds of morphologies and separation properties to be obtained. Thus most commercially available membranes are obtained by phase inversion due to the mentioned advantages.

2.7.1 **Phase inversion induced asymmetric membranes**

Loeb and Sourirajan developed the first asymmetric, high-flux RO membrane which is now well known as the Loeb–Sourirajan technique. Phase inversion is the most important asymmetric membrane fabrication method. Phase inversion is the most popular for preparing polymeric membranes due to it being a versatile technique that allows several kinds of morphologies and structures. Therefore, it is not surprising to see that most of the commercially available membranes especially in desalination industries are synthesized via phase inversion. In this process, the polymer solution is precipitated into two phases: (1) solid phase, polymer-rich phase that forms the membrane substrate, and (2) a liquid phase, where pores form under polymer-poor phase. Those phases will be further explored through a ternary phase diagram (Figure 2.12).

A variety of membranes with different pore morphologies can be fabricated for different applications via phase inversion. They can vary from porous microfiltration membranes, to a much denser membrane such as RO and gas separation membranes. In order to fabricate suitable membranes for water desalination especially osmotic membranes, understanding the fundamental theories on membrane precipitation through phase inversion is essential (Tsay & McHugh 1990; Wijmans et al. 1983). Generally, in phase inversion, polymer is transformed from a liquid phase to a solid phase in a manner that can be controlled by solvent, non-solvent and polymer concentration rate (Chickering III et al. 2000).

The ternary phase diagram illustrated in Figure 2.12 can explain the pathway the polymer solution has followed in the phase inversion step. The phase regions and boundaries are illustrated in a ternary phase diagram.

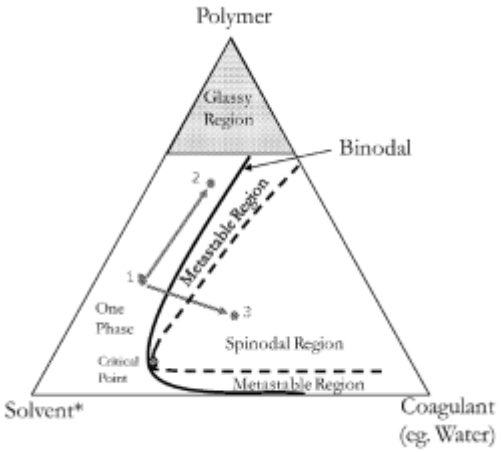

Figure 2.12: Ternary phase diagram of system with three component used in Loeb–Sourirajan membranes fabrication (Husain 2012).

The points 2 and 3 represent the change in polymer dope composition for the skin layer and the porous sublayer respectively after the polymer film with initial composition (point 1) is immersed in a nonsolvent bath such as water. Point 1 shows the initial polymer dope composition and the skin layer formation is believed to form before phase inversion in the air gap through the evaporation of volatile solvent from the surface of casted film at an arbitrary composition point 2 closer to the glassy region of the phase diagram. The interior porous sub layers, beneath the skin layer, form through the spinodal region around point 3 (Baker 2000; Husain 2012; Tsay & McHugh 1990).

A polymer solution with approximately 20% by weight of dissolved polymer can form a dense, selective skin layer on top of the membrane surface (metastable region in the ternary diagram, Figure 2.12). As a consequence, the dense skin layer slows down the entry of non-solvent in precipitation bath (water bath) into the underlying polymer solution. Thus it precipitates more slowly and forms a more porous substructure. Factors which determine the pore size and the porosity of membranes developed by this method are polymer concentration rate, additives and solvent /non

solvent compatibility. Decreasing the polymer concentration or increasing the non-solvent content of the casting solution enhances porosity. It is important that the non-solvent be completely incompatible with the polymer. Semi-compatible non-solvents encourage the slow precipitating which results in a dense rather than a microporous film (Guillen et al. 2011).

2.7.1.1 **Immersion precipitation process (Loeb–Sourirajan process)**

As described in the previous section, polymer precipitation can be achieved in several ways. However, precipitation by immersion in a non-solvent bath which is well known as the Loeb–Sourirajan process is the most important membrane-preparation technique for membrane fabrication. In fact, the Loeb–Sourirajan process is a subcategory of the general class of phase inversion membranes. Figure 2.13 shows Loeb–Sourirajan membrane casting setup equipment used to fabricate RO and UF membranes. A casting knife is used to coat the casting solution onto a moving backing fabric or polyester web which is then immersed in the water bath tank for precipitation. (Miller et al. 1966).

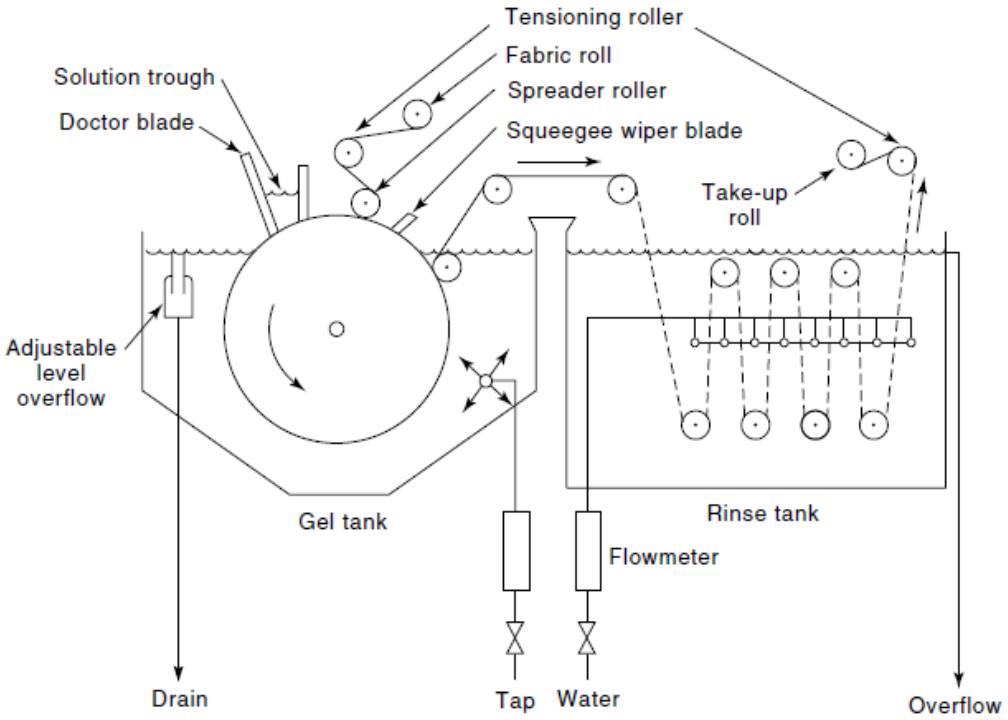

Figure 2.13: Schematic of Loeb–Sourirajan membrane casting machine used to fabricate RO and UF membranes (Miller et al. 1966).

2.8 **Forward osmosis membrane fabrication methods**

Optimizing the membrane material and the fabrication procedure are two common methods to improve the membrane performance. Based on previous studies, there are at least two different fabrication techniques to produce polymeric membranes for FO application and one distinguished fabrication technique to produce non polymeric, inorganic membranes. Polymeric membranes are divided in to: (1) integral asymmetric membranes which were fabricated via one-step non-solvent induced phase separation (NIPS); polybenzimidazole (PBI) and cellulose acetate (CA), cellulose triacetate (CTA) and (2) composite membranes which were fabricated via a two or more step preparation using phase inversion followed by interfacial polymerization. The third type of novel non-polymeric membranes has been listed as inorganic membranes for engineered osmosis.

2.8.1 **Phase inversion membranes**

The fabrication of asymmetric and symmetric membranes through one stage precipitation of a polymer solution is called phase inversion. Phase inversion is one of the most versatile membrane fabrication techniques to prepare vast varieties of different polymeric membranes including FO. In the following section the most popular membrane for FO that is fabricated through phase inversion will be presented.

2.8.1.1 **Cellulose acetate (CA)**

Cellulose ester polymers, especially cellulose acetate (CA) have attracted attention in order to fabricate a suitable membrane for the FO process due to their availability, low cost and high resistance to chlorine. Initially, CA has been used to fabricate RO membranes since Loeb-Sourirajan introduced it in the mid-1960's (Zhao. et al. 2012). CA RO membrane could not perform in the FO process due to a thick non-woven fabric support and low porosity of CA structure support. Therefore, CA material was not implemented for FO until recently. The Hydration Technology Innovations, HTI Company improved the structure design and applied woven polyester mesh with a high open area as a backing support fabric (Herron 2008). CTA FO membrane has an asymmetric structure that is formed via phase inversion. The membrane has been fabricated through a different fabrication method than the CTA RO membrane. Therefore, embedding a polyester mesh woven fabric with high open rate was successful without any appearance of air bubble or polymer penetration that can cause defect points on the membrane surface (Herron 2008). CTA FO membrane fabricated by HTI is relatively thin (90μm) compared to the similar CA RO membrane (250 μm). Cross section morphology of CTA FO

membrane on woven polyester mesh has been shown in Figure 2.14. Porous open polyester mesh and thinner CA support material greatly reduced the ICP compared to the RO membranes. HTI CTA membranes were extensively evaluated in various FO application in the past decade in lab and pilot scale studies (Cath et al. 2006).

Few research groups have tried to develop a FO hollow fiber membrane based on CA material as well. In recent years, Chung's group has developed CA hollow fiber membranes through phase inversion (Su et al. 2010). Also further studies and a few other groups have tried to modify the CA membrane in both flat sheet and hollow fiber. However, low water flux, low rejection, poor resistance and hydrolysis are the drawbacks for CA based membranes. These problems have diverted research focus **from the CA material to** screening better materials for a FO membrane.

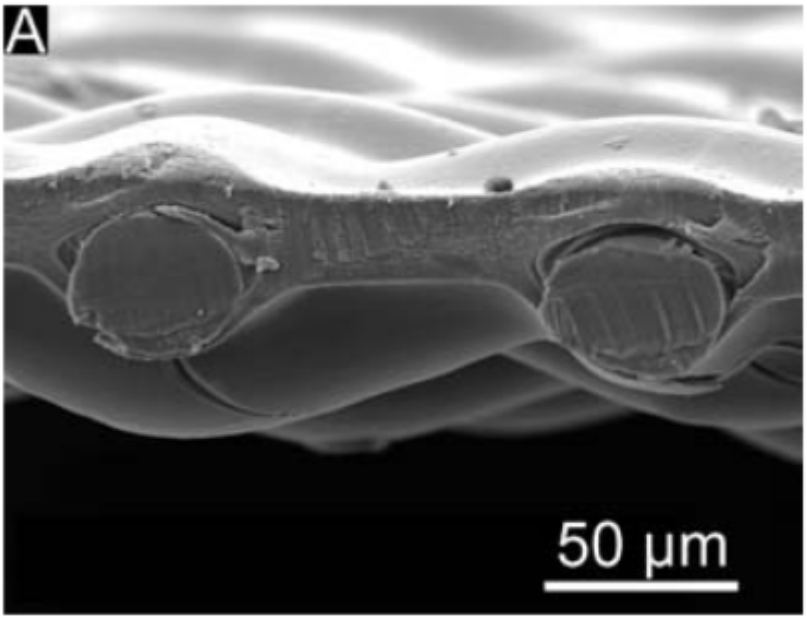

Figure 2.14: Schematic of CTA FO membrane from HTI on woven polyester mesh (Yip et al. 2010).

2.8.1.2 **Polybenzimidazole (PBI)**

Hydrophilic polybenzimidazole (PBI) is another material that has been used to develop a membrane for FO through phase inversion (Wang et al. 2009). Also in terms of hydrophilicity it is similar to CA material but its excellent chemical stability and self-charged properties make it a promising material for the FO membrane. However, similar to the CA material low rejection is common with the PBI membrane. Further modification has been applied through manufacturing a double skin PBI membrane or the dual-layer structure PBI-PES to increase membrane performance in terms of rejection (Yang et al. 2009).

2.8.1.3 **Polyamide-imide (PAI)**

Polyamide-imide has been used as a base support material to fabricate FO hollow fibre and flat membranes through phase inversion in recent years (Setiawan et al. 2011). The advantage for this kind of membrane is that it has a capability to easily crosslink to materials like polyethyleneimide (PEI) molecules for further modifications. PAI crosslinking greatly depends on several conditions which include PEI molecular weight, concentration, casting temperature and crosslinking time (Setiawan et al. 2011). However, in terms of rejection and water flux performance it was not promising. Performance results for the flat sheet PAI membrane were better than hollow fibre membrane due to the ease of further modification of the flat sheet PAI layer. For instance, a positively charged selective layer using the PAI on a woven fabric shows a better performance compared to a similar hollow fibre membrane due to modification (Qiu et al. 2012a).

Table 2.2: Recent FO membranes made through phase inversion. DI water was used as the feed.

Membrane	Materials	Draw solution [M]	Flux L m^{-2} h^{-1}	References
Flat sheet cellulose acetate membrane	CA	1.0 NaCl	12	(Yip et al. 2010)
Flat sheet double skinned	CA	2.0 NaCl	22	(Wang et al. 2010)
Flat sheet with an NF-like selective layer	polyamide-imide	0.5 $MgCl_2$	95	(Qiu et al. 2012a)
PBI-PES dual layer hollow fiber	PBI-PES	5.0 $MgCl_2$	24.5	(Yang et al. 2009)

2.8.2 **Composite membranes**

Composite membranes are composed of multiple layers and are fabricated in multiple stages. They are usually prepared in two steps, (1) fabrication of base support substrate and, (2) formation of a selective layer on top of the support through the next step which can be interfacial polymerisation, spin coating, etc (Kedem & Katchalsky 1963). The advantage for the composite membrane is the ability to modify and control both support and selective layers for membrane custom design. Based on selective layer formation methods, a composite membrane for FO can be divided in to three categories.

2.8.2.1 **Thin film composite (TFC)**

Thin-film composite (TFC) membranes are principally designed for use in water desalination or water purification. Also it has other applications such as fuel cells and batteries (Baker 2000; Lonsdale 1982). A TFC membrane is fabricated through two or more multiple fabrication stages (Petersen 1993). Developing TFC membranes for various applications including desalination was introduced by Cadotte in the 1970s (Cadotte 1977). However, the earliest work on fabrication of TFC for FO membrane application dated back to 2010 (Wei et al. 2011a; Yip et al. 2010). Generally, TFC FO membranes consist of porous membrane support and a top thin rejection layer mainly polyamide. This structure can be supported by backing support fabrics for additional mechanical strength. The formation of a thin rejection layer of polyamides can be formed via interfacial polymerization (IP). IP occurs between two monomer solutions such as m-phenylenediamine (MPD) monomer dissolved in nonpolar organic solvent, for example water and trimesoyl chloride (TMC) monomer in a polar organic solvent, e.g. hexane. Reaction occurs when MPD saturated membrane substrate is exposed to the TMC solution which results in forming a thin selective layer on the top of the membrane support (Cadotte 1981).

Resulting TFC membranes exhibit a high performance (Wei et al. 2011a). However, TFC membranes typically suffer from compaction effects especially for a pressure based membrane such as RO, PRO and possibly PAO process. Due to constant applied hydraulic pressure, the polymers are compacted which results in a lower porosity. In general, the higher the pressure, the greater the compaction and this can affect membrane performance in the long term (Pendergast et al. 2010). Although the procedures for fabrication of FO and RO TFC membrane are similar, the fabrication

schemes are quite different. They have different essential requirements for preparing the support structure that stands as a cushion for the selective layer. Therefore, the main difference between FO and RO TFC membrane is: (1) different polymeric support nature and structure, and (2) supporting backing fabric. Unlike RO with hydrophobic dense polymeric support, FO requires a hydrophilic and porous support structure (Cath et al. 2006). Furthermore, the FO membrane requires a very thin and porous support fabric which can be woven mesh or non-woven PET fabrics. However, RO membranes require a thick support fabric commonly a nonwoven PET fabrics to withstand high hydraulic pressure. Therefore, poor TFC RO membrane performance in FO application can be related to both RO support structure and thick backing fabric support (McCutcheon & Elimelech 2008a). Based on this fundamental, research groups have tried to develop a TFC membrane that can perform in the FO process. Initial efforts show that a finger-like support structure is preferred to form TFC FO membranes (Yip et al. 2010).

Further studies evaluated the porous support hydrophilicity and its effect on FO performance. Results confirm the important role of hydrophilic support characteristics on FO performance (Wang et al. 2012b). Increased hydrophilicity can be achieved either by choosing more hydrophilic materials such as polyethersulfone (PES) or direct sulphonation post treatment through thermal sulphonation or blending with sulphonated polymers (Ariza. et al. 2002). A new comprehensive approach to fabricate high performance TFC FO membranes using sulphonated materials in the preparation of membrane supports was demonstrated by Widjojo et al. (Widjojo et al. 2011, 2013). From this finding it can be concluded that membrane hydrophlicity has more effect on and that it has a performance than support structure

morphology. Resultant hydrophilic membrane (sulphonated membrane) also shows fully sponge-like structure but attains a superior performance in terms of water fluxes and salt reverse fluxes (Widjojo et al. 2011). Earlier research on TFC FO membrane has related the membrane performance to the membrane finger-like structure (Tiraferri et al. 2011a). Also this can be true for hydrophobic polysulfone polymers used in that study but when other modification factors such as increasing the substrate hydrophilicty are considered, the role of membrane structure in terms of morphologies on membrane performance may be less important. Furthermore, in addition to sulphonation, polydopamine (PDA) coating on the Psf support layer can enhance hydrophilic properties of the membrane (Arena et al. 2011; Han. et al. 2012). TFC support membrane surface coated with PDA before interfacial polymerization showed improved performance in both water flux and salt rejection (Han. et al. 2012). Also earlier work using PDA on TFC RO membrane showed significant improvement. PDA coated TFC RO membrane structure after removing their nonwoven fabric layer showed remarkable performance improvement. Water flux was enhanced by eight to fifteen fold in comparison with the uncoated membranes (Arena et al. 2011) .

These findings provide an opportunity for screening new hydrophilic materials as an FO support. Few studies evaluate the capability of hydrophilic cellulose acetate materials as support for fabricating TFC FO membrane (Li et al. 2012). Further studies confirmed that cellulose-based polymers can perform as a reliable hydrophilic support for a TFC FO membrane (Alsvik. et al. 2013). In addition, an alternative concept of using electrospinning nanofibers as a support structure for the FO membrane can remarkably decrease ICP and structural parameter. Lower structural parameter in those nanofiber supports is related to its high porosity and low

tortuosity characteristics of membrane films that are fabricated through electrospinning. Results show relatively high water fluxes which are attributed to the high porosity and a relative thin thickness of the eletrospun nanofiber supports (Bui et al. 2011; Bui & McCutcheon 2013; Song et al. 2011). For instance, using the same types of CTA polymer material for producing nanofiber supports water fluxes improved significantly more than the commercial HTI-CTA FO membrane (Song et al. 2011). Furthermore, close performance in different mode of FO and PRO in FO process indicated a significant reduction of ICP within the membrane substrate was made through electrospinning. In conclusion, TFC membranes have higher performance but unlike the cellulose triacetate membrane, TFC membranes consist of polyamide that are not tolerant to chlorine (Sagle & Freeman 2004).

2.8.2.1.1 **Thin Film Nanocomposite (TFN)**

Principally, thin film nanocomposite membranes (TFN) are a modified form of TFC through applying nanoparticles such as zeolites, carbon nano particulates and, etc. on the membrane support structure or selective layer to obtain higher performance (Jeong et al. 2007). Figure 2.15 shows TFC and TFN membranes conceptual illustration. A wide verities of carbon based nano materials can be used to fabricate TFN membranes.

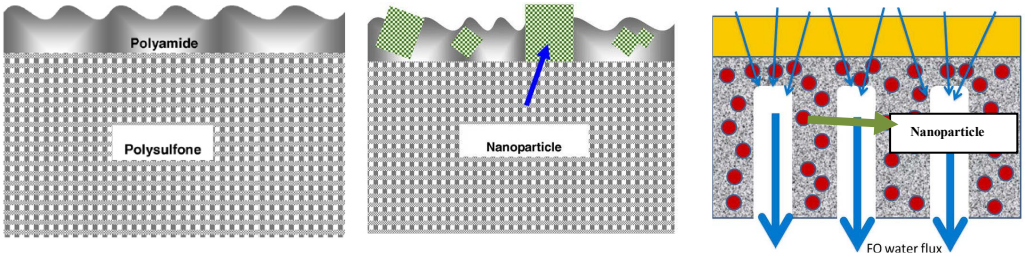

Figure 2.15: Illustration of (a) TFC and (b) TFN membrane with nano particles on selective layer (Jeong et al. 2007), and TFN membrane with nano particles within support structure layer (Ma et al. 2013).

For instance, developing thin film nanocomposite (TFN) FO membranes using multi-walled carbon nanotubes in the membrane selective layer or graphene oxide in the membrane support structure (Amini. et al. 2013). This is explained in the section 2.10 (custom designs of flat sheet FO membranes).

2.8.2.2 **Layer-by-layer composite membranes (LbL)**

The LbL self-assembly occurs through an electrostatic force hydrophobic attraction which is a covalent bonding force (Decher 1997; Johnson et al. 2012; Lojou & Bianco 2004). This is a simple, robust and flexible process to fabricate a membrane for specific separation purposes. LbL fabrication can be assembled via dip-coating, spin-coating, or spraying methods with the aid of electrostatic interaction. The membrane performance properties can be controlled by deposition time, the ionic strength of the polyelectrolyte solution and the pH of the polyelectrolyte solutions (Decher 1997) . Results show that an FO membrane fabricated through the LbL method has a high performance. For instance, water flux up to 100 LMH was achieved using a 2 M $MgCl_2$ with good rejections (Duong et al. 2013; Saren et al. 2011). However, it has poor performance in terms of monovalent ion rejection such

as NaCl. Further studies have improved the rejection performance for monovalent ions by applying an additional layer of polyelectrolyte (Duong et al. 2013).

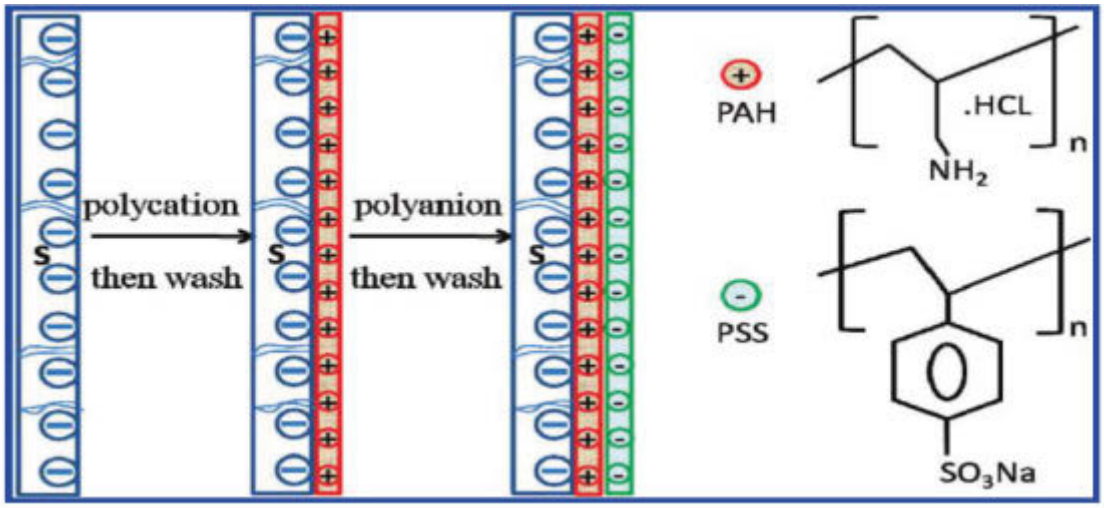

Figure 2.16: Shows layer-by-layer assembly of poly (allylamine hydrochloride) (PAH) and poly(sodium 4-styrene-sulfonate) (PSS) membrane, PSS was used as the polyanion and PAH as the polycation (Saren et al. 2011).

2.8.2.3 **Biomimetic membranes**

Despite a promising result for the CNT and vertically stand CNT membrane (Kar et al. 2012; Wang et al. 2013), currently the highest performance belongs to the successfully made biomimetic membrane (Honglei et al. 2012). Biomimetic membranes have been copied through the function of the biological membranes in the cells that are characterized by their high permeability and specific selectivity towards water and different solutes (Xie, He, et al. 2013). Their unique performance is related to the proteins known as Aquaporins (AQPs). Membrane design has been achieved by mimicking nature through coating of vesicles and black lipid membranes on the top surface of a membrane substrate (Kaufman et al. 2010). Still, however, incorporation of aquaporin remains important (Rigaud et al. 1995).

Regarding FO application, a novel study demonstrates an outstanding performance

by coating aquaporin-containing proteoliposomes or proteopolymersome on the surface of the membrane support followed by interfacial polymerization (Sun et al. 2013; Xie, He, et al. 2013). Also, further study achieved mechanically robust Aquaporin Z-embedded biomimetic membranes for FO with high performance (Xie & Tong). Fabricated flat sheet biomimetic FO membrane showed 142 LMH in PRO mode when 2 M NaCl was used as a DS (Honglei et al. 2012). Figure 2.17 (a) shows preparation procedure of aquaporin based biomimetic membranes prepared through an interfacial polymerization process. A thin layer (yellow line) which contains aquaporin forms the active layer supported by a porous support layer. Figure 2.17 (b) shows permeability values for FO, RO and EE-EO (polyethylethylene polyethylene oxide diblock membrane) to ABA and AqpZ-ABA with incorporated AqpZ Biomimetic membrane. It shows that incorporation of AqpZ increases the performance more than a fold over existing RO and FO membranes. (Kumar et al. 2007).

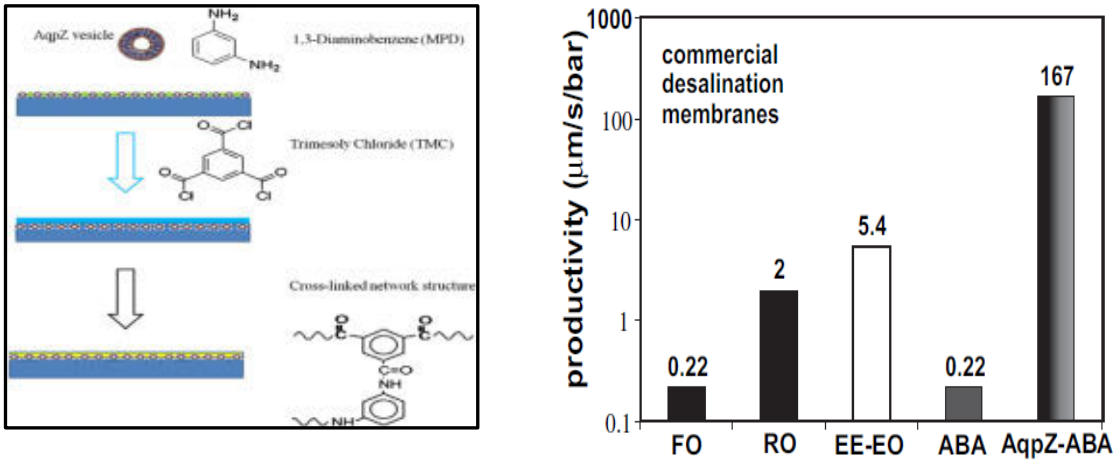

(a) (b)

Figure 2.17: (a) Aquaporin based biomimetic membranes fabricated through interfacial polymerization (Tang et al. 2013), and **(b)** Comparison of permeability for polymeric membranes of FO, RO and EE-EO membrane to ABA and AqpZ-ABA with incorporated AqpZ biomimetic membrane (Kumar et al. 2007).

2.8.3 **Inorganic membranes**

FO membranes prepared through organic polymers are subjected to low stability and severe internal concentration polarization (You et al. 2013). Thin film inorganic (TFI) membranes such as zeolite membranes have been widely studied in recent decades for liquid pervaporation and gas separation (Caro et al. 2000; Tavolaro & Drioli 1999). For example, tetra ethylorthosilicate (TEOS)-driven silica membrane has networks with micro-pores of nanometers (0.3−0.8 nm) for gas separation (Coterillo et al. 2008). Compared to polymeric membranes they possess a narrow pore size distribution and specific pore structure, a potential factor for higher performance in terms of higher permeability and selectivity in desalination. Furthermore, they show better resistance to chemical conditions. However, the performance of zeolite membranes can be affected by hydraulic pressure, ion concentration, feed solution propriety and temperature. Zeolite NaA membrane has been fabricated supported on a porous a-Al_2O_3 ceramic for RO application (thickness 5 ≈ mm). Rejection and water flow performs through inter-crystal pores and zeolite pores in zeolite membranes. However, synthesis of an asymmetric inorganic membrane using a supporting substrate with large thickness (1−5 mm) will promote severe ICP in FO application. Thick porous α-Al_2O_3, γ-Al_2O_3, and TiO_2 for pressure-driven membrane processes have been developed on a substrate with low flexibility (You et al. 2013). In a recent study, Shijie et al. have developed a TFI-FO membrane by LBL deposition of micro-porous silica xerogels on a stainless steel mesh (SSM) support for the FO process. They demonstrated that the ability of TFI membrane to sustain the FO process without any wrinkling, cracking or deformation under the severest conditions. This also suggests TFI has superiority over a polymeric FO membrane. Figure 2.18 shows TFI membrane which is made of micro-

porous silica xerogels on a stainless steel mesh (SSM) frame. The results show that the TFI membrane could obtain water flux of 60.3 L m^{-2} h^{-1} driven by 2.0 M NaCl DS. The specific solute flux was (0.19 g L^{-1}) which is lower than (CTA) membrane (0.46 g L^{-1}) (You et al. 2013).

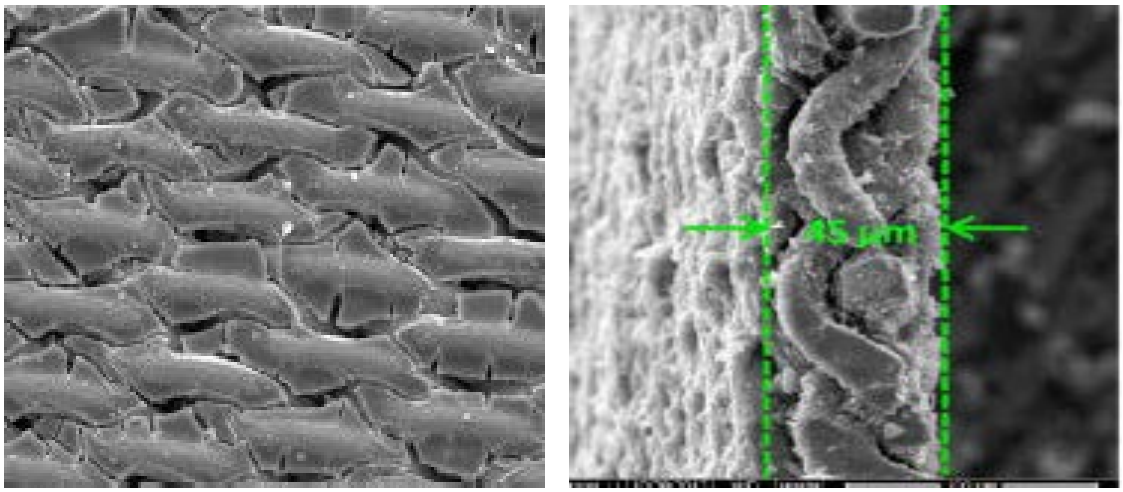

(a) (b)

Figure 2.18: SEM images of TFI FO membrane (a) top surface, and (b) membrane cross section (You et al. 2013).

Table 2.3: Recent FO composite membranes. DI water was used as a feed.

Membrane	Materials	Draw solution [M]	Flux L m^{-2} h^{-1}	References
Flat sheet TFC membrane	Psf, PA	2.0 NaCl	19	(Yip et al. 2010)
CA double-skin flat sheet	CA	2.0 NaCl	22	(Wang et al. 2010)
Flat sheet nanocomposite	Psf, PA, CNT	2.0 NaCl	95	(Amini. et al. 2013)
TFC-FO membrane	Psf+ sulfonated	2.0 NaCl	39	(Zhou. et al. 2014)
LbL flat sheet	-------	2.0 $MgCl_2$	49	(Qiu et al. 2011)
Biomimetic flat sheet	-------	2.0 NaCl	142 (PRO)	(Wang et al. 2012b)

Table 2.3 shows a summary of recent FO composite membranes made via different material and fabrication methods Biomimetic flat sheet composite membrane shows the highest performance so far while typical flat sheet membrane using CA or Psf for the substrate has moderate flux 20-50 L m^{-2} h^{-1}.

2.9 **Custom designs of flat sheet FO membranes**

Based on FO fundamentals and requirements, three factors can increase the water flux in FO. As mentioned in Section 2.3.2.1, TFC membranes usually consist of three distinct layers which include: (1) thin active layer, (2) support polymeric layer and (3) support backing fabric for additional mechanical strength. There are several options for manufacturing high performance FO membrane through separate design and modification for each layer.

Before discussing the possibilities and technical approach for designing and modifying each layer in a thin film flat sheet membrane, the basic procedure involved for fabrication of TFC FO membrane which involved two steps is briefly explained:

1) Casting support layer through phase inversion

Polymer solution is prepared from 12-20 % Polysulfone (Psf) in NMP/DMF solvent with or without pore former. The dope solution will be degased before it is cast onto a thin PET fabric. The PET fabric is attached to a glass plate. PET or woven polyester mesh will be treated with NMP before casting. Then the excess NMP solvent is dried out using an air knife or paper filter. The polymer solution is then carefully poured on top of the fabric and casted by a casting knife. Figure 2.19 shows a typical hand casting knife for fabricating a FO membrane. Immediately, the whole glass plate is immersed into a precipitation bath contain DI water at room temperature to initiate the phase inversion. The resulting membrane film is allowed to rest in the precipitation bath for at least 10 minutes. Then it will be stored in DI water for 24 h before the forming of the polyamide rejection layer on the top surface of the membrane film (Yip et al. 2010). This will be explained in the next step.

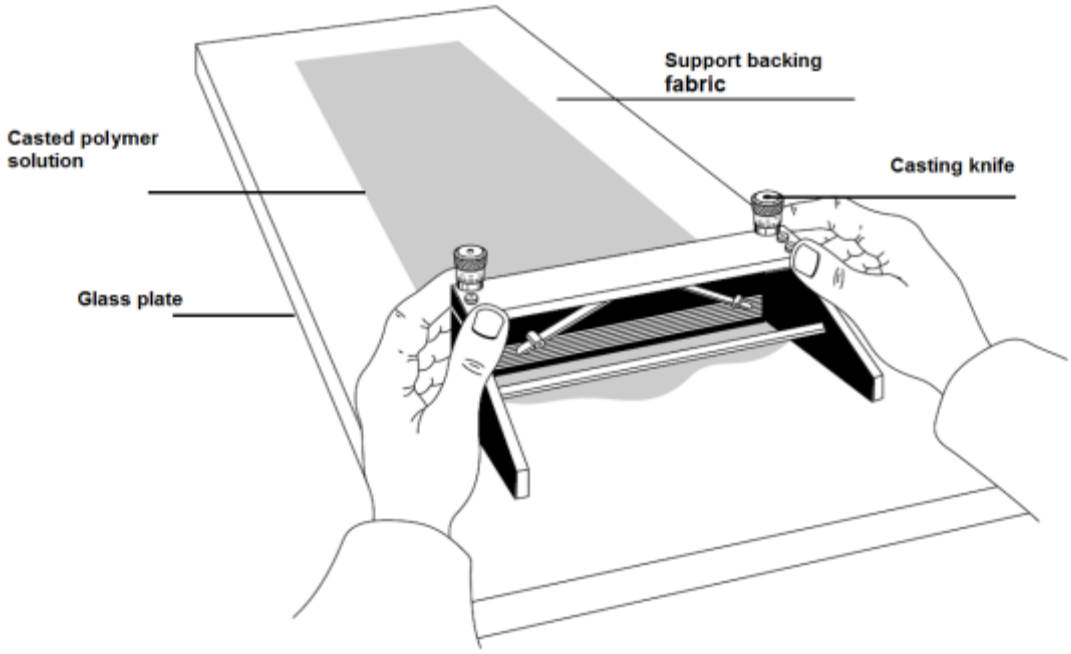

Figure 2.19: A typical hand casting knife for fabricating FO membrane by Paul N. Gardner Company, Inc.

2) Forming the polyamide rejection layer through interfacial polymerisation (IP)

The membrane film is acquired from phase inversion submerged into 3% (w/v) aqueous solution of MPD for 2 min. Then excess MPD solution will be removed through an air knife. The mesh-embedded Psf substrate will be placed into a sealed frame to allow coating for the top surface of the membrane film only. TFC FO membrane modification is possible through both phase inversion and phase inversion steps that will be discussed in the following sections in more detail.

2.9.1 **Selective rejection layer**

The ideal FO membranes should have a large water permeability and good ions rejection. Water permeability is mainly determined by the properties of the support structure and the rejection layer while rejection is mainly obtained by a thin

polyamide selective layer. Therefore an ultrathin rejection layer is required to increase selectivity without hindering water flux. Depending on FO application and feed solution characteristics, the requirements for membranes thin layer properties and selectivity are different. For example for desalination proposes using brackish or sea water as a feed, the selective layer should be more and less similar to the RO membranes to allow the passage of water but reject most of the sodium and chloride ions (Wei et al. 2011a; Yip et al. 2010). For this purpose similar to RO the suitable materials are limited. They include cross linked polyamide formed by interfacial polymerization or cellulose acetate (CA) / cellulose triacetate (CTA) through phase inversion (Lee et al. 2011). Similarly, selective layer modification is limited as well. There are studies that have tried to improve the selective layer by chemical modification, applying PDA or Graphene nanosheet coating or incorporating nanoparticles such as zeolite and CNT on the thin PA selective layer. Those modifications can occur during or after interfacial polymerization for increasing performance or improving the selective layer properties for fouling resistance. For example, Ning et al. developed a Zeolite-polyamide thin film nanocomposite membrane by incorporating 0.02–0.1 wt. % zeolite in PA layer. TFN membrane with 0.1 wt./v% zeolite loading performance increased almost 80% higher compared to the baseline TFC membrane (Ma et al. 2012). Materials such as layer-by-layer polyelectrolytes and polybenzimidazole (PBI) with hydrophilic nature can be used for FO application other than desalination.

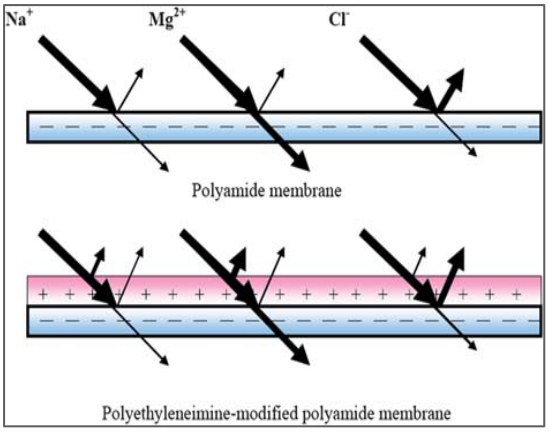

(a)

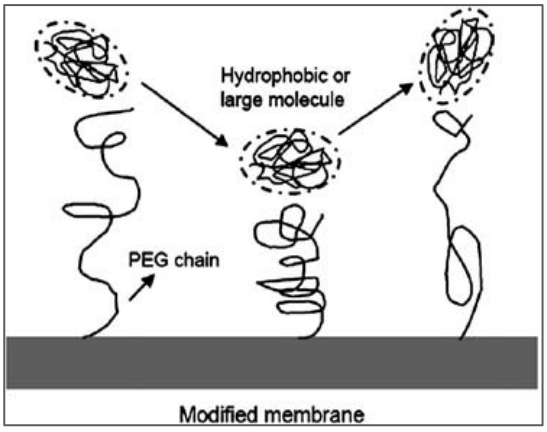

(b)

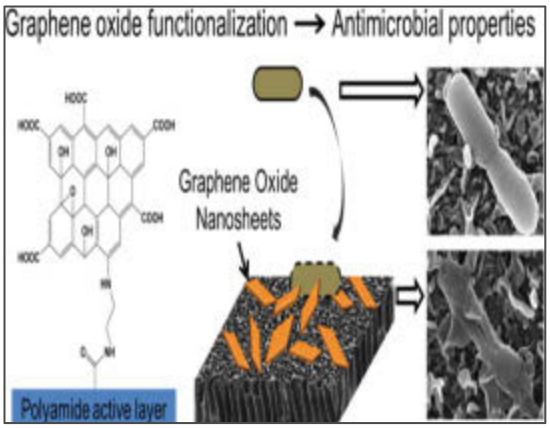

(c)

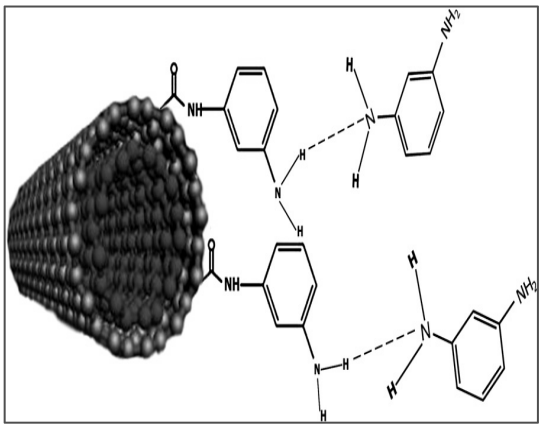

(d)

Figure 2.20: (a) Diagram shows ion transport through and modified and unmodified membranes (Zhou. et al. 2009), (b) poly(ethylene glycol)-modified nascent TFC membranes and surface grafted poly(ethylene glycol) chain to repulsion of macromolecule (Kang et al. 2007), (c) Polyamide TFC membranes functionalized with graphene oxide for fouling control (Perreault et al. 2013), and (d) amine functionalized MWCNTs in MPD solution reacting with TMC to form better selective thin layer (Amini. et al. 2013).

Figure 2.20 shows the possibilities of membrane selective layer modification through several different methods. Figure 2.20 (a) shows ion transport through modified and unmodified polyamide membranes. This TFC membrane was modified by self-

assembly of polyethyleneimine on the membrane surface. Modification improved antifouling properties to cationic foulants due to the application of the polyethyleneimine layer on the membrane surface (Zhou. et al. 2009). Figure 2.20 (b) shows the rejection layer modification in TFC membranes through surface grafted poly (ethylene glycol). Figure 2.20 (c) illustrates polyamide membranes functionalized with graphene oxide nanosheets for fouling control and finally Figure 2.20 (d) shows membrane rejection layer modified through functionalized MWCNTs in MPD aqueous solution. Amini et al. reported that this particular modification can significantly improve the selective layer permeability and thus the performance. This novel TFN membrane was fabricated by interfacial polymerization through multi-walled carbon nanotubes (F-MWCNTs) and functionalized amine used as additive in the MPD solution during interfacial polymerisation for forming the selective layer. The loaded F-MWCNTs were 0.01–0.1 wt%. Using 10 mM NaCl solution as feed solution along with 2 M NaCl solution as DS, the TFN membranes showed high water flux of 95.7 $Lm^2 h^{-1}$ with acceptable salt rejection (Amini. et al. 2013).

2.9.2 **Support polymeric layer**

In the phase inversion membranes such as CTA or PBI membranes, the support layer functions as both the support structure and the rejection layer (Zhang et al. 2010). However, regarding the composite membranes for FO, the support structure is not carrying both burdens. The ideal TFC FO membrane can be semi-permeable without the porous polymeric layer; however, without the support polymeric structure, the selective layer will not be able to stand independently (Chou et al. 2010). The polymeric substrate gives the membrane its frame and mechanical strength and a cushion for a selective thin rejection layer and without it, the rejection layer will not

be able to be free-standing.

The main differences between RO and FO membranes are in support polymeric properties in addition to support backing fabrics which will be discussed in the next section (section 2.10.3). High structural parameter (S value) and thick backing fabric support are the main factors that limit use of RO membrane for FO application. S values for the RO membranes are usually bigger than a few mm (1<S) while it is a few hundred μm (200-700 μm) for FO membranes (Mccutcheon & Elimelech 2007; Yip et al. 2010).

Previous studies suggest that more hydrophilic membrane and finger like structures can enhance the membrane performance (Yip et al. 2010). Furthermore, ICP and ECP play a crucial role in the FO membrane. Thus to minimize this effect especially ICP, the supporting FO membrane polymeric layer requires special chemical properties and structure designed to minimize the ICP effect (McCutcheon & Elimelech 2006c, 2007). Structural parameter which can be obtained through tortuosity, porosity and thickness of the membrane supporting layer, is the main element to improve FO membrane design. This can be achieved by designing a membrane with high porosity, small tortuosity and lower thickness to decrease structural parameter (Yip et al. 2010).

The main approaches to decrease the S value for FO membranes can be achieved by fabricating a thin membrane which is supported by a highly porous woven/non-woven backing fabric thus increasing the porosity and the hydrophilicity of polymeric support by adding pore formers such as PEG and EG. Furthermore, enhancing membrane hydrophilic nature is possible through modification by a hydrophilic agent such as direct thermal sulphonation or blending with sulphonated

polymers. This is in addition to the casting condition in phase inversion that has an obvious role in reducing ICP and structural parameter by producing a more porous membrane through precipitation bath components and conditions (Tiraferri et al. 2011a; Yip et al. 2010).

Figure 2.21 shows a poly (phthalazinone ether sulfone ketone), PPESK, and sulfonated poly (phthalazinone ether sulfone ketone), SPPESK. Regardless of the membrane finger or sponge like morphology, substrate hydrophilicity plays a greater role than membrane morphology. Hydrophilic sulfonated membrane with a sponge-like structure can perform better than a hydrophobic finger like structure FO membrane. Thus higher performance may depend more on support hydrophilicity than substrate morphology (Han et al. 2012; Widjojo et al. 2011, 2013).

In addition to support polymeric film through phase inversion, electrospinning has been recognized as an efficient versatile technique for the fabrication of polymer nanofiber matrix in recent years (Ma et al. 2005; Ramakrishna et al. 2006). Their potential application is based on the use of such fibres as reinforcement in nanocomposite development for medical and separation industries (Ramakrishna et al. 2005). Due to the precise control on the fibre size, shape and morphology, electrospun fibrous membranes have been used for filtration and MD processes successfully (Tijing et al. 2014). Regarding electrospun nanofibre film for FO application, the concept is relatively new. The nanofiber support layer is a porous structure, which provides direct routes for water and salt diffusion. Figure 2.23 shows the schematic of FO membrane with a scaffold-like nanofiber as a support layer (Song et al. 2011).

Through (1) fabrication method (electrospinning), (2) choosing and modifying hydrophilic support materials, and (3) incorporating nanomaterials in membrane substrate during phase inversion, custom design of support layer for FO membrane is possible.

Firstly, conventional thin film composite (TFC) membrane possesses the polymeric sponge and finger like structure substrate as support. Support membrane properties are the main cause for the membrane high ICP which results in poor water flux. Even using the same materials in an electrospun nanofiber FO membrane, the conventional polymeric support (sponge or finger like structure) will be replaced with a thinner, more porous and less tortuous nanofiber film structure (Bui & McCutcheon 2012). TFC membrane fabricated through nanofiber as their membrane support showed 2-5 times higher water flux depending on fabrication condition and post treatment (Bui et al. 2011). Xiaoxiao et al. has reported that using polyethersulfone (PES) nanofiber as support layer can greatly enhance the membrane performance. Using 1M NaCl as a DS, water flux of 46 LMH with a reverse solute flux of 0.6 GMH was achieved (Song et al. 2011). The diameters of nanofibers were in the range of 50–150 nm for this PES nanofiber support layer with 45 μm thickness.

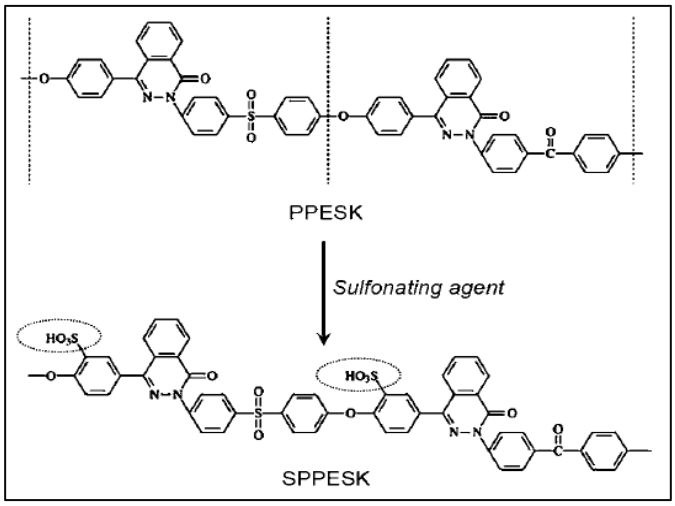

Figure 2.21: Poly (phthalazinone ether sulfone ketone), PPESK reaction into sulfonated poly(phthalazinone ether sulfone ketone), SPPESK.

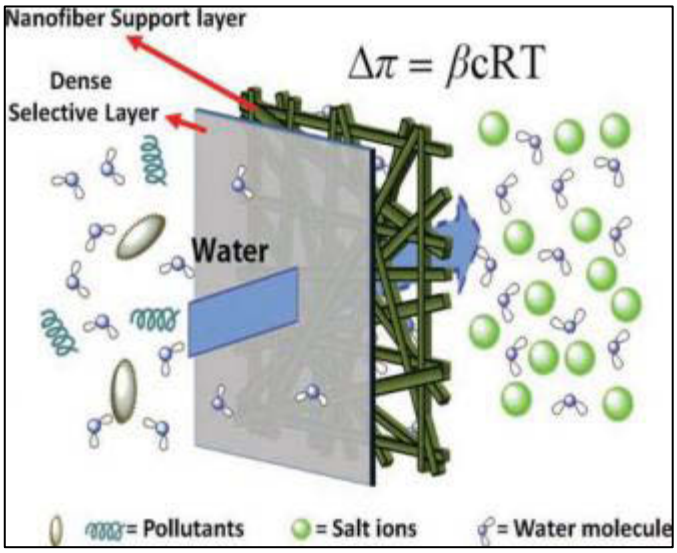

Figure 2.22: Schematic of FO membrane made of nanofiber (Song et al. 2011).

Further studies tried to use more hydrophilic materials such as nylon 6,6 to produce a nanofiber matrix for the FO application (Bui & McCutcheon 2012). Nylon 6,6 polymer was the choice of material for the support layer, mainly due to its hydrophilicity, good mechanical strength, and excellent compatibility with a polyamide selective film (Huang et al. 2013). This significantly reduces the structural parameter to 250 μm.

Secondly, custom design of an FO membrane is possible by choosing more hydrophilic materials like CTA or PES than hydrophobic Psf materials. Furthermore, modifying support with hydrophilic nature through sulphonation can modify the substrate properties. Incorporating nanomaterials in support polymeric layer can enhance and specialise the membrane properties for a specific purpose which can include performance enhancement or fouling resistance. This kind of membrane is commonly called thin film nanocomposite membrane (TFN). Figure 2.23 shows membrane formation from a polymer solution with graphene oxide (GO) through phase inversion.

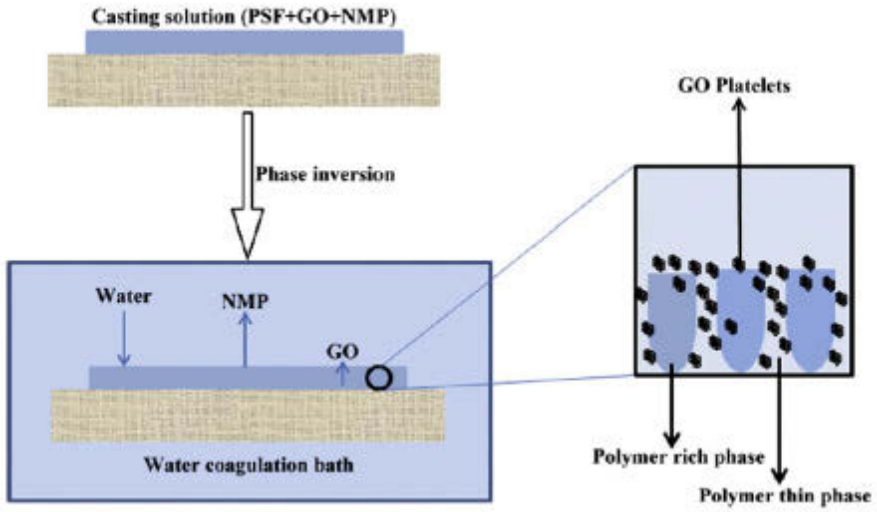

Figure 2.23: Schematic illustration of membrane formation from polymer solution with graphene oxide (GO) through phase inversion (Ganesh et al. 2013).

2.9.3 **Support backing fabric**

Membrane mechanical strength is the most important characteristic for the membrane to be industrialised (Yip et al. 2010). However, most of research works have not incorporated backing fabrics in their casted membrane. The composite membrane support acts as a support for the rejection layer and is comprised of two

elements, the backing fabric support and the porous polymeric material (Lee & Liu 1976). The backing that is incorporated into the porous polymeric matrix is preferably woven, but may be non-woven in most RO membranes. For the FO, the woven backing is preferred over a non-woven backing material for two key reasons, (1) the woven backing yields membranes with sufficient mechanical integrity required for standard membrane manufacturing practices, and (2) the woven backing simultaneously minimizes water transport resistance due to the inherent large openings in the backing structure (Farr, Bharwada, et al. 2013). For instance, commercial CTA and TFC FO membrane from HTI both possess a woven polyester mesh. Figure 2.24 (a) shows CTA FO membrane from HTI with woven polyester mesh, (b) CTA FO from HTI with non-woven backing fabric, (c) thin film comosoite FO membrane on non-woven from Woongjin, (d) thin film comosoite FO membranbe on woven poleyster mesh from University of Tecnhlogy Sydney.

Based on FO fundamental requirements for achieving high flux, the backing fabric should be thin and porous preferably woven fabrics. CTA FO membrane from HTI shows better performance than CTA FO on non-woven fabric (Wei et al. 2011b).

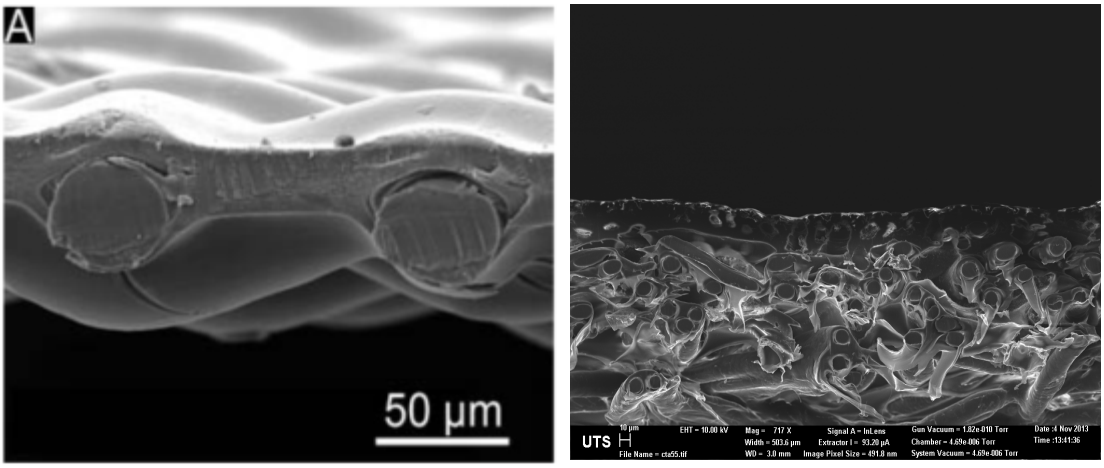

(a) (b)

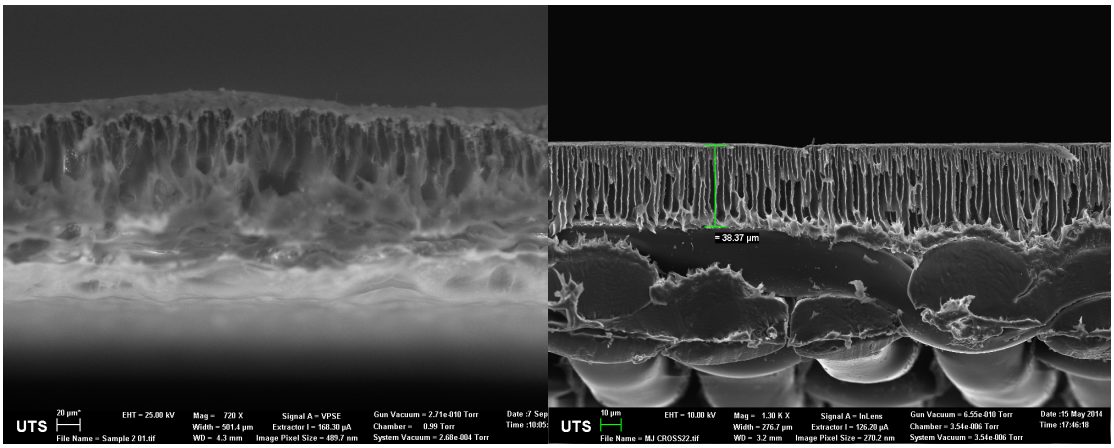

(c) (d)

Figure 2.24: (a) shows CTA FO membrane from HTI with woven polyester mesh, (b) CTA FO from HTI with non-woven backing fabric, (c) thin film composite FO membrane on a non-woven fabric from Woongjin, (d) thin film comosoite FO membrane on woven polester mesh from University of Technology Sydney.

The woven-backed membranes show a distinct advantage over the non-woven backing due to the overall thinness of the membrane that can be produced as well as reduced diffusional barrier to osmotic agent migration within the support layer (Farr et al. 2014). However, casting a FO membrane on fabric with this property seems to be challenging due to certain obstacles including:

1) Firstly by removing any RO membrane backing fabric for quick observation and

comparison with the conventional backing fabric used for FO membrane fabrication, it is clear that the RO backing fabric is thick non-woven **(**200 μm) and more importantly it doesn't appear to be porous (similar to note taking paper with open pores ≈ 1 μm). However, conventional backing fabrics either woven or non-woven for FO are thinner **(**40-70 μm**)** and more importantly they are porous with big open pores ≈ 100 μm (Figure 2.25).

2) Due to the FO membrane backing support fabric high porosity, polymer solution penetrates to the back of the fabric which can cause defect points, creasing and wrinkling on the membrane top surface skin layer.

3) Backing fabric pre-treatment with NMP solution will improve the casting and can remove the defect points to some extent, however, combining backing material and a porous polymer-based support into an inseparable matrix to form a defect free composite support layer is still a challenge.

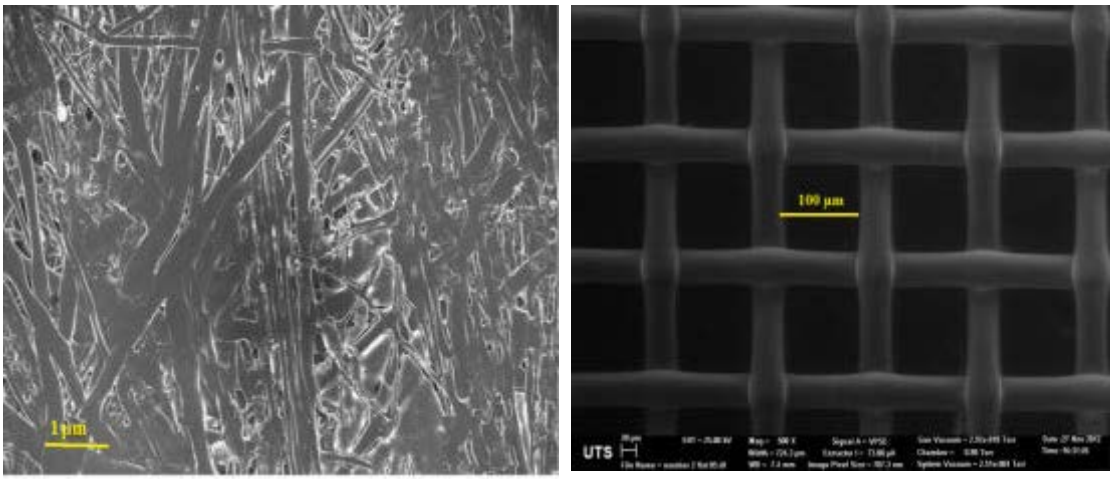

(a) (b)

Figure 2.25 (a) non woven backing fabric used in RO membrane, (b) poleyster mesh woven backing fabric used in TFC-HTI FO membrane.

On a commercial scale, FO membrane is fabricated by casting the solution on a rotating drum and pulling the backing material into the solution from the top. In this

case, polymer penetration through the fabric will be limited because of the casting method this will be explained in the next section) (Herron 2008). However, simulating this fabrication method under laboratory conditions is challenging. Therefore, either using hand cast or automatic casting knife, the polymer solution will be poured on top of the fabric similar to the commercial RO membrane fabrication method. For fabrication of FO, PAO or PRO membranes to be able to be tested in a regular FO cell (2.7cm -8 cm) a large piece of membrane that was reinforced with backing fabric support is required.

Regarding the backing fabric custom design, there are various potential materials that can be used for membrane backing support. So far, metal mesh (You et al. 2013), woven and non-woven fabrics have been used for developing FO membranes (Qiu et al. 2012a; Yip et al. 2010). Also there are patented works that suggest a spacer fabric or polyaniline as backing support (Farr, Herron, et al. 2013). Furthermore, there are materials like nanocellulose or microfibrillated cellulose (MFC) that may be a suitable option as a backing fabric support for an engineered osmosis membrane. Nanocellulose stands out as a unique choice among those options. MFC has been around since the early 1980s and is composed of nanosized cellulose fibrils that can be extracted from wood. Due to good stability, durability and high surface area they are expected to be a promising functional entity in the next generation of membrane separation technologies (Mathew et al. 2013), including MFC-enabled FO membranes, considering the following point:

1) There are a large number of functional groups that are present on the surface of the nanocelluloses substrate that gives a positive approach to modify the surface according to needs.

2) MFC substrate is similar to electrospinning nanofibers. However, it may function

as both a support polymeric structure and a backing fabric support due to it stiffness; this may lead to a fully bio based FO membrane for different FO applications.

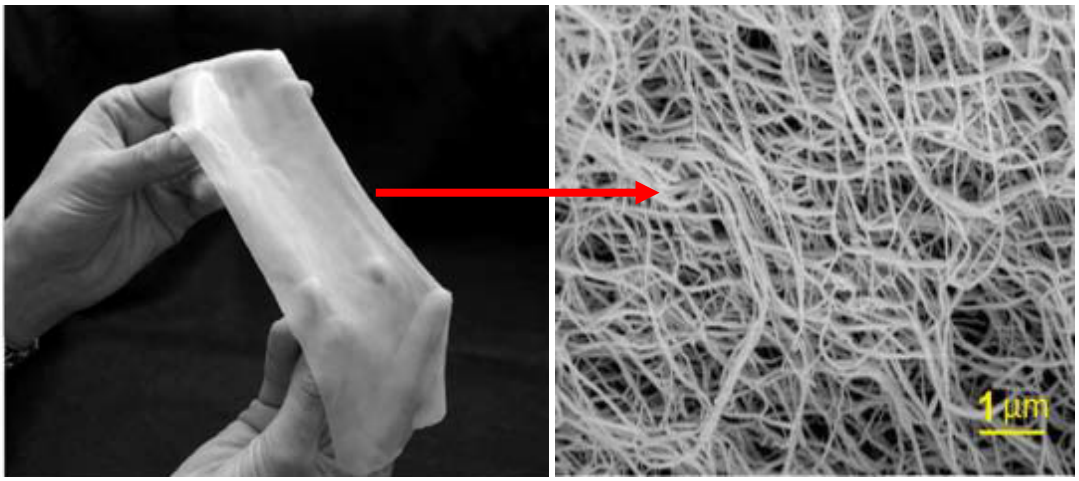

(a) (b)

Figure 2.26 Schematic of Nanocelluloses thin membrane film (a) and SEM image of Nanocelluloses fibre (b) (Klemm et al. 2006).

2.10 **Important factors in fabricating TFC FO membrane**

2.10.1 **Membrane wrinkling, creasing and defect points**

Wrinkling and creasing occur in the phase inversion stage during polymer precipitation. It is common when woven or non-woven backing support fabric is used for additional mechanical strength. Wrinkling is frequently related to the fabric used for the FO membrane fabrication because without it or using RO membrane thick nonwoven backing fabric, defect point and wrinkles disappear significantly. There are several factors that can create defect points and wrinkles. This may be the reason that most of the research groups had not used any backing fabrics for the FO membrane or if they were used, there would be a lot of defect points which would make only a small piece of the fabricated membranes suitable for the test. Therefore, making similar membrane (cast on the woven or non-woven backing fabrics) in the

lab condition is very challenging. However, fabrication of FO, PAO and PRO membrane reinforced with backing fabric support is crucial in the laboratory condition for further research development on engineered osmosis.

It is worth noting that the FO fabrication method on a commercial scale is quite different from the method for the RO membrane and this may explain this FO membrane fabrication adoption for limiting the problem. The main reasons for the FO membrane unique fabrication style on the rotating roll related to several factors involved for fabrication. First of all, backing fabric support in the RO membrane is thick nonwoven fabric while for the FO membrane thin non-woven or woven mesh can be used. Therefore, due to more porous fabric with bigger pore size, polymer penetration is common during the FO membrane fabrication. Although it is not proven that this polymer penetration is the reason for the defect point appearance and membrane wrinkles during phase inversion, however, due to the nature of the backing fabric required for the FO and lower polymers concentration (less viscose casting solution) for the FO membrane, the fabrication method in a commercial scale is quite different to prevent and limit the casting solution strike through the backing fabric. Figure 2.27 (a) shows the membrane fabrication RO-style where the backing fabric will turn on the rotating roll and then the polymer solution will be poured on the top surface of the fabric. In contrast, Figure 2.27 (b) shows membrane fabrication FO-style where the polymer solution is cast on the rotating roll then backing support fabric will be pulled on the top surface of the casted polymer. This FO membrane fabrication technique includes all three commercial FO membranes currently manufactured and distributed by the HTI Company.

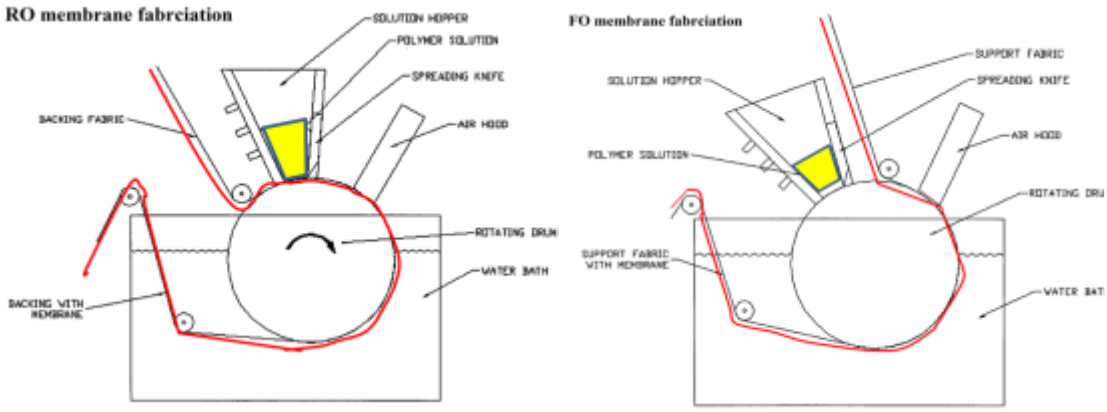

(a) (b)

Figure 2.27: (a) Membrane fabrication RO-style, and (b) FO style. Modified figure from (Herron 2008).

Based on literatures, there are suggestions for fabric pre-treatment to increase polymer and backing fabric compatibility or changing the precipitation bath component and temperature (Tiraferri et al. 2011a).

Although wrinkle and defect points can be minimised by making the backing fabric compatible with the polymer solution or softening precipitation bath by NMP but still it exists to the point that interfacial polarization becomes very difficult or impossible due to various defect points and wrinkles on the membrane top surface.

To this point, for preventing the polymer penetration, high polymer concentration solution will stay on the fabrics but the outcome structure will be a dense support with low water flux while with low polymer concentration solution will penetrate the back of the fabric, resulting in shrinkage, wrinkles and defect points.

2.10.2 **Membrane pore size in support layer**

Based on membrane fabrication methods, factors for controlling the membrane pore size in the support layer are different. For instance, for the polymer precipitation by solvent evaporation which was the earliest methods of making micro porous membranes, pore size mostly depends on evaporation time before non-solvent treatment. Figure 2.28 (a) shows SEM images of cellulose acetate membranes fabricated from acetone and 2-methyl-2,4-pentanediol. If the evaporation step is extended before phase inversion by plunging in water, average non-solvent droplet diameter will be larger and as a consequence the average pore size will be larger. It seems polymer concentration and non-solvent miscibility in the precipitation bath with solvent in polymer dope plays a crucial role in achieving the finger-like structure. Figure 2.28 (b) shows a polysulfone membrane obtained by phase inversion through precipitation bath. The schematic diagrams shows phase inversion in two different precipitation baths and their effect on membrane structure. Precipitation bath contains non solvent with high miscibility with solvent exit in the polymer solution that leads to fast solvent non solvent exchange during phase inversion which results in finger-like morphology in the membrane substrate (Mark & Kroschwitz 1989; Miller et al. 1966).

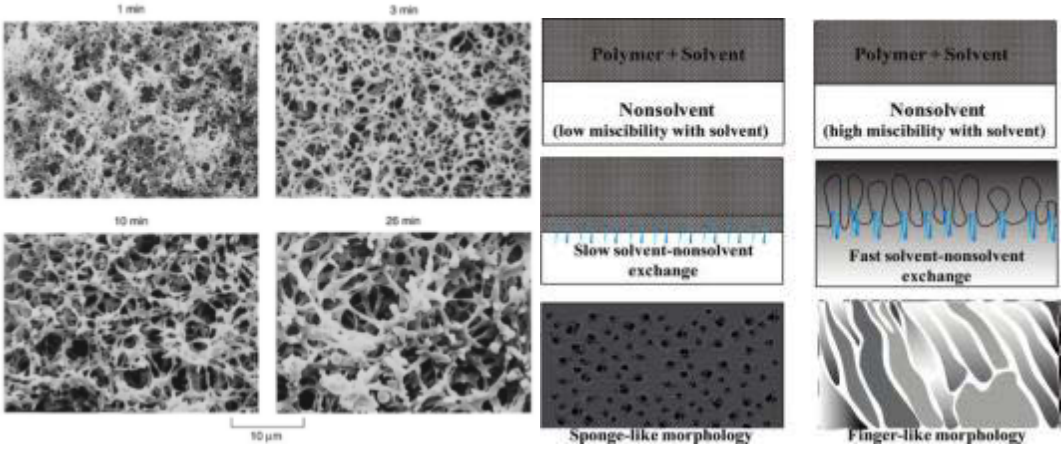

(a) (b)

Figure 2.28: (a) SEM images of CA membranes fabricated from acetone and 2-methyl-2,4-pentanediol. The evaporation time is different for four samples (Mark & Kroschwitz 1989), (b) SEM images of PSF membranes fabricated from a solution of NMP and different non solvent in the precipitation bath (Guillen et al. 2011).

Then, membrane pore distribution and pore size, first can be controlled (1) through different non-solvent and solvent components in the precipitation bath, and (2) through polymer casting solution concentration and pore former additives like PEG, EG and $LiCl_3$. Lower polymer concentration leads to a membrane with macrovoid and finger- like morphology in their structure while higher polymer concentration leads to a dense membrane substrate (Wang et al. 2012b; Yip et al. 2010). Thus, applying additives is usual for preparing a membrane with a higher concentration to produce micro and nano pores across the membrane substrate. Custom design of membrane support layer is possible through a different protocol, precipitation bath conditions to obtain the desired structure, porosity and morphology. FO membrane porosity and optimum pore size are crucial factors especially at the membrane top surface skin layer for successful interfacial polymerization (this will be discussed in the next section).

2.10.3 **Membrane pore size in skin layer**

The possible ways to control the membrane pore size in the membrane skin layer and then the role of porous skin layer properties and pore size on membrane fabrication (successful interfacial polymerization) and performance are important.

Membrane pore size on the skin layer has a greater effect on interfacial polymerization than pore size in the membrane substrate. Interfacial of TFC membrane was used to produce RO membranes with improved performance in terms of salt rejections and water fluxes compared to those fabricated by the Loeb–Sourirajan method in the early 60s. For the FO membrane, a selective polyamide layer can be formed via interfacial polymerization similar to the RO membrane. Rejection PA layer forms through the reaction of MPD saturated membrane film when exposed to TMC solution either in hexane or ISOPAR-G solution (zinc salt of mono-2-butyloctyl phosphate). As a result, the MPD and TMC then react at the interface of the two solutions (on the top surface of a membrane film) to form an extremely thin membrane rejection layer. Figure 2.29 shows the interfacial polymerization process in the TFC FO membrane.

Based on these fundamentals, the following points can be obtained; (1) a porous membrane skin layer is essential to initiate the IP reaction, (2) IP reaction is a result of MPD eruption from pores when the membrane surface is exposed to the TMC solution.

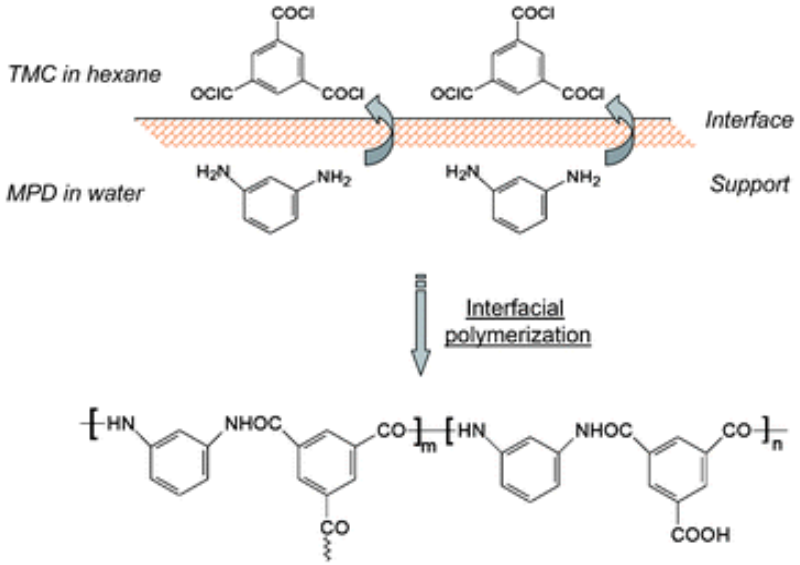

Figure 2.29: Schematic diagram of the interfacial polymerization process.

Surface porosity of polysulfone membrane and pore size are important parameters for developing different kinds of TFC membranes. Figure 2.30 shows an illustration of polyamide–polysulfone layers from Type 1 (smaller pore size) and Type 2 (bigger pore size) TFC membranes. The TFC membrane marked as type 1 shows superior salt rejection than type 2. This study shows a two-fold thicker skin layer in type 1 membrane because of decreased penetration of polyamide into the pores of Psf with smaller pore size than type 2. However, in the type 2 membrane, the polyamide filled the pores while the skin layer is relatively thinner. PA layer was 0.2 µm for type 1 versus 0.1µm for type 2.

This increases the possibility of higher defect points across the membrane thin PA layer, consequently, lower salt rejection is achieved (Singh et al. 2006). Membrane with larger hydrophilicity used in type 2 favours penetration of the diamine monomer into the pores. Thus polyamide formation is accomplished inside the pore.

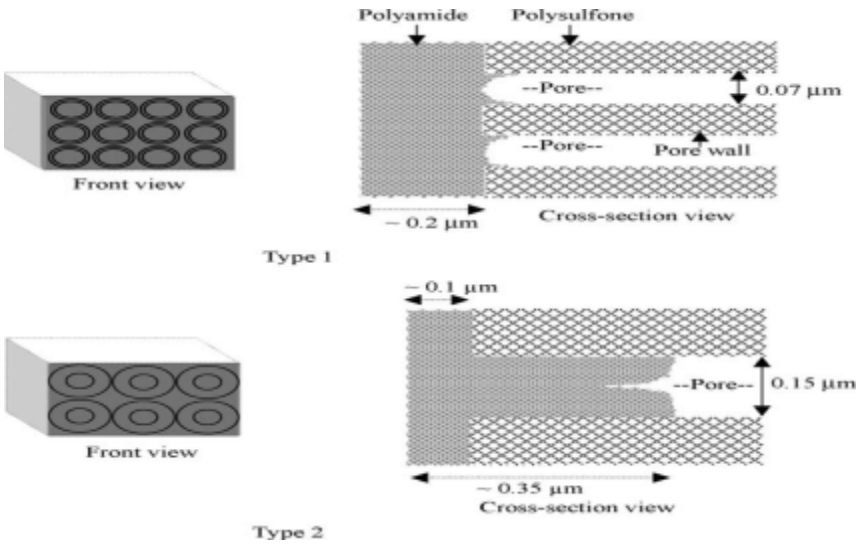

Figure 2.30: Illustration of polyamide–polysulfone layers for two type TFC membrane (Singh et al. 2006).

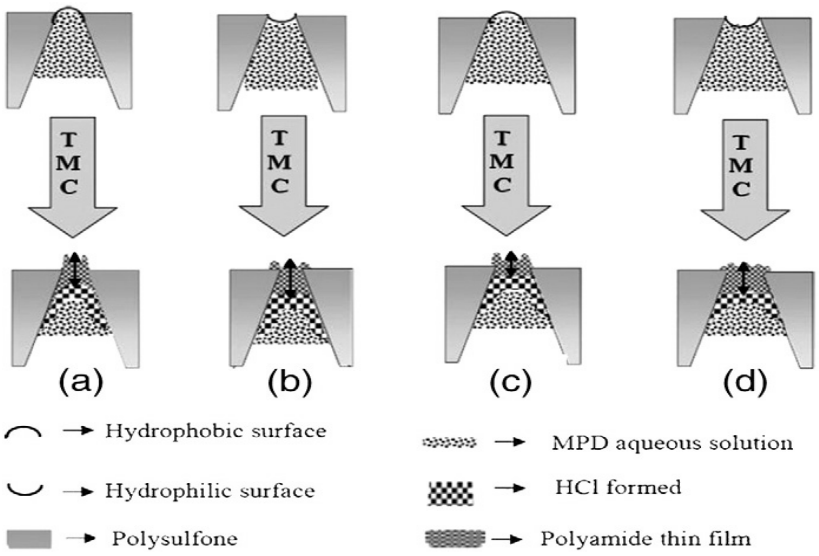

Figure 2.31: The effects of PSF substrate and chemistry in producing TFC membrane through MPD-TMC reaction (a) higher permeability and surface with relative roughness, (b) relatively impermeable and medium surface roughness, (c) the highest permeability and the highest roughness, and (d) the lowest permeability and medium surface roughness (Ghosh & Hoek 2009a).

Another comprehensive study evaluated the membrane pore size and chemical properties on interfacial polymerisation (Ghosh & Hoek 2009a). Figure 2.31

illustrates the scenario of interfacial polymerisation on PSF support with different chemical properties and pore size. Substrates (a) and (b) have the same pore size and so on for (c) and (d) but with pores at least twice as large as samples (a and b). Substrate (a) is a more permeable TFC membrane with rougher surface than (b) membrane. Generally, hydrophobic skin layer pores produced a membrane which is more permeable with rougher surface due to less polyamide formation within the pores. Similarly for the substrates (c) and (d) that had similar pores size but different hydrophilic properties. Substrate (c) was more permeable than (d) sample and had the most permeable substrate with highest surface roughness among all samples. This is related to bigger pore size compared to (a) and (b) substrates and its hydrophobic property compares to the (d) substrate. Pores with hydrophilic properties are prone to polyamide formation inside thus produced thinner PA layer, less rough surface with much lower permeability. These results can help for a better design of FO membranes, which requires porous and hydrophilic substrate (Ghosh & Hoek 2009a).

2.11 **Concluding remarks and recommendations**

Engineered osmosis processes have risen as an emerging technology in recent years. It has potential in several applications such as water purification, desalination, wastewater treatment, power generation and food processing. It is unlikely for FO to take over the dominant desalination technology such as RO in the near future. However, it is still attractive considering its fast growing application and hybrid FO systems for desalination and energy production due to FO advantages over pressure based membrane technologies. Nevertheless, FO needs to overcome challenges before practical large scale application. Development of suitable FO membranes and

suitable draw solutes can significantly shift the commercial interest and FO competition capability to the other desalination technologies. Application of FO on hybrid systems is a very good opportunity to expand engineered osmosis. Although DS and fluid management are not limiting factors in hybrid systems as much as single stand FO. However, finding a suitable membrane with a high mechanical strength remains as an important issue. Any successful FO application particularly in PAO and hybrid FO units depends on a novel customized enhanced robust FO membrane.

Chapter 3

MATERIALS AND METHODS

3.1 Introduction

The experimental work covers fabricated forward osmosis (FO) and pressure assisted osmosis (PAO) membranes and a comprehensive investigation of the PAO process using CTA membrane with different feed solution (FS) and draw solution (DS). Developed FO and PAO membranes were evaluated using mainly NaCl as DS and DI and brackish water (BW) as FS. The PAO process was investigated as a post-treatment process for the fertiliser drawn FO (FDFO) desalination process. The new pressure assisted fertiliser drawn osmosis (PAFDO) process was assessed to potentially eliminate NF post-treatment in the FDFO desalination unit.

Basic membrane properties such as salt rejection and water permeability for the fabricated membranes as well as the commercial membrane were determined by the RO process. Membrane fabrication materials and characterisation procedures for the FO and PAO process were carried out in this chapter. Descriptions of the detailed fabrication method and developing procedures specific to certain work can be found in their respective chapters.

3.2 Experimental Materials

3.2.1 Membranes fabrication materials

Polyethersulfone (PES) granules (Mn: 55,000 - Good fellow, UK), Polysulfone (Psf) 25000 (Sigma–Aldrich Pty. Ltd, Australia), and Polyester mesh woven fabric (PETEX 07-11/5, 07-40/25, SEFAR Pty. Ltd, Australia) was used for preparing the membrane polymeric support. 1-methyl-2- pyrrolidinone (NMP, anhydrous, 99.5%), Polyethylene glycol (PEG, MW 400) (Sigma–Aldrich Pty. Ltd, Australia) were used in the casting solution. M-phenylenediamine (MPD, >99%), 1,3,5-

benzenetricarbonyl trichloride (TMC, 98%) and n-hexane (Sigma–Aldrich Pty. Ltd, Australia) were used for interfacial polymerization.

The sulphonated Polyethersulfone (SPES) polymer was prepared by a method described by Zhou and Xiao et al (Xiao et al. 2010). The detail procedure will be discussed in the respective chapter. The sulphonated PES polymer was synthesized and prepared at the National University of Singapore (NUS). The detailed procedure will be presented at the respective chapter. Chemicals were used as received for the synthesis of SPES polymer; 4,40-difluorobenzophenone (DFBP) and 2,2-Bis(4-hydroxy-3,5-dimethyl-phenyl) propane (TMBPA) were obtained from (Sigma–Aldrich Pty. Ltd, Singapore). Sodium hydroxide and fuming sulphuric acid of 50% were received from Wako Junyaku Kogyo Co. Ltd. CTA FO membranes were obtained from HTI (Albany, OR) and FO and RO membranes from Woongjin Chemicals, Korea were used for comparison and validation purposes.

3.2.2 **Chemicals used as draw and feed solution**

Sodium chloride (99.5%) was utilized as the draw solute to prepare the feed and draw solutions for the fabricated membrane performance evaluation. The deionized (DI) water was produced by a Milli-Q unit (Millipore) with a resistivity of 15 MΩ cm. Three other draw solutes for the PAO investigation were fertilisers. Mono ammonium phosphate (MAP) or $NH_4H_2PO_4$, ammonium sulphate (SOA) or $(NH_4)_2SO_4$, and potassium chloride or KCl were just used in the PAO experiment. The thermodynamic properties of the solutions such as osmotic pressure, viscosity, diffusion coefficient and density were analysed using a thermodynamic modelling software OLI Stream Analyser 3.2 (OLI Systems Inc., Morris Plains, NJ, US).

3.2.3 **Membrane fabrication procedure**

The PAO flat sheet TFC substrates were fabricated on a woven polyester mesh fabric. However, the sulphonated PES membrane was fabricated without any backing fabrics and evaluated as a FO membrane. Both TFC PAO and TFC FO membrane fabrication procedures required two stages. First, the casting of a membrane polymer support with or without backing support was prepared via phase inversion. The second stage was the formation of a thin rejection layer through interfacial polymerization.

Prepared polymer dopes were degassed using digital bench top ultrasonic cleaners (Soni clean Pty Ltd, Australia) before using the solution for casting. Flat glass plate was used as a fabrication ground for the stainless steel film applicator (Sheen Instruments Ltd, UK) with an adjustable gate. Figure 3.1 shows the film applicator used to fabricate membranes in this study. The casted membrane was sunk immediately into a water bath to initiate the first stage which is phase inversion to prepare the membrane polymeric support.

The resultant membrane was soaked in a solution of 3.4% wt aqueous MPD solution for 120 seconds. Air knife was used to remove the excessive MPD solution on the membrane surface. Figure 3.2 shows the membrane frame which was used for interfacial polymerization. The membrane substrate was placed in a frame that was sealed around the corners and bottom but open on the top side. This allows the TMC solution just to react with the top surface of the substrate where the rejection layer is needed. N-hexane solution of 0.15-0.3 wt % TMC was gently poured onto the membrane top surface and was allowed to react for 60 sec to form the ultra-thin PA rejection layer. The resultant composite membrane was rinsed with DI water to remove the residual solution and stored in DI water at 4◦C for characterization.

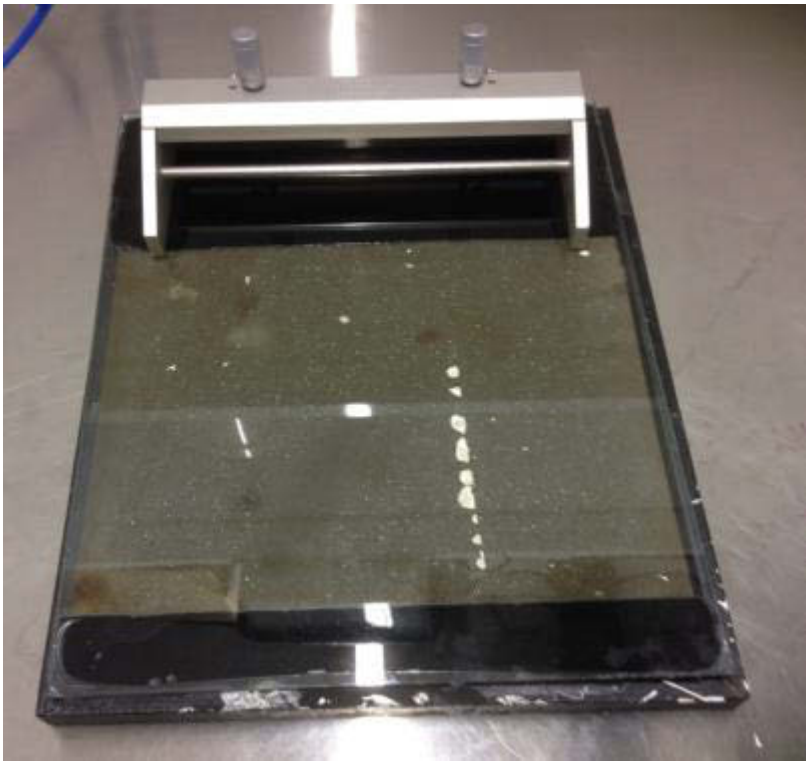

Figure 3.1: Stainless steel film applicator and the glass plate.

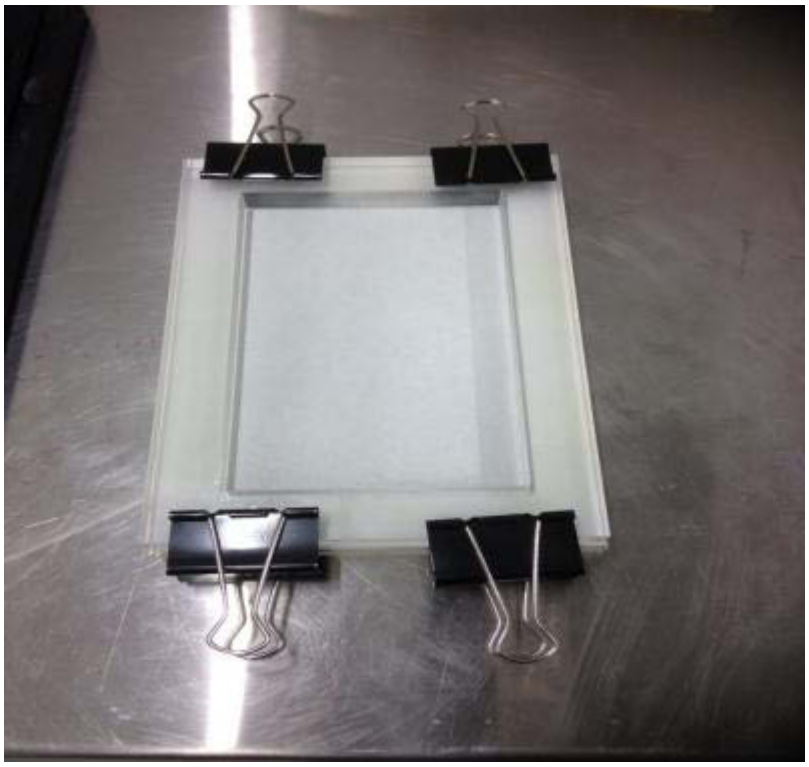

Figure 3.2: Membrane frame which was used for the interfacial polymerization.

3.3 Membrane characterizations

3.3.1 Basic characterisation

Thickness was measured by digital micrometre (Model 293-330 Mitutoyo, Japan). Water permeability and membrane salt rejection which was relevant to this study was carried out through the RO unit.

3.3.2 Field Emission Scanning Electron Microscope (FESEM)

Membrane cross section and rejection layer surface morphology was obtained via high-resolution Schottky Field Emission Scanning Electron Microscope (SEM, Zeiss Supra 55VP, Carl Zies AG, Germany). The membrane was dried at vacuumed condition then samples were flash frozen in liquid nitrogen before fracturing. For the membrane with a backing fabric a sharp razor was used for a decent cut. For better SEM images resolution, all samples were sputter coated with a thin layer of carbon before observation, using Balzers Sputter Coater (SCD 050, BAL-TEC, Germany) with applied operating 10-15 kV. Figure 3.3 shows the high-resolution Schottky field emission scanning electron microscope to obtain the SEM images.

Figure 3.3: High-resolution Schottky field emission scanning electron microscope (SEM Zeiss Supra 55 VP).

3.4 Forward osmosis (FO) and pressure assisted osmosis (PAO) test

3.4.1 FO lab scale set up and performance tests

Fabricated FO membranes and all related experiments were carried out using the FO lab scale set up. Figure 3.4 shows the lab scale FO unit used for the experimental studies. The illustrated FO unit is comprised of an FO cell with a carved channel in both sides. Effective membrane area of 2.002 x 10^{-3} m^2 dimensions is 7.7 cm length x 2.6 cm width x 0.3 cm depth.

Crossflow rate for all FO and PAO experiments was 400 ml/min. Crossflow was controlled by two variable speed peristaltic pumps (0.07 HP, Thermo Fisher Scientific, USA and Cole Palmer model 75211-15, 50-5000 RPM). The temperature of all feed and draw solutions was controlled heater/chiller. It was maintained at

25±1°C for all FO and PAO experiments. Performance of the membrane in terms of water flux in all experiments was measured from the continuous changes in the DS tank. A digital mass scale was connected to a computer and the accumulated flux data was printed on excel sheet via software at three-minute intervals. Each test was run for a period of at least four hours.

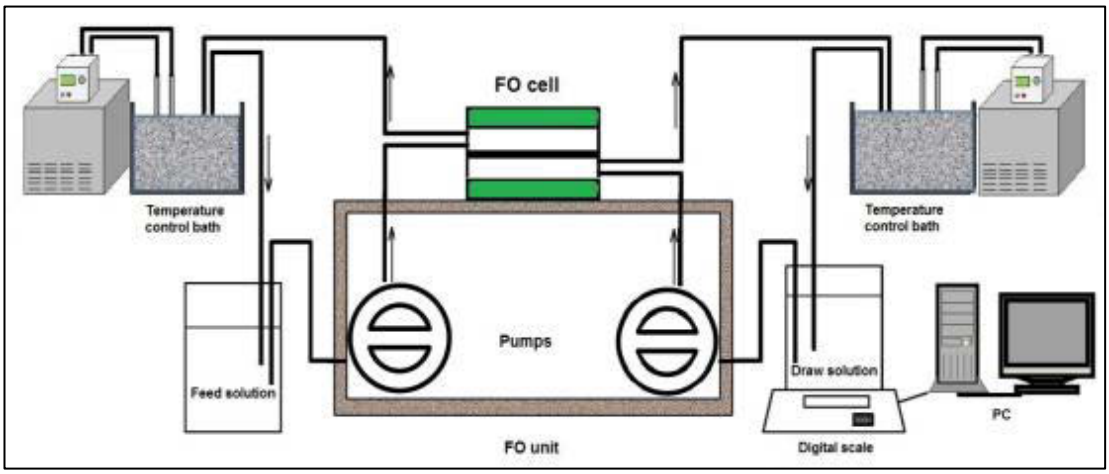

Figure 3.4: Schematic of the lab-scale crossflow forward osmosis experimental setup.

DS with different molar concentrations and FS solution with different properties were used to evaluate the fabricated membranes. A balance (EK-4100i, A&D Company Ltd., Japan) connected to a computer continuously printed down the change in the DS tank every 3 min. The permeated water flux was calculated from the average volume change of the FS and DS:

$$Jw = \frac{\Delta V}{\Delta t.Me} \quad (1)$$

Where ΔV (L) is the permeated water to a DS tank Δt is the time (h) for the collected water and Me is the membrane surface area (m^2). Fabricated membranes were evaluated under two FO modes. In the PRO mode, the DS was in direct contact with

the rejection layer and the feed solution was in contact with the membrane backing support while in the FO mode it was vice versa.

The initial volume for the DS and FS were 2.0 L for each tank. The solutions were pumped by gear pump passing through a flow-meter and then the membrane in the FO cell. Solutions were returned to their respective tanks after passing through a temperature controlling bath. Thus the DS was continuously diluted while the FS concentration was increased. This was continued for a period of time and it was declined until both solutions had reached an osmotic equilibrium state. Each experiment was run for duration of at least four hours to achieve a reliable data reading especially in regards to the reverse diffusion of draw solutes.

3.4.2 **PAO lab scale set up and performance tests**

Performance of the fabricated TFC-PAO membranes and all related PAO experiments was obtained through a bench-scale crossflow filtration unit. The schematic layout of the bench-scale crossflow PAO lab scale setup is shown in Figure 3.5. It is similar to the bench scale FO unit used in this study in terms of cell dimension. It consisted of one gear pump and one pressure pump each connected to the crossflow membrane cell with channel dimensions of 2.6 cm width and 7.7 cm length. However, in all PAO experiments, the channel on the DS side of the membrane cell was filled with 6 razor cut layers of polystyrene spacers to prevent membrane damage. For generating applied hydraulic pressure on the feed side in the PAO experiments, a nanofiltration pressure pump was used for producing hydraulic pressure. The amount of hydraulic pressure was regulated manually via a pressure valve.

The pressure pump could generate 10 bars at the maximum capacity. For the PAO the applied pressure was varied between 0 and 10 bar. The crossflows and temperature for both the DS and FS were similar to the bench scale FO experiments. The reverse diffusion of the draw solutes was obtained by measuring the electrical conductivity (EC) through a multimeter (CP-500L, ISTEK, Korea) when DI was used as feed. In the case when BW was used as FS, cations were analysed using ICP-MS.

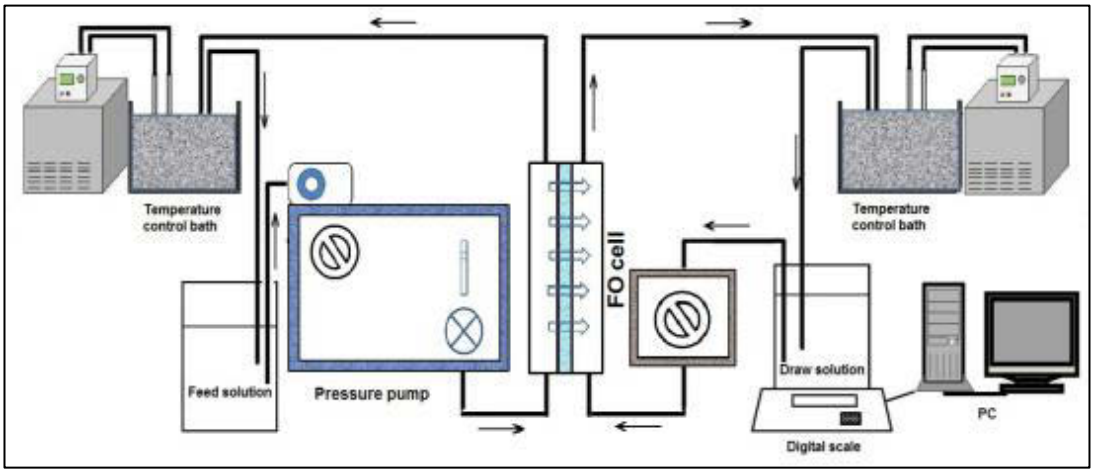

Figure 3.5: Schematic of the lab-scale experimental setup for pressure assisted osmosis process.

3.4.3 **Water contact angle**

The contact angles of membranes were obtained with the sessile drop method, using an Optical Tensiometer (Attension Theta Lite 100, Biolin Scientific, Finland). Figure 3.6 shows an Optical Tensiometer to measure contact angles in this study. Membrane samples were dried in a vacuum at room temperature for 24 h. Small deionized water droplets (5-7µL) were applied onto a levelled membrane surface and water drops reaction were captured by a camera and the imaging software determines the contact

angles. At least 3 measurements were obtained to get the average value in order to minimize the measurement error.

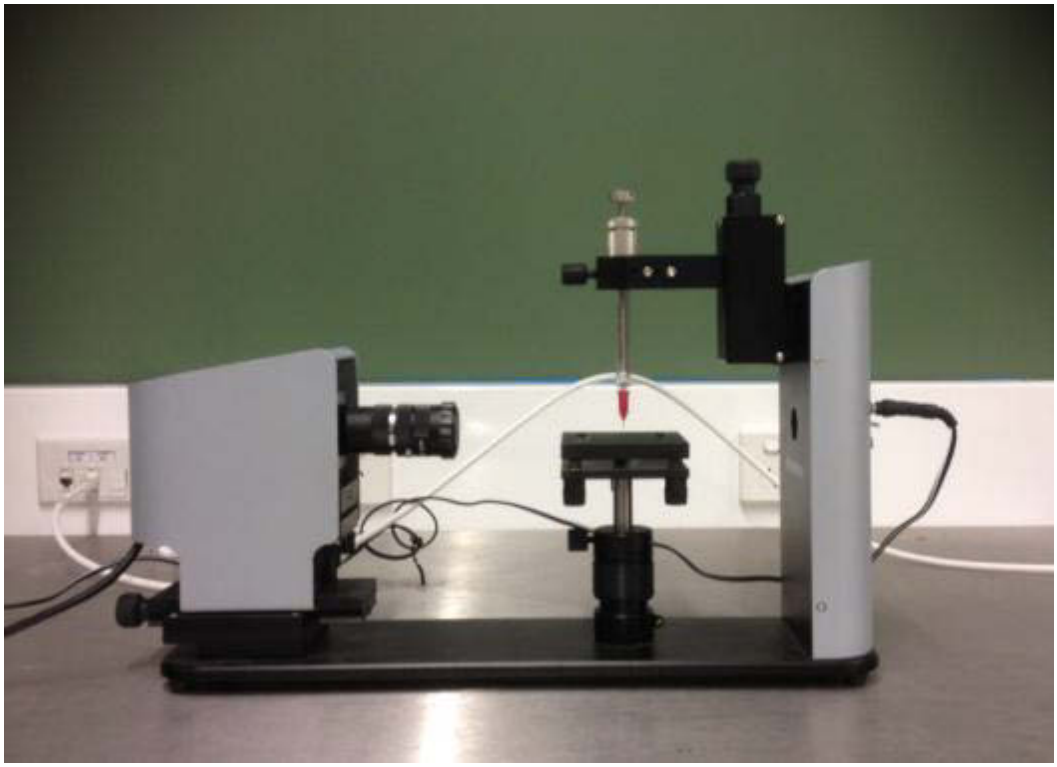

Figure 3.6: Optical tensiometer using the sessile drop method to measure membrane contact angles.

3.4.4 **Membrane porosity**

The membrane was fully wetted overnight. Excess water from the membrane surface was removed using tissue paper and then the membrane was weighed. After drying at a vacuum condition for 24 hours the membrane weight was measured again. Membrane porosity (ε) was obtained by measuring the dry mass (W_2) and wet mass (W_1) of membrane samples according to the following equation (Sukitpaneenit & Chung 2009) :

$$\varepsilon = \frac{(W1-W2)/\rho i}{\left[\frac{W1-W2}{\rho i}\right],+[W2/\rho m]} \times 100 \qquad (2)$$

Where ρi and ρm are density of wetting solvent (Isopropanol ethanol in the current study) and membrane, respectively (Sukitpaneenit & Chung 2012; Wang et al. 2012b).

3.4.5 **Mechanical strength**

Tensile strength was evaluated using an Instron bench-type tensile test machine (LR5K Plus).

Figure 3.7 shows the bench-type tensile test machine used in this study. The maximum load limit was 100 N according to ASTM D882-10 while the crosshead speed adjusted to 5 mm/min. At least three sticky tape shaped specimens for each fabricated membrane sample were tested and the average was reported as the tensile property for each sample.

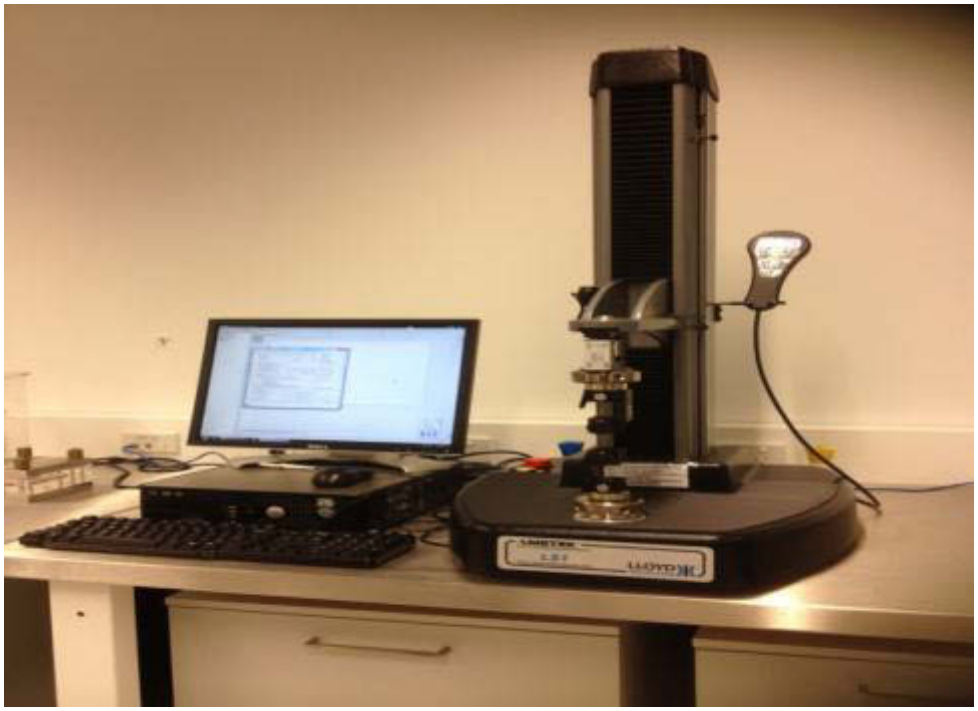

Figure 3.7: Bench-type tensile test machine for measuring membrane tensile strength.

3.5 Measurement and data analysis

3.5.1 Pure water permeability

Pure water permeability (PWP) or A coefficient properties of fabricated TFC membranes and CTA membrane used in the PAO process were measured in the same cross-flow filtration setup used for the PAO test (Figure 3.5), in the RO testing mode. The A value can be reported on (LMH bar^{-1}) or (L $M^{-2}h^{-1}$). The water permeability coefficient (A) was calculated through an applied pressure range of 1–10 bar on the membrane selective layer with DI water as a feed. The A value was obtained according to the following equation:

$$PWP\ (A) = \frac{Q}{Mem * \Delta P} \quad (3)$$

Where Δp is the applied pressure, Q (L h^{-1}) is the water permeation volumetric flow rate, Mem (m^2) is the membrane area.

3.5.2 Salt rejection and salt permeability tests

The membrane salt rejection and salt permeability, B values of the FO/PAO membrane were measured in the same PAO setup (Figure 3.5) in RO mode over 1–10 bar. BW10 NaCl was used as the feed solution. Rejection was determined based on conductivity measurement (Ultra Meter IITM 4P, Myron L Company, CA) of the feed and permeate.

$$R = \frac{Cf - Cp}{Cf} \times 100\% \quad (4)$$

Where C_f is the salt concentrations in the feed tank and C_p is the salt concentrations in the permeated flux. Accordingly, B value, the salt permeability was calculated according to the following equation (Lee et al. 1981b):

$$B = \frac{A(1-R)(\Delta p - \Delta \pi)}{R} \quad (5)$$

Where ΔP the applied pressure and R is the salt rejection of the membrane during rejection test in the RO mode, Δπ is the difference in the osmotic pressure across the membrane.

3.5.3 **Measurement of the reverse solute flux**

FO and PAO are associated with two different solution concentrations on each side of the membrane. Bidirectional movement of solutes is possible in membrane used in the FO and PAO process. However, this bidirectional movement is measured and named differently. Salt rejection is referred to the amount of solute fluxes that can pass through the rejection layer for the feed to the other side of the membrane while the reverse solute flux (RSF) is referred to the amount of solute fluxes in the feed permeated from draw solutes. The specific RSF (SRSF) is measured as a ratio (SRSF=J_s/J_w) of reverse draw solute flux (J_s) and the water flux (J_w) while J_s (where $J_s = B*\Delta C$) is given as a function of the solute permeability coefficient B and the concentration difference ΔC (where $\Delta C=C_D-C_F$) (Phillip et al. 2010). Feed solution conductivity is measured via conductivity meter (Model: H270G-BNDL, Hach). The conductivity meter probe was placed in the FS tank and conductivity of the FS was recorded every 3 minute using data logging features. This data was then used to evaluate the RSF trend. Standard conductivity curve was used to find the RSF values for particular sets of experiment where the DI water was used as feed and the single component solute such NaCl was used as the DS.

3.5.4 **Determining membrane structural parameter**

A large structural parameter is responsible for severe ICP in the FO membrane. In general, the membrane structural parameter or S value can be measured by calculating the support layer thickness (t) and tortuosity (τ) over its porosity (ε):

$$S = \frac{t\tau}{\varepsilon} \quad (6)$$

However, calculating the S value based on Eq (5) is challenging when the membrane tortuosity (τ) is not clear. In this study, the membrane structural parameter for the FO and PAO membrane was measured through the following calculation.

Based on the classical ICP model developed by Loeb et al. (Loeb et al. 1997), the water flux can be calculated by the following equations in the FO process:

$$J_w = \frac{D}{S}\left[ln\frac{A\pi_{D,b}+B}{A\pi_{F,b}+Jw+B}\right] \quad (7)$$

Where D is the bulk diffusion coefficient of the draw solute, B is the salt permeability coefficient of the membrane active layer, and $\pi_{D,b}$ is the bulk osmotic pressure of the FS and DS respectively. In the experimental tests, the membrane effective structural parameter can be determined using the empirical equation previously described. The water flux, Jw, was measured with the membrane in the FO mode (rejection layer facing the feed solution) using a 1 M NaCl DS and DI water as FS. Based on equation 7, the membrane support structural parameter was calculated using the following equation:

$$S = \left(\frac{Ds}{Jw}\right) ln\frac{A\pi_{D,b}+B}{A\pi_{F,b}+Jw+B} \quad (8)$$

However, the solute diffusion resistivity, K, within the porous support can be used to obtain the structural parameter as well. It can be defined as in the following equation.

$$K = \frac{t\tau}{\tau D} = \frac{S}{D} \quad (9)$$

D is the bulk diffusion coefficient of the draw solute, and S is the structural parameter of the membrane referred to in equation 1. This equation can be used to estimate the structural parameter as well.

Chapter 4

PRESSURE ASSISTED FERTILISER DRAWN OSMOSIS PROCESS TO ENHANCE FINAL DILUTION OF FERTILSER DRAW SOLUTION BEYOND OSMOTIC EQUILIBRIUM

4.1 **Introduction**

Forward osmosis (FO) has been recently emerging as an alternative membrane process for desalination. Unlike the reverse osmosis (RO) process, which operates at very high hydraulic pressure, FO simply utilises osmotic pressure difference between the concentrated draw solution (DS) and the feed solution (FS) as a driving force to transfer water across the semipermeable membrane without using pressure or energy (Cath et al. 2006; Holloway et al. 2007; Shuaifei et al. 2012). The only energy required is simply for maintaining adequate crossflows that provides dynamic contact with the FO membrane which otherwise would result in severe concentration polarisation (CP) effects, thereby reducing the water flux. Several research works have been published on the potential applications of the FO process including desalination for potable water, water treatment, wastewater treatment, membrane bio-reactor, food industries, pharmaceutical industry and recently in desalination for irrigation (Achilli et al. 2009; Garcia-Castello et al. 2009; Holloway et al. 2007; Phuntsho et al. 2011).

However, FO is a concentration-based process because of which it has its own process limitations. One of the major limitations is that, the water fluxes in the FO process have been observed to be much lower than the expected water flux based on the bulk osmotic pressure difference between the DS and FS. This low process efficiency is caused by severe CP effects present on both sides of the FO membrane unlike in the pressure based membrane process where CP effect is present only on the feed side of the membrane. The second major limitation of the FO process is that, the transfer of water across the membrane towards the DS from FS occurs until the point at which the osmotic pressure of the DS reaches equilibrium with the FS. Once

osmotic equilibrium is attained, the water flux becomes zero and therefore further dilution of the DS beyond this equilibrium concentration is not possible without providing external driving force. This means that, the final concentration of the diluted DS will still have osmotic pressure equivalent to the osmotic pressure of the FS. The lowest possible concentration of the diluted DS in the FO process is at osmotic equilibrium with the incoming fresh FS for FO modules operated with the DS and FS under counter-current crossflow directions. If the FO process is operated with DS and FS under the co-current crossflow directions, the final concentration of the diluted DS will in fact have osmotic pressure equal to the feed concentrate, much higher than the osmotic pressure of the fresh FS(Phuntsho. et al. 2014). This final concentration of the diluted DS will have a significant bearing on the post-treatment process especially where complete separation of draw solutes and the pure water is necessary. Unless the FO process is used, in which the diluted DS can be directly used without the need to separate the draw solutes and the pure water, FO cannot be used as a standalone process. Recently, the integration of several other processes with FO were reported such as with RO (Bamaga. et al. 2011; Choi et al. 2009), nanofiltration or NF (Phuntsho et al. 2013; Tan & Ng 2010), ultrafiltration or UF (Ling & Chung 2011a), membrane distillation or MD (Wang et al. 2011; Xie, Nghiem, et al. 2013), etc.

One of the practical applications of the FO process is in the desalination for irrigation purpose since the cost of RO desalinated water remains high and commercially not viable for irrigation. Phuntsho et al. has reported several studies on the fertiliser drawn FO (FDFO) process in which a concentrated fertiliser solution is used as DS (Phuntsho et al. 2011; Phuntsho. et al. 2013). The advantage of this process is that,

the final diluted fertiliser solution can be applied directly for fertigation of crops without requiring additional process to separate and remove the fertiliser draw solutes from the diluted DS unlike for the potable purpose. Fertilisers DS can be even customised as per the requirements of a particular crop or growth stage. However, when a saline feed water with high TDS is used for desalination, the final diluted fertiliser DS at osmotic equilibrium could contain fertiliser or particular nutrient concentrations much higher than acceptable limits for fertigation. Several approaches were suggested in our earlier studies to reduce the fertiliser concentrations in the diluted fertiliser DS. These included using blended or mixed fertilisers containing multiple nutrients as DS to reduce the concentration of particular nutrient (Phuntsho. et al. 2012), using NF as either pre-treatment or post-treatment to reduce the fertiliser concentration (Phuntsho et al. 2013; Phuntsho. et al. 2012), using dual stage FO process for desalination and wastewater treatment (Cath et al. 2010; Phuntsho, HoKyong, et al. 2012) and applying pressure on the FS during the FO process (Sahebi et al. 2015) .

Few studies have recently reported on the concept of introducing an applied hydraulic pressure during the FO process with the aim of enhancing the water flux (Blandin et al. 2013; Choi et al. 2009; Coday et al. 2013; Oh et al. 2014; Yun et al. 2013a). This approach exploits the synergies of the two driving forces (osmotic pressure and the hydraulic pressure) in a single stage. Such study was driven mainly by the desire to enhance water flux and feed recovery rate to compensate the low efficiency of the FO process due to CP effects and the dilutive internal CP (ICP) effect in particular. The in-situ combination of the FO and RO process in a single stage may offer other advantages such lower footprint of the FO process and

enhanced dilution of the final DS that can reduce energy for the post-treatment process. In the published literature so far, several different terms are used to describe this particular mode of FO process using applied pressure such as pressure assisted osmosis (PAO) (Oh et al. 2014), pressure assisted FO (PAFO) (Yun et al. 2013a), assisted FO (AFO) (Blandin et al. 2013) and pressurised FO (PFO) by Cody et al. (Coday et al. 2013) although the term PFO was used only in the form of graphical abstract and not exactly defined in their paper. Although, all these terms describe the same osmotic process, we have used the term pressure assisted osmosis or PAO in this study as this term seems to more consistently distinguishes it from the pressure retarded osmosis (PRO) for osmotic power generation, a closely related process but where the pressure is applied on the DS side of the membrane. This is similar to the preferred use of term forward osmosis to more consistently distinguish it from the term reverse osmosis. In other terms used for the FO process include direct osmosis, osmotic dilution, etc. However, all other terms used in describing the FO process with hydraulic pressure applied on the FS is considered to have identical meaning with the PAO process.

The use of combined driving forces could be more advantageous particularly for FDFO desalination process where the maximum dilution of the fertiliser DS is preferred for meeting the nutrient concentrations acceptable for direct fertigation rather than to separate the fertiliser DS. The main objective of this study is therefore to evaluate the potential application of PAO in the FDFO process, hereby termed as pressure assisted fertiliser drawn osmosis or PAFDO process. The hydraulic pressure applied during the FDFO process could enhance the dilution of the fertiliser DS so that final diluted fertiliser solution can then be applied directly for fertigation

potentially eliminating the need for an additional post-treatment process such as NF for nutrient reduction. The specific objectives of the study are therefore to validate PAO process through lab-scale experiments and theoretical models, evaluate the effective gain in water flux in the PAFDO process under different DS and FS concentrations and assess the significance of the PAFDO process and its implications for modular applications. We report here how PAFDO process could be very effective in generating water flux even after the DS concentration has reached the point of osmotic equilibrium with the FS, thereby achieving much higher dilution of the fertiliser DS.

4.2 **Classification of osmotic processes and modelling**

Solutions containing dissolved solutes in water generate osmotic pressure. When a hydraulic pressure higher than the osmotic pressure of the FS is applied, the water comes out of the membrane rejecting and leaving the salt behind and this process is termed as RO. Osmosis, on the other hand however, refers to the spontaneous flow of the water through a semi-permeable membrane from a low concentrated solution to higher concentrated solution. This same principle is adopted in the FO process where the concentrated DS is used as a driving force for desalination.

The general equation for the water transport through the salt rejecting membranes is given by the following equation (Ling & Chung 2011a; McCutcheon. & Elimelech. 2007).

$$J_w = A\,[\Delta P - \sigma\Delta\pi] \quad (1)$$

Where J_w is the water flux, A is the pure water permeability coefficient, $\Delta\pi$ is the net pressure between the feed and the permeate (or filtrate), ΔP is the applied hydraulic or trans membrane pressure and σ is the reflection coefficient (generally assumed unity for salt rejecting membranes). The net osmotic pressure ($\Delta\pi$) can be written as follows:

$$\Delta\pi = \pi_F - \pi_p \quad (2)$$

Where π_F is the osmotic pressure on the FS and the π_p is the osmotic pressure of the permeate or filtrate.

Based on hydraulic pressure applied either on the FS side or the DS side, the osmotic processes may be classified into four different types, which may be described by the conditions stated below. This same processes have been presented in Figure 4.1, modified from the osmotic processes phenomenon described by Lee et al. (Lee et al. 1981b):

Forward osmosis (FO): $\Delta P = 0$, driving force = $\pi_D - (\pi_F - \pi_p)$

Reverse osmosis (RO): $\Delta P > \Delta\pi$, driving force = $\Delta P - (\pi_F - \pi_p)$

Pressure retarded osmosis (PRO): $\Delta P < \Delta\pi$, driving force = $\pi_D - (\pi_F - \pi_p) - \Delta P$

Pressure assisted osmosis (PAO): $\Delta P < 0$, driving force = $\Delta P - (\pi_F - \pi_p - \pi_D)$

Where π_D is the osmotic pressure of the DS. While the principles of the PRO and FO processes are similar however, in the PRO process, the pressure is applied on the DS side ($\Delta P < \Delta\pi$) opposite to the osmotic gradient that partially retards the water crossing the FO membrane generated by the osmotic driving force. This creates

hydraulic pressure within the DS chamber that in turn can be used to drive a hydraulic turbine to generate osmotic power. The DS in the PRO process is located on the active layer side of the membrane so that the membrane can withstand the hydraulic pressure in the DS chamber.

For the PAO process however, the hydraulic pressure ΔP is applied on the FS side unlike in the PRO process where ΔP is applied on the DS side although in both the processes, the ΔP is applied on the active layer side of the membrane. The PAO process can therefore be described as an in-situ combination of RO and FO processes. The total osmotic pressure on the permeate side is therefore a combination of both the osmotic pressure of the permeate (π_p) and the DS (π_D) that is already present on the permeate side of the membrane. Hence, $\Delta\pi$ can be re-written by adding the osmotic pressure of the DS (π_D) on the permeate side of the membrane as below.

$$\Delta\pi = \pi_F - (\pi_p + \pi_D) \tag{3}$$

Equation (1) can therefore be re-written as follows for the PAO process:

$$J_w = A\left[\Delta P - \left(\pi_F - \pi_p - \pi_D\right)\right] \tag{4}$$

Osmotic pressure of the permeate is comparatively lower than the DS and hence can also be safely neglected ($\pi_p = 0$).

Equation (4) is however relevant only under static condition. Once the process starts and becomes under dynamic condition, the transfer of water across the membrane alters the solute concentrations at the membrane surface boundary layer, phenomenon we know as CP effects. Two independent solutions exist on each side

of the membrane in the FO or PAO process that results in two different types of CP phenomena: concentrative CP on the membrane surface towards facing the FS and dilutive CP on the membrane surface facing the DS. Given that the synthetic polymeric membranes are generally asymmetric (thin active layer on the porous support layer), each of these CP effects could occur either on the active layer (external CP or ECP) or inside the support layer (ICP). For FO process operated in FO mode (FS facing the membrane active layer and DS facing the porous support layer), CP phenomena involve both concentrative ECP and dilutive ICP. Concentrative ECP occurs at the membrane active layer because the concentration or the osmotic pressure of the feed at the membrane surface increases due to permeation of water through the membrane and rejecting the salt. The feed osmotic pressure at the membrane rejecting surface ($\pi_{F,m}$) is described by the following equation :

$$\pi_{F,m} = \pi_{F,b} \exp\left(\frac{J_w}{k}\right) \tag{5}$$

where $\pi_{F,b}$ is the bulk osmotic pressure of the FS and k_F the mass transfer coefficient, given by the following relationship:

$$k_F = \frac{Sh\, D_F}{d_h} \tag{6}$$

Where Sh is the Sherwood number, D_F is the feed solute diffusion coefficient and d_h the hydraulic diameter of the feed channel. The Sherwood number relates to flow conditions in the membrane channel (McCutcheon & Elimelech 2006):

$$Sh = 1.85\left(\mathrm{Re}\, Sc \frac{d_h}{L}\right)^{0.33} \quad \text{(Laminar flow)} \tag{7}$$

$$Sh = 0.04\ \mathrm{Re}^{0.75}\, Sc^{0.33} \quad \text{(Turbulent flow)} \tag{8}$$

Where Re is the Reynolds number, *Sc* the Schmidt number and *L* the length of the channel .The Schmidt number (*Sc*) can be calculated using the following relationship:

$$Sc = \frac{\nu}{D_F} = \frac{\mu}{\rho D_F} \tag{9}$$

where ν is the kinematic viscosity of the solution, ρ the solution density and μ the dynamic viscosity.

On the other hand the dilutive ICP occurs inside the membrane support layer facing the DS due to back diffusion of draw solutes by the convective water flux coming from the feed displacing the draw solutes away from the membrane active layer interface. This lowers the DS concentration near the active layer thereby reducing the effective osmotic driving force. The osmotic pressure ($\pi_{D,i}$) near the membrane active layer interface, inside the support layer is given by the following equation :

$$\pi_{D,i} = \pi_{D,b} \exp\left(-J_w K_D\right) \tag{10}$$

where K_D is the solute resistivity for diffusion of draw solutes within the porous support which can be defined as:

$$K_D = \frac{t\tau}{D_D \varepsilon} \tag{11}$$

where t, τ and ε represent thickness, tortuosity and porosity of the support layer, respectively. The value of K_D can be however determined by the following flux relationship described by Loeb et al. (McCutcheon. & Elimelech. 2007) for FO mode:

$$K_D = \left(\frac{1}{J_w}\right) \ln \frac{B + A\pi_{D,b}}{B + J_w + A\pi_{F,m}} \tag{12}$$

Wherein B is the salt permeability coefficient of the membrane active layer.

Therefore, the water flux shown by Equation (4) has been modified to take into account the concentrative ECP and dilutive ICP phenomenon under PAO mode as follows (Lee et al. 1981b):

$$J_w = A\left[\Delta P + \pi_{D,i} - \pi_{F,m}\right] \tag{13}$$

Combining equations (5) and (10) with (13), the modified water transport in the PAO can be represented by the following relationship.

$$J_w = A\left[\Delta P + \pi_{D,b} \exp(-J_w K) - \pi_{F,b} \exp\left(\frac{J_w}{k}\right)\right] \tag{14}$$

The second term in equation (14) takes into account the dilutive ICP effects $\pi_{D,b}$ exp ($-J_w K$) for DS facing the support layer side of the asymmetric FO membrane. In the earlier studies with the PAO process (Choi et al. 2009; Oh et al. 2014; Yun et al. 2013a), the second term used was $\pi_{D,b}$ exp ($-J_w/k_D$) which accounts for dilutive ECP for symmetric membrane and not dilutive ICP for asymmetric membrane. This could

have been one of the reasons why their model and the experimental data on water flux had slightly poorer correlation.

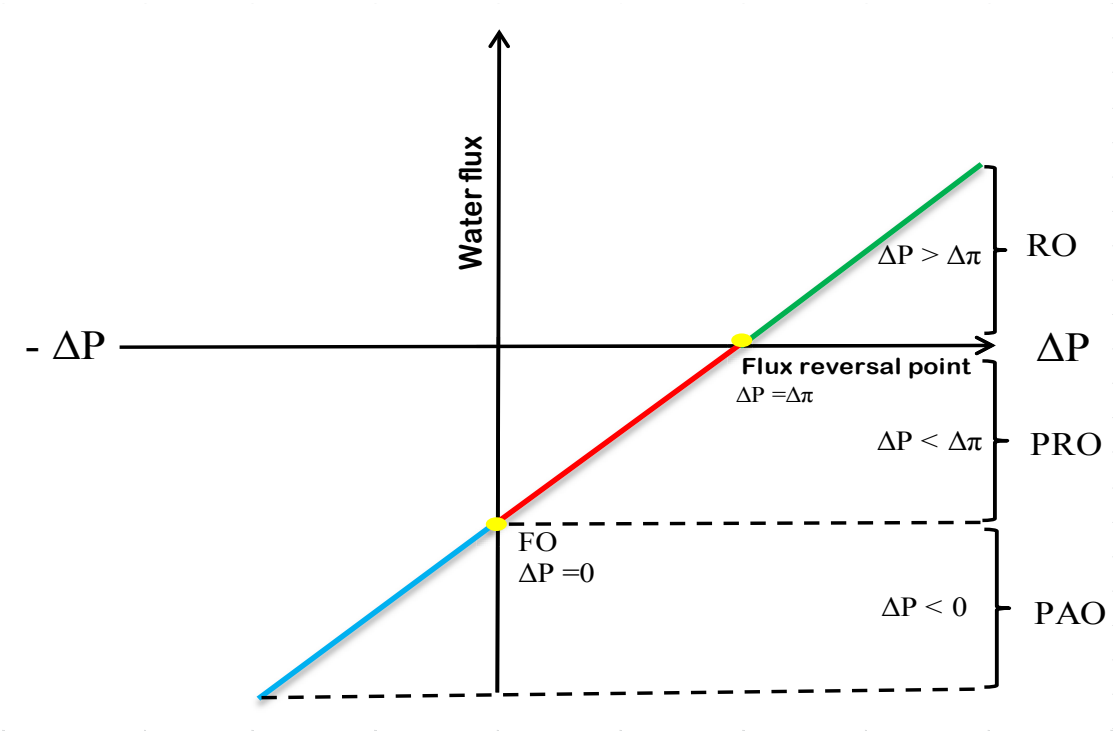

Figure. 4.1: The relationship and direction of water flux as a function of applied pressure in FO, PRO, RO and PAO for an ideal semipermeable membrane. Figure modified from (Lee et al. 1981b).

4.3 Materials and Methods

4.3.1 Feed and draw solutions

Four different types of draw solutes were used in this study. While NaCl was mainly used for validating the theoretical model, the other three draw solutes were fertilisers such as ammonium sulphate (SOA) or $(NH_4)_2SO_4$, monoammonium phosphate (MAP) or $NH_4H_2PO_4$ and potassium chloride or KCl and all these fertilisers were

used as DS in the earlier studies (Phuntsho et al. 2013; Phuntsho et al. 2011). All the chemicals used for the lab-scale experiments in this study were of reagent grade supplied by Sigma–Aldrich, Australia. The DS of specified concentrations were prepared by dissolving the solutes in deionised water (DI) with the help of a magnetic stirrer. Depending on the objective, a wide range of DS concentrations were used in this study and they are all specified in the figures and discussion. NaCl solution was used as FS that simulates brackish water (BW) representing FS of different total dissolved solids (TDS). In most cases, BW in the study refers to the NaCl concentration of 10 g/L unless stated otherwise. The thermodynamic properties of the solutions such as osmotic pressure, viscosity, diffusion coefficient, density, etc. were analysed using a thermodynamic modelling software OLI Stream Analyser 3.2 (OLI Systems Inc., Morris Plains, NJ, US).

4.3.2 Bench-scale pressure assisted osmosis (PAO) experimental setup and its operation

The schematic layout of the bench-scale crossflow FO/PAO experimental setup shown in Figure 4.2, consisted of two pumps (one each for DS and FS), each connected to the crossflow membrane cell with channel dimensions of 2.6 cm width, 7.7 cm length and 0.3 cm depth on both sides of the membrane. All the FO and PAO experiments were conducted using flat sheet cellulose triacetate (CTA) FO membrane supplied by Hydration Technology Innovations (HTI, Albany, OR). The pure water permeability coefficient (A) and salt rejection of the CTA FO membrane were determined in the RO mode using the same membrane cell at pressures ranging from 0 to 10 bar. The permeability coefficient A was found to be 0.91 $Lm^{-2}h^{-1}bar^{-1}$ (2.52 x 10^{-7} m/s/bar) while salt rejection was 97.5% and salt permeability coefficient

B =1.29 x 10^{-7}m/s. The other characteristics of the CTA FO membrane have been widely reported including in our earlier studies (Cath et al. 2006; Tang. et al. 2010). The channel on the DS side of the membrane cell was filled with 6 layers of diamond shaped polystyrene spacers to prevent membrane deformation and damage when hydraulic pressure was applied on the active layer side of the membrane.

Pressure pump was used for the FS and the applied hydraulic pressure was adjusted manually using pressure valve installed at the outlet of the membrane cell and the valve located in the bypass. Both FO and PAO experiments were conducted with membrane active layer facing the FS and support layer facing the DS. The applied pressure on the feed side varied between 0 and 10 bar only as the maximum pressure rating for the pump was only up to 11 bar. The crossflow for the DS was maintained using a low-pressure variable speed gear pump (Cole Parmer). The DS and FS temperatures were maintained at 25 °C with the help of water bath connected to heating/chilling system. The crossflows for both the DS and FS were maintained at 400 mL/min in counter-current direction. Each experiment was carried out for an average of 4 h duration. The water flux was measured by recording the change in the weight of the DS tank held on the digital mass scale connected to PC for online data logging. The FO and PAO experiments were carried out in the batch mode where both the diluted DS and feed concentrate were recycled back to their respective tanks. The reverse diffusion of the draw solutes was evaluated either by observing the electrical conductivity (EC) using a multimeter (CP-500L, ISTEK, Korea) when DI was used as feed or by analysing the cations using inductively coupled plasma mass spectrometry (ICP-MS) when BW was used as FS.

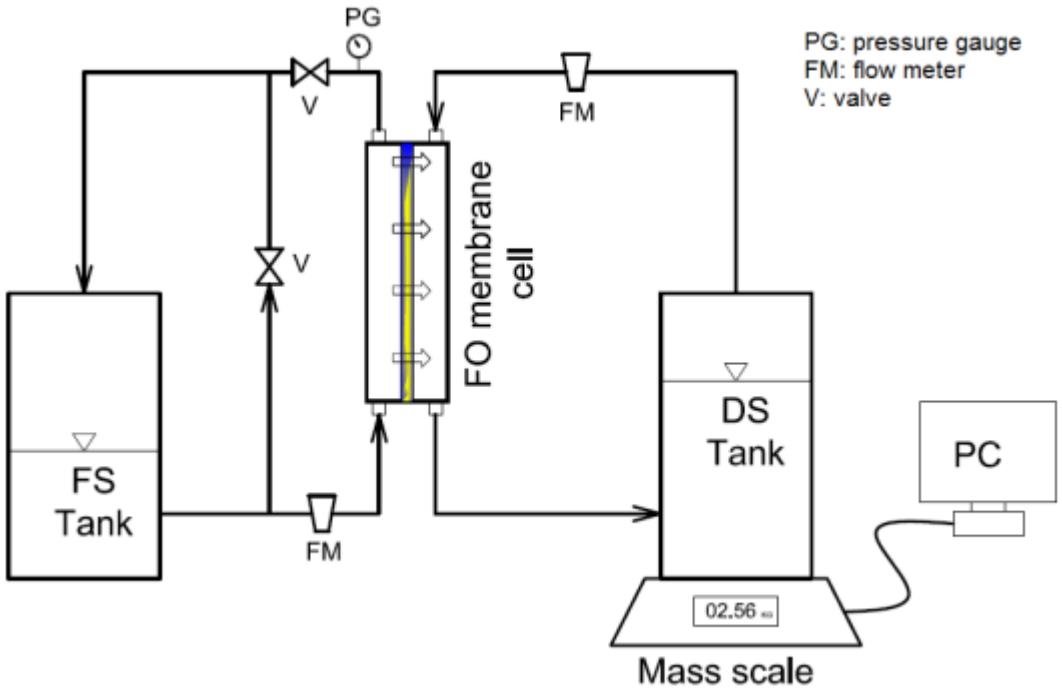

Figure 4.2: Schematic of the lab-scale experimental setup for PAO process.

4.4 **Results and discussion**

This study can be divided in to two parts. In the first one, FO/PAO experiments were conducted using NaCl as both DS and FS mainly to validate the PAO process with the help of models discussed under section 2. The experimental and theoretical water fluxes were comparatively studied. In the second part, fertiliser DS were used to study the PAFDO process and finally the significance and implications of the results are discussed in relation to the modular applications.

4.4.1 **Validating the pressure assisted osmosis (PAO) process**

PAO experiments were conducted under different solute concentrations using NaCl for both the DS and FS. NaCl solute was chosen because the thermodynamic properties of NaCl are well known and widely studied and hence found easier for

modelling works. Moreover, NaCl was used as solutes in our earlier study with the FO modelling and the same modelling approach has been adopted here for the PAO process (Phuntsho. et al. 2014). Theoretical water flux was calculated using equation (14) and the parameters listed in Table 4.1.

The variations or increase in the water flux with the hydraulic pressure in the PAO process are presented in Figure 4.3 (a) using NaCl solution either as DS or FS or both. PAO experiments were conducted under four different DS-FS conditions, (DI-DI, BW-DI, DI-BW and BW-BW) with the applied pressure varying from 0 to 10 bar. Here BW refers to NaCl solution with a concentration of 10 g/L. The results in Figure 4.3 show that, the applied hydraulic pressure not only has a positive influence on the water flux in the PAO process as reported in the earlier studies (Blandin et al. 2013; Coday et al. 2013; Yun et al. 2013a) but also shows good correlation between the experimental water flux and the theoretical water flux calculated using the proposed model. The water flux in the PAO process increased significantly compared to FO process depending on the applied pressure and the DS-FS conditions.

Table 4.1: Essential parameters used for mathematical modelling for FO and PAO processes.

Parameters	**Values**
Membrane material (HTI, Albany, OR)	CTA
Pure water permeability coefficient, A ($Lm^{-2}h^{-1}bar^{-1}$)	0.91
Salt (NaCl) permeability coefficient, B ($Lm^{-2}h^{-1}$)	0.46
Salt rejection (1000 mg/L NaCl at 10 bar)	97.2%
Thermodynamic properties of 1.0 M NaCl (from OLI Stream Analyser 3.2)	
Diffusion coefficient (m^2/s)	1.4096×10^{-9}
Density at 0.11 M NaCl (kg/m^3)	1035.97
Dynamic viscosity (cP)	0.9735
Solution temperature (both DS and FS)	25^oC

In the first set of experiments, DI water was used on both sides of the membrane, which simulates the pure water permeability test conducted in the RO mode of operation. The results in Figure 4.3 (a) show that the water flux increased linearly with the applied pressure and the average water flux determined from the slope of the flux versus pressure plot was found to be 0.91 $Lm^{-2}h^{-1}bar^{-1}$ and this value has been used as a pure water permeability coefficient (A) for calculations of the models.

In the second set of experiments under the BW-DI condition, the water flux is positive (3.47 Lm^{-2} h^{-1}) in the FO process (ΔP=0) and we know that this flux is generated solely by the osmotic pressure difference between the BW as DS and DI as FS. When the pressure was however introduced on the feed side, the water flux was observed to increase linearly with the pressure at an average of 0.66 Lm^{-2} $h^{-1}bar^{-1}$. This translates to about 19% gain in water flux per unit applied pressure in addition to the water flux generated by the osmotic driving force. In the third set of experiments under the DI-BW condition, the water flux was negative in the FO process (ΔP=0) and this is expected because the osmotic pressure of the DS is lower (DI) than the FS (BW). This mode is generally termed as PRO mode of operation applied mainly for osmotic power generation. When the pressure is however applied on the BW feed side, the negative water flux decreases until the water flux was observed to reverse towards positive indicating that, the applied pressure (ΔP) has overcome the osmotic pressure of the FS. Extrapolation of the flux data with the applied pressure indicates that the water flux is zero at about 7.8 bar applied pressure, which is equal to the osmotic pressure of the BW (10 g/L NaCl). Water flux increased somewhat linearly with the applied pressure up to 10 bar tested in this study. This DI-BW condition for the PAO process is similar to the RO process with the only difference being that, DI water is already present on the DS side of the membrane in the PAO process. In the RO process however, the permeate is released only after adequate hydraulic pressure (higher than osmotic pressure of the FS) is introduced on the feed side and hence negative flux is not expected to occur in the RO process.

For the last conditions tested (BW-BW), the water flux is zero in the absence of applied pressure because of the equal concentration between the DS and the FS.

However, when the pressure was applied on the FS side, the water flux increased linearly with the applied pressure at an average of 0.6 $Lm^{-2}\ h^{-1}bar^{-1}$. This increase in the water flux due to applied pressure is quite significant given that the two solutions were under osmotic equilibrium and with zero water flux there was no possibilities of further reducing the DS concentrations. The results in Figure 4.3 (a) therefore show the suitability of the applied pressure in generating additional water flux after the FO process has reached osmotic equilibrium. The presence of DS on the permeate side with equal osmotic pressure as the FS, reduces the net osmotic pressure difference which the applied pressure has to overcome to zero ($\Delta\pi = 0$) and hence produce water flux much higher than under the condition in which the solution is absent on the DS or the permeate side of the membrane. This advantage is clearly visible when we compare the differences in the water flux between BW-BW and DI-BW experimental conditions. DI-BW simulates the RO process and hence it requires applied pressure higher than the osmotic pressure of the BW (7.8 bar for 10,000 mg/L NaCl) to generate a positive permeate flux. At the same applied pressure however, the water flux for BW-BW is much higher than DI-BW condition even though both used the FS of the same osmotic pressure.

Figure 4.3 (a) also presents the theoretical water flux (shown in dashed lines) modelled using equation (14). The theoretical water flux matches fairly well with the experimental water flux indicating that equation (14) can be useful in predicting the water flux in for the PAO process as long as the thermodynamic properties of the DS and FS are known.

The next sets of experiments were conducted to see the differences in the net gain in the water flux when PAO is operated under different DS concentrations or the

osmotic pressure difference. The water fluxes obtained under the FO mode (ΔP=0) and the PAO mode (6 bar) of operations under different NaCl DS concentrations with BW10 (10 g/L NaCl) as the FS are presented in Figure 3(b). Under the FO mode of operation, the water flux increases with the increase in the NaCl DS concentrations although this increase was non-linear and but rather logarithmic. This non-linearity of flux is consistent with many earlier studies which is attributed to the enhanced dilutive ICP and concentrative ECP effects at higher water flux that in turn reduces the effective driving force when higher DS concentrations are used (Gray et al. 2006; McCutcheon & Elimelech 2006a; Tan & Ng 2008; Tang. et al. 2010; Zhao et al. 2011). When a pressure of 6 bar is however applied under the PAO mode of operation, the water flux increases significantly at all the DS concentrations tested. Although the water flux under the applied pressure showed a similar logarithmic trend with the DS concentrations as in the FO process however, a closer observation reveals a significant difference in the actual increase or percentage gain in the water flux due to the applied pressure under different DS concentrations. The actual gain in water flux due to applied pressure of 6 bar in the PAO process is presented in Figure 4.3 (b) as a percentage of the water flux increase beyond the FO process. These results indicate that, the total increase or gain in the water flux on applying pressure is slightly higher at lower DS concentration than at higher DS concentrations confirming earlier studies by Oh et al. (2014). For example, the net gain in the water flux at 0.5 M DS concentration (BW10 as FS) on applying 6 bar pressure is 85% whereas at this same applied pressure, the net gain at 3 M DS concentration is only 9%. The experimental water fluxes in Figure 4.3 (b) also closely matched with the theoretical flux calculated using model presented by equation (14). More detailed

discussions on this can be found in the next Section (4.2) using three fertilisers solutions as DS in the FDFO process.

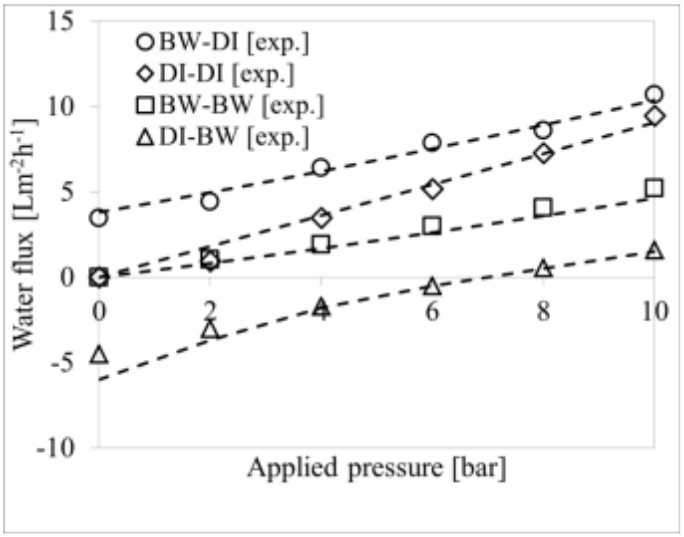

(a)

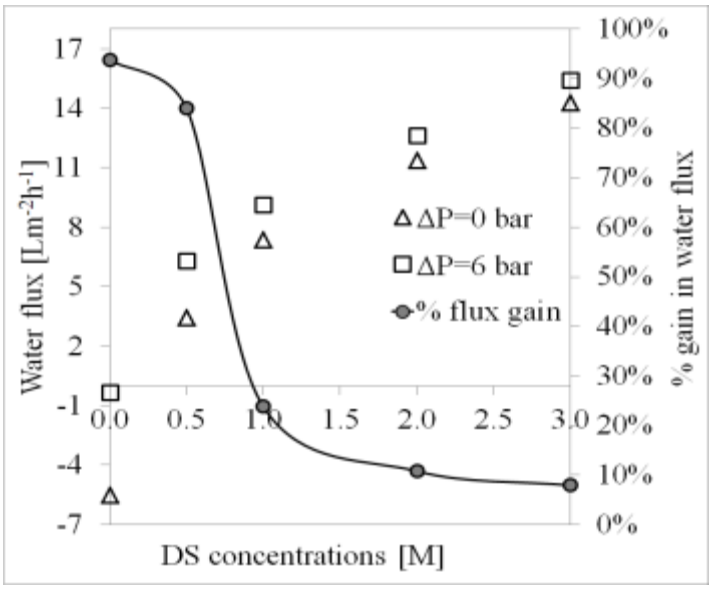

(b)

Figure 4.3: Variation of water flux in the FO/PAO processes (a) at different applied pressures under different DS-FS combinations (BW refers to 10 g/L NaCl solution) and (b) at different DS concentrations using BW as FS at an applied pressure of 6 bar. The data points refer to the experimental water flux while dotted lines refer to the theoretical flux calculated using models discussed under Section 2.

4.4.2 PAO process for the pressure assisted fertiliser drawn osmosis (PAFDO) desalination

The water fluxes under the FDFO mode (ΔP=0) and the PAFDO mode (10 bar) of operations using three types of fertilisers as DS and BW10 as the FS are presented in Figure 4.5. Similar to the earlier results with NaCl in Figure 4.3 (b), the water flux increases non-linearly with the increase in the DS concentrations for all these fertiliser DS tested as shown in Figures 4.4 (a), 4.4 (b) and 4.4 (c) for SOA, KCl and MAP, respectively. On the application of 10 bar hydraulic pressure, the water flux increased significantly for all the three fertiliser DS tested. Several interesting observations are made from the results presented in Figure 4.4 and are discussed below.

The comparison of the water fluxes under FDFO process (ΔP = 0) for the three fertilisers shows that, KCl generates the highest water flux followed by SOA and MAP at the same bulk osmotic pressure difference, consistent with our earlier studies on the fertiliser DS (Cath et al. 2010; Coday et al. 2013; Oh et al. 2014; Yun et al. 2013a). The trend in the water flux increase with the DS concentration under both FDFO mode and PAFDO mode of operations is non-linear for all the three fertilisers tested as shown in Figures 4.4 (a) to 4.4 (c). A summary of the net gain in water flux entirely due to 10 bar applied pressure is presented in Figure 4.4 (d) for all the three fertiliser DS. Similar to the earlier results with NaCl in Figure 4.3 (b), the results in Figure 4.4 (d) indicate that, the gain in the water flux due to applied pressure is higher at lower DS concentration than at higher DS concentrations. For example, the net gain in water flux due to applied pressure of 10 bar are 7.38, 8.62 and 9.42 $Lm^{-2}h^{-1}$ at 0.1 M fertiliser DS which decreases to 4.93, 5.22 and 5.87 at 3 M DS

concentrations for SOA, KCl and MAP, respectively. In fact, this translates to 1928%, 345% and 237% increase in the water flux at 0.1 M DS compared to only 38%, 29% and 69% increase at 3 M for SOA, KCl and MAP, respectively at 10 bar applied pressure. These results clearly demonstrate the advantages if the applied pressure is introduced at the lower stages of the osmotic process (when the net osmotic driving force becomes significantly reduced) rather than applying throughout the stages. This also indicates that, the applied pressure in the PAO process could be more effective when the DS concentration approaches closer to the osmotic equilibrium, where the driving force becomes significantly reduced.

However, the results in Figures 4.3 and 4.4 also indicate that, although water flux can be increased under the PAO or PAFDO mode by applying pressure nevertheless, this increased water flux is also likely to further exacerbate the severity of both the dilutive ICP and concentrative ECP effects. Perhaps this explains why the net gain in water flux at higher DS concentrations is much lower than the net gain at lower DS concentrations for similar feed concentrations used in the PAO/PAFDO process. This study therefore shows that, applying hydraulic pressure to enhance the FO water flux irrespective of the available osmotic driving force may not be an effective option and hence must be targeted at the lower end of the FO process where the driving force decreases due to continuous dilution of the DS.

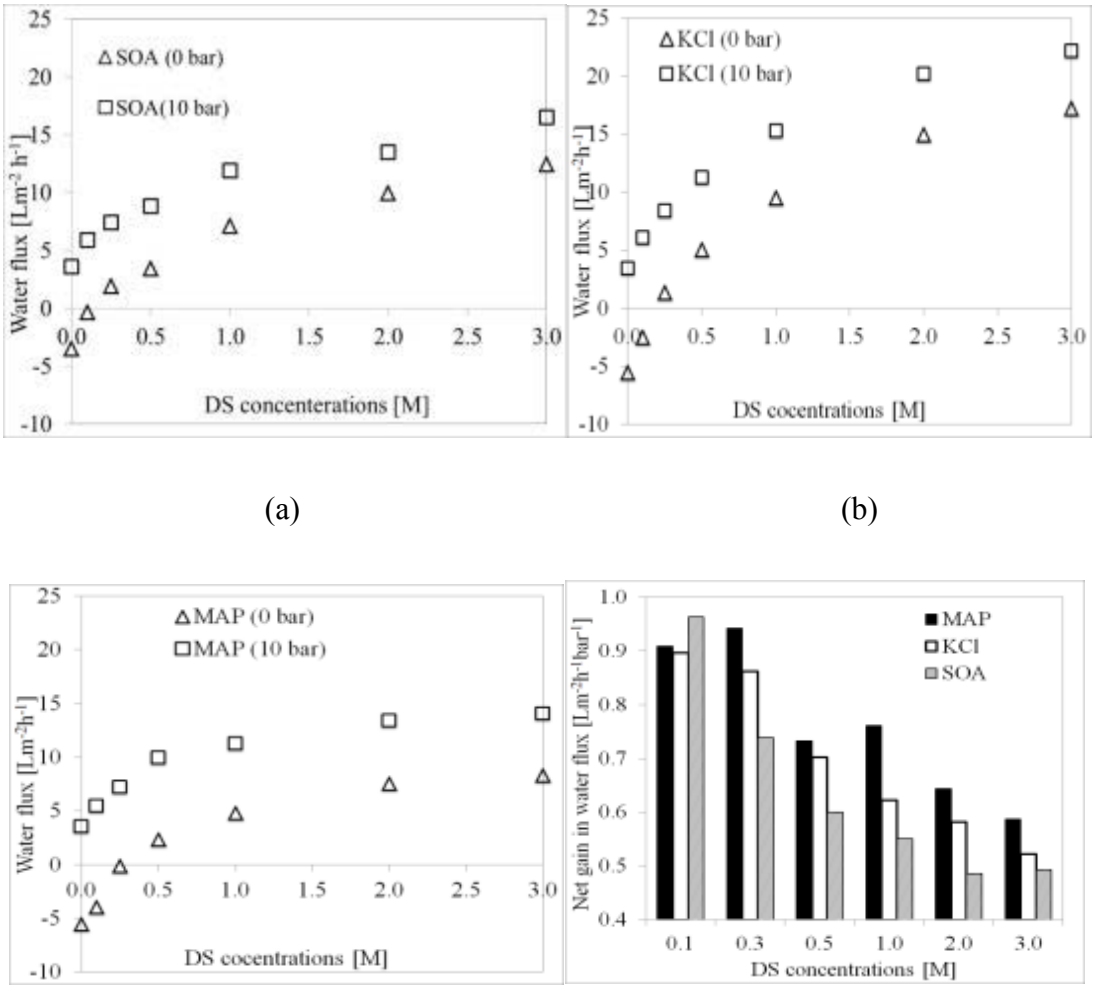

(a) (b)

(c) (d)

Figure 4.4: Influence of applied pressure on the water flux and the net gain in water flux under various DS concentrations for the three fertilisers used as DS using 10 g/L NaCl solution as FS. (a) For SOA, (b) for KCl, (c) for MAP and (d) the net gains in the water flux per unit applied pressure (specific water flux) when a hydraulic pressure of 10 bar was applied on the feed side of the membrane. In Figure 4.3 (b), the applied pressure of 6 bar was used since during the initial stage of the study, a lower applied pressure was preferred until it was realised later that higher applied pressure was possible and hence 10 bar was used in this experiment.

Comparing the three fertilisers DS used in this study, the effective gain in the water flux (in terms of specific water flux) at 10 bar applied pressure was highest for MAP followed by KCl and SOA. For example, the effective gains in water flux for MAP were 0.94 $Lm^{-2}h^{-1}bar^{-1}$ at 0.1 M and 0.57 $Lm^{-2}h^{-1}bar^{-1}$ at 3 M. The same gains in water flux for SOA were 0.74 $Lm^{-2}h^{-1}bar^{-1}$ for 0.1 M and 0.47 $Lm^{-2}h^{-1}bar^{-1}$ for 3 M concentrations. The water flux under the FO process is lowest for MAP amongst the three DS tested however; it has the highest effective gain in water flux under the PAFDO mode. This might be explained due to the less severity of dilutive ICP effects under the combined driving force (osmotic pressure difference and the applied pressure) for MAP. Even though, MAP has the highest effective gain in water flux nevertheless, it still has much lower water flux both in the FDFO and PAFDO modes and hence the severity of dilutive ICP effect should be lower than the other two fertiliser DS which has much higher water flux under both modes of operation.

Osmotic equilibrium occurs when the osmotic pressure of the solutions on both sides of the membrane becomes equal and the net transfer of water across the membrane becomes zero. At this point, the ultimate dilution of the DS has been achieved and any further dilution of the DS is not possible by the natural osmotic process. The hydraulic pressure of 10 bar was applied on the feed side under the condition in which the fertiliser DS was at osmotic equilibrium with the BW and the results are presented in Figure 4.5 for all the four different DS used in this study. The FS concentrations ranged 0 - 35 g/L NaCl and the DS concentrations for SOA, MAP and KCl with equal osmotic pressure as FS were determined using OLI Stream Analyzer

3.2. Experimental flux at these bulk DS and FS concentrations were observed zero, which confirmed that the selected fertiliser DS concentrations using OLI Stream Analyser were at osmotic equilibrium with the NaCl FS.

The results in Figures 4.5 (a) and 4.5 (b) indicate that, a significant water flux can be obtained by applying a slight hydraulic pressure on the feed when the DS reaches osmotic equilibrium with the FS. For example, when MAP DS and BW5 (5 g/L NaCl) FS are in osmotic equilibrium, the water flux becomes zero however, when a hydraulic pressure of 10 bar is applied, the water flux of 9.46 $Lm^{-2}h^{-1}$ was gained which could significantly help in further diluting of the DS beyond the concentrations at the point of osmotic equilibrium. Although, all the three fertiliser DS showed a significant increase in water flux however, the gain in water flux decreased somewhat exponentially with the increase in the feed concentrations. Similar results were obtained using NaCl as FS under the applied pressure of 6 bar and moreover, the theoretical water flux obtained using model fitted very closely (shown by dashed lines) with the experimental water flux as presented in Figure 4.5 (b). This is interesting given that the net bulk osmotic pressure, which the applied pressure has to overcome, is zero for all cases under osmotic equilibrium irrespective of the level of concentrations at which the equilibrium is reached. The exponential decrease in the flux at higher osmotic equilibrium concentrations can be explained due to the different extent of dilution and concentration of solutes at the membrane surface that decreases the effective driving force due to increase in the net osmotic pressure.

At static osmotic equilibrium condition, the net osmotic pressure between the FS and DS (permeate side) is zero (i.e $\Delta\pi = \pi_{F,b} - \pi_{b,D} = 0$) and this is true irrespective of the

concentration levels at which the osmotic equilibrium has reached. However, once the applied pressure generates the water flux, the process becomes dynamic which then alters the concentration profiles of both the FS and DS at their respective membrane surfaces. This change in the DS and FS concentrations (both using NaCl) under dynamic condition at 6 bar applied pressure at different levels of osmotic equilibrium has been simulated and presented in Figure 4.5 (b). The simulation results indicate that, the net osmotic pressure which the applied pressure has to overcome not only becomes positive ($\Delta\pi>0$) but its value increases with the increase in the concentration level at which the osmotic equilibrium has attained. This explains the reason for lower gain in water flux when the hydraulic pressure is applied at higher level of concentrations under osmotic equilibrium.

The net gain in water fluxes at 10 bar applied pressure is different for the three fertiliser DS even though, the osmotic equilibrium occurred under the same FS (5 g/L NaCl) condition as shown in Figure 4.5 (a). Comparing these net gain in water fluxes for the three fertiliser DS, it is found that the trend is similar to the water fluxes under FDFO or PAFDO modes of operations presented in Figure 4.4. This indicates that the differences in the net gain in water fluxes for the three fertiliser DS is likely due to other thermodynamic properties such as diffusion coefficient, viscosity, density, speciation and ionisation, etc., which could influence the mass transfer and the CP effects to different degree thereby significantly affecting their performances.

It is however significant to note that, water flux of 4.08, 3.60 and 1.83 was generated from a feed with salt concentration as high as the seawater TDS (35 g/L) using a hydraulic pressure of meagre 10 bar which is impossible in the RO mode of

operation and (where the applied pressure has to be more than 29.3 bar). This clearly shows the advantage offered by the presence of DS on the permeate side of the FO membrane during the PAFDO process which reduces the net osmotic pressure which the applied pressure has to overcome thereby increasing the net driving force. The analogy to the PAO process could be, like as if a vacuum is applied on the permeate side of the FO membrane and this vacuum is generated by the osmotic pressure of the draw solution.

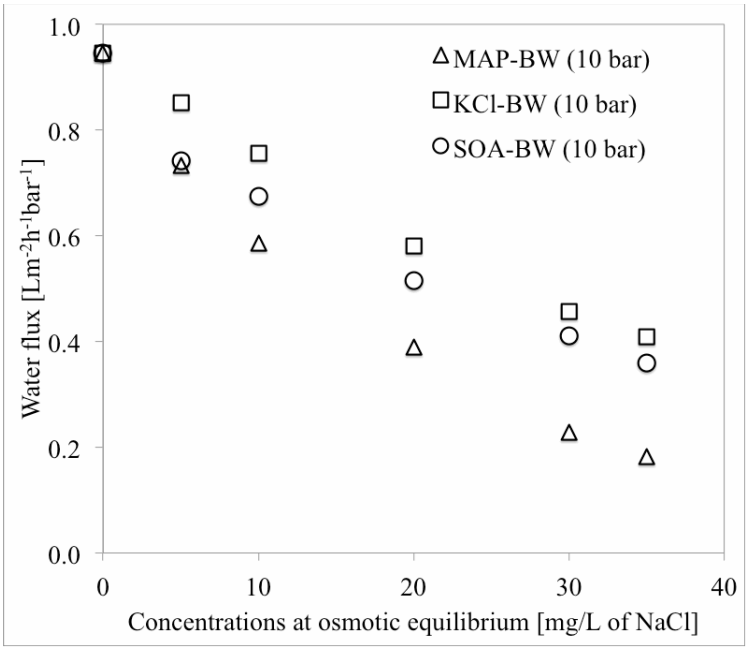

(a)

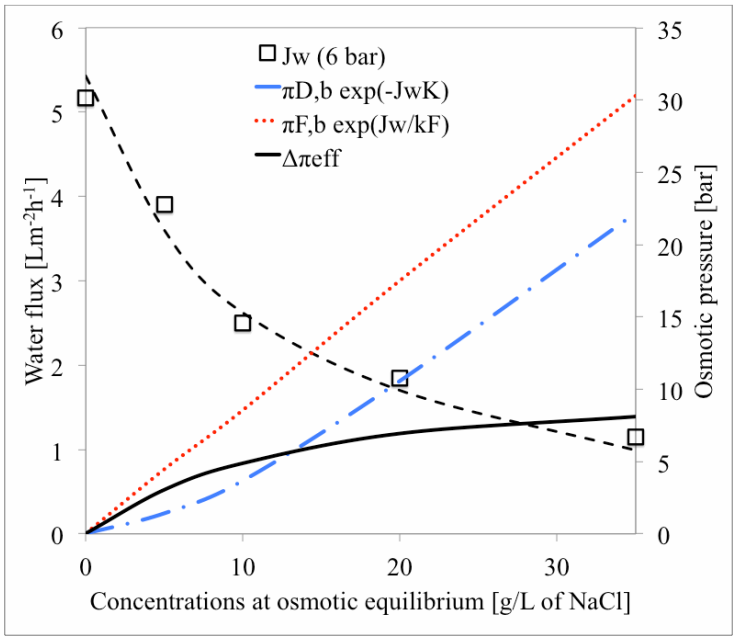

(b)

Figure 4.5: Variation of the water fluxes when the hydraulic pressure is applied under the condition in which the osmotic equilibrium occurs at different DS-FS concentrations levels (a) using three fertilisers as DS with BW as FS (with concentrations ranging from 0 to 35 g/L NaCl at an applied pressure of 10 bar and (b) using NaCl as DS with FS ranging from 0 to 35 g/L NaCl at an applied pressure of 6 bar and the variation of the effective osmotic pressures of the DS and FS at the membrane surface. The equivalent concentrations of SOA, KCl and MAP were determined using OLI Stream Analyser 3.2.

4.4.3 Reverse draw solute diffusion and feed solute rejection in the PAO process

In addition to the water flux, it is important to assess the performance of the PAO process in terms of solute flux. As in any osmotic process, PAO is associated with two independent solutions on each side of the membrane and hence there is a

bidirectional movement of solutes. The solute fluxes are usually assessed in terms of salt rejection for feed solutes and the specific reverse solute flux (SRSF) for draw solutes. The SRSF is measured as a ratio (SRSF=J_s/J_w) of reverse draw solute flux (J_s) and the water flux (J_w) while J_s (where $J_s = B*\Delta C$) is given as a function of solute permeability coefficient B and the concentration difference ΔC (where $\Delta C = C_D - C_F$) (Phillip et al. 2010; Tan & Ng 2010). The assessment of the SRSF is significant given its implications to the FO process such as its potential to accelerate membrane scaling and fouling on interaction with the feed solutes, economic loss of the draw solutes and the likely contamination of the feed concentrate which could complicate the brine management (Boo et al. 2012; Hancock & Cath 2009; Phillip et al. 2010; She, Jin, Li, et al. 2012). To assess the SRSF for the PAO process, two sets of experiments were conducted: one set with BW10-DI and another set with 0.5 M KCl-BW at pressures ranging from 0 to 10 bar.

The SRSF for both NaCl and KCl, and the feed rejection data for the PAO experiments are presented in Figure 4.6. The results show a slight decrease in the SRSF with increase in the applied pressure for the PAO process compared to the FO process. For example, the SRSF for FO process ($\Delta P=0$) is 0.77 g/L and 0.60 g/L for NaCl and KCl, respectively however, it decreases to 0.49 g/L and 0.45 g/L, respectively in the PAO process on the application of 10 bar pressure. These results are consistent with the earlier studies on the PAO process where a generally decreasing trend in the solute flux was observed with the increase in the applied pressure under the PAO process.

The decline in the SRSF in the PAO process is likely due to either change in the B value or change in the ΔC or both. Although, the membrane deformation was not

assessed in this study, Blandin et al. (Blandin et al. 2013) observed a slight stretching of the membrane that led to increase in the pure water permeability coefficient (A) and the solute permeability coefficient (B) of the membrane although this issue was not reported in the other studies for the PAO process (Coday et al. 2013; Yun et al. 2013a). However, membrane deformation has been reported in some of the earlier studies with the PRO process, a process quite similar to the PAO process (Kim & Elimelech 2012; She, Jin & Tang 2012).

The study however, observed a decrease in the reverse diffusion of the draw solutes with applied pressure indicating that the increased water permeability likely limits the diffusivity of the draw solutes through the membrane due to enhanced convective water flux that drives the draw solutes away from the membrane due to back diffusion (Phuntsho. et al. 2012).

The alternative explanation is that, increasing the applied pressure increases the water flux which in turn alters the solute concentrations at the membrane boundary layer on both sides of the membrane due to enhanced CP effects. This reduces the concentration difference ($\Delta C=C_D-C_F$) between the DS and FS that determines the rate of reverse diffusion of the draw solutes. The DS concentration decreases due to increased dilution while FS concentration increases due to more feed solute rejection thereby reducing the ΔC and ultimately the SRSF (Coday et al. 2013).

Figure 4.6 also presents the variation in the feed solute rejection due to applied pressure in the PAO process. The results are presented for experiments conducted using 0.5 M KCl as DS and BW10 as FS. The results indicate that the NaCl feed rejection increases with the increase in the applied pressure, a trend that could be considered consistent to the SRSF. This increased rejection is a result of the

enhanced water flux due to applied pressure in addition to the water flux generated by the osmotic driving force. This can also be explained due to dilution effect from the enhanced water flux at higher applied pressure, a similar phenomenon observed with the RO process when operated at higher applied pressure (Hancock & Cath 2009; Lee et al. 2014; Phillip et al. 2010).

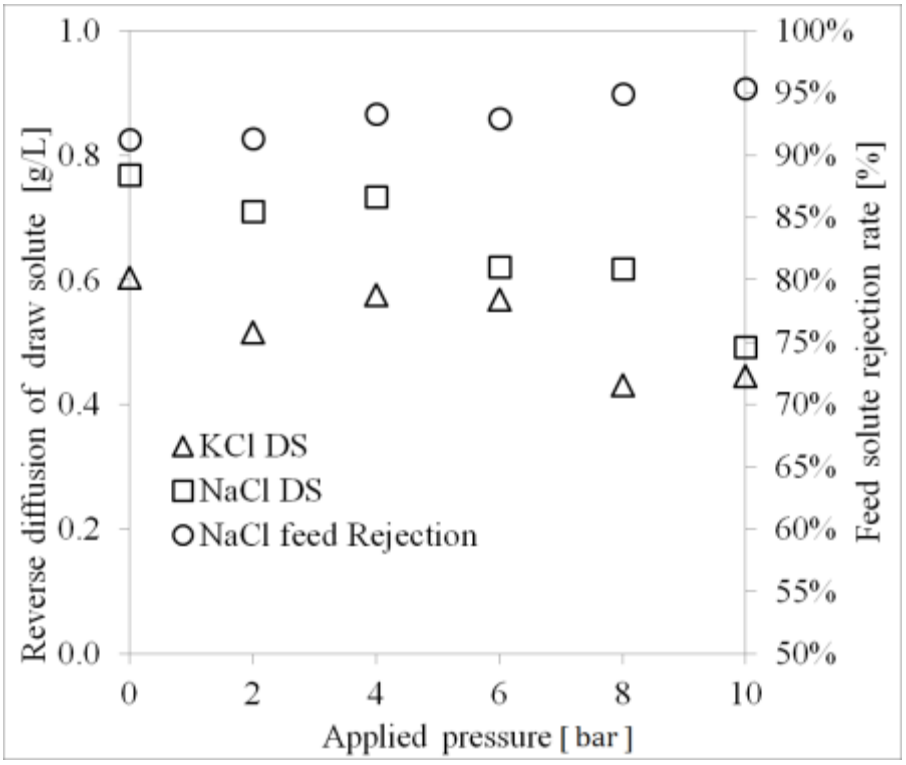

Figure 4.6: Influence of reverse diffusion of draw solutes and the feed solute rejection due to applied pressure in the PAFDO process.

4.4.4 **Understanding the significance and implications of the PAFDO process**

In the FDFO desalination process, it is impossible to achieve fertiliser concentrations acceptable for direct fertigation especially when a feed with higher TDS or osmotic pressure is used. One of the options is to integrate NF with the FDFO process where NF is used as post-treatment process to reduce fertiliser concentration to acceptable limit before fertigation. However, NF becomes an additional process that not only

requires energy but also increases its footprint. One of the objectives of this study was therefore to evaluate whether the pressure assisted fertiliser drawn osmosis or PAFDO could substitute FDFO-NF hybrid process thereby removing the footprint of NF post-treatment system completely. There are several positive implications of introducing in-situ hydraulic pressure in the PAFDO process rather than the FDFO-NF process, which are worth discussing here.

The synergies from the two driving forces (osmotic driving force and the hydraulic applied pressure) enhances the water flux which can then reduce the number of elements required for the desalination up to the point of osmotic equilibrium thereby decreasing the capital cost and foot print of the membrane modules. Alternatively, for the fixed number of membrane elements designed to reach osmotic equilibrium under the FO process alone, the in-situ introduction of hydraulic driving force would reach osmotic equilibrium earlier along the elements in the module and hence the additional water flux due to applied pressure could dilute the DS beyond the point of osmotic equilibrium or have higher dilution factor. PAFDO process should therefore be able to operate at a much higher feed recovery rate and final DS dilution factor because of the additional flux generated due to the applied pressure.

However, applying hydraulic pressure throughout the FDFO process may not be optimum based on the results in Figures 4.3 (a) and 4.5 since applied pressure is more effective at lower DS concentration when the FDFO process approaches closer towards osmotic equilibrium. Therefore, based on these results, applying the hydraulic pressure in the later stages of the membrane elements would provide the optimum gain in water flux rather than applying throughout. However, applying the hydraulic pressure only after the osmotic equilibrium has attained completely would

mean that, a separate PAO stage is necessary that would add to the cost of membrane modules and hence may appear not much different from having a separate NF process. However, a separate PAFDO will be more advantageous than a separate NF process given the synergies of the two driving forces in PAFDO against only single driving force for the NF stage. However, for example, if the FDFO process is designed to achieve osmotic equilibrium in two stages, the optimum design could be to have PAFDO in the second stage instead of both the stages. However, it is worthwhile to note the earlier findings that, the water flux under PAO mode is slightly lower than the water fluxes added for FO and RO process operated separately and this has been attributed due to slightly enhanced dilutive ICP and concentrative ECP effects for FO operated under the enhanced water flux. Therefore, a comparative economic assessment of the PAFDO versus FDFO-NF could only provide the true advantages of each process over the other.

Figure 4.7 presents the simulation of how the concentrations of the diluted SOA DS that comes of the FO membrane module would vary depending on the membrane area and applied hydraulic pressure used in the PAFDO process. For the simulation, PAFDO (10 bar) data for SOA DS obtained in this study was applied to the 8040 CTA FO membrane element (membrane area of 9.0 m^2) reported in the earlier study (Eun et al. 2014). Simulation was performed by assuming that the PAFDO was operated after the diluted DS and FS have reached osmotic equilibrium at which point the water flux due to osmotic driving force is zero. The simulation results in Figure 4.7 indicate that, as the membrane area increases with the addition of number of membrane elements, the dilution of the DS will increase as shown by the exponential decrease in the diluted SOA DS concentrations compared to FDFO process (without pressure) where the diluted DS concentration would remain same at

osmotic equilibrium. Using 10 numbers of 8040 membrane elements in series (total membrane area of 90 m^2), PAFDO can achieve additional dilution factor of almost 7 compared to the SOA concentration at osmotic equilibrium with 10 g/L NaCl FS. Using higher applied hydraulic pressure could further enhance the DS dilution factor with the simulation showing a dilution factor of about 14 at an applied pressure of 20 bar that results in the final diluted DS concentrations of 1.2 g/L SOA which is very close to acceptable nitrogen concentration of 275 mg/L for fertigation of tomato plants (Phuntsho. et al. 2012). Therefore, by optimising the total membrane area, feed recovery rates and the applied hydraulic pressure, it is possible that PAFDO could achieve the final diluted DS concentrations suitable for direct fertigation of crops thereby potentially eliminating the need for the NF post-treatment process.

However, most polyamide based thin film composite (TFC) FO membranes recently reported have comparatively weak tensile strength. This is because, effort on membrane fabrication has been mainly focussed on improving the water flux by reducing the membrane thickness and the porosity of the membrane support layer resulting in low tensile strength. The tensile strength of the CTA FO membrane used in this study did not show any evidence of extensive damage when tested up to hydraulic pressure of 10 bar however; CTA membranes have low comparatively lower permeability than the TFC membranes. Therefore, deformation may become an issue especially when TFC FO membranes are used for the PAO process and are subject of interest for future investigations.

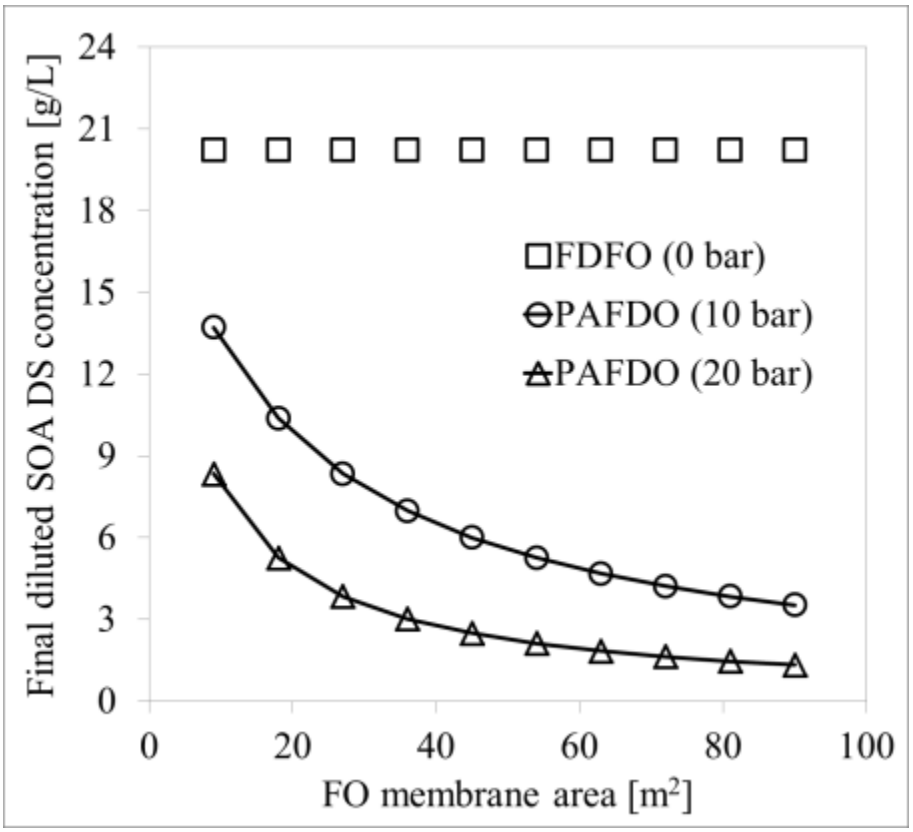

Figure 4.7: Variations in the expected concentrations of the diluted SOA fertiliser DS with total membrane area in the PAFDO process under the hydraulic pressures of 10 and 20 bar applied at the osmotic equilibrium between diluted SOA DS (20.2 g/L) and 10 g/L NaCl FS. Simulations were performed for 8040 CTA FO membrane element with an effective membrane area of 9.0 m^2 per element. Initial DS flow rate for 8040 CTA element was assumed at 120 L/h. For this particular simulation, influence of feed recovery rate was neglected for convenience and hence the results may slightly vary in the values although the trend would be similar. Readers are advised to consider the relative trend rather than the absolute data in this figure as more accurate simulation would require taking many other factors into considerations.

4.5 **Concluding remarks**

In this study, the pressure assisted osmosis or PAO was evaluated for its application in the fertiliser drawn forward osmosis or FDFO desalination process. Termed in this study as pressure assisted fertiliser drawn osmosis or PAFDO, the main objective of introducing pressure simultaneously during the FDFO process is to enhance the final osmotic dilution of the fertiliser DS by generating water flux beyond the point of osmotic equilibrium. PAFDO is expected to produce final diluted fertiliser DS that meets acceptable nutrient concentrations for direct fertigation potentially eliminating the need for an additional post-treatment process such as NF to reduce the fertiliser concentrations. The following specific conclusions have been drawn from this study:

- Application of small hydraulic applied pressure on the FS could help significantly gain water flux for the FO process and the experimental water flux closely fit with the models suggested.
- The study on the PAO using NaCl and PAFDO using three different fertilisers DS $(NH_4)_2SO_4$, $NH_4H_2PO_4$ and KCl suggests that, the hydraulic pressure could be more suitable when applied at lower DS concentrations especially when the osmotic driving force gradually decreases and the DS and FS approaches closer towards osmotic equilibrium.
- The additional water flux generated by the applied pressure could help dilute the fertiliser DS concentrations beyond the point of osmotic equilibrium making the PAFDO process potential for application as a standalone process without the need of additional post-treatment process such as NF to reduce the final fertiliser concentration to acceptable level for direct fertigation.

- The net gain in water flux under the PAO or PAFDO however decreases when the TDS of the feed increases.
- The specific reverse solute flux was lower and feed solute rejection was higher in the PAO or PAFDO mode compared to FO or FDFO mode of operations.
- Nevertheless, further work including long-term operations are required for better understanding the effects of hydraulic pressure on the FO membrane and membrane fouling and scaling, and the effect of pressure on ICP, which reduces the efficiency of the PAO.

Chapter 5

THIN FILM COMPOSITE FORWARD OSMOSIS MEMBRANE ON A SULPHONATED POLYETHERSULFONE SUBSTRATE

5.1 **Introduction**

The forward osmosis (FO) process has been emerging as an alternative technology for desalination, water treatment and power generation in recent years (Cath et al. 2006; Chung 2012). FO utilizes osmotic pressure for spontaneous water diffusion from the feed to the draw solution across a semi-permeable membrane. Compared to the pressure based driven membrane technology such as reverse osmosis (RO), the FO process displays several merits that can potentially surpass the RO technology for certain applications (Liu et al. 2009). Practically, FO can be used as a pre-treatment or in hybrid units for desalination. Applying FO as a pre-treatment can minimize reverse osmosis (RO) fouling and energy by treating raw feed water to much cleaner feed water (Yangali-Quintanilla et al. 2011). Furthermore, FO hybrid system has been proposed for desalination for fertigation by using fertilizer as the draw solution (DS) (Phuntsho et al. 2013; Phuntsho et al. 2011). Other potential and more practical applications of the FO process include juice or food concentration (Garcia-Castello et al. 2009), protein and pharmaceutical enrichment (Ling & Chung 2011b), and power generation (Achilli. et al. 2009; Lee et al. 1981b; Loeb 2002; Peinemann et al. 2008). Lack of high performing membranes and draw solution (DS) that can be recycled effectively still remains as major obstacles for the commercialisation of the FO technology (Cath et al. 2006; McCutcheon et al. 2005; Phuntsho et al. 2011). The flat-sheet cellulose triacetate (CTA) FO membrane produced by Hydration Technologies Inc. (HTI, Albany, OR) is the only FO membrane which is commercially available in the market at larger scale although few more companies such as Oasys (Boston, MA) have started to make FO membranes in the market in limited quantities. Regardless of its broad applications for the FO process, CTA FO

membrane has relatively lower water flux than the few reported polyamide based thin film composite (TFC) FO membranes (Cath et al. 2006). Recently, attention has been drawn to the development of asymmetric flat sheet or hollow fibre FO membranes via phase inversion technique followed by interfacial polymerization (Rong et al. 2010; Yip et al. 2010). This TFC FO membrane has been inspired from membrane approach that was originally developed for the RO process. It contains a very thin polyamide rejection layer and a polysulfone (Psf) support layer casted on a fabric support (usually made of non-woven polyethylene terephthalate or PET fabric) that gives additional mechanical strength to the membrane structure (Cadotte 1981). Chemically modified TFC-RO membrane has also been investigated for the FO process and it has been found that existing RO membrane can be used for all engineered osmosis applications (Arena. et al. 2011). However, the thick nonwoven support fabric and the hydrophobic Psf support layer results in very high internal concentration polarization (ICP) effects that significantly reduces the water flux during the FO process (Arena. et al. 2011). Tiraferri et al. (Tiraferri et al. 2011a), and Yip et al. (Yip et al. 2010), hypostasized that an optimal FO membrane should consist of a very thin polyamide rejection layer on top of a highly porous finger-like structure substrate to decrease the ICP. Afterward, investigations have demonstrated that membrane hydrophilicity plays a major role in inducing water flux across semi-permeable membranes (McCutcheon & Elimelech 2008b). Reports by Wang et al. confirmed that FO performance can be further enhanced in TFC membranes by increasing membrane hydrophilicity (Wang et al. 2012a). Hence, in addition to a finger-like structure, hydrophilicity has been added to the hypothesis for enhancement of water flux in the FO process. However, hydrophilic polymers have several disadvantages as membrane substrates: (1) swelling that is the super water

uptake that can negatively affect membrane substrate strength and PA rejection layer stability with the over stretched substrate; and (2) interfacial polymerization formation inside pores instead of membrane top surface (Ghosh & Hoek 2009b). Also increased hydrophilicity can improve binding between the PA rejection layer and the substrate top surface compared to the substrate with a relatively hydrophobic nature and rough surface (Ghosh et al. 2008; Wang et al. 2012a). Furthermore, membrane casting materials and interfacial polymerization have a great effect on permeability regardless of hydrophilicity (Ghosh & Hoek 2009b). Based on polymer solution and casting condition, each substrate can produce a different skin layer and pores morphology. Herein, substrate physical and chemical properties can affect polyamide rejection layer formation resulting in different membrane performance (Ghosh & Hoek 2009b).

Recently, sulphonated polyethersulfone (SPES) has been studied as a promising material in the proton exchange membrane fuel cell (PEMFC) applications and also for both RO and FO membranes to increase hydrophilicity and fouling resistance (Blanco et al. 2001; Wen et al. 2009). It is also assumed that the sulphonation of the polymer materials can introduce not only the hydrophilic nature to the membrane substrate which enhance water flux of the resultant FO membranes, but also may help change its membrane substrate morphology. Therefore, the objectives of this study are: (1) to investigate the influence of PES sulphonation on the formation of substrate morphology and its mechanical strength and (2) to investigate the effect of blended sulphonated materials as membrane substrates on FO performance. The synthesized SPES could be directly blended with PES at specific ratios to prepare modified membranes. As a benchmark, a non-sulphonated polyethersulfone (PES)

material was also assessed. The effects of membrane substrate structure on water flux and salt transports were investigated and compared.

5.2 Material and methods

5.2.1 Chemicals

Polyethersulfone (PES) granules (Mn: 55,000 - Good fellow, UK) have been used as materials for the synthesis of membrane substrates. N-methyl-2-pyrrolidone (NMP) (Sigma–Aldrich Pty. Ltd, Australia) was used for the fabrication of membrane substrates. M-phenylenediamine (MPD) with >99% purity and trimesoyl chloride (TMC) with 98% purity (Sigma–Aldrich Pty. Ltd, Australia) were used as received in this study for the interfacial polymerisation process. N-hexane from Sigma–Aldrich with >99.0% purity was utilized as the solvent for TMC. Sodium chloride (NaCl) reagent grade was used to prepare draw solution and feed solution supplied by Sigma–Aldrich, Australia. NaCl was dissolved in deionized (DI) to prepare 0.5, 1 and 2 M concentrations for use as draw solutions with DI water as feed solution (FS).

5.2.2 Synthesis of SPES polymer

The sulphonated polyethersulfone (SPES) polymer was synthesized following the method described by Xiao et al. (Li et al. 2007; Xiao et al. 2010). The chemical structures of PES and SPES are illustrated in Figure 5.1. A mixture containing 772 g of DMSO, 257 g of toluene, 16.47 g (0.039 mol) of 5, 50 –carbonylbis (2-fluorobenzene sulfonic acid) sodium salt, 76.59 g (0.351 mol) of DFBP, 99.98 g (0.390 mol) of TMBPF and 67.38 g (0.488 mol) of potassium carbonate were poured into a five-necked reactor equipped with a reflux condenser, a stirrer, a nitrogen-introducing tube and a thermometer. The reactor was heated to 140°C and maintained at this temperature for 12 h under constant stirring, then a nitrogen

atmosphere for 8 h to remove water generated out of the system followed by distilled toluene for another 2 h. The mixture was diluted with 180 g of N-methylpyroridinone (NMP) after it cooled down to room temperature. The mixture was discharged into 2000 g of methanol to precipitate the polymer solution followed by filtration and washing with water several times to remove residual methanol. The collected polymer was dried at 80°C for 10 h and 150°C for 8 h under nitrogen atmosphere. Figure 5.2 shows the flow chart for the PES sulphonation reaction and preparation procedure (Li et al. 2007).

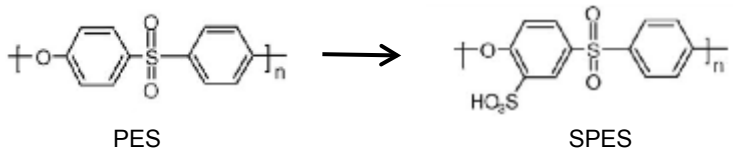

Figure 5.1: Chemical structure of PES and SPES synthesized in this study.

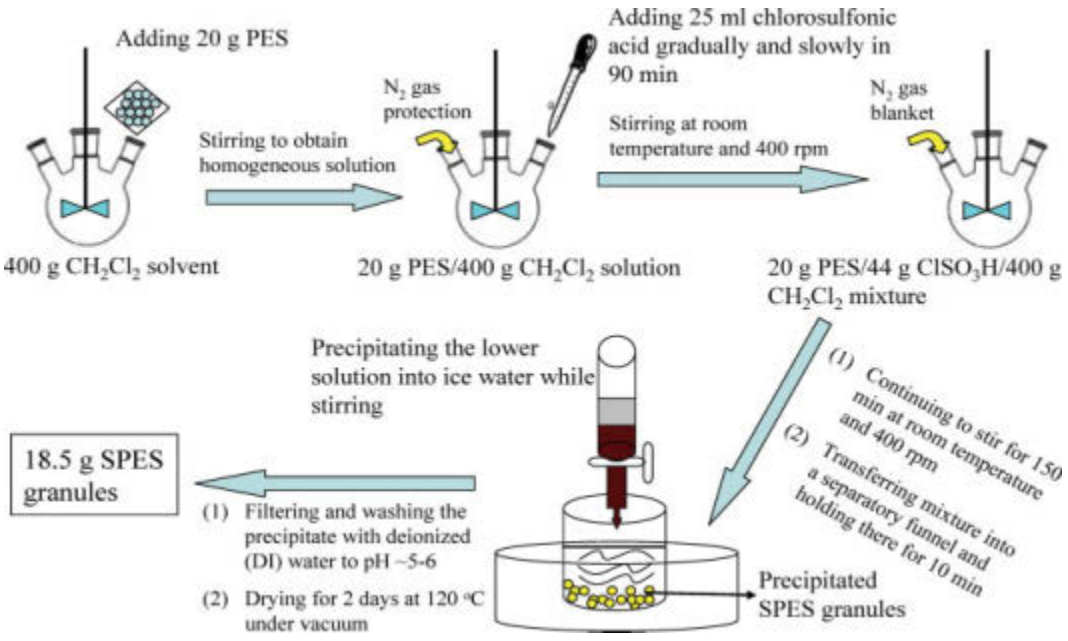

Figure 5.2: PES sulphonation reaction and preparation procedure (Li et al. 2007).

5.2.3 **Fabrication of flat-sheet TFC FO membranes**

5.2.3.1 **Fabrication of FO membrane substrates via phase inversion**

Casting solutions were prepared using certain amount of PES and SPES as shown in Table 5.1. Polyethersulfone (PES) and sulphonated PES (SPES) were dissolved in NMP then stirred by magnetic stirrers at room temperature for 24 hours. The polymer solutions were then degassed using digital bench top ultrasonic cleaner (Soniclean Pty Ltd, Australia) for 60 min. They were stored in a desiccator for over 48 hours before casting. Casting was performed on a glass plate using a stainless steel film applicator (Sheen Instruments Ltd, UK) with an adjustable gate height fixed at 200 μm. The casted substrate was immersed immediately into a DI water bath to initiate phase inversion and it remained in the bath for 10 minutes. The resultant substrates were then kept in DI water before conducting the next stage which was formation of the polyamide rejection layer on top of this substrate.

Table 5.1: TFC-FO casting solutions composition with different sulphonated polymer blending ratio.

Membrane ID	Casting solution composition			Sulphonated polymer (%)
	PES (wt%)	MNP (wt%)	SPES (wt%)	
TFC_1	12	88	0	0
TFC_2	8	88	4	25
TFC_3	6	88	6	50

5.2.3.2 **Forming of rejection layer via interfacial polymerization**

The rejection layer on the top surface of the membrane substrates was formed by interfacial polymerisation. The substrate was soaked first in 3.4 wt % aqueous MPD solution for 120 seconds and then with the help of an air knife the excessive MPD solution was removed from the membrane top surface. Then n-hexane solution of 0.15 wt % TMC was gently poured onto the top surface of substrates that were sealed in a frame for 60 sec to form the ultra-thin PA rejection layer. Sealed frame will allow TMC solution to react with the MPD just on the top surface of the membrane. Figure 5.3 shows the polyamide formation by reaction between TMC and MPD. The resultant TFC-FO composite membrane was rinsed with DI water to remove the residual solution and stored in DI water at 4 ◦C for characterization and for conducting performance experiments.

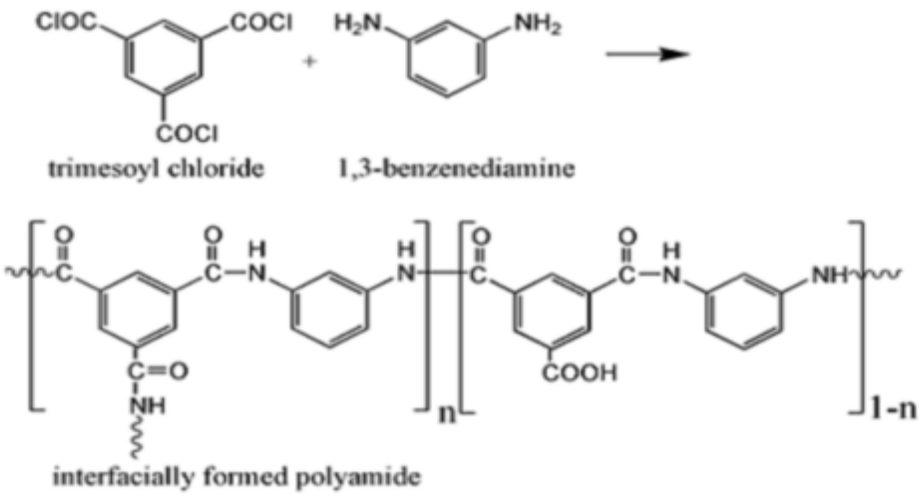

Figure 5.3: Polyamide formation by reaction between TMC and MPD (Tang. et al. 2009).

5.2.4 **Membrane characterizations**

5.2.4.1 **Membrane substrate characterisation**

Membrane substrate morphologies were studied using a high-resolution Schottky Field Emission Scanning Electron Microscope (SEM, Zeiss Supra 55VP, Carl Zies AG, Germany). Membrane substrates were first dried in a vacuum condition at room temperature for 24 h. To view the cross sections of the membranes, samples were then flash-frozen in liquid nitrogen to preserve the pore structure then coated with a thin layer of carbon using Balzers Sputter coater (SCD 050, BAL-TEC, Germany) before SEM imaging.

The contact angles of the membranes were measured by the sessile drop method, using an Optical Tensiometer (Attension Theta Lite 100, Biolin Scientific, Finland). Membrane samples were first dried in vacuum at room temperature for 24 h. Small distilled water droplets (5-7μL) were applied onto a levelled membrane surface and profiles of the water drops were captured by a camera and the imaging software determined the contact angles. At least 3 measurements were obtained to get the average value of the contact angle. Membrane thicknesses were measured using a digital micrometre (293-330 Mitutoyo, Japan). Membrane porosity (ε) was obtained by measuring the dry mass (W_2) and wet mass (W_1) of membrane samples according to the following equation (Sukitpaneenit & Chung 2009):

$$\varepsilon = \frac{(W1-W2)/\rho i}{\left[\frac{W1-W2}{\rho i}\right],+[W2/\rho m]} \times 100\% \quad (1)$$

Where ρi and ρm are density of wetting solvent and membrane, respectively.

The mechanical property of the membrane substrate was measured in terms of its tensile strength using LS_1 tensile testing equipment (AMETEK, Lloyd instruments

ltd, UK). The membranes substrates were cut into strips of 10 mm width and 25 mm length and the testing was conducted at the rate of 10 mm/min.

5.2.4.2 **TFC-FO membrane characterizations**

The water permeability coefficient (*A*) and salt rejection of the fabricated TFC membrane were determined based on the pure water fluxes obtained in the RO mode using the same membrane cell at pressures ranging from 0-10 bar. Salt rejection (*Rs*) property of the TFC-FO membranes was determined by measuring the electrical conductivity of the permeate and the feed water (200 ppm NaCl) at 1 bar applied pressure. The salt permeability coefficient (*B*) was then determined based on the following equation:

$$\frac{1-Rs}{Rs} = \frac{B}{A(\Delta P - \Delta \pi)} \quad (2)$$

5.2.5 **FO performance experiments**

FO experiments were conducted on a crossflow bench-scale FO experimental setup as per the schematic experimental layout shown in a previous study (Phuntsho. et al. 2013). It consisted of two pumps (one each for DS and FS), each connected to the crossflow FO membrane cell. The volumetric flow rates of both sides were 200 mL/min. The FO water flux *Jw* was determined by measuring the weight change of the feed tank using a digital mass balance connected to a data logging system. Heating/chilling unit maintained DS and FS temperatures at 25 °C.

The membranes performances were evaluated under two different modes: (1) FO mode where the active layer faced the FS (AL-facing-FS), (2) pressure retarded osmosis (PRO mode) where the active layer faced DS (AL-facing-DS). For salt permeability, the reverse solute flux was evaluated by observing the increase in the electrical conductivity (EC) of the DI feed water using a multimeter (CP-500L,

ISTEK, Korea). A thermodynamic modelling software OLI Stream Analyser 3.2 (OLI Systems Inc., Morris Plains, NJ, US) was used to analysis the thermodynamic properties of the solutions such as viscosity, osmotic pressure, density and diffusion coefficient.

Based on the classical ICP model developed by Loeb et al, the water flux can be predicted by the following equations in the FO process for the FO mode (AL-FS) (Loeb et al. 1997):

$$J_w = \frac{1}{K_D}\left[ln\frac{A\pi_{D,b}+B}{A\pi_{Fm}+Jw+B}\right] \qquad \text{(AL-FS)-FO} \qquad (3)$$

For the PRO mode (AL-DS), the water flux in FO processes can be obtained by the following equations.

$$J_w = \frac{1}{K_D}\left[\ ln\frac{A\pi_{D,m}+Jw+B}{A\pi_{F,b}+B}\right] \qquad \text{(AL-DS)-PRO mode} \qquad (4)$$

Where $\pi_{F,b}$ and $\pi_{D,b}$ are the bulk osmotic pressure of the FS and DS, π_{Dm} and π_{Fm} are the osmotic pressures on membrane surfaces facing the DS and FS, respectively, B is the salt permeability coefficient of the membrane, K_D is the solute resistivity for diffusion of draw solutes within the porous support which can be defined as:

$$K_D = \frac{t\tau}{\varepsilon D} = \frac{S}{D} \qquad (5)$$

Where t, ε and τ represent thickness, porosity and tortuosity of the support layer, respectively. This equation shows the relationship among solute diffusion resistivity within the porous layer K_D, diffusivity D, membrane structural parameter S, membrane porosity ε and membrane thickness t. This equation can be used to obtain the membrane structural parameters as well.

5.3 Results and discussion

5.3.1 Characteristic of membrane substrates

Sulphonated PES membrane substrate was synthesized by blending PES with the SPES and compared with the pure PES substrate. The effect of sulphonation on the PES substrate formation by phase inversion was investigated in terms of its membrane morphology and changes in membrane hydrophilicity, and mechanical strength. Figure 5.4 shows the SEM images of membrane substrates casted with different concentrations of sulphonated polymer as explained in Table 5.1. The thicknesses of these membrane substrates were in the range 65–80 μm although the height of the casting knife was adjusted to 200 μm for all the substrate samples.

Figure 5.4 (a) shows the cross-section, top and bottom SEM images of the membrane substrate casted from pure PES (no sulphonation) showing clearly the presence of a large number of finger-like pore structures which is in parallel with previous reported studies (Tiraferri et al. 2011b; Yip et al. 2010). With sulphonation however, the membrane substrate formed loses its finger like morphology although it was still faintly visible at 25 wt% as shown in Figure 5.4 (b). At higher sulphonation, (50 wt %), SPES substrates did not exhibit any finger like structures but rather a sponge-like structure with few macrovoids were observed as presented in Figure 5.4 (c). Membrane substrates formed during the phase inversion stage usually have few distinguished structures and morphologies (Mark 1968). Several pathways may occur for the original polymer solution during the phase inversion stage which can be explained using a ternary diagram (Wijmans et al. 1985b). Based on the ternary diagram, delayed demixing in the phase inversion can affect the substrate morphology. Adding sulphonated material would cause delayed demixing which

results in a sponge like substrate and significantly reduces macrovoid formation as the sulphonated material content increases.

Figure 5.4 also shows that while changes in membrane substrate cross section are obvious under different casting solution composition with a different degree of sulphonation, changes in the membrane top surface cannot be clearly visualised from SEM images even at a magnification of 10,000. However, previous studies have shown that as the sulphonation concentration increases, membrane surface roughness decreases (Widjojo et al. 2011). The top skin layer and the more porous sub layer can be formed by two separate pathways during the phase inversion stage. The top skin layer that forms on the surface of the porous membrane film is hypothesized to occur when the solvent diffusion from the membrane exceeds the non-solvent infusion. This process can increase the polymer concentration on the top side and form a slight denser skin during phase inversion on the membrane top surface (Wijmans et al. 1985a). Therefore, delayed demixing due to increase sulphonated materials not only significantly changes the membrane substrate and morphology but it can affect the surface properties such as pore size and roughness as has previously been reported (Widjojo et al. 2011).

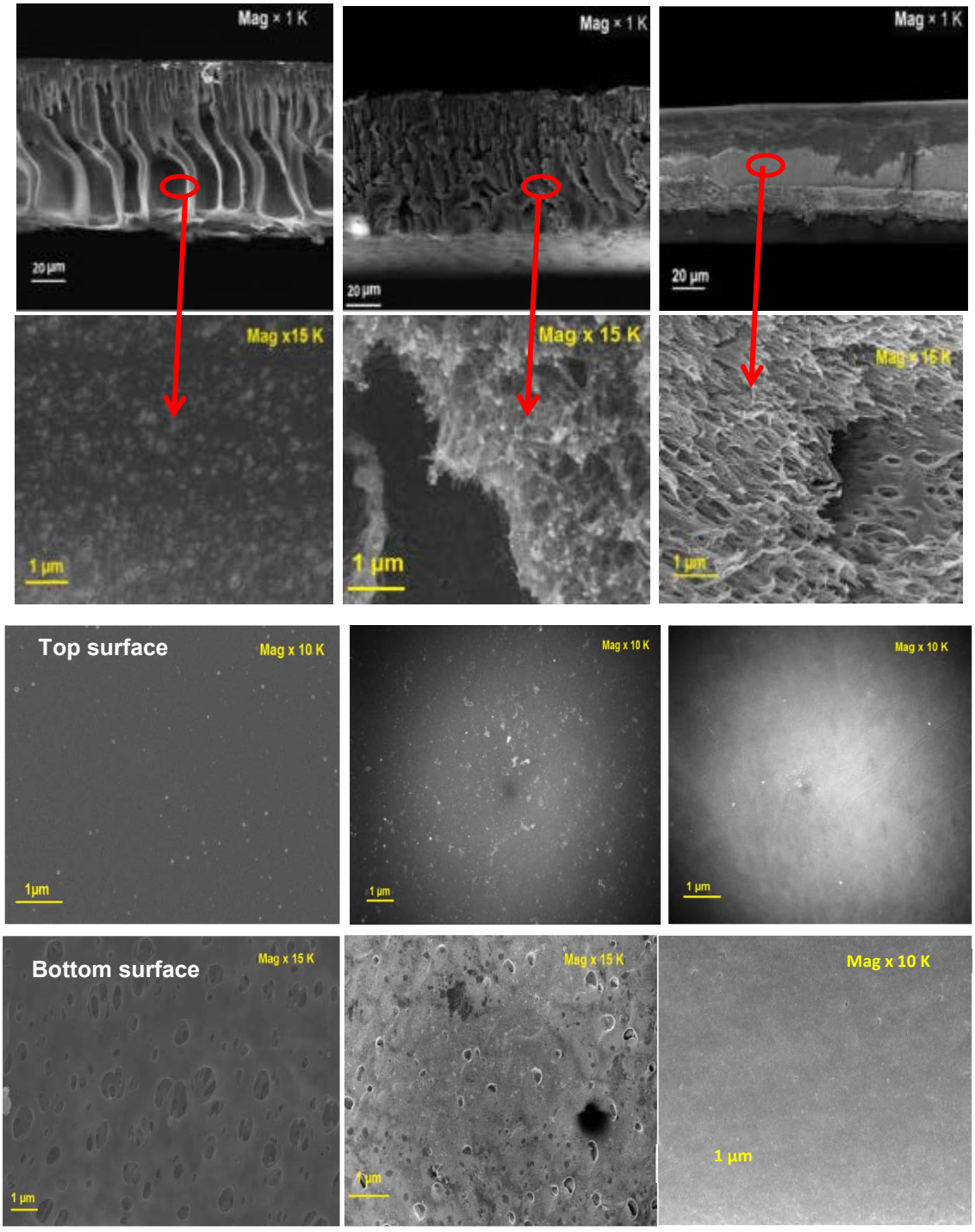

(a) PES (b) SPES (25 wt%) (c) SPES (50 wt%)

Figure 5.4: SEM images of membrane substrates with different blending ratio of sulphonated polymer for TFC fabrication: (a) no sulphonated polymer; (b) 25 wt% sulphonated material; (c) 50 wt% sulphonated material. All samples were fabricated through 12 wt% polymer concentration in NMP.

The membrane bottom surface morphology in Figure 5.4 (a) shows traces of macrovoids in the substrate sample without sulphonation (TFC_1) and this macrovoids seem to decrease with sulphonation as shown in Figure 5.4 (b) for TFC_2 (25 wt %). No such macrovoids can be found with the substrate sample TFC_3, (50 wt %) as shown in Figure 5.4 (c). A closer SEM observation of the membrane cross section reveals that the sulphonation increases the porosity of the membrane substrate.

Table 5.2 presents the membrane substrates characteristics at different degree of sulphonation. The results confirm the hypothesis that the sulphonation of PES increases the hydrophlicity and relatively porosity of the membrane substrate. The contact angle of PES membrane substrate (without sulphonation) has a contact angle of 77.3◦, while the contact angles for sulphonated substrates showed relatively lower contact angles in the range of 15–20◦ due to the increased hydrophilicity. Thus these results show that the higher degree of hydrophilicity can be achieved by increasing the degree of sulphonation on the PES.

Table 5.2: Characteristics of membrane substrates at different sulphonation rates.

Sample ID	Thickness (μm)	Porosity%	Contact angle (º)	
			Active layer	Support layer
TFC_1-(PES)	80± 3.0	77 ± 1	52 ± 1	65 ± 1
TFC_2-(SPES-25%)	71± 2.0	75 ± 1	27 ± 1	26 ± 2
TFC_3-(SPES-50%)	65± 3.0	79 ± 3	20 ± 1	20 ± 2

Table 5.3: Mechanical properties of membranes with a different degree of sulphonation.

Membrane ID	Tensile strength	Modulus	Elongation break (%)
TFC_1-(PES)	7.8	241	17.9
TFC_2-(SPES-25%)	3.6	72.1	36.2
TFC_3-(SPES-50%)	1.1	12	43.3

Table 5.3 shows the mechanical strengths of fabricated membrane substrates with a different sulphonation ratio. With an increase in the sulphonation, the tensile strength and Young's modulus decreases while the elongation at break increases. From these results, it is clear if the sulphonation is increased beyond 50 wt%, the membrane substrate would have very poor mechanical strength. Earlier studies have suggested that, the reduction in tensile strength due to sulphonation may be related to two factors: (1) the binding of strong polar sulfonic acid to the polymer chain may decrease the aggregative state and (2) the polymer matrix is expanded due to sulphonation thereby augmenting the polymer chain movements which gives the polymer material more flexibility (Guan et al. 2005; Smitha et al. 2003).

Figure 5.5 shows the comparative FTIR spectra of PES and SPES (50 wt%) membrane substrate samples to confirm the presence of SO_3H group on the polymer chains. The symmetrical stretching vibrations of sulfonic acid groups and aromatic SO_3H symmetric appear at ~1180 cm^{-1} and ~1025 cm^{-1}, respectively (Guan et al. 2005; Kim et al. 1999) however, based on Figure 5.5, we could not detect the peaks distinctly probably because of near overlapping band. However, absorption peak at

3420 cm^{-1} is due to stretching vibrations link to the hydroxyls of sulfonic acid groups which confirm the presence of sulfonic acid groups in the SPES membrane samples.

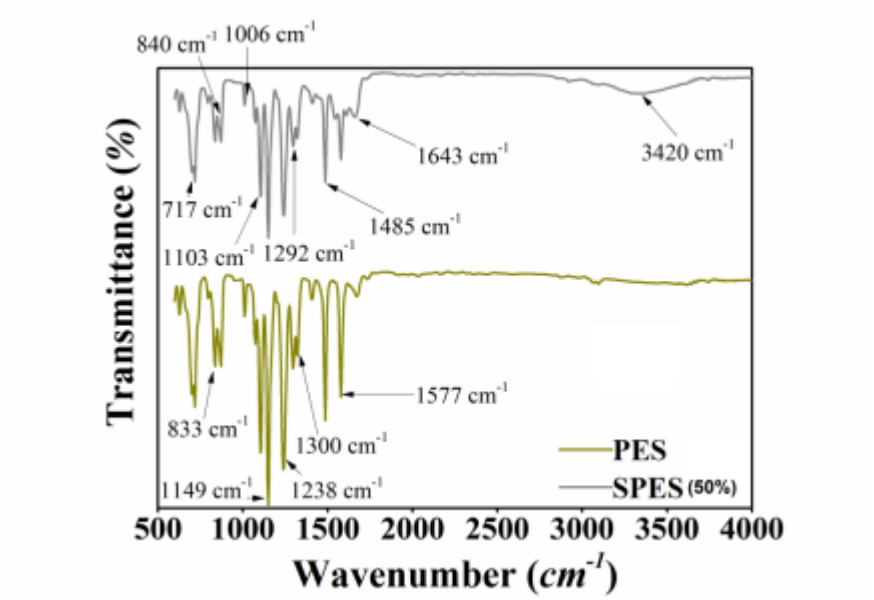

Figure 5.5: FTIR spectra of membrane substrate sample for PES and SPES 50 wt%.

5.3.2 **Characterization of TFC-FO membranes**

TFC-FO membranes were prepared via interfacial polymerisation on the top surface of prepared membrane substrates. Table 5.4 summarizes the TFC-FO membrane transport properties and their structural parameters. The pure water permeability coefficient of the TFC-FO membranes increases with the increase in sulphonation rates. For example, the *A* values of 1.1 $Lm^{-2}h^{-1}bar^{-1}$ with the TFC_1 (substrate without sulphonation) increased to 2.1 $Lm^{-2}h^{-1}bar^{-1}$ and 2.9 $Lm^{-2}h^{-1}bar^{-1}$ for TFC_2 (25 wt% sulphonation) and TFC_3 (50 wt% sulphonation), respectively.

The salt permeability coefficient (*B*) also slightly increased for TFC_2 and TFC_3 with a higher degree of sulphonation. However, regardless of degree of substrate sulphonation, all the TFC membranes showed a reasonable salt rejection of 93.3 %, 91.3 %, 91.1 % with TFC_1, TFC_2 and TFC_3, respectively.

The membrane A and B parameters are intrinsic membrane properties related to the top rejection layer independent the substrate properties. However, the increase in the *A* and *B* values with the degree of sulphonation is probably related to the characteristics of the top skin layer of the membrane substrate formed during the phase inversion stage that likely effected the formation of polyamide rejection layer. It was discussed earlier under Section 5.3.1 that, at higher degree of sulphonation, a much smother top skin surface is formed that likely provided a more suitbale conditions for the formation of a PA rejection layer with much more uniform thickness. At no sulphonation or at lower degree of sulphonation, the top skin layer of the substrate is more rough which may likely result in the formation of much thicker PA layer (average) thereby reducing the membrane permeability.

Lower structural parameter is preferable for membrane based osmotic process such as FO. The membrane structural parameter is related to the degree of ICP and hence the membrane performances under the FO process. Table 5.4 shows the structural parameters (*S* value) of the three TFC-FO membranes. These results indicate that the S values of the TFC-FO membrane decrease with an increase in the degree of sulphonation. The *S* value for TFC_1 was 1096 μm which decreased to 335 μm and 245 μm for TFC_2 and TFC_3, respectively with sulphonation.

Generally, higher degree of sulphonation resulted in more porous and hydrophilic substrate which lowers the structural parameter and the ICP effects. Most previous works indicate that the membrane porosity and water permeability is related to the polymer concentration and additives such as pore formers (McGinnis & McGurgan 2013); however, the findings in Table 5.2 show that, sulphonation also makes the membrane substrate more porous for the sample prepared at similar polymer

concentrations (all the three membrane substrate samples were fabricated with 12 % polymer concentration). Furthermore, Table 5.4 shows that, the permeability of the TFC membrane active layer increases with the increase in the sulphonation degree although both the TFC membranes with 25 wt % and 50 wt % sulphonation composed of similar polymer concentration as the TFC_1 without sulphonation.

Membrane with different degree of sulphonation has different chemical properties and top surface pore size and topologies which consequently effect the interfacial polymerisation and PA layer formation (Widjojo et al. 2011). Although it is hard to differentiate the effect of sulphonation on interfacial polymerisation through SEM images however, the performance in terms of water flux and salt permeability can greatly help in interpreting the rejection layer properties under increased sulphonation rate. For example, the intrinsic pure water permeability (*A* value) for TFC_1 (without substrate sulphonation) was 1.1 $L/m^2\ h^{-1}\ bar^{-1}$ which increases to 2.1 $L/m^2\ h^{-1}\ bar^{-1}$ for TFC_2 (25 wt%) and 2.9 $L/m^2\ h^{-1}\ bar^{-1}$ for TFC_3 (50 wt%) membrane samples. However, this also correspondingly led to slight decrease in the salt rejection or increases in the salt permeability (*B* value) of the sulphonated TFC membranes compared to un-sulphonated TFC_1 membrane. The higher water permeability and higher salt permeability for TFC_3 compared to TFC_2 also indicate that at higher sulphonation degree, it results in the formation of thinner PA rejection layer due to smoother substrates.

Table 5.4. Transport properties and structural parameters of fabricated membrane samples in comparison with CTA-HTI membrane.

Sample ID	[a] Water permeability (A)		[b] Salt permeability B (10^{-8} m/s)	NaCl rejection (%)	[c] S value
	$L/m^2\ h^{-1}\ bar^{-1}$	$\times^{10-12}$ m/s Pa			
TFC-1	1.1 ± 0.15	3.1±0.5	2.6±0.1.3	93.2	1096
TFC-2	2.1 ±0.26	5.1±0.5	4.1±0.1.3	91.3	335
TFC-3	2.9 ±0.25	8.1±0.5	5.1±0.1.3	91.1	245

[a] Evaluated in the RO testing mode over an applied pressure range of 1bar with DI water as feed water .
[b] Evaluated in the RO testing mode over an applied pressure range of 1bar for a feed water containing 200 ppm NaCl .
[c] Evaluated based on experiments under the FO mode using 2 M NaCl as the draw solution with DI water as feed water.

5.3.3 **Performance of TFC-FO membranes for FO process**

The performances of synthesized TFC-FO membranes with different sulphonation degree were assessed under both FO and PRO mode of operations using 0.5 – 2.0 M NaCl as DS and DI water as feed. Their comparative performances in term of water fluxes and reverse solute fluxes are presented in Figure 5.6. Figure 5.6 (a) compares the membrane performance in terms of water flux and reverse solute flux for the TFC membrane samples under the FO and PRO mode of membrane orientation at various NaCl DS concentrations with DI FS.

As expected, the water flux presented in Figure 5.6 (a) increases with an increase in DS concentration for all the TFC membrane samples due to a greater driving force generated by higher DS concentration.

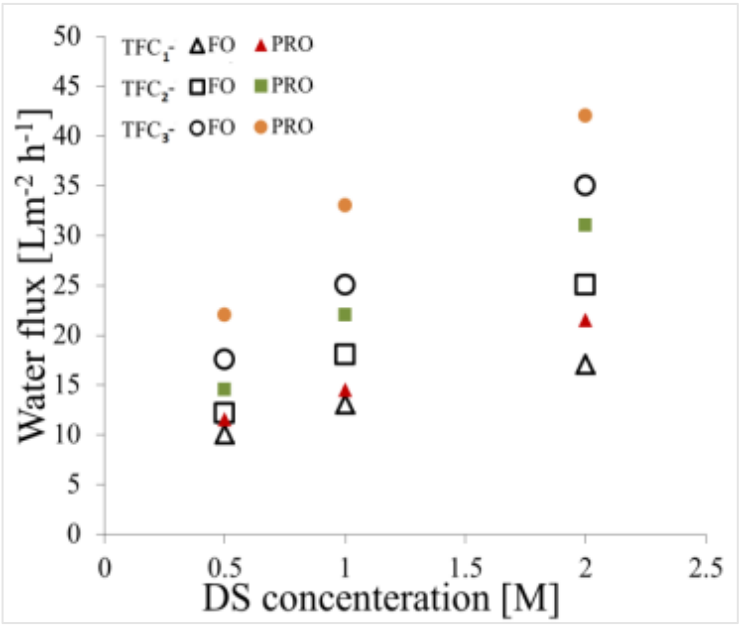

(a)

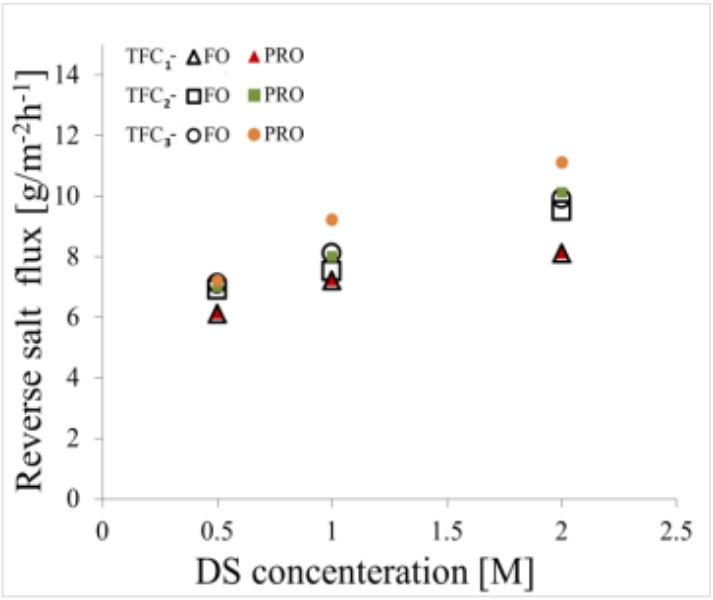

(b)

Figure 5.6: Performance comparison of fabricated membranes in terms of water flux and reverse solute flux under FO and PRO with various NaCl concentrations as DS and DI water as feed. (a) performance of membrane samples in terms of water flux, (b) performance of membrane samples in terms of reverse solute flux. (TFC_1 contains 0 wt % sulphonated material in the membrane substrate while TFC_2 and TFC_3 have 25 wt % and 50 wt % sulphonated material in the membrane substrates respectively).

As shown in Figure 5.6 (a), the water flux performances of the TFC FO membrane improve significantly by sulphonation with higher performances at higher degree of sulphonation. Table 5.5 shows the summary of water fluxes using 2 M NaCl as DS and DI water as FS under two different modes of membrane orientations. For example, the water flux of the TFC_3 FO membrane at 2 M NaCl was 35.1 $Lm^{-2}h^{-1}$ compared to 25 $Lm^{-2}h^{-1}$for TFC_2 and 17.12 $Lm^{-2}h^{-1}$ for TFC_1. These results clearly show the benefits of sulphonation of the PES substrate on FO water flux. Similar improvement in water flux for the sulphonated TFC membranes were also observed under the PRO mode of membrane orientation. For example, the water flux for TFC_1 FO membrane at 2 M NaCl DS and DI as FS under the PRO mode was 21.5 $Lm^{-2}h^{-1}$ which increased to 31.0 $Lm^{-2}h^{-1}$ and 42.1 $Lm^{-2}h^{-1}$for TFC_2 and TFC_3, respectively. These water fluxes under the PRO mode of membrane orientation are only about 20% – 26% higher than water fluxes under the FO mode of membrane orientation. This is slightly lower than significant differences in the water fluxes observed between FO and PRO modes of membrane orientation with PRO mode generally producing twice or more water fluxes compared to under FO modes of membrane orientations with the PA based TFC FO membranes (Phuntsho. et al. 2013). This lower water flux differences between the FO and PRO modes of membrane orientation indicates that, the extent of dilutive ICP during the FO mode is not very significant probably further supporting the positive influence of substrate sulphonation. However, as pointed out earlier, although sulphonation increases the water flux by improving its substrate structure and hydrophilicity however, the mechanical strength (tensile strength) of TFC membrane decreases with the increase in the degree of sulphonation (Table 5.3).

Table 5.5: Performance of fabricated TFC-FO membrane using 2 M NaCl as DS and DI as FS under FO and PRO mode.

Membrane ID	FO mode			PRO mode		
	Water flux	RSF(g $m^{-2}h^{-1}$)	SRSF (gL^{-1})	Water flux	RSF(g $m^{-2}h^{-1}$)	SRSF (gL^{-1})
TFC_1	17	7.5	0.44	21.5	8.1	0.37
TFC_2	25	9.5	0.38	31	10	0.32
TFC_3	35.1	9.9	0.28	`42.1	11.1	0.26

Based on the water flux performances under the FO and PRO modes of membrane orientations presented in Figure 5.6 and Table 5.5, it is clear that, substrate sulphonation can significantly help improve the performances of the TFC FO membranes in terms of water flux. This increase in water flux is due to two main reasons: change in the membrane support morphology and the improvement in its hydrophilic property however, a closer observation on the membrane cross section morphologies for the three TFC FO membrane samples reveals interesting points. TFC_3 membrane possesses a denser sponge-like support layer structure compared to finger-like support structures for TFC_2 and TFC_1 and yet TFC_3 resulted in the best performance in terms of water flux. This result therefore indicates that, the performances of the FO membranes can be improved by not only having a finger-like membrane substrate structure morphology but also by improving the hydrophilicity of the sponge-like membrane substrate such as through optimum sulphonation. The main advantage of the sponge-like substrate compared to the finger-like substrate could be in the form of better resistance to membrane compaction during the

operations such as in the pressure retarded osmosis for power generation and pressure assisted osmosis.

Reverse solute flux (RSF) is another important performance parameter for assessing the performance of the FO membranes. It measures the extent of draw solute that reversely diffuses through the FO membrane during the osmotic process. A high RSF of the FO membrane may have significant implications on the loss of draw solutes towards the feed water complicating the concentrate management, membrane fouling/scaling and water flux performance. Figure 5.6 (b) and Table 5.5 show the RSF of three fabricated TFC FO membrane samples under the FO and PRO modes of membrane orientations. Although the water flux increases with the increase in the degree of membrane substrate sulphonation however, this also correspondingly increased the RSF of the TFC FO membranes. For example, the RSF of the TFC_1 membrane (at 2 M NaCl as DS and DI as FS under FO mode) was 7.5 g $m^{-2}h^{-1}$ which then increased to 9.5 g $m^{-2}h^{-1}$ and 9.9 g $m^{-2}h^{-1}$ with sulphonation for TFC_2 and TFC_3, respectively. Likewise under the PRO mode of membrane orientation using similar DS-FS condition, the RSF for the TFC_1 membrane sample was 8.1 g $m^{-2}h^{-1}$ which increased to 10 g $m^{-2}h^{-1}$ and 11.1 g $m^{-2}h^{-1}$ for TFC_2 and TFC_3 FO membranes, respectively. Although the RSF under the PRO mode of membrane orientation is higher than under the FO mode however, the ratio of RSF generally termed as the specific RSF (SRSF) is fairly constant irrespective of the membrane orientations of the DS concentrations. However, the SRSF remained fairly similar (0.25 – 0.45 gL^{-1}) for both the un-sulphonated and sulphonated TFC FO membranes. Table 5.6 presents the comparative performances of three fabricated TFC FO membranes in this study with other works reported in the literature. It is clear from these

comparative data that, sulphonated TFC FO membrane fabricated in this study has comparable performance in terms of water flux and SRSF.

Table 5.6: Performance comparison of flat sheet TFC-FO membranes in FO mode of operation.

Membrane types	Materials	Water flux ($Lm^{-2}h^{-1}$)	Specific reverse salt flux (gL^{-1})	DS (M) NaCl	FS	References
SPES TFC-FO	PES	18/25	0.4/ 0.32	1/2	DI	Present work
SPES TFC-FO	PES	26/35	0.36/0.28	1/2	DI	Present work
TFC flat-sheet (HTI)	Psf	13	0.81	2	DI	(Phillip et al. 2010)
TFC flat-sheet membrane	Psf	12	0.4	1	---	(Wei et al. 2011a)
TFC flat-sheet membrane	Psf	20.5	--	1	DI	(Tiraferri et al. 2011a)
TFC flat-sheet membrane	Psf	15.1	-	1	DI	(Yip et al. 2010)
SPSf TFC FO	Psf	26	0.3	2	DI	(Wang et al. 2012a)
SPSf TFC FO	Psf	18	0.2	1	DI	(Wang et al. 2012a)

5.4 **Concluding remarks**

The effect of sulphonation on the PES substrate to synthesise TFC-FO membranes was studied through substrate characterisation such as morphology, tensile strength and TFC membrane performances. The following summary is drawn from this work:

- Sulphonation of PES substrate resulted in significant influence on the substrate morphology by changing the substrate morphology from finger-like to more sponge-like substrate at higher degree of sulphonation, increase in substrate hydrophilic property, improvement in membrane permeability coefficient (*A* value) and decrease in membrane structural parameter (*S* value)

and tensile strength although it resulted in increased salt permeability (B value) and salt rejection.

- The performances of the TFC-FO membranes in terms of water flux and specific reverse solute flux increased with the increase in the degree of sulphonation. The TFC FO membrane at 50 wt % sulphonation showed the best performance with water fluxes of 35.1 L $m^{-2}h^{-1}$ (FO mode) and 42.1 L $m^{-2}h^{-1}$ (PRO mode) using 2 M NaCl as DS and DI water as FS compared to 17.0 L $m^{-2}h^{-1}$ (FO mode) and 21.5 L $m^{-2}h^{-1}$ (PRO mode) for un-sulphonated TFC FO membrane under the same operating conditions.

Chapter 6

THIN-FILM COMPOSITE MEMBRANE SUPPORTED ON A COMPACTED WOVEN FABRIC MESH SUPPORT FOR PRESSURE ASSISTED OSMOSIS

6.1 **Introduction**

Forward Osmosis (FO) has drawn significant research attention as an alternative membrane process for desalination, osmotic energy generation and treating impaired water sources (Achilli et al. 2009; Holloway et al. 2007; Phuntsho. et al. 2012; Zhao et al. 2012). Unlike pressure based membrane processes such as RO and NF, FO utilises osmotic pressure generated by Draw Solution (DS) as a driving force to transfer water across a semipermeable membrane without applying hydraulic pressure (Chung et al. 2012). However, since the FO process is based on concentration difference, the water flux decrease is due to the continuous decline in the DS concentration during the process (Ge et al. 2013; McCutcheon et al. 2006; Zhao et al. 2012). Furthermore, the water flux is also limited due to other factors such as concentration polarisation (CP) phenomena that occur on both sides of the membrane (Gray et al. 2006; Phuntsho. et al. 2013). CP is particularly more significant when it occurs within the support layer of the asymmetric polymer membrane where the hydrodynamic mixing cannot be provided during the FO process and is known as ICP. ICP can substantially impact the net osmotic pressure ($\Delta\pi$), which is the main driving force in the FO process, and hence, the transfer of water across the membrane in the FO process. Water flux occurs until the osmotic pressure of the DS attains equilibrium with the Feed Solution (FS) (Achilli et al. 2009; Garcia-Castello et al. 2009). Extensive design modification efforts have been made to optimize the operating factors and the membrane materials in order to reduce the limiting factors, particularly the ICP hindrance. However, the ICP and appropriate membrane remain major issues in the FO process (Gray et al. 2006).

Recently, a few studies on the combined processes of applied hydraulic pressure and osmosis have reported attempts to exploit the synergies of the two processes in a single stage to overcome low flux in the FO process (Blandin et al. 2013; Coday et al. 2013; Yun et al. 2013b). The concept of Pressure Assisted Osmosis (PAO) is applied in an expanding FO process application. In this process, pressure is applied to the feed side to enhance the water flux albeit at a lower energy cost (Yun et al. 2013b). Previous work has demonstrated that applied hydraulic pressure can increase the FO performance (Oh et al. 2014; Yun et al. 2013b); however, performance also depends on the FO membranes properties such as type, structure and materials (Coday et al. 2013).

To date, most of the published papers have used cellulose triacetate with embedded polyester support screen membrane (CTA-ES) from HTI to investigate the process (Oh et al. 2014; Yun et al. 2013b). Low water flux is common in the CTA membranes. Furthermore, only recently, HTI has designed and produced a large scale, new thin film composite membrane with embedded polyester screen support (TFC-ES). However, these membranes are still largely unavailable to researchers. Therefore most of the PAO process has been validated using the CTA-ES membrane from the HTI (Coday et al. 2013; Yun et al. 2013b). One exception is a study by Coday et al. in which TFC-ES from HTI has been used in addition to the CTA membrane (Coday et al. 2013). Based on the HTI operating limits and guideline (OLG) sheet for supplied membrane kits and casting procedures for the FO membrane on a large scale (described in US Patent 7,445,712 B2), the TFC membrane for FO seems to have been fabricated in a similar way to that of the CTA-FO membrane (Herron 2008). The polymer solution is casted on a roll which is followed by pulling the fabric from the top to embed it in the casted polymer

solution. This unique fabrication method for the FO membrane confines the polymer penetration to the back of the porous fabric support and prevents the formation of air bubbles as explained in the patent (Herron 2008). However, the commercial scale solution of embedding the woven polyester mesh on the roll is generally difficult at a lab scale level using manual casting knife and flat glass plate.

The FO membrane can be made with or without any backing fabric support. Nevertheless, the membrane needs adequate mechanical strength to perform sustainably under certain hydraulic pressure. Most recent efforts for fabricating high performance membrane have been devoted to modifying the structural morphology and chemical properties of the polymeric support to enhance the membrane performance. A thin film composite FO membrane fabricated under lab conditions is not effective in the PAO process due to the likely compaction of the polymeric membrane substrate and lack of backing fabric support (Wang et al. 2012a; Widjojo et al. 2011). Although most of the new FO membranes have reported enhanced water flux and salt rejection properties compared to the CTA membrane but they have low tensile strength**,** particularly for the PAO process (Wang et al. 2012a; Widjojo et al. 2011). Furthermore, even the commercial TFC-FO membrane with finger like morphology supported by PET nonwoven backing fabric may not be effective for the PAO process due to the likely compaction of substrate which could lead to crack and defect points on the membrane surface and rejection layer. Thus, the membrane substrate with finger-like structures may not be appropriate when subjected to applied hydraulic pressure in the PAO process.

Few studies have reported the successful reinforcement of the FO substrate with backing fabric support (highly porous non-woven PET) (Tiraferri et al. 2011b; Yu et

al. 2011). However, following their protocols, producing large pieces of defect and wrinkle free membrane substrate by using a highly porous nonwoven fabric support was challenging due to polymer penetration and wrinkle formation. R.Mc Ginnis, and G. Mcguregan (Herron 2008; McGinnis & McGurgan 2013) have used bilayer backing fabric to make the support layer sturdier and thicker. The use of bilayer backing fabric can block the polymer solution from penetrating the backing layer and limit the appearance of wrinkles and defect points. Furthermore, in the commercial scale membrane fabrication additional strategies in machine design such as optical alignment are considered in order to prevent the creasing and folding over of the membrane (McGinnis & McGurgan 2013). This strategy is very challenging in terms of duplicating FO membranes fabrication supported by backing fabric under lab conditions.

Understanding how the applied pressure influences the membrane and the performance in PAO is crucial for the development of a suitable membrane for the PAO processes. Considering the nature of the PAO process, such a membrane would have intermediate characteristics between RO and FO membranes suitable under both the FO and RO modes of operation. Like the FO membrane, an ideal PAO membrane should possess high water flux, low solute flux and good chemical stability. This is in addition to mechanical strength which is indispensable for this pressurised process.

The present work is therefore aimed at solving the above problems by incorporating woven mesh fabric into the substrate to reinforce and produce a wrinkle and defect free TFC membrane for the PAO process. The compacted woven polyester mesh fabrics may reduce wrinkle formation since it is relatively impervious to the polymer

solution. Furthermore, this study has systematically investigated the possible solutions for embedding woven mesh fabric to the membrane polymeric support by applying lab scale and commercial scale FO membrane fabrication methods to produce a defect free membrane. The morphologies and physical characteristics of the resultant TFC membranes were investigated and compared to commercial CTA-ES, WJ-FO and WJ-RO membranes to illustrate the potential of the fabricated membrane for the PAO process and the relative importance of the backing fabric support properties and membrane support structure.

6.2 Materials and Methods

6.2.1 Chemicals and membrane materials

Polyethersulfone (PES) granules (Mn: 55,000 - Good fellow, UK) and Polyester mesh woven fabric (PETEX 07-11/5, 07-40/25, SEFAR Pty. Ltd, Australia) were used for preparing the membrane substrates. 1-methyl-2-pyrrolidinone (NMP, anhydrous, 99.5%) andPolyethylene glycol (PEG, MW 400) (Sigma–Aldrich Pty. Ltd, Australia) were used in the casting solution. Chemicals used for interfacial polymerization included m-phenylenediamine (MPD,>99%), 1,3,5-benzene tricarbonyl trichloride (TMC, 98%) and n-hexane (Sigma–Aldrich Pty. Ltd, Australia). CTA FO membranes were obtained from HTI (Albany, OR) and the FO and RO membranes from Woongjin Chemicals, Korea were used for comparison and validation purposes.

6.2.2 **Synthesis of flat-sheet TFC PAO membranes**

6.2.2.1 **Polymer concentration and additives rate**

In this study, the PES polymer concentration for fabricated TFC membranes ranged from 12-18%. At a higher polymer concentration, pore former agents such as $LiCl_3$ or other additives like PEG are necessary to make the membrane more permeable (Qiu et al. 2012b; Tang et al. 2014; Wang et al. 2012a). In this study, the optimum level of PEG as an additive was 10-20 wt %. The casting solution component for five types of fabricated TFC membranes (denoted T_1 to T_5) and their preparation conditions are summarized in Table 6.1.

Table 6.1: Synthesis conditions for TFC PAO membranes.

Membrane ID	Open area (%)	Substrate layer via phase inversion			Fabrication methods
		PES (Wt.%)	NMP (Wt.%)	PEG (Wt.%)	
T_1	5	18	72	10	M_1
T_2	5	18	62	20	M_1
T_3	5	12	88	--	M_1
T_4	25	18	72	10	M_2
T_5	25	18	72	10	M_1

***Note**: Woven polyester mesh fabric for all fabricated samples was 60 μm in thickness

6.2.2.2 **Fabrication methods**

Figure 6.1 demonstrates the two fabrication methods on the roll (rotating drum) used for the fabricating of the RO and FO membranes at a commercial scale. Method 1 (M_1) is used for casting the RO membrane using a thick non-woven fabric support with highly viscose solution containing a high polymer concentration. In this method, the non-woven backing fabric support is firstly placed on the roll and then the

polymer solution is poured on the top of the thick nonwoven fabric and cast by a casting knife on top of the roll (Herron 2008; Tiraferri et al. 2011b). Due to thick non-woven fabric and the viscose polymer solution used in the RO membrane, polymer penetration to the back of the fabric is limited. The whole structure is then immersed in the water bath for the initiating phase inversion. Similar method but on a glass plate instead of a rotating drum is used for the casting of T_1,T_2,T_3 and T_5 samples illustrated in the Table 6.1. However, the fabrication procedure for the FO membrane at the commercial scale follows the casting method 2 (M_2) as depicted at Figure 6.1. In this method, the polymer solution is firstly, poured onto a rotating drum and then; the polymer solution is casted through a casting knife on the roll followed by pulling the woven or nonwoven fabric into the casted polymer solution from the top so that the backing fabric is fully embedded (Herron 2008). The whole structure is immersed in a water bath to initiate phase inversion. This method is used for casting the T_4 sample. The fabrication method 1 (RO style) and method 2 (FO style) are investigated to fabricate a defect and wrinkle free TFC membrane for the PAO process using woven mesh fabric on the glass plate instead of the rotating drum.

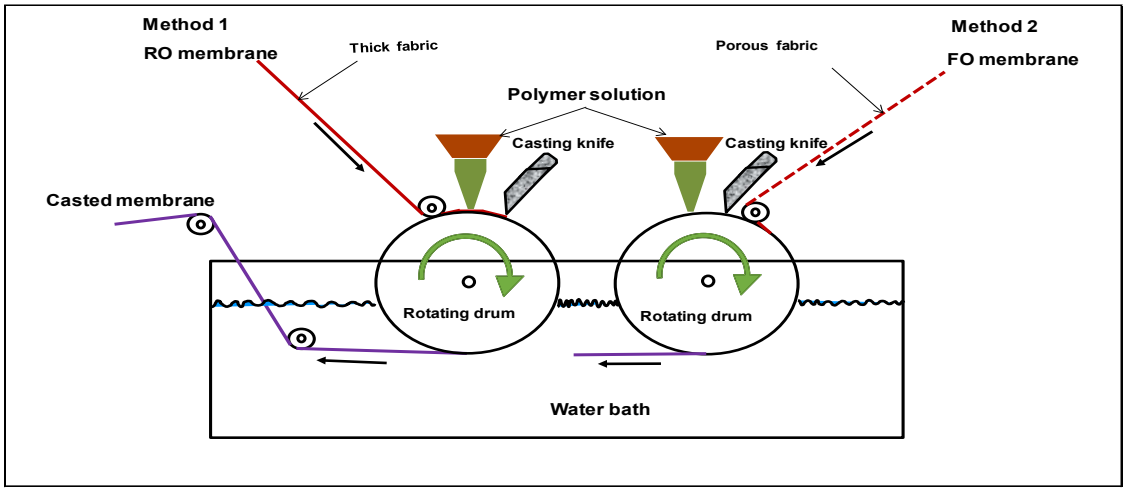

Figure 6.1: Schematic of RO and FO membrane fabrication methods in commercial scale. Modified from (Herron 2008).

6.2.2.3 **Casting polymer solution on woven polyester mesh fabric support**

The choices of backing fabric support for the fabricated samples (T_1-T_5) are presented in Table 6.1. The flat sheet TFC substrates are fabricated on woven polyester mesh over two stages. First, the casting of a membrane polymer support layer embedded on woven fabric mesh through a phase inversion stage is followed by a second stage; the formation of a polyamide (PA) thin selective layer through interfacial polymerization.

For the first stage, casting solutions are prepared by applying a certain amount of PES and PEG as a pore former (Table 6.1). Polyethersulfone (PES) is dissolved in NMP and PEG then stirred by magnetic stirrers at 60 ◦C for 24 hours. The polymer dopes are then degassed using digital bench top ultrasonic cleaners (Soniclean Pty Ltd, Australia) for 60 min and stored in a desiccator for at least 48 hours before casting. To prepare the membrane support (samples T_1-T_3), the woven polyester mesh with a 5 % open area is placed on top of a flat glass plate, and then the fabric is treated with NPM (except T_3). Thereafter the fabric is dried carefully by an air knife

to remove the excess NPM. Casting is performed on a glass plate using a stainless steel film applicator (Sheen Instruments Ltd, UK) with an adjustable gate height fixed at 200 μm (~8 mils). The casted substrate is immersed immediately into a precipitation bath that contains DI water at room temperature to initiate phase inversion and remains in the bath for at least 10 minutes. The resultant substrate is stored in DI water before undertaking the next stage which is the formation of an active rejection layer. All samples (T_1, T_2, T_3, T_5) in this study are fabricated through this casting method (M_1- RO style) except the T_4 sample which is fabricated through the casting method (M_2 - FO style).

6.2.2.4 **Formation of a polyamide rejection layer**

The rejection layer of TFC membranes is formed by interfacial polymerization on the top surface of the hand-cast PES film embedded with polyester woven fabric mesh. The substrate is soaked in a solution of 3.4% wt aqueous MPD solution for 2 minutes and then the excessive MPD solution on the substrate surface is removed using an air knife. Next, the membrane substrate is placed in a frame that is sealed around the corners and bottom but is open on the top side, allowing the TMC solution to react with the top surface of the MPD saturated substrate membrane where the active layer is needed. N-hexane solution of 0.15 wt% TMC is gently poured onto the substrate and this is allowed to react with the membrane top surface for 60 sec to form an ultra-thin PA rejection layer. This protocol was used for all fabricated samples. The resultant TFC composite membranes are rinsed with DI water to remove the residual solution and are then stored in DI water at 4 ◦C before characterization.

6.2.3 **Membrane characterization**

6.2.3.1 **Characterization of membrane morphology, contact angle, porosity and tensile strength**

Membrane cross-sections and surface morphologies are examined using a high-resolution Schottky Field Emission Scanning Electron Microscope (SEM, Zeiss Supra 55VP, Carl Zies AG, Germany). First, membrane samples are dried in a vacuum at room temperature for 24 h. To view the cross sections of the membranes, samples are then flash-frozen in liquid nitrogen to preserve the pore structure. Woven fabric mesh support stiffness makes it difficult for a decent cut thus a sharp razor blade is used. All samples are sputter coated with thin layer of carbon before SEM imaging using Balzers Sputter coater (SCD 050, BAL-TEC, Germany) which is operated at the 10-15 Kv applied voltage.

The contact angles of the membranes are measured with the sessile drop method, using an Optical Tensiometer (Attension Theta Lite 100, Biolin Scientific, Finland). Membrane samples are dried in a vacuum at room temperature for 24 h. Small deionized water droplets (5-7μL) are applied onto a levelled membrane surface and profiles of the water drops are captured by a camera and the imaging software to determine the contact angles. At least 3 measurements are obtained to get the average value.

Membrane thicknesses are measured using a digital micrometre (293-330 Mitutoyo, Japan). Membrane porosity (ε) is obtained by measuring the dry mass (W_2) and wet mass (W_1) of the membrane samples and calculated based on the following equation (Sukitpaneenit & Chung 2009) :

$$\varepsilon = \frac{(W1-W2)/\rho i}{\left[\frac{W1-W2}{\rho i}\right],+[W2/\rho m]} \times 100\% \quad (1)$$

Where ρi and ρm are the density of the wetting solvent (Isopropanol ethanol in the current study) and membrane, respectively. Tensile strength is evaluated using an Instron bench-type tensile test machine (LR5K Plus). The maximum load limit is 100 N according to ASTM D882-10 while the crosshead speed is adjusted to 5 mm/min. At least five dog-bone-shaped specimens for each fabricated membrane sample are tested, and the average of these is used as the tensile property for each sample.

6.2.3.2 **Measurement of pure water permeability and rejection properties**

Pure water permeability of TFC membranes are measured in the same cross-flow filtration setup used in the PAO test, in the RO testing mode. Pure water permeability coefficient (A) is evaluated at an applied pressure range of 1–10 bar with DI water as a feed. The A value is calculated according to the following equation:

$$\mathrm{A} = \frac{\mathrm{Jw}}{\Delta \mathrm{p}} \tag{2}$$

Where Δp is the applied pressure and Jw is the permeate water flux. The pure water permeability of the embedded substrate was also determined through Equation (2). Sodium chloride rejection and salt permeability, B value of a membrane is measured in the PAO setup under the RO mode at 1–10 bar, using 10 g/L NaCl solution as feed. For all tests conducted in the RO mode a diamond patterned feed spacer was used. Rejection is determined based on conductivity measurement (Ultra Meter IITM 4P, Myron L Company, CA) of the feed and permeate by the following equation.

$$R = \frac{Cf - Cp}{Cf} \times 100\% \tag{3}$$

where C_f and C_p are the salt concentrations in the feed and the permeate, respectively.

The salt permeability B value of a membrane is calculated according to the following equation (Lee et al. 1981b):

$$B = \frac{A(1-R)(\Delta p - \Delta \pi)}{R} \quad (4)$$

Where ΔP is the applied pressure and R is the salt rejection of the membrane during the rejection test in the RO mode, Δπ is the osmotic pressure difference across the membrane.

6.2.3.3 Determining the membrane structural parameter

S value is one of the critical properties of the TFC-PAO membranes given by the following relationship that depends on the support layer thickness (t) and tortuosity (τ) and its porosity (ε):

$$S = \frac{t\tau}{\varepsilon} \quad (5)$$

In the experimental tests, the membrane effective structural parameter can be determined using the empirical equation. Based on the classical ICP model developed by Loeb et al. (Loeb et al. 1997), the water flux can be calculated by the following equations in the FO process:

$$J_w = \frac{D}{S}\left[ln\frac{A\pi_{D,b}+B}{A\pi_{F,b}+Jw+B}\right] \quad (6)$$

Where D is the bulk diffusion coefficient of the draw solute, B is the salt permeability coefficient of the membrane active layer, and $\pi_{F,b}$ and $\pi_{D,b}$ are the bulk osmotic pressures of the FS and DS respectively. Based on equation 6, the membrane support structural parameter is determined using the following equation:

$$S = \left(\frac{Ds}{J_w}\right) ln\frac{A\pi_{D,b}+B}{A\pi_{F,b}+J_w+B} \quad (7)$$

6.2.3.4 **Membrane tests in PAO process**

Membrane tests in the PAO process are carried out in FO/PAO cell similar to the cell used in our previous work (Sahebi et al.). Two variable-speed gear pumps are used to supply the feed and draw solutions respectively. Each pump is connected to the cross flow membrane cell with channel dimensions of 2.6 cm width, 7.7 cm length and 0.3 cm depth on both sides of the membrane. The volumetric flow rates of both sides are 400 mL/min. All PAO experiments are performed under FO mode configurations: active layer facing FS (AL-FS) at 25 °C in which the pressure was applied on the feed. The active layer facing DS (AL-DS) (PRO mode) orientation is ignored because of possible damage to the active layer of the membrane as a result of a rejection layer collision with the spacer in the PRO mode. The channel on the DS side of the membrane cell is filled with 6 layers of diamond shaped polystyrene spacers to prevent membrane deformation and damage due to applied hydraulic pressure on the feed side. Concentrated NaCl solutions (0.11, 0.5, 1 and 2.0 M) are used as draw solutions. The feed solution contains 10 g/L NaCl and DI water. The water flux *Jw* is determined by measuring the changes in the volume of the DS tank connected to a digital mass balance data logging system and a PC. A pressure pump is used for the feed solution side and the applied hydraulic pressure is adjusted manually using the pressure valve. The applied pressure on the feed varies between 0 and 10 bars; the maximum pressure rating for the pump is only up to 11 bars. The reverse diffusion of the draw solutes is evaluated by observing the electrical conductivity (EC) using a multimeter (CP-500L, ISTEK, Korea) when DI is used as feed. In this study, to validate the derived water flux produced by the fabricated TFC-PAO membrane, a commercial cellulose triacetate (CTA-ES) FO membrane (Hydration Technology Inc., Albany, OR) and a TFC-FO/TFC-RO from Woongjin

Chemicals is tested under the PAO mode of different ranges of applied hydraulic pressure. The thermodynamic properties of the solutions such as osmotic pressure, viscosity, diffusion coefficient, density, etc. are analysed using thermodynamic modelling software OLI Stream Analyser 3.2 (OLI Systems Inc., Morris Plains, NJ, US).

6.3 Results and discussion

In these sections, a systematic analysis of a fabricated wrinkle free TFC membrane for the PAO process will be presented. Fabrication methods and backing fabric support properties affect membrane formation and the appearance of wrinkle and defect points. Consequently, they affect interfacial polymerization. Understanding these fundamentals provides a basis for the rational selection of a backing fabric support and fabrication method in order to effectively embed the backing fabric support to produce a wrinkle and defect free TFC membrane for the PAO or FO process under the lab conditions. For a better membrane performance comparison under the PAO process, fabricated samples have been compared to commercially available FO and RO membranes.

6.3.1 Membrane substrate layer

6.3.1.1 Role of polymer concentration, backing fabric properties and casting method on membrane support structure formation

Polymer solution concentration and viscosity can affect the casting of membrane support layer particularly when it is embedded with backing fabrics. Low polymer concentration forms dilute polymer dope that can penetrate to the back of the fabric support during membrane casting (Lee et al. 1981b; S. et al. 2012; Wang et al. 2012a), which can cause seve\ral problems including creases, wrinkles and defect

points. Furthermore, low polymer concentration rate plus additives has a significant effect on membrane permeability and desirable for FO membranes (McGinnis & McGurgan 2013).

Lower polymer concentrations have been used to fabricate finger like structures to minimize the impact of ICP and the support layer on diffusion in the FO membrane as evidenced by previous studies (S. et al. 2012; Tang et al. 2014; Tiraferri et al. 2011b). Membrane performance in terms of water flux has an inverse relationship with polymer concentration (McGinnis & McGurgan 2013). However, in the PAO process due to the required applied hydraulic pressure, membranes need to be denser to prevent rupture and compaction during the process. Therefore, higher polymer concentration is required to produce a membrane free of a finger like structure. However, to maintain permeability, PEG is used as a pore former in a higher polymer concentration for our fabricated TFC membranes (Table 6.1).

The support layer of the FO membrane is typically polymeric micro porous support membranes, which may (or may not) be supported by a non-woven or woven backing fabric. In the PAO membranes since higher mechanical strength is essential, a structural supports by backing fabric is necessary due to withstand hydraulic pressure required in the PAO process. A comprehensive explanation of the casting procedure for fabricating FO membranes supported by backing fabric on a commercial scale is described in the HTI patent (Herron 2008) which is similar to the fabrication method (M_2) presented in Figure 6.1. This method has been chosen in commercial scale in order to prevent the polymer solution penetration through the backing woven mesh fabric in the CTA-FO membrane which otherwise leads to defect points across the FO membrane substrate due to trapped air bubbles.

Figure 6.2 (a) shows the images of the T_5 sample on woven mesh fabric with a 25 % open area as compared to Figure 6.2 (b), a membrane film without backing fabric. As evident, regular backing fabric for casting a membrane has a severe effect on membrane support during phase inversion which causes very unsmooth surface. The membrane film without backing fabric support is smooth and free of wrinkles and defect points while wrinkle and defect points appeared for the membrane sample casted with the same polymer solution on woven fabric with a regular opening mesh. Figure 6.2 (c) shows the same images of the T_5 sample and is compared with the Figure 6.2 (d), the T_1 (T_2 and T_3 had a similar appearance) membrane sample using compacted woven mesh fabric with a 5 % open area. A similar fabrication protocol but different backing fabric supports in terms of open area was used. Casting solution, casting method (M1), and fabric thickness (60 μm) were the same but the woven mesh fabric had a 25% open area for Figure 6.2 (c) while it was 5% in Figure 6.2 (d) (Table 6.1). This can indicate the effect of the backing fabric properties in terms of the open area and mesh opening on the membrane support layer formation during phase inversion. This has been confirmed during our observation when the polymer solution is casted on fabrics with 1%, 5%, 10%, 25% and 50% open areas. Membrane support casted on a woven mesh fabrics with a smaller open area (1%, 5%) was wrinkle free due to limited polymer solution penetration while on fabrics with a bigger open area (10%, 25%), severe wrinkles appeared.

Figure 6.2: Picture and SEM images of membranes substrate displaying (a) T_5 sample on backing fabric support casted through method 1 and (b) substrate caste without backing fabric (Both (a, b) fabricated from 18 wt % PES in 72 % NMP and 10% PEG solvent). Picture and SEM images of membranes substrate displaying (c) T_5 sample cast on woven polyester mesh with 25% precent open area and (d) T_1 sample cast on compacted woven polyester mesh with 5% precent open area (Both (c, d) fabricated from 18 wt % PES in 72 % NMP and 10% PEG solvent and casting method (1)).

In this study, woven mesh backing fabric used for the T_1-T_3 membrane samples were different from the T_4, T_5 samples in terms of open area percentage but all have a similar thickness of 60 µm (Table 6.1). Firstly, attempts to fabricate the TFC membrane with regular woven mesh backing fabric (25% open area) for T_4, T_5 samples using both casting methods will be explained. Both fabrication methods (M_2) and (M_1) were used to fabricate T_4 and T_5 samples respectively. T_5 sample was fabricated through casting method (M_1) which is similar to the T_1-T_3 samples (Table 6.1). Due to a large open area (25%) in the backing fabric, penetration occurred even at very high levels of polymer concentration (higher viscosity) for T_5 sample. However, it could not be utilized for our PAO process due to complete penetration that caused wrinkles. Furthermore, trapped air bubbles led to the formation of air pockets and defect points at the membrane surface. However, these membrane

samples were tested in a smaller FO unit which only required a smaller membrane area (3 cm^2) while for the PAO unit at least 21 cm^2 of defect free TFC membrane required.

The T_4 sample was fabricated using a similar procedure presented at the commercial scale (M_2) to resolve the penetration problem and validation of the FO membrane fabrication method on a large scale. Instead of a rotating drum, a flat glass plate was used. The casting method is similar to the commercial FO membrane fabrication on the roll and a few previous research works (Herron 2008; Qiu et al. 2012b). The fabricated T_4 membrane sample was wrinkle free and appeared to be a defect free membrane; however, samples could not be utilized for interfacial polymerisation due to membrane skin layer properties as this will be discussed later under the characterization section 3.2. Therefore from findings on T_5 sample, in this study, backing fabric with 5% was chosen to obtain a wrinkle free membrane and from findings on T_4 sample, casting method (M_1) was chosen which is suitable for interfacial polymerisation under lab condition.

Previous studies have used different strategies to mitigate the impact of polymer solution penetration for FO membrane fabrication supported by backing fabric. For example, choosing unique fabrication method (Herron 2008), or a double layer backing fabric to confront the polymer penetration challenge (McGinnis & McGurgan 2013). However, in this study, TFC membrane for the PAO process (T_1, T_2) and T_3 developed on a distinguished woven fabric mesh support that not only improved the membrane mechanical strength but limited the polymer penetration and prevent wrinkle formation on the membrane substrate. However, despite the compacted appearance (Figures 6.2 (c) and (d)) and low fabric open rate (5%), it has

shown high water permeability of 1554 $L/m^2 h^{-1}$ bar due to overlapped fabric knitting instead of tangled knitting. Thus, this specific fabric dose not hinders water passage significantly.

6.3.1.2 **Characterization of membrane substrates layer**

Five TFC membranes were fabricated in this study. In order to better understand and compare the role of support structures on the structural parameter S (the current section) and the PAO performance (Section 3.3) in our TFC (T_1-T_3), tow commercial FO membranes (CTA-ES, WJ-FO) plus WJ- RO membrane were also characterized. Regarding polymer penetration to the fabric in addition to casting solution concentration and backing fabric properties, there are other factors to consider. For instance, fabric pre-treatment by NMP can facilitate penetration by diluting the casted polymer solution through residual NMP close to the fabric thread. All fabricated membranes on the woven fabric mesh were pre-treated with NMP prior to the casting except the T_3 sample. In addition to compatibility, this allows slight penetration of the casting solution into the backing layer, without allowing complete "strike through". This also prevents the detachment of PES support layer from the backing fabric in cases where the compacted fabric is used for T_1 and T_2 samples.

Figures 6.3 (b), 6.4 (b), and 6.5 (b) show the bottom surface of membrane samples fabricated through casting method (M_1) for T_1, T_2, T_3 respectively. Figures 6.3 (b), 6.4 (b) show a slight penetration in T_1 and T_2 samples. Although their polymer concentration was higher than T_3 sample, the fabric pre-treatment with NMP caused a slight penetration due to residual NMP around the fabric filament. NMP pre-treatment can help join the backing fabric to the PES substrate in order to prevent

membrane film detachment from the support backing fabric. Furthermore, residual NMP on the fabric from the pre-treatment can dilute the polymer solution a few micrometres near the bottom of the substrate close to the fabric filament. Subsequently, the bottom can become more porous and less ICP may occur at the bottom surface. Sub-micrometre pores were observed for both T_1, T_2 substrates along with big pores where cast polymer did not cover the bottom surface, although the pores for both substrates appeared to be similar. Figure 6.5 (b) also shows the T_3 sample, casted with a dilute polymer of 12% without any fabric pre-treatment. As a result, a finger like structure morphology forms but it has only slightly penetrated to the woven mesh fabric due to lack of fabric pre-treatment with NMP. However, for the T_3 sample with NMP pre-treated backing fabric, casting was not successful (result not shown). Due to the low polymer dope used for T_3 sample (Table 6.1), residual NMP from the pre-treatment causes a further dilution of the polymer dope in a few micrometres around the fabric filament and facilitates the penetration. This indicates that complete penetration of the polymer solution is closely related to polymer solution viscosity in addition to fabric physical properties.

Figure 6.6 shows the cross section, top and bottom membrane surface of the T_4 sample casted through casting method (M_2), FO style in commercial scale. A unique fabrication method made it possible, firstly to eliminate membrane wrinkle and defect points that can be detected by the naked eyes and secondly to reduce the thickness of the substrate to even less than 100 μm. M_2 is a unique FO membrane manufacturing method in a large scale which is compactable by incorporating backing fabric support and low polymer solution concentration. Thus, the polymer penetration through the back of the fabric due to dilute polymer solution and open mesh fabric can be avoided (Herron 2008). However, as Figure 6.6 shows the SEM

images of bottom and top surface of the T_4 sample using casting method (M_2) under lab condition had a severe effect on membrane top and bottom surface morphology and pore size which probably make it unsuitable for interfacial polymerisation.

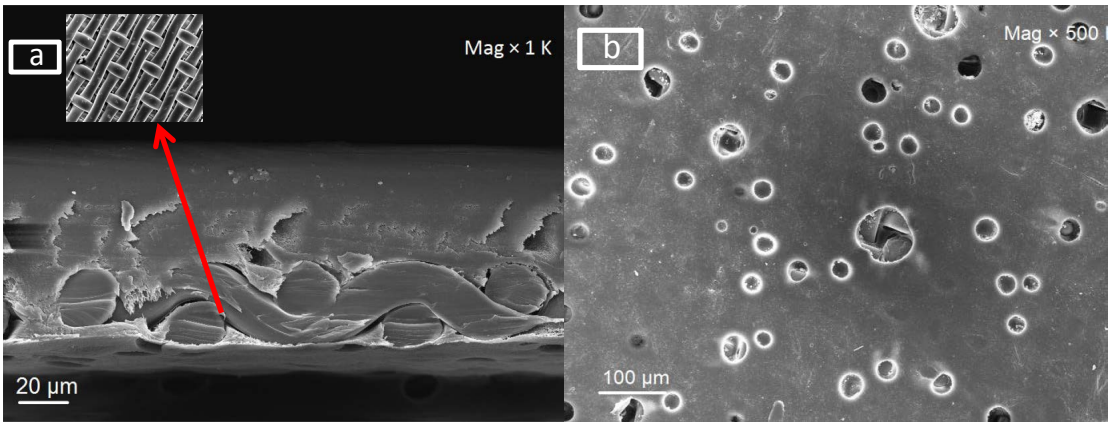

Figure 6.3: SEM images of T_1 membrane substrate displaying (a) cross-section and (b) bottom surface cast on compacted woven polyester mesh fabric support fabricated from 18 wt % PES in 72 % NMP and 10 % PEG solvent. This sample was fabricated through casting method 1.

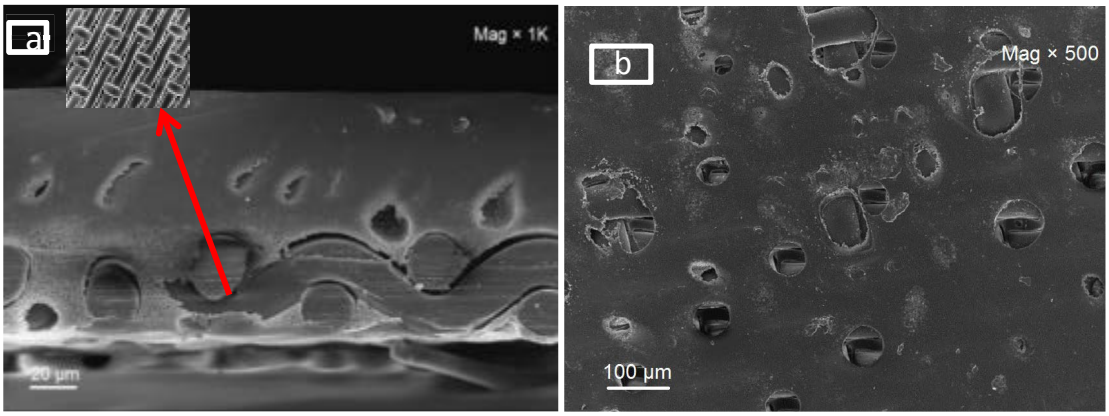

Figure 6.4: SEM images of T_2 membrane substrate displaying (a) cross-section and (b) bottom surface cast on compacted woven polyester mesh fabric support fabricated from 18 wt % PES in 62 % NMP and 20 % PEG solvent. This sample was fabricated through casting method 1.

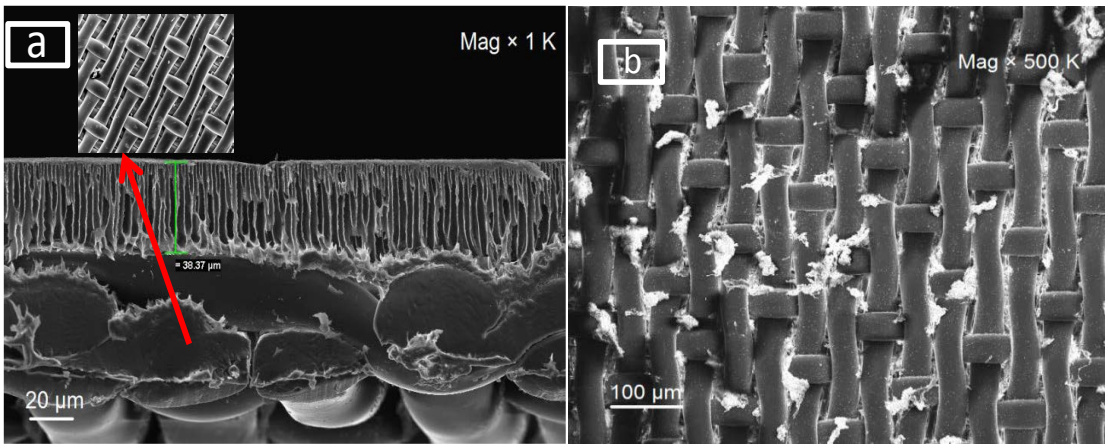

Figure 6.5: SEM images of T_3 membrane substrate displaying (a) cross-section and (b) bottom surface cast on compacted woven polyester mesh fabric support fabricated from 12 wt % PES in 88 % NMP solvent, without PEG as pore former. This sample was fabricated through casting method 1 and backing fabric was not pre-treated with NMP solvent prior to casting.

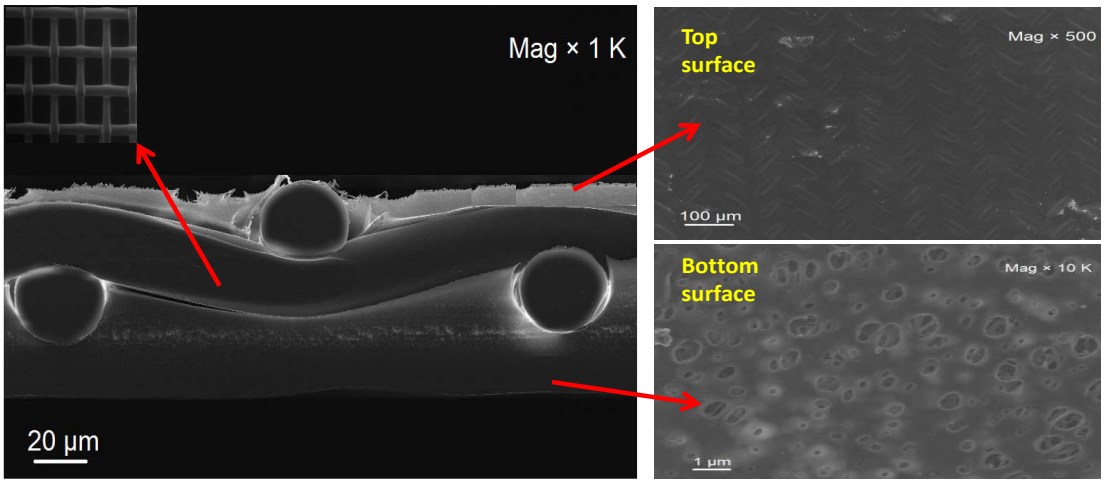

Figure 6.6: SEM images of T_4 membrane substrate displaying (left) cross-section and (right) bottom and surface cast on compacted woven polyester mesh fabric support fabricated from 18 wt % PES in 72 % NMP and 10 % PEG solvent. This sample was fabricated through casting method 2 (FO style on large scale).

WJ-FO membrane seems to be very fragile compared to the other membranes evaluated in this study. Although it is supported by non-woven backing fabric, however, the backing fabric seems to be very thin (unknown materials). Presumably due to the lack of applied hydraulic pressure in typical FO applications there is no need for a membrane that can withstand significantly higher applied pressure. However, the WJ-FO membrane shows significant changes even under the FO test. Figures 6.7 (a) and 6.7 (b) show the SEM cross section images of new and used membrane, respectively. Although there was no applied hydraulic pressure during the FO process, however, the membrane with the finger like structure is vulnerable to compaction even with the slight pressure created by flux cross flow. The thickness reduced from ~140μm to almost ~70μm. Thus, applied hydraulic pressure in the PAO process can further compress the whole membrane and causing severe damage to both the membrane substrate and the active layer similar to the T_3 substrate.

WJ-FO and T_3 membrane samples were used to validate the hypothesis of this study which is the need for stable membrane free of finger like structures for the PAO process. The finger-like pores are preferred for FO membranes to minimize the structural parameter; as such pores have a tortuosity of near unity. However, due to possible compaction of finger like structure, a denser substrate with higher structural parameters can perform sustainably under PAO process.

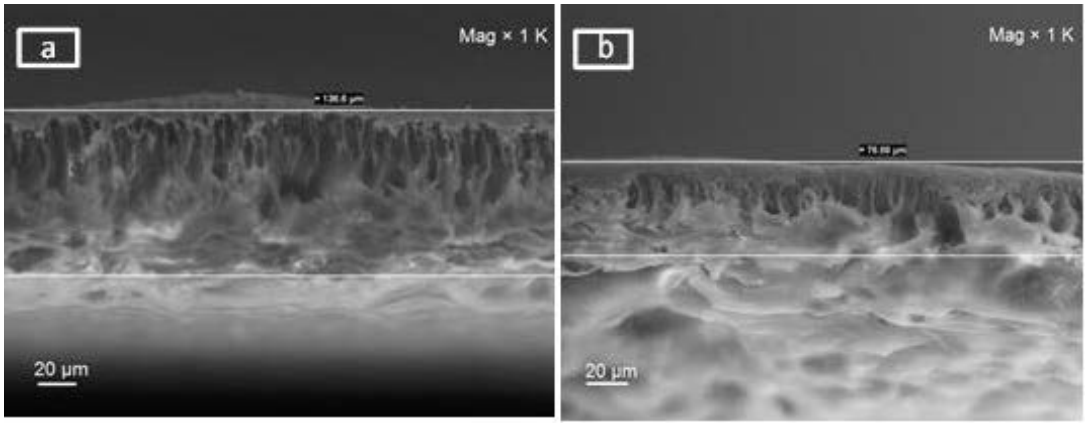

Figure 6.7: SEM cross section images of Woongjin FO membrane substrate displaying (a) new membrane and (b) after few FO experiments. Woongjin membrane is a TFC-FO membrane cast on unknown nonwoven fabric support.

Table 6.2 shows the thickness measurement and effect of applied pressure on the membrane physical property in terms of compaction and thickness. T_1 and T_2 substrates had overall thickness ~150µm while T_3, T_4 and T_5 substrates had overall thickness of ~100µm. Under the PAO process, the T_1 was less compacted than the T_2 substrate which is related to the composition of PEG additive as a pore-former additive in the T_2 sample which was 20% against 10 % for the T_1 sample. The addition of the PEG to the polymer solution support layer may increase the tendency of the membrane to become more compacted under applied hydraulic pressure. Furthermore, it may lose permeability faster overtime and be slightly less resistant against damage and distortion compared to the T_1 sample. The WJ-FO membrane thickness was reduced by more than 50 % even under the FO process and similarly T_3 thickness was decreased by 30 % due to the substrate's finger like structure. The CTA membrane did not show any noticeable change in thickness due to applied pressure.

Table 6.2: Characterisation of membrane substrates.

Sample ID	Thickness (μm)		Porosity%	S Value (mm)	Contact angle (º)	
	New membrane	Used membrane			Active layer	Support layer
T_1	150.2 ± 3.0	142±2	77 ± 1	2.72 ± 0.15	56 ± 1	75 ± 1
T_2	155.3 ± 1.2	141±3	79 ± 1	2.21 ± 0.15	57 ± 1	76 ± 2
T_3	103.2 ± 3.2	72±4	74 ± 3	0.72 ± 0.17	55 ± 1	75 ± 2
T_4	99.3 ± 3.3	____	57 ± 1		54 ± 1	74 ± 2
T_5	105.2 ± 3.1	____	59 ± 1		51 ± 3	72 ± 1
CTA-ES	103.2 ± 1.2	102±3	55 ± 1	0.85 ± 0.15	76 ± 2	81 ± 3
WJ-FO	141.2 ± 3.6	70±3	84 ± 3	0.55 ± 0.21	65 ± 1	65 ± 3
WJ-RO	155.2 ± 2.5	151±2	61±1	16.5 ± 2	96 ± 1	105 ± 2

Other characterisations of membrane substrates are summarised in Table 6.2. The low value of the structural parameter is desired to minimize the detrimental effects of ICP in the FO membranes. Between T_1 and T_2 samples, T_2 performed better under the PAO test. This substrate was slightly more porous than the T_1 sample with lower *S* value (T_1 2.72mm, T_2 2.21mm) (Table 6.2). The improved pore structure and porosity of T_2 was likely due to the use of higher volume of PEG (Table 6.1) (Wang et al. 2012a). Gravimetric measurements in Table 6.2 confirmed that both substrates (WJ-FO and T_3) had high porosities (74±3% for T_3 and 84±3% for WJ-FO).

Corresponding to the high porosity and the finger-like pore structures, relatively small *S* values were obtained for both substrates (0.72 ±0.17 mm for T_3 and 0.55±0.21 mm for WJ-FO). There is a large difference between the measured overall S values for T_3, 0.72 mm and the estimated values for T_1 and T_2. This can be attributed to the finger-like pores, higher porosity and lower membrane thickness in the T_3 sample. Denser substrate, lower porosity and the tortuous nature of the T_1 and T_2 samples contributed to the overall higher structural parameter compared to the T_3 sample ($S \approx 0.72$ mm) or WJ-FO membrane ($S \approx 0.55$ mm). Furthermore, Table 6.2 also shows that WJ-RO had the highest structural parameter ($S \approx 16.5$ mm) which is the main reason for RO membranes in general for their poor performance in the FO process despite their higher water permeability.

The hydrophilicity of the substrates prepared in the current studies was characterised by using contact angle measurements (Table 6.2). The contact angle of fabricated T_1 and T_2 was ~56◦, lower than those of the CTA (~76◦) and the WJ-FO (~65◦) membrane. The relatively low contact angles for the T_1 and T_2 could be attributed to the hydrophilic nature of PES and the addition of PEG in the membrane casting

solutions (Wang et al. 2012a; Widjojo et al. 2011). Additional substrate samples prepared without the addition of PEG had much higher contact angle values and lower porosity which resulted in poor performance under the FO and PAO process (results not shown). Previous studies also confirm that hydrophilic substrates tend to have better water flux as a result of improved substrate wetting (McCutcheon & Elimelech 2008b). Therefore a higher water flux is expected from the composite membranes (T_1- T_3). Results in Table 6.4 demonstrate that water permeability for the T_1 and T_2 is 2.2 L/m^2 h^{-1} bar and 3.7 L/m^2 h^{-1} bar respectively which is several times greater than water permeability of the CTA membrane (0.9 L/m^2 h^{-1} bar) indicating the direct relationship between membrane hydrophilicity and water permeability. The relationship between the membrane structural parameter and water permeability with the membrane performance under FO and PAO process is discussed in the section 3.3.

Table 6.3: Mechanical properties of TFC membrane substrates.

Membrane ID	Tensile strength (MPa)	Young's Modulus (MPa)	Elongation break (%)
TFC-1	148.6	1323.23	41.68
TFC-2	111.4	1132.82	43.34
TFC-3	84.4	749.19	45.53
CTA	61.9	532.55	63.68
WJ-RO	35.8	141.69	37.76
WJ-FO	25.8	90.66	41.45

Table 6.3 summarises tensile strengths of fabricated TFC-PAO membranes and it was compared with the commercial FO and RO membrane. Young's modulus and

tensile strength were highest for T_1 and T_2 and lowest for the WJ- FO membrane. CTA membrane tensile strength and modulus were lower than fabricated TFC-PAO samples in this study and higher than WJ-RO membrane while elongation at break was the highest among all samples.

6.3.2 **Membrane rejection layer**

6.3.2.1 **Relating substrate morphology to forming polyamide thin layer**

The top skin layer and pore size of the membrane surface play a major role in forming the polyamide rejection layer (Tang et al. 2009; Tiraferri et al. 2011b; Wijmans et al. 1985b). For a better illustration of the rejection layer morphology's requirements, the T_3 and T_4 skin layer samples have been chosen for the purposes of comparison. Figure 6.8 (a) shows SEM images of the T_3 membrane fabricated by casting method (M_1). The finger like structure and spongy sub layer pores beneath the top skin layer are attributed to the low polymer concentration used for T_3 sample. Such a smooth top skin layer with small pore size (<50 nm) is necessary to have better results in interfacial polymerization. Figure 6.8 (b) shows the membrane surface (bottom surface) of the T_4 sample fabricated by M_2 casting method. Similar to commercial FO membrane fabrication presented in the patent (Herron 2008), the skin layer was in contact with glass plate which leads to large pore size on the membrane bottom surface where rejection layer is supposed to form. SEM images of the T_4 top and bottom surface together have been shown in Figure 6.7 in the previous section.

Generally, polyamide layer forms as a result of MPD solution eruption from the membrane pores, reacts with TMC that results in the formation of a thin skin PA rejection layer. However, in the membrane surface with a large pore size, such as our

T_4 sample, TMC can penetrate the pores and result in PA formation inside the pores and formation of PA layer with uneven thickness increasing the chance of some uncoated area and defect points on the membrane rejection layer (Tang et al. 2014). Top skin layers with optimum pore size are critical for optimum rejection layer formation, otherwise membrane rejection will be compromised (Petersen 1993). It was not possible to fabricate a PA layer on the T_4 embedded polyester mesh membrane either on the top or bottom surface of the substrate. Figures 6.7 and 6.8 (b) show large pore size (~1μm) on the surface that was in contact with glass plate. SEM image of T_4 membrane sample top side reveals a defect point that caused by M_2 fabrication method and woven polyester mesh embedding. Also through the literature review and previous studies, we could not confirm what would be the optimum pore size for forming the rejection layer on the membrane top skin layer. However, some studies suggest that there is a relationship between morphology and rejection surface properties of the PA layer to the top skin pore size (Singh et al. 2006). Findings show surfaces with a smaller pore size will form a smoother rejection layer compared to surfaces with a larger pore size (Ghosh & Hoek 2009b).

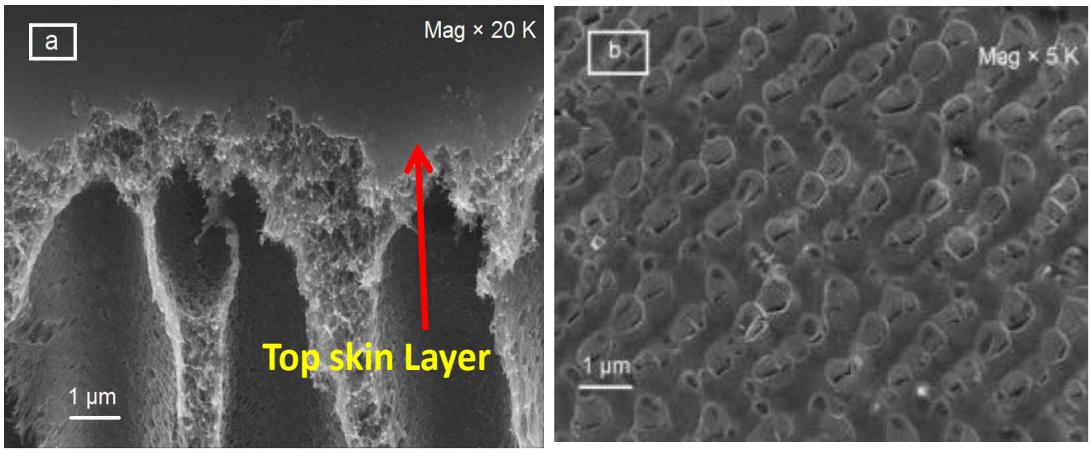

Figure 6.8: SEM images of membrane substrate displaying (a) cross-section for T_3 sample on compacted woven polyester mesh fabric fabricated through casting method 1 and (b) bottom surface for T_4 sample cast on regular woven polyester mesh fabric fabricated through casting 2. Complete casting solution condition presented in Table 6.1.

Generally, low polymer concentration results in a finger like structure and have a higher chance of big open pores at the top skin layer depending on their phase inversion pathway (Tiraferri et al. 2011b). Figure 6.8 (a) shows the cross section for the T_3 sample. The polymer concentration was low for this sample compared to the other substrate (Table 6.1), however, the top skin layer with a porous sub layer is evidence that liquid-liquid phase separation occurred as it was expected for low polymer concentrations during the phase inversion stage (Singh et al. 2006). The polymer concentration rate at the membrane top surface became more concentrated as a result of air exposure during the casting. It means solvent evaporation occurred in the gap between casting and the precipitation bath. Thus, as it is evident from Figure 6.8 (a), big pores in the membrane porous sub layer couldn't extend to the membrane surface.

Gelation usually takes place at high polymer concentrations (Singh et al. 2006). Figures 6.4 (a) and 6.5 (a) show T_1 and T_2 fabricated samples with high polymer

concentrations (18 %) where the gelation pathway occurred in the phase inversion stage. In those samples, the membrane substrate is less porous and free of finger like structures, thus membrane surfaces are usually denser at the top skin and sub layer. Similarly, the polymer concentrations in the T_4 and T_5 samples were high (Table 6.1) and gelation pathways are expected for the membrane substrate. However, the liquid–liquid phase inversion occurs for the bottom surface which is the last part of the casted membrane to solidify in the precipitation bath. Here, the precipitation pathway intersects the binodal before crossing into the gelation region, causing a lower polymer concentration and an open skin layer with larger pores in the bottom surface (Bokhorst et al. 1981; Tiraferri et al. 2011b). This may help to explain the fail interfacial polymerisation attempt when duplicating the FO membrane fabrication on commercial scale in T_4 membrane sample under lab condition. Bottom surface morphology and optimum pore size were not critical in our fabricated TFC membrane (T_1, T_2 T_3). However, it was a fundamental requirement in the T_4 membrane sample to form a rejection layer on the surface that was in contact with the glass plate.

6.3.2.2 **Characterization of membrane rejection layers**

The active rejection layers of the TFC PAO membranes were fabricated on top of the PES substrates via interfacial polymerization as explained under section 3.2.1. Figures 6.9 (a) and 9.6 (b) show the SEM images of polyamide layers form on the top of T_1 membrane sample and cross section view of the T_2 membranes sample. It showed a ridge-valley morphology which is typical for TFC polyamide membranes formed by interfacial polymerization (Tang et al. 2009). The separation properties (water permeability A, NaCl rejection R and NaCl permeability B) of membranes T_1,

T_2 and T_3 are characterized (T_4 and T_5 samples ignored) and compared with commercial CTA-ES , WJ- FO and RO membranes presented in Table 6.4.

Table 6.4: Properties of fabricated TFC and other commercial membranes.

Sample ID	Support material	[a] Water permeability (A)		[b] Salt permeability B (10^{-8} m/s)	NaCl rejection (%)	B/A (kPa)
		$L/m^2\ h^{-1}\ bar^{-1}$	$\times^{10-12}$ m/s Pa			
T_1	PES	2.2	6.1±0.5	5.6±0.1.3	96.2	9.15
T_2	PES	3.7	10.1±0.5	14±0.1.3	94.3	14.2
T_3	PES	4.5	11.1±0.5	18±0.1.3	91.2	18.2
CTA	CTA	0.91	2.6±0.5	16± 1.3	78 ± 4	61
WJ-FO	PSF	2.71	7.2±0.5	23± 1.3	85 ± 1	32.2
WJ-RO	PSF	1.15	3.19±0.5	2.9± 1.3	96 ± 5	9.1

[a] Evaluated in the RO testing mode over an applied pressure range of 1–10 bar with DI water as feed water.
[b] Evaluated in the RO testing mode over an applied pressure range of 1–10 bar for a feed water containing BW10 NaCl.

According to data tabulated in Table 6.4, both the T_1 and T_2 exhibited much higher water permeability and better NaCl rejection compared to the commercial CTA membrane. As a result of its higher porosity and possibly thinner rejection layer (presented in Table 6.2), the T_2 had a relatively higher pure water permeability and was nearly triple the amount of the CTA membrane. Also, the WJ-FO membrane shows better results in terms of water permeability compared to CTA membrane. However, it could not be used for the PAO process due to its fragile structure. The T_3 also shows water permeability of 4.5 ±0.25 $L/m^2\ h^{-1}\ bar^{-1}$ which is higher than the T_1 and T_2 membrane samples. However, similar to the WJ-FO membrane, it could not be used in the PAO process because of the finger like structure properties and compaction under applied hydraulic pressure. However, the T_3 sample could endure higher pressure compared to the WJ-FO membrane of up to 4 bar (performance data will be discussed in the next section) which could be attributed to the presence of the

polyester woven mesh fabric support that provides more mechanical strength than thin non-woven backing fabric support in WJ-FO.

At an applied pressure of 10 bar in the RO testing mode, T_1 and T_2 had decent NaCl rejection of 96.2% and 94.3%, respectively as shown in Table 6.4. It is worth noting that the solute rejection under applied hydraulic pressure can increase significantly at higher testing pressures as confirmed by the previous study (Tang. et al. 2010). T_2 had improved water permeability over T_1 but it also causes higher salt permeability and lower rejection compared to the T_1 sample as shown in Table 6.4. Compared to the CTA membrane that had relatively low water permeability, the TFC-PAO membrane samples (T_1, T_2) exhibited superior separation properties and water permeability.

Table 6.4 also summarized the B/A ratio which is a direct indicator of the selectivity of an FO membrane. A larger B/A ratio indicates lower selectivity and is likely to increase draw solution reverse diffusion which can accelerate the possibility of membrane fouling on the membrane surface in addition to the economic loss of the draw solutes (Tang. et al. 2010; Xiao et al. 2011). Furthermore, due to the nature of PAO and effect of applied hydraulic pressure on the process, with increases in applied hydraulic pressure, there was a decrease in the reverse solute flux that will be elaborated upon in section 3.3. Generally, a lower B/A ratio is preferred. In the current study, both T_1 and T_2 had relatively low B/A ratios of 9 and 14 respectively compared to 61 for the CTA membrane and 32 for the WJ-FO membrane hence, this indicates their superior separation properties alongside their high water permeability.

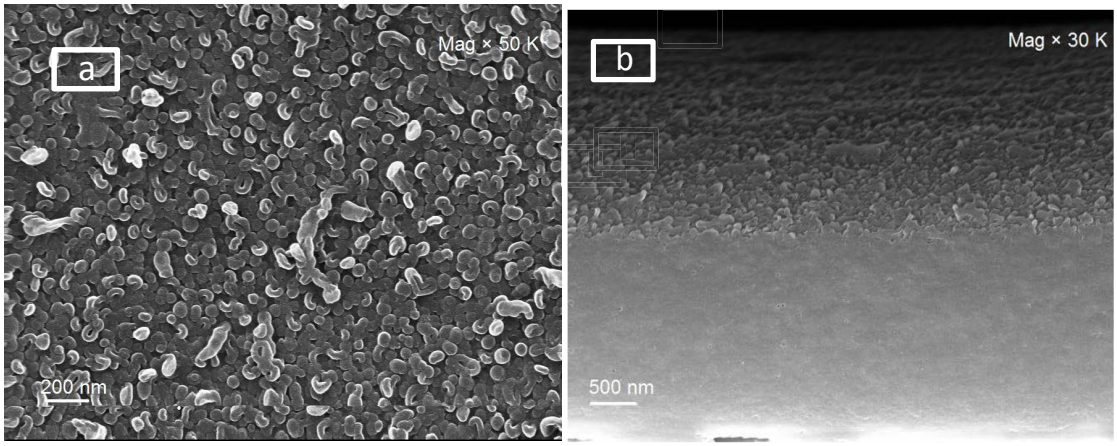

Figure 6.9: SEM images of membrane rejection thin layer displaying (a) top surface view for T_1 sample and (b) cross section view for T_2 sample cast on PES membrane substrate through interfacial polymerisation. Thin polyamide cross-linked rejection layer formed through reaction between 3.5 wt % MPD in water and 0.15 % TMC in hexane.

Overall, compared to the CTA membrane, TFC membrane is chemically tolerant and they have superior permeability and separation properties (Lee et al. 2011). Obtained data illustrated in Table 6.4 for the T_1 and T_2 membrane samples show that TFC polyamide based membranes can be promising alternatives to existing CTA based FO membranes for newly developed PAO process.

6.3.3 **PAO performance evaluation**

Fabricated TFC membranes performances were validated by a comparison with the commercial FO (CTA-ES, WJ-FO) and WJ-RO membrane under the FO and PAO process using various FS and DS conditions. For the fabricated TFC membranes (T_1, T_2, T_3) alongside other membranes used for validation, the net increase in water flux per unit pressure was higher at higher hydraulic pressure. Increasing applied pressure did impact the performance of our membrane samples under the PAO process (T_1, T_2). The external hydraulic pressure has a significant impact on CTA water flux in the PAO process, and the results for fabricated membrane samples evaluated with the

PAO process (T_1, T_2) were more considerable. Using 0.5 M NaCl as a DS, CTA flux improved approximately two times by increasing pressure up to 10 bar on the feed side while improvement for the T_1 and T_2 membrane was approximately 10 times and roughly twice that of the CTA membrane when hydraulic pressure was increased up to 10 bar. It is worth noting that among all the membranes evaluated in the current study, the T_1 and T_2 substrates had a poor water flux in the FO process despite their superior water permeability (T_1 , 2.21 L/m^2 h bar^{-1} and T_2, 3.7 L/m^2 h bar^{-1}). This can be related to the higher structural parameters of those substrates (T_1=2.72 mm, T_2=2.21 mm) and the compacted woven fabric mesh support. Support fabric can hinder the water flux in the FO process; also, it shows a less significant effect on water flux under PAO performance due to applied hydraulic pressure.

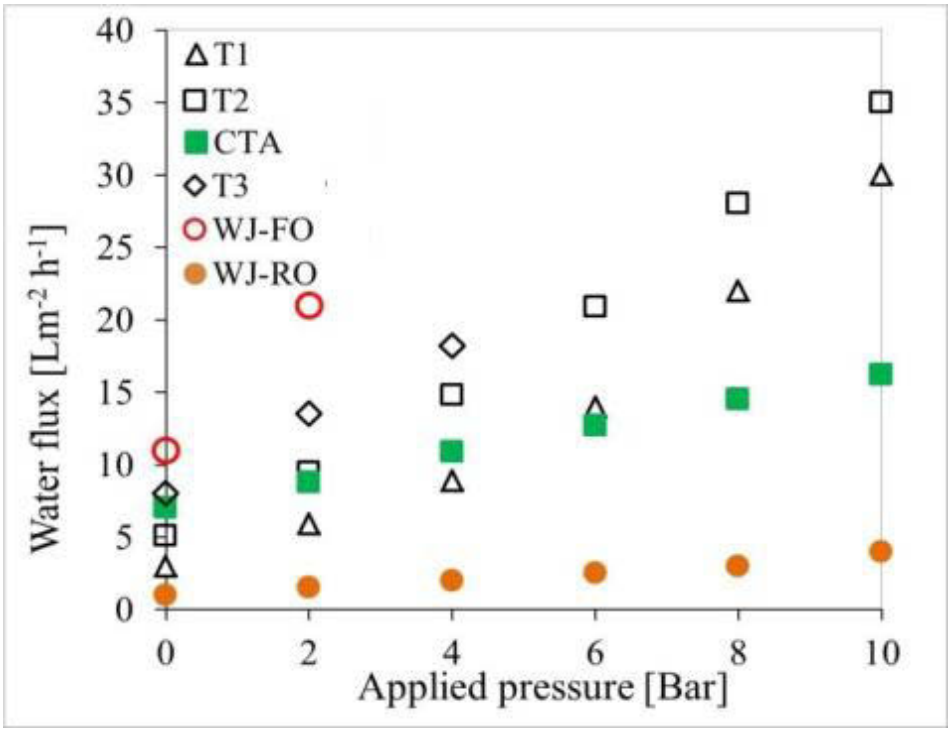

(a)

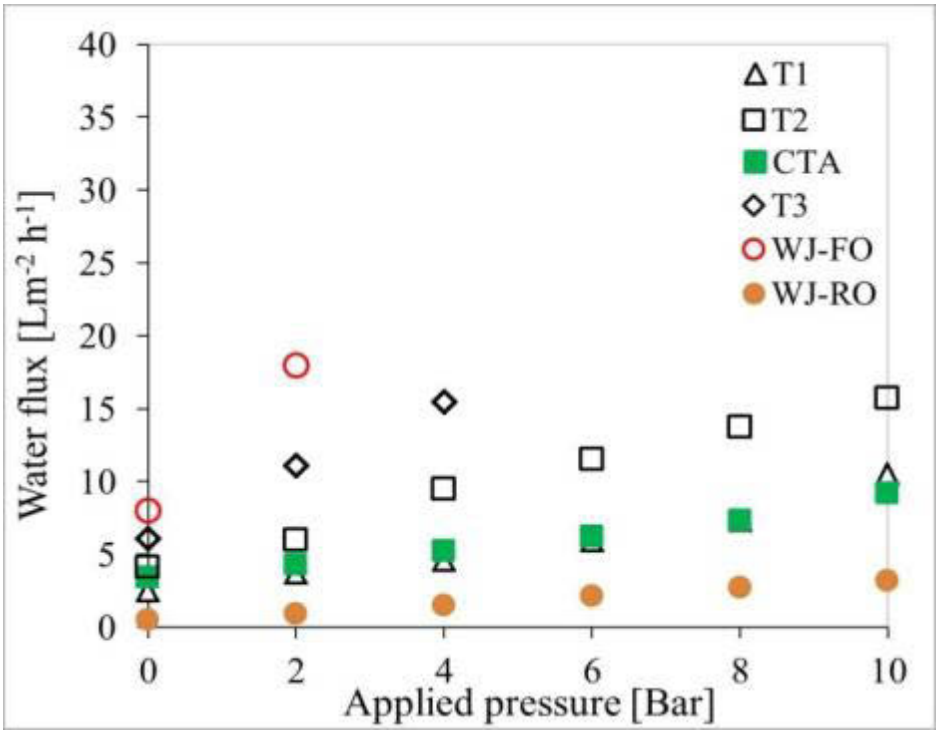

(b)

Figure 6.10: Performance comparisons of fabricated membranes with commercial membranes in terms of water flux (a) with 0.5 M NaCl as DS and DI water as FS and (b) 0.5 M NaCl as DS and BW10 as FS at different applied hydraulic pressure.

Figure 6.10 (a) shows the water flux for T_1, T_2, CTA and Wj-RO membranes under the PAO process with 0.5 M NaCl concentration as DS and DI as FS at an applied pressure of 0 to 10 bar. T3 and WJ-FO could not perform under applied hydraulic pressure of 10 bar. However, WJ-FO and T_3 membrane had the highest water flux in the FO mode. This can be explained by their lower structural parameter compared to the CTA, RO and our fabricated TFC membrane samples. Furthermore, high performance during FO process in the WJ-FO substrate is attributed to its higher porosity and membrane finger like structure supported on thin non-woven fabric in comparison with other membrane samples evaluated in this study (Table 6.2 and Figure 6.7). While the commercial WJ-FO membranes were optimized in terms of permeability, finger like and porous substrates to achieve a low structural parameter,

its support layer was far from optimal for enduring applied hydraulic pressure under the PAO process and hence this customized design for the FO process could not perform under the PAO process. Required applied pressure in the PAO process can cause compaction and distortion across the membrane substrate.

Between the T_1 and T_2 substrates, the T_2 shows a better result in both the FO and PAO processes due to it more porous structure in addition to its higher water permeability and lower structural parameter than the T_1 substrate (Tables 6.2 and 6.4). Using 0.5 M NaCl as DS and DI water as FS, T_2 obtained a flux of 37 $L/m^2\ h^{-1}$ when applied hydraulic pressure was10 bar, which was 300% higher compared to that of CTA membrane. This is more than 3 times that of the CTA membrane that is currently used for the PAO process. Furthermore, similar results were observed when brackish water used as a feed solution. Using 0.5M NaCl as DS and 10 g/L NaCl as FS, T_2 obtained a water flux of 17 $L/m^2\ h^{-1}$ against 11 $L/m^2\ h^{-1}$ for CTA membrane when applied hydraulic pressure was10 bar. Figures 6.10 (b) shows the water flux increased linearly for T_1 and T_2 substrates at an average of ≈1.1 $Lm^{-2}\ h^{-1}bar^{-1}$ and 1.05 $Lm^{-2}\ h^{-1}bar^{-1}$, respectively.

T_1 and T_2 had an S value in the range of 2.72 and 2.21 mm respectively which was much larger than the CTA of 0.85 mm (Table 6.2). However, results illustrated in Figure 6.10 (a) and (b) indicate that despite the bigger S value, the T_1 and T_2 had better results under the PAO process in terms of water flux. Better performance under the PAO process can be attributed to those membrane properties such as higher hydrophilicity and porosity in addition to higher water permeability and better rejection property (Tables 6.2 and 6.4). In addition, the WJ-RO membrane has a higher A value (1.15 $L/m^2\ h^{-1}\ bar^{-1}$) compared to the CTA-ES (0.91 $L/m^2\ h^{-1}\ bar^{-1}$)

used in this study. However, the higher S value for the tested RO membrane (16.55 mm) makes it impractical for FO or PAO application (Table 6.2 and 6.4 -Figures 6.10 and 6.11). Our optimum TFC-PAO membranes had a higher A value than the CTA membrane while their *S* value was much lower than the RO membrane. Such a membrane can be located between the FO and RO membrane characteristics.

In the FO membrane, a higher A value (water permeability) and lower S value (structural parameter) are favourable for obtaining higher water flux. However, the PAO needs a stable, dense and porous membrane with high water permeability. It seems that unlike the FO, membranes with a higher S value are more appropriate for the PAO due to the need to withstand required applied hydraulic pressure during the process. Based on results from the Figure 6.10 and Tables 6.2 and 6.4, we can conclude that membranes free of finger like structures with higher water permeability than the CTA membrane and a lower S value than the RO are more favourable for PAO applications.

For assessing the poor results of T_1 and T_2 during FO process, the compact woven backing of two samples of T_1 and T_2 were carefully removed and tested in similar experiments. Results show a significant water flux increase under FO experiments (results not shown). This confirms that reinforcing the membrane support layer with backing fabric (woven or non-woven) can sacrifice a large portion of flux enhancement in the FO process. However, T_1 and T_2 shows better water flux compare to the other membrane in the PAO process. Their better PAO water flux over other membranes was mainly due to their superior separation properties and higher water permeability (Table 6.4) as predicted by equation (6). The current results suggest that the TFC-PAO membranes offer significant advantages over

integral asymmetric membranes like CTA-ES from HTI or the WJ-FO membrane for the PAO process. Also reinforcement with fabric support can hinder some of the water flux through the membrane structure. However, due to increased strength through applying woven mesh fabric, it is possible to produce a thinner support membrane meaning shorter paths for flux flow that can amend the portion of flux decline due to applied fabric support.

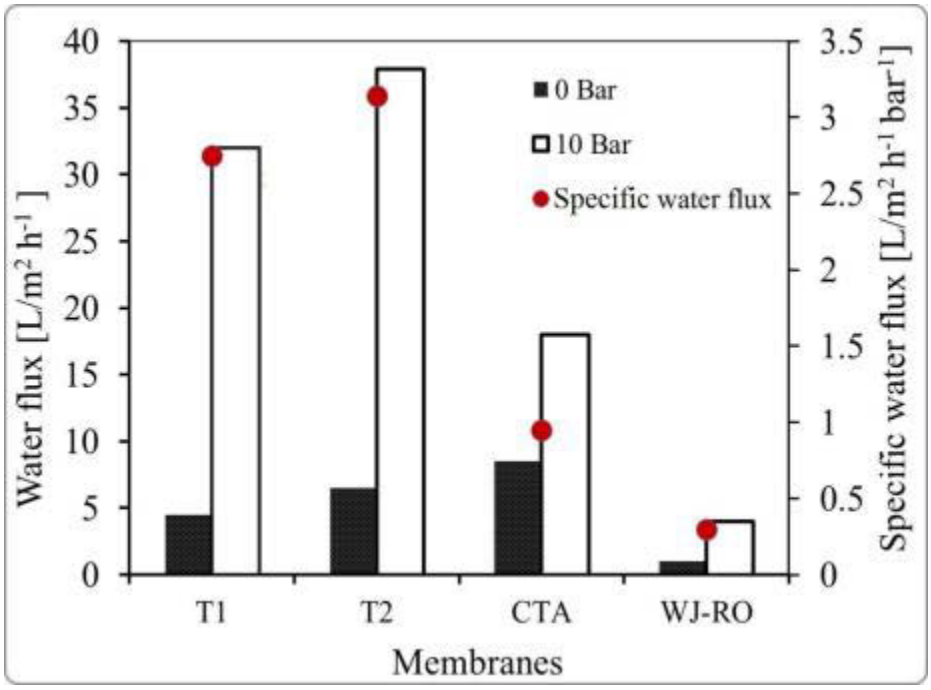

Figure 6.11: Variation of water flux in the fabricated membrane with commercial membranes with 0.5 M NaCl as DS and DI water as FS at an applied pressure of 0 and 10 bar.

Figure 6.11 shows variation of water flux in the fabricated membrane with commercial membranes at applied hydraulic pressure of 0 and 10 bar and the gain illustrated in terms of water flux and specific water flux (SWF). SWF is defined here as permeate flux per unit applied pressure that gives an indirect comparison toll to measure membrane performance and effectiveness under the PAO process. Higher

SWF is favourable for the PAO membranes. Interesting observations are made from results illustrated and are discussed below.

Firstly, the T_2 substrate had the highest water flux which was 37 LMH at applied pressure of 10 bar, almost 800% net water gain compare to the FO process ($\Delta P = 0$) with the specific water flux of 3.3 $L/m^2\ h^{-1}\ bar^{-1}$. That is the highest water flux and net gain among all other tested membrane under the PAO process. CTA water flux was 16.5 $L/m^2\ h^{-1}$ at the similar condition which was 85% net water gains with the specific water flux of 1.05 $L/m^2\ h^{-1}\ bar^{-1}$. Secondly, WJ-RO had the lowest water flux 4.5 $L/m^2\ h^{-1}$ under PAO process at a similar condition .Interestingly, the net water gain for the WJ-RO membrane was much higher than the CTA membrane which was 300% and an 85% increase in net gain water flux respectively. However in terms of SWF, RO was much lower than the CTA and fabricated TFC samples T_1 and T_2 samples. Obtained results from Figure 6.11 for the WJ-RO membrane revealed the interesting design criteria for the PAO membrane. In general, RO membranes have very high structure parameter (15-30 mm), however, they have higher water permeability compared to the commercially available CTA-FO membrane. A higher structure parameter makes RO membranes inappropriate for the FO process. However, under applied pressure, the net gain percentage in water flux was higher than the CTA membrane due to its higher water permeability, 1.15 $L/m^2\ h^{-1}\ bar^{-1}$ (Table 6.4).

Figure 6.12 shows the salt permeability (B value) against water permeability (A value) for the fabricated and other commercial membranes in this study. In general, membrane substrates with higher water permeability but lower NaCl permeability are preferred (Wei et al. 2011a). Based on William A et al. 2010, membranes for

desalination contain two important transport parameters, which are structure parameter (S) and active layer salt permeability coefficient (B). Referring to their described equation, a higher S value will decrease the draw solute reverse flux (Phillip et al. 2010). Therefore lower salt permeability in the T_1, T_2 samples in comparison to the CTA and WJ FO membranes can be related to their higher structural parameter alongside their thin film polyamide rejection layer properties.

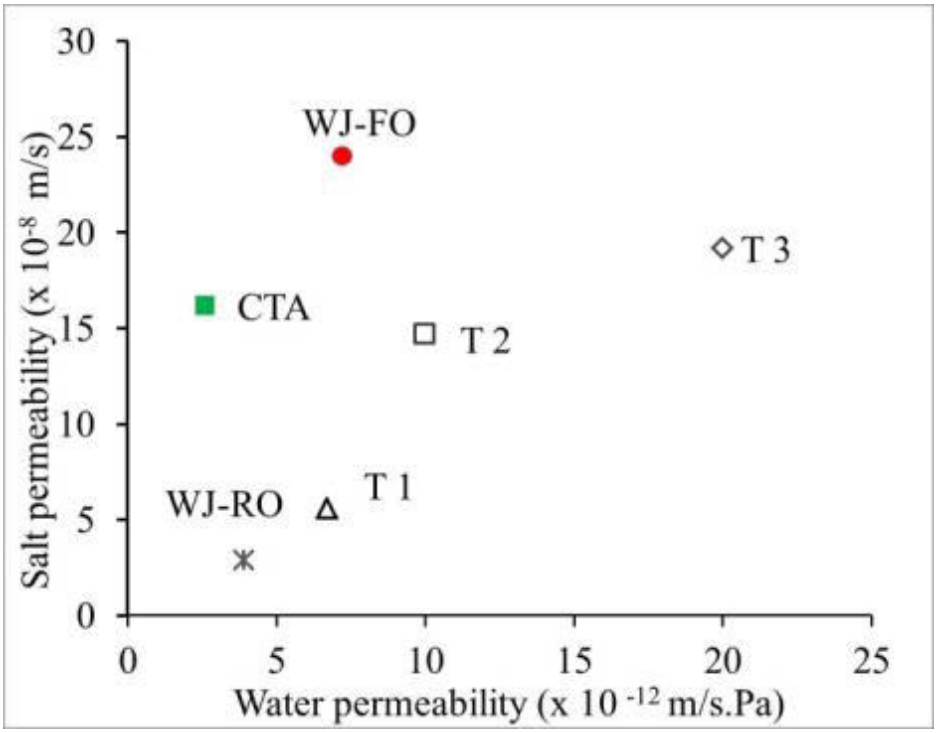

Figure 6.12: Salt permeability versus water permeability for the synthesized TFC and commercial membranes.

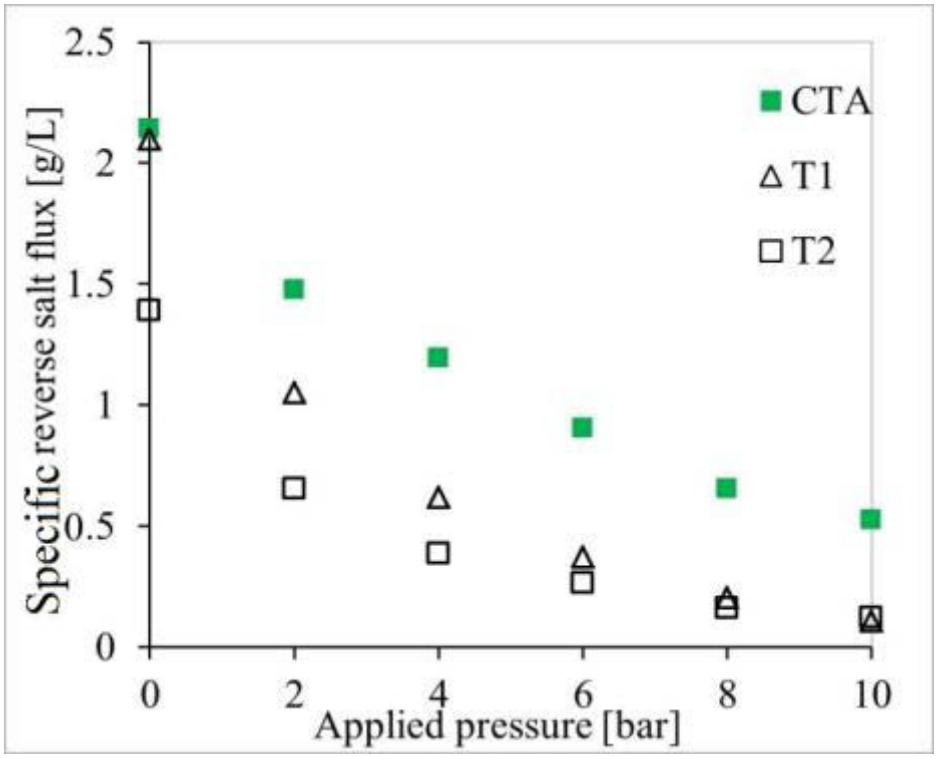

Figure 6.13: Influence of reverse salt flux due to applied pressure in the PAO process using 05M NaCl as draw solution and DI water as FS.

The solute fluxes across the semipermeable FO membrane are usually assessed in terms of salt rejection for feed solutes which has been presented in the previous section (section 3.3 Table 6.2) and reverse solute flux (RSF) or specific reverse solute flux (SRSF) for draw solutes. The SRSF is calculated as a ratio ($SRSF=J_s/J_w$) of reverse draw solute flux (J_s) and the water flux (J_w). The SRSF for NaCl as DS and DI as FS for the PAO experiments at pressures ranging from 0 to 10 bar are presented in Figure 6.13. Obtained data shows the SRSF for T_1, T_2 membrane is compared to the CTA membrane under PAO process. The T_3 and WJ-FO membrane could not perform under the PAO process due to their fragile substrate and hence their results are excluded. SRSF was generally declining for the T_1, T_2 sample and the CTA FO membranes under the PAO process with an increase in applied

hydraulic pressure. Similar results have been confirmed through a previous study on the PAO process which is in contrast to the conventional FO process (Blandin et al. 2013; Oh et al. 2014). Declining RSF or SRSF with increased hydraulic pressure can be attributed to the force of water flowing from the feed side by applied pressure in the PAO process. This is in addition to osmotic pressure produced by osmotic agents which may reduce the concentration difference close to the membrane surface, the main driving force for reverse solute flux. For example, the SRSF for the T_1, T_2 sample under the FO process ($\Delta P=0$) is 1.4 g/L and 1.60 g/L respectively. However, it decreases to 0.18 g/L and 0.20 g/L, respectively where applied hydraulic pressure is increased to 10 bar. Meanwhile, SPRF for the CTA FO membrane was higher than both the T_1 and T_2 samples. Also it declined at a similar rate where it decreases from 2.1 g/L for the FO process ($\Delta P=0$) to and 0.62 g/L under the PAO process at 10 bar hydraulic pressure. In addition to the effect of PAO process on RSF or SRSF due to the increased water permeability, the T_1 and T_2 substrates had a higher S value and tortuosity that can limit the draw solute diffusion further compared to the CTA membranes with lower structural parameters (Table 6.2).

6.4 **Concluding remarks**

In this study, TFC-PAO membrane fabricated on specific compacted woven polyester mesh was shown to have a superior performance when compared to the CTA membrane that has been often used in recent PAO studies. The membrane substrate, prepared by phase inversion was free of finger-like structures and reinforced by woven mesh fabric to produce a membrane substrate with suitable structural parameter for which could be utilized in the PAO process.

- The resulting PAO membranes T_1 and T_2 also had larger structural parameters 2.7 mm and 2.2 mm compared to the FO membranes but they had higher water permeability (A value) and high selectivity which leads to a higher net water flux gain in the PAO process.
- Compared to the commercial CTA-ES from HTI, both T_1 and T_2 exhibited superior performance under the PAO process. With a 0.5 M NaCl as DS, T_2 achieved a flux of ~37 L/m^2 h, which was 300% higher than the commercial CTA membrane at an applied pressure of 10 bar.
- Water flux through the TFC-PAO membranes significantly increased with applied hydraulic pressure while reducing the specific reverse solute flux.
- The PAO process requires a membrane that can endure applied hydraulic pressure. Therefore it should be a dense but porous and permeable substrate that is free of finger like structures and reinforced by backing fabrics.
- Unlike for the FO process which requires membrane which has a very low structural parameter, higher structure parameter seems to be more appropriate for the PAO process. Further development taking the form of modified membrane designs will be needed for improving the overall PAO membrane performance.

Chapter 7

CONCLUSIONS AND RECOMMENDATIONS

Based on the results obtained from this study, the following conclusions and recommendations are presented useful for future study for further development of high performance and sustainable FO membrane for different engineered osmosis applications.

7.1 Pressure assisted fertilizer drawn osmosis process

Use of external hydraulic pressure alongside the osmotic gradient across the membrane in the Pressure Assisted Osmosis (PAO) proved to be effective in terms of water flux enhancement and further DS dilution. The concept of PAO is applied in an expanding FO process application. In this process, pressure is applied to the feed side to enhance the water flux albeit at a lower energy cost (Yun et al. 2013b). Previous work has demonstrated that applied hydraulic pressure can increase the FO performance (Oh et al. 2014; Yun et al. 2013b); however, performance also depends on the FO membranes properties such as type, structure and materials (Coday et al. 2013). In this study, the combined processes of applied hydraulic pressure and osmosis have been reported to exploit the synergies of the two processes in a single stage to overcome low flux in the FO process (Blandin et al. 2013; Coday et al. 2013; Yun et al. 2013b).

One of the practical applications of the FO process is in the desalination for irrigation through novel concept of using fertilizer as draw solution. The use of hybrid FO-PAO system could be more advantageous where dilution of the fertiliser DS is to meet the nutrient concentrations acceptable for direct fertigation rather than to separate the fertiliser DS. The additional water flux generated by the applied pressure could help dilute the fertiliser DS concentration beyond the point of osmotic equilibrium making the PAFDFO process for application as a standalone process

without the need of additional post-treatment process such as NF to reduce the final fertiliser concentration to acceptable level for direct fertigation.

In this study, the PAO was evaluated for its application in the FDFO desalination process. The study on the PAO using NaCl and PAFDFO using three different fertilisers DS, $(NH_4)_2SO_4$, $NH_4H_2PO_4$ and KCl suggests that, the hydraulic pressure could be more suitable when applied at lower DS concentrations especially when the osmotic driving force gradually decreases and the DS and FS approaches closer towards osmotic equilibrium.

The specific reverse solute flux was lower and feed solute rejection was higher in the PAO or PAFDO mode compared to FO or FDFO mode of operations. However, further work including long-term operations using different membrane materials is required for better understanding the effects of hydraulic pressure on the FO membrane and membrane fouling and scaling, and the effect of pressure on ICP, which reduces the efficiency of the PAO.

7.2 **Thin film composite forward osmosis membrane**

In this work, sulphonated polyethersulfone (SPES) has been synthesized and then blended with PES to increase the membrane hydrophilicity. Then comprehensive investigation was conducted to evaluate the FO performance, formation, morphology, and mechanical strength of flat sheets membrane made of sulphonated materials with different degrees of sulphonation.

Introducing sulphonated polymer results in a higher degree of hydrophilicity and relatively higher porosity. The contact angle of PES membrane substrates without any sulphonation material (TFC_1) has an average contact angle of 77.3◦, while the substrates comprising 25 or 50 wt % sulphonation material have relatively low

contact angles in the range of 15–20◦ due to the increased hydrophilicity. Fabricated substrates with more hydrophilic nature performed better under the FO process.

Study by previous research groups suggested that the ideal membrane substrate for FO should have finger-like structure morphology to enhance the water transport and limit the ICP. However, in this study, membrane substrate with finger-like structure has the lowest water flux compared to the dense substrate which possesses sponge morphology. Higher water flux in the membrane sample with sponge morphologies can be attributed to a much more hydrophilic nature due to higher rate of sulphonated materials. Furthermore, this study reveals that membrane substrate with higher degree of sulphonation has sponge morphology compared to the non-sulphonated materials which possess a finger-like structure. Therefore, this work suggests that membrane properties like hydrophilicity have a greater effect on water transport within the membrane substrate than the membrane structure morphologies. Membrane morphology is not a governing factor in achieving higher performance in FO membrane and other membrane properties such as hydrophilicity are major factors as well.

The following points summarize the findings in this work:

The TFC_3 membrane sample blended with the 50 wt % sulphonated materials shows the best performance in terms of water flux, while it possesses fully sponge-like structure morphology. However, it was the most hydrophilic substrate which is the reason for high water flux of 42.0 35 L $m^{-2}h^{-1}$ under PRO and 35 L $m^{-2}h^{-1}$ under FO modes when 2 M NaCl as DS and DI water as FS were used. The TFC_1 membrane casted without sulphonated material contains finger-like structure in the membrane substrate with water fluxes of 13.5 and 10.5 $Lm^{-2}h^{-1}$ tested under PRO and FO modes, respectively, when DI water as FS and 2 M NaCl as DS were used.

With an increase in sulphonated material ratio in the membrane substrates, the membrane porosity increased and the structural parameter decreased. This caused the internal concentration polarization (ICP) to decrease within the membrane substrate. However, with an increase in membrane sulphonation ratio, membrane tensile strength decreased. Thus finding new materials to increase hydrophilicity without sacrificing membrane tensile strength and stability will lead to high performance and sustainable TFC-FO membrane in the future.

Finally this study concludes that high performance membrane for osmotically driven membrane processes can be achieved not only through optimum design of structural characteristics of the support layer but via chemical properties that can affect the substrates characteristics as well. Membrane with hydrophilic support will be critical to minimise the ICP and to improve the flux performance in future process technologies such as FO, PRO and PAO that rely on osmotic force to induce water across polymeric asymmetric membranes. In the meantime, due to the nature of PAO and PRO, membranes with finger-like structure are not stable due to compaction. Thus, developing a high performance membrane free of macro-avoid structure is worthwhile investment.

7.3 Thin film composite supported on woven fabric for pressure assisted osmosis

To date, most of the published papers have used cellulose triacetate with embedded polyester support screen membrane (CTA-ES) from HTI to investigate the PAO process (Oh et al. 2014; Yun et al. 2013b). Low water flux is common in the CTA membranes.

For developing thin film composite membrane on a backing fabric two fabrication methods and a backing fabric support with different properties were investigated. Understanding fundamentals provides a basis for the rational selection of a backing fabric support and fabrication method in order to effectively embed the backing fabric support to produce a wrinkle and defect free TFC membrane for the PAO or FO process under the lab conditions.

The support layer of the FO membranes is typically polymeric micro porous support membranes, which may (or may not) be supported by a non-woven or woven backing fabric. In the PAO membranes since higher mechanical strength is essential, a structural supports by backing fabric is necessary due to withstand hydraulic pressure required in the PAO process.

Polymer penetration through the backing fabric seems to be a challenge in casting FO membrane. Previous studies have used different strategies to mitigate the impact of polymer solution penetration for FO membrane fabrication supported by backing fabric. For example, choosing unique fabrication method (Herron 2008), or a double layer backing fabric to confront the polymer penetration challenge (McGinnis & McGurgan 2013). However, in this study, TFC membrane for the PAO process T_1, T_2 and T_3 developed on a distinguished woven fabric mesh support that not only improved the membrane mechanical strength but limited the polymer penetration and prevent wrinkle formation on the membrane substrate. Membrane support casted on a woven mesh fabrics with a smaller open area (1%, 5%) were wrinkle free due to limited polymer solution penetration while on fabrics with a bigger open area (10%, 25%), severe wrinkles appeared.

This work is therefore aimed at solving the above problems by incorporating woven mesh fabric into the substrate to reinforce and produce a wrinkle and defect free TFC membrane for the PAO process. The compacted woven polyester mesh fabrics reduced wrinkle formation since it is relatively impervious to the polymer solution. In addition to a specific fabric, 2 fabrication methods also have been investigated for fabricating PAO membrane.

Compared to the commercial CTA-ES from HTI, both T_1 and T_2 exhibited superior performance under the PAO process. With a 0.5 M NaCl as DS, T_2 achieved a flux of ~37 L/m^2 h, which was 300% higher than the commercial CTA membrane at an applied pressure of 10 bar. Furthermore, with an increase in applied hydraulic pressure and RSF declines which is in contrast to the conventional FO process. Declining RSF or SRSF with increased hydraulic pressure can be attributed to the force of water flowing from the feed side by applied pressure in the PAO process. This is in addition to osmotic pressure produced by osmotic agents which may reduce the concentration difference close to the membrane surface, the main driving force for RSF.

The study on fabricating thin film composite membrane for pressure assisted osmosis indicates that unlike FO process which requires membrane with a very low structural parameter, higher structure parameter and a membrane free of finger-like structure seems to be more appropriate for the PAO process. In the FO membrane, a higher *A* value (water permeability) and lower S value (structural parameter) are favourable for obtaining higher water flux. However, the PAO needs a stable, dense and porous membrane with high water permeability due to the need to withstand required applied hydraulic pressure during the process. Based on the results, we can conclude

that membranes free of finger like structures with higher water permeability than the CTA membrane and a lower S value than the RO are more favourable for PAO applications.

7.4 Recommendations and future work

FO application in standalone and hybrid system has expanded tremendously in recent years. FO seems to be a promising technology not only to obtain sustainable potable water but also to desalinate brackish water for the agricultural sector. However, several questions need to be answered to enable FO to be used on a commercial scale. For example how much energy is needed to run a FO or hybrid FO to produce water for drinking or other usage. Except for the gear pumps that need to flow the DS and FS solution across the membrane sides, no further energy is required to draw and desalinate water in FO process. However, depending on the product water end use, extra stages are needed to recover the draw solute. This is the most energy intensive part of the FO process especially when the target product is drinking water. That is why; desalination using fertilizer for fertigation seems to be attractive since it does not require DS recovery in the end use product. However, to reduce the fertiliser concentration in the end use product to meet the nutrient level for fertigation, NF is integrated as post-treatment to reduce the fertiliser concentration. Since then further development has been made by this study which suggests and tests the potential of PAO integration instead of FO. This is believed to be a step in the right direction for other units to improve the FDFO desalinating efficiency and reduce the overall energy consumption required for the process. However, a comprehensive economic investigation is needed to evaluate the both integrated systems. The economic efficiency of DS recovery (in the case of FDFO fertigation) or DS full separation (in

the case of potable water as a final product) using RO, NF and UF is not clear enough. Thus, proper investigation is needed to evaluate the PAO economic efficiency to remove the NF as post-treatment in the FDFO desalination unit.

Secondly, PAO has the potential to produce much higher water flux compared to the FO since it exploits the synergies of the two driving forces (osmotic pressure and the hydraulic pressure) in a single stage. It is well-known that higher water flux can increase fouling propensity and consequently the fouled membrane subjected to severe concentration polarization. Thus systematic investigation should be considered regarding the membrane fouling in the PAO and hybrid FO-PAO processes.

Finally, FO membrane has been developed significantly in terms of water flux using hydrophilic membrane substrate through incorporating nanoparticle and chemical treatment such as sulphonation. However, FO and PAO membranes need high selectivity and tensile strength to function sustainably. Therefore, much more investigation is required to develop a hydrophilic membrane substrate without sacrificing those two important factors.

REFERENCES

Achilli, A., Cath, T.Y., Marchand, E.A. & Childress, A.E. 2009, 'The forward osmosis membrane bioreactor: A low fouling alternative to MBR processes', *Desalination*, vol. 239, no. 1-3, pp. 10-21.

Achilli., Cath, T.Y. & Childress, A.E. 2009, 'Power generation with pressure retarded osmosis: An experimental and theoretical investigation', *Journal of Membrane Science*, vol. 343, no. 1–2, pp. 42-52.

Achilli., Cath, T.Y. & Childress, A.E. 2010, 'Selection of inorganic-based draw solutions for forward osmosis applications', *Journal of Membrane Science*, vol. 364, no. 1, pp. 233-41.

Alsvik., Zodrow, K.R., Elimelech, M. & Hägg, M.-B. 2013, 'Polyamide formation on a cellulose triacetate support for osmotic membranes: Effect of linking molecules on membrane performance', *Desalination*, vol. 312, pp. 2-9.

Amini., Jahanshahi, M. & Rahimpour, A. 2013, 'Synthesis of novel thin film nanocomposite (TFN) forward osmosis membranes using functionalized multi-walled carbon nanotubes', *Journal of Membrane Science*, vol. 435, pp. 233-41.

Arena, J.T., McCloskey, B., Freeman, B.D. & McCutcheon, J.R. 2011, 'Surface modification of thin film composite membrane support layers with polydopamine: enabling use of reverse osmosis membranes in pressure retarded osmosis', *Journal of Membrane Science*, vol. 375, no. 1, pp. 55-62.

Arena., McCloskey, B., Freeman, B.D. & McCutcheon, J.R. 2011, 'Surface modification of thin film composite membrane support layers with polydopamine: Enabling use of reverse osmosis membranes in pressure retarded osmosis', *Journal of Membrane Science*, vol. 375, no. 1–2, pp. 55-62.

Ariza., Jones, D.J. & Rozière, J. 2002, 'Role of post-sulfonation thermal treatment in conducting and thermal properties of sulfuric acid sulfonated poly (benzimidazole) membranes', *Desalination*, vol. 147, no. 1, pp. 183-9.

Baker, R.W. 2000, *Membrane technology*, Wiley Online Library.

Bamaga., Yokochi, A., Zabara, B. & Babaqi, A.S. 2011, 'Hybrid FO/RO desalination system: Preliminary assessment of osmotic energy recovery and designs of new FO membrane module configurations', *Desalination*, vol. 268, pp. 163-9.

Banchik, L.D., Sharqawy, M.H. & Lienhard V, J.H. 2014, 'Limits of power production due to finite membrane area in pressure retarded osmosis', *Journal of Membrane Science*.

Banchik. 2013, 'Osmotic mass exchangers for power generation and energy recovery: analysis and analogy to heat exchangers', Massachusetts Institute of Technology.

Banchik., Sharqawy, M.H. & Lienhard V, J.H. 2014a, 'Effectiveness-mass transfer units (ε-MTU) model of a reverse osmosis membrane mass exchanger', *Journal of Membrane Science*, vol. 458, no. 0, pp. 189-98.

Banchik., Sharqawy, M.H. & Lienhard V, J.H. 2014b, 'Limits of power production due to finite membrane area in pressure retarded osmosis', *Journal of Membrane Science*, vol. 468, no. 0, pp. 81-9.

Batchelder, G.W. 1965, 'Process for the demineralization of water', Google Patents, <https://www.google.com/patents/US3171799>.

Beaudry, E.G. & Herron, J.R. 1997, *Direct osmosis for concentrating wastewater*, SAE Technical Paper.

Blanco, J.F., Nguyen, Q.T. & Schaetzel, P. 2001, 'Novel hydrophilic membrane materials: sulfonated polyethersulfone Cardo', *Journal of Membrane Science*, vol. 186, no. 2, pp. 267-79.

Blandin, G., Verliefde, A.R.D., Tang, C.Y., Childress, A.E. & Le-Clech, P. 2013, 'Validation of assisted forward osmosis (AFO) process: Impact of hydraulic pressure', *Journal of Membrane Science*, vol. 447, no. 0, pp. 1-11.

Bokhorst, H., Altena, F.W. & Smolders, C.A. 1981, 'Formation of asymmetric cellulose acetate membranes', *Desalination*, vol. 38, no. 0, pp. 349-60.

Boo, C., Lee, S., Elimelech, M., Meng, Z. & Hong, S. 2012, 'Colloidal fouling in forward osmosis: Role of reverse salt diffusion', *Journal of Membrane Science*, vol. 390–391, no. 0, pp. 277-84.

Bui, N.-N., Lind, M.L., Hoek, E. & McCutcheon, J.R. 2011, 'Electrospun nanofiber supported thin film composite membranes for engineered osmosis', *Journal of Membrane Science*, vol. 385, pp. 10-9.

Bui, N.-N. & McCutcheon, J.R. 2012, 'Hydrophilic Nanofibers as New Supports for Thin Film Composite Membranes for Engineered Osmosis', *Environmental science & technology*, vol. 47, no. 3, pp. 1761-9.

Bui, N.-N. & McCutcheon, J.R. 2013, 'Hydrophilic nanofibers as new supports for thin film composite membranes for engineered osmosis', *Environmental science & technology*, vol. 47, no. 3, pp. 1761-9.

Cadotte, J.E. 1977, 'Reverse osmosis membrane', Google Patents, <https://www.google.com/patents/US4039440>.

Cadotte, J.E. 1981, 'Interfacially synthesized reverse osmosis membrane', Google Patents, <http://www.google.com.au/patents/US4277344>.

Caro, J., Noack, M., Kölsch, P. & Schäfer, R. 2000, 'Zeolite membranes–state of their development and perspective', *Microporous and mesoporous materials*, vol. 38, no. 1, pp. 3-24.

Cath, T.Y., Childress, A.E. & Elimelech, M. 2006, 'Forward osmosis: principles, applications, and recent developments', *Journal of Membrane Science*, vol. 281, no. 1, pp. 70-87.

Cath, T.Y., Elimelech, M., McCutcheon, J.R., McGinnis, R.L., Achilli, A., Anastasio, D., Brady, A.R., Childress, A.E., Farr, I.V. & Hancock, N.T. 2013, 'Standard methodology for evaluating membrane performance in osmotically driven membrane processes', *Desalination*, vol. 312, pp. 31-8.

Cath, T.Y., Gormly, S., Beaudry, E.G., Flynn, M.T., Adams, V.D. & Childress, A.E. 2005, 'Membrane contactor processes for wastewater reclamation in space: Part I. Direct osmotic concentration as pretreatment for reverse osmosis', *Journal of Membrane Science*, vol. 257, no. 1, pp. 85-98.

Cath, T.Y., Hancock, N.T., Lundin, C.D., Hoppe-Jones, C. & Drewes, J.E. 2010, 'A multi-barrier osmotic dilution process for simultaneous desalination and purification of impaired water', *Journal of Membrane Science*, vol. 362, no. 1-2, pp. 417-26.

Chickering III, D., Jacob, J.S., Jong, Y.S. & Mathiowitz, E. 2000, 'Process for preparing microparticles through phase inversion phenomena', Google Patents.

Choi, Y.-J., Choi, J.-S., Oh, H.-J., Lee, S., Yang, D.R. & Kim, J.H. 2009, 'Toward a combined system of forward osmosis and reverse osmosis for seawater desalination', *Desalination*, vol. 247, no. 1-3, pp. 239-46.

Chou, S., Shi, L., Wang, R., Tang, C.Y., Qiu, C. & Fane, A.G. 2010, 'Characteristics and potential applications of a novel forward osmosis hollow fiber membrane', *Desalination*, vol. 261, no. 3, pp. 365-72.

Chung, J.-S. 2012, 'Forward osmosis processes: yesterday, today and tomorrow', *Desalination*, vol. 287, pp. 78-81.

Chung, T.-S., Li, X., Ong, R.C., Ge, Q., Wang, H. & Han, G. 2012, 'Emerging forward osmosis (FO) technologies and challenges ahead for clean water and clean energy applications', *Current Opinion in Chemical Engineering*, vol. 1, no. 3, pp. 246-57.

Coday, B.D., Heil, D.M., Xu, P. & Cath, T.Y. 2013, 'Effects of Transmembrane Hydraulic Pressure on Performance of Forward Osmosis Membranes', *Environmental Science & Technology*, vol. 47, no. 5, pp. 2386-93.

Coday, B.D., Xu, P., Beaudry, E.G., Herron, J., Lampi, K., Hancock, N.T. & Cath, T.Y. 2014, 'The sweet spot of forward osmosis: Treatment of produced water, drilling wastewater, and other complex and difficult liquid streams', *Desalination*, vol. 333, no. 1, pp. 23-35.

Coterillo, C.C., Mendia, A. & Uribe, I.O. 2008, 'Pervaporation and gas separation using microporous membranes', *Inorganic Membranes: Synthesis, Characterization and Applications: Synthesis, Characterization and Applications*, vol. 13, p. 217.

Decher, G. 1997, 'Fuzzy nanoassemblies: toward layered polymeric multicomposites', *Science*, vol. 277, no. 5330, pp. 1232-7.

Duong, P.H., Zuo, J. & Chung, T.-S. 2013, 'Highly crosslinked layer-by-layer polyelectrolyte FO membranes: understanding effects of salt concentration and deposition time on FO performance', *Journal of Membrane Science*, vol. 427, pp. 411-21.

Elimelech, M. 2007, 'Yale constructs forward osmosis desalination pilot plant', *Membrane Technology*, vol. 2007, no. 1, pp. 7-8.

Eun, K.J., Sherub, P., Fezeh, L. & Kyong, S.H. 2014, 'Investigation of pilot-scale 8040 FO membrane module under different operating conditions for brackish water desalination', *Desalination and Water Treatment*, vol. doi: 10.1080/19443994.2014.931528.

Farr, I.V., Bharwada, U.J. & Gullinkala, T. 2013, 'Method to improve forward osmosis membrane performance', Google Patents, <http://www.google.com/patents/WO2013016574A1?cl=en>.

Farr, I.V., Bharwada, U.J. & Gullinkala, T. 2014, 'Method to improve forward osmosis membrane performance', Google Patents, <http://www.google.com/patents/EP2736959A1?cl=en>.

Farr, I.V., Herron, J.R., Bharwada, U.J. & Gullinkala, T. 2013, 'Forward osmosis membrane based on an ipc spacer fabric', Google Patents, <http://www.google.com/patents/WO2013110087A2?cl=en>.

Field, R.W. & Wu, J.J. 2013, 'Mass transfer limitations in forward osmosis: Are some potential applications overhyped?', *Desalination*, vol. 318, pp. 118-24.

Frank, B.S. 1972, 'Desalination of sea water', Google Patents, <https://www.google.com/patents/US3670897>.

Fritzmann, C., Löwenberg, J., Wintgens, T. & Melin, T. 2007, 'State-of-the-art of reverse osmosis desalination', *Desalination*, vol. 216, no. 1, pp. 1-76.

Gadelha, G., Nawaz, M.S., Hankins, N.P., Khan, S.J., Wang, R. & Tang, C.Y. 2014, 'Assessment of micellar solutions as draw solutions for forward osmosis', *Desalination*, vol. 354, pp. 97-106.

Ganesh, B., Isloor, A.M. & Ismail, A. 2013, 'Enhanced hydrophilicity and salt rejection study of graphene oxide-polysulfone mixed matrix membrane', *Desalination*, vol. 313, pp. 199-207.

Garcia-Castello, E.M., McCutcheon, J.R. & Elimelech, M. 2009, 'Performance evaluation of sucrose concentration using forward osmosis', *Journal of Membrane Science*, vol. 338, no. 1, pp. 61-6.

Ge, Q., Ling, M. & Chung, T.-S. 2013, 'Draw solutions for forward osmosis processes: developments, challenges, and prospects for the future', *Journal of Membrane Science*, vol. 442, pp. 225-37.

Ghaffour, N., Missimer, T.M. & Amy, G.L. 2013, 'Technical review and evaluation of the economics of water desalination: current and future challenges for better water supply sustainability', *Desalination*, vol. 309, pp. 197-207.

Ghosh, A.K. & Hoek, E. 2009a, 'Impacts of support membrane structure and chemistry on polyamide–polysulfone interfacial composite membranes', *Journal of Membrane Science*, vol. 336, no. 1, pp. 140-8.

Ghosh, A.K. & Hoek, E.M.V. 2009b, 'Impacts of support membrane structure and chemistry on polyamide–polysulfone interfacial composite membranes', *Journal of Membrane Science*, vol. 336, no. 1–2, pp. 140-8.

Ghosh, A.K., Jeong, B.-H., Huang, X. & Hoek, E.M.V. 2008, 'Impacts of reaction and curing conditions on polyamide composite reverse osmosis membrane properties', *Journal of Membrane Science*, vol. 311, no. 1–2, pp. 34-45.

Glater, J. 1998, 'The early history of reverse osmosis membrane development', *Desalination*, vol. 117, no. 1, pp. 297-309.

Global Water Intelligence (GWI/IDA DesalData), 'Market profile and desalination

markets', *2009–2012 yearbooks and GWI website*

http://www.desaldata.com/.

Gray, G.T., McCutcheon, J.R. & Elimelech, M. 2006, 'Internal concentration polarization in forward osmosis: role of membrane orientation', *Desalination*, vol. 197, no. 1, pp. 1-8.

Greenlee, L.F., Lawler, D.F., Freeman, B.D., Marrot, B. & Moulin, P. 2009, 'Reverse osmosis desalination: water sources, technology, and today's challenges', *Water research*, vol. 43, no. 9, pp. 2317-48.

Guan, R., Zou, H., Lu, D., Gong, C. & Liu, Y. 2005, 'Polyethersulfone sulfonated by chlorosulfonic acid and its membrane characteristics', *European Polymer Journal*, vol. 41, no. 7, pp. 1554-60.

Guillen, G.R., Pan, Y., Li, M. & Hoek, E.M. 2011, 'Preparation and characterization of membranes formed by nonsolvent induced phase separation: a review', *Industrial & Engineering Chemistry Research*, vol. 50, no. 7, pp. 3798-817.

Han, Chung, T.-S., Toriida, M. & Tamai, S. 2012, 'Thin-film composite forward osmosis membranes with novel hydrophilic supports for desalination', *Journal of Membrane Science*, vol. 423, pp. 543-55.

Han., Zhang, S., Li, X., Widjojo, N. & Chung, T.-S. 2012, 'Thin film composite forward osmosis membranes based on polydopamine modified polysulfone substrates with enhancements in both water flux and salt rejection', *Chemical Engineering Science*, vol. 80, pp. 219-31.

Hancock, N.T. & Cath, T.Y. 2009, 'Solute Coupled Diffusion in Osmotically Driven Membrane Processes', *Environmental science & technology*, vol. 43, no. 17, pp. 6769-75.

Helfer, F., Lemckert, C. & Anissimov, Y.G. 2014, 'Osmotic power with Pressure Retarded Osmosis: Theory, performance and trends–A review', *Journal of Membrane Science*, vol. 453, pp. 337-58.

Herron, J. 2008, 'Asymmetric forward osmosis membranes', Google Patents, <https://www.google.com/patents/US7445712>.

Hickenbottom, K.L., Hancock, N.T., Hutchings, N.R., Appleton, E.W., Beaudry, E.G., Xu, P. & Cath, T.Y. 2013a, 'Forward osmosis treatment of drilling mud and fracturing wastewater from oil and gas operations', *Desalination*, vol. 312, pp. 60-6.

Hickenbottom, K.L., Hancock, N.T., Hutchings, N.R., Appleton, E.W., Beaudry, E.G., Xu, P. & Cath, T.Y. 2013b, 'Forward osmosis treatment of drilling mud and fracturing wastewater from oil and gas operations', *Desalination*, vol. 312, no. 0, pp. 60-6.

Hoek, E.M. & Elimelech, M. 2003, 'Cake-enhanced concentration polarization: a new fouling mechanism for salt-rejecting membranes', *Environmental science & technology*, vol. 37, no. 24, pp. 5581-8.

Holloway, R.W., Childress, A.E., Dennett, K.E. & Cath, T.Y. 2007, 'Forward osmosis for concentration of anaerobic digester centrate', *Water research*, vol. 41, no. 17, pp. 4005-14.

Honglei, W., Tai-Shung, C., Wah, T.Y., Kandiah, J., Arunmozhiarasi, A., Zaichun, C., Minghui, H. & Wolfgang, M. 2012, 'Highly Permeable and Selective Pore-Spanning Biomimetic Membrane Embedded with Aquaporin Z', *Small*, vol. 8, no. 8, pp. 1185-90.

Huang, L., Bui, N.-N., Meyering, M.T., Hamlin, T.J. & McCutcheon, J.R. 2013, 'Novel hydrophilic nylon 6, 6 microfiltration membrane supported thin film composite membranes for engineered osmosis', *Journal of Membrane Science*, vol. 437, pp. 141-9.

Hughes, R. 1996, *Industrial membrane separation technology*, Springer.

Husain, S. 2012, 'Methods of preparing a crosslinked fiber membrane', Google Patents, <http://www.google.com.ar/patents/CA2808616A1?cl=en>.

Jeong, B.-H., Hoek, E., Yan, Y., Subramani, A., Huang, X., Hurwitz, G., Ghosh, A.K. & Jawor, A. 2007, 'Interfacial polymerization of thin film nanocomposites: a new concept for reverse osmosis membranes', *Journal of Membrane Science*, vol. 294, no. 1, pp. 1-7.

Jiao, Y., Yang, C. & Kang, Y. 2014, 'Energy Conversion from Salinity Gradients by Forward Osmosis–Electrokinetics', *The Journal of Physical Chemistry C*, vol. 118, no. 20, pp. 10574-83.

Johnson, P.M., Yoon, J., Kelly, J.Y., Howarter, J.A. & Stafford, C.M. 2012, 'Molecular layer-by-layer deposition of highly crosslinked polyamide films',

Journal of Polymer Science Part B: Polymer Physics, vol. 50, no. 3, pp. 168-73.

Kang, G., Liu, M., Lin, B., Cao, Y. & Yuan, Q. 2007, 'A novel method of surface modification on thin-film composite reverse osmosis membrane by grafting poly (ethylene glycol)', *Polymer*, vol. 48, no. 5, pp. 1165-70.

Kar, S., Bindal, R. & Tewari, P. 2012, 'Carbon nanotube membranes for desalination and water purification: Challenges and opportunities', *Nano Today*, vol. 7, no. 5, pp. 385-9.

Kaufman, Y., Berman, A. & Freger, V. 2010, 'Supported lipid bilayer membranes for water purification by reverse osmosis', *Langmuir*, vol. 26, no. 10, pp. 7388-95.

Kedem, O. & Katchalsky, A. 1963, 'Permeability of composite membranes. Part 1.—Electric current, volume flow and flow of solute through membranes', *Trans. Faraday Soc.*, vol. 59, pp. 1918-30.

Kessler, J. & Moody, C. 1976, 'Drinking water from sea water by forward osmosis', *Desalination*, vol. 18, no. 3, pp. 297-306.

Kim, I., Choi, J. & Tak, T. 1999, 'Sulfonated polyethersulfone by heterogeneous method and its membrane performances', *Journal of Applied Polymer Science*, vol. 74, no. 8, pp. 2046-55.

Kim, J.-j., Chung, J.-S., Kang, H., Yu, Y.A., Choi, W.J., Kim, H.J. & Lee, J.-C. 2014, 'Thermo-responsive copolymers with ionic group as novel draw solutes for forward osmosis processes', *Macromolecular Research*, vol. 22, no. 9, pp. 963-70.

Kim, Y., Han, S. & Hong, S. 2011, 'A feasibility study of magnetic separation of magnetic nanoparticle for forward osmosis', *Water Science & Technology*, vol. 64, no. 2, pp. 469-76.

Kim, Y.C. & Elimelech, M. 2012, 'Adverse impact of feed channel spacers on the performance of pressure retarded osmosis', *Environmental science & technology*, vol. 46, no. 8, pp. 4673-81.

Kimura, S. & Nakao, S.-I. 1975, 'Fouling of cellulose acetate tubular reverse osmosis modules treating the industrial water in Tokyo', *Desalination*, vol. 17, no. 3, pp. 267-88.

Klemm, D., Schumann, D., Kramer, F., Heßler, N., Hornung, M., Schmauder, H.-P. & Marsch, S. 2006, 'Nanocelluloses as innovative polymers in research and application', *Polysaccharides Ii*, Springer, pp. 49-96.

Kravath, R.E. & Davis, J.A. 1975, 'Desalination of sea water by direct osmosis', *Desalination*, vol. 16, no. 2, pp. 151-5.

Kumar, M., Grzelakowski, M., Zilles, J., Clark, M. & Meier, W. 2007, 'Highly permeable polymeric membranes based on the incorporation of the functional

water channel protein Aquaporin Z', *Proceedings of the National Academy of Sciences*, vol. 104, no. 52, pp. 20719-24.

Lacey, R.E. & Loeb, S. 1972, *Industrial processing with membranes*.

Lee, J.J., Woo, Y.C. & Kim, H.-S. 2014, 'Effect of driving pressure and recovery rate on the performance of nanofiltration and reverse osmosis membranes for the treatment of the effluent from MBR', *Desalination and Water Treatment*, pp. 1-7.

Lee, K., Baker, R. & Lonsdale, H. 1981a, 'Membranes for power generation by pressure-retarded osmosis', *Journal of Membrane Science*, vol. 8, no. 2, pp. 141-71.

Lee, K.L., Baker, R.W. & Lonsdale, H.K. 1981b, 'Membranes for power generation by pressure-retarded osmosis', *Journal of Membrane Science*, vol. 8, no. 2, pp. 141-71.

Lee, K.P., Arnot, T.C. & Mattia, D. 2011, 'A review of reverse osmosis membrane materials for desalination—Development to date and future potential', *Journal of Membrane Science*, vol. 370, no. 1–2, pp. 1-22.

Lee, L.T. & Liu, K.-J. 1976, 'Method of making permselective interpolymer membranes', Google Patents.

Li, D., Zhang, X., Yao, J., Simon, G.P. & Wang, H. 2011, 'Stimuli-responsive polymer hydrogels as a new class of draw agent for forward osmosis desalination', *Chem. Commun.*, vol. 47, no. 6, pp. 1710-2.

Li, X., Wang, K.Y., Helmer, B. & Chung, T.-S. 2012, 'Thin-film composite membranes and formation mechanism of thin-film layers on hydrophilic cellulose acetate propionate substrates for forward osmosis processes', *Industrial & Engineering Chemistry Research*, vol. 51, no. 30, pp. 10039-50.

Li, Y., Krantz, W.B. & Chung, T.S. 2007, 'A novel primer to prevent nanoparticle agglomeration in mixed matrix membranes', *AIChE Journal*, vol. 53, no. 9, pp. 2470-5.

Lin, S., Yip, N.Y., Cath, T.Y., Osuji, C.O. & Elimelech, M. 2014, 'Hybrid Pressure Retarded Osmosis–Membrane Distillation System for Power Generation from Low-Grade Heat: Thermodynamic Analysis and Energy Efficiency', *Environmental science & technology*, vol. 48, no. 9, pp. 5306-13.

Ling, M.M. & Chung, T.-S. 2011a, 'Desalination process using super hydrophilic nanoparticles via forward osmosis integrated with ultrafiltration regeneration', *Desalination*, vol. 278, pp. 194-202.

Ling, M.M. & Chung, T.-S. 2011b, 'Novel dual-stage FO system for sustainable protein enrichment using nanoparticles as intermediate draw solutes', *Journal of Membrane Science*, vol. 372, no. 1–2, pp. 201-9.

Ling, M.M., Wang, K.Y. & Chung, T.-S. 2010, 'Highly Water-Soluble Magnetic Nanoparticles as Novel Draw Solutes in Forward Osmosis for Water Reuse', *Industrial & Engineering Chemistry Research*, vol. 49, no. 12, pp. 5869-76.

Liu, L., Wang, M., Wang, D. & Gao, C. 2009, 'Current Patents of Forward Osmosis Membrane Process', *Recent Patents on Chemical Engineering*, vol. 2, no. 1, pp. 76-82.

Loeb, S. 2002, 'Large-scale power production by pressure-retarded osmosis, using river water and sea water passing through spiral modules', *Desalination*, vol. 143, no. 2, pp. 115-22.

Loeb, S., Bloch, M.R. & Isaacs, J.D. 1978, 'Salinity Power, Potential and Processes, Especially Membrane Processes', *Advances in oceanography*, Springer, pp. 267-88.

Loeb, S., Titelman, L., Korngold, E. & Freiman, J. 1997, 'Effect of porous support fabric on osmosis through a Loeb-Sourirajan type asymmetric membrane', *Journal of Membrane Science*, vol. 129, no. 2, pp. 243-9.

Loeb, S., Van Hessen, F., Levi, J. & Ventura, M. 1976, 'The osmotic power plant', *11th Intersociety Energy Conversion Engineering Conference*, vol. 1, pp. 51-7.

Logan & Elimelech 2012, 'Membrane-based processes for sustainable power generation using water', *Nature*, vol. 488, no. 7411, pp. 313-9.

Lojou, É. & Bianco, P. 2004, 'Buildup of polyelectrolyte-protein multilayer assemblies on gold electrodes. Role of the hydrophobic effect', *Langmuir*, vol. 20, no. 3, pp. 748-55.

Lonsdale, H. 1982, 'The growth of membrane technology', *Journal of Membrane Science*, vol. 10, no. 2, pp. 81-181.

Lutchmiah, K., Verliefde, A., Roest, K., Rietveld, L. & Cornelissen, E. 2014, 'Forward osmosis for application in wastewater treatment: A review', *Water research*, vol. 58, pp. 179-97.

Ma, N., Wei, J., Liao, R. & Tang, C.Y. 2012, 'Zeolite-polyamide thin film nanocomposite membranes: Towards enhanced performance for forward osmosis', *Journal of Membrane Science*, vol. 405–406, no. 0, pp. 149-57.

Ma, N., Wei, J., Qi, S., Zhao, Y., Gao, Y. & Tang, C.Y. 2013, 'Nanocomposite substrates for controlling internal concentration polarization in forward osmosis membranes', *Journal of Membrane Science*, vol. 441, pp. 54-62.

Ma, Z., Kotaki, M. & Ramakrishna, S. 2005, 'Electrospun cellulose nanofiber as affinity membrane', *Journal of Membrane Science*, vol. 265, no. 1, pp. 115-23.

Mallevialle, J., Odendaal, P.E. & Wiesner, M.R. 1996, *Water treatment membrane processes*, American Water Works Association.

Mark, H.F. 1968, 'Encyclopedia of polymer science and technology; Plastics, resins, rubbers, fibers. Vol. 8. Keratin to modacrylic fibers'.

Mark, H.F. & Kroschwitz, J.I. 1989, *Encyclopedia of polymer science and engineering*, Wiley.

Mathew, A.P., Karim, Z., Liu, P. & Oksman, K. 2013, 'Nanocellulose for water purification membranes', *Production and Applications of Cellulose Nanomaterials*.

McCormick., Pellegrino, J., Mantovani, F. & Sarti, G. 2008, 'Water, salt, and ethanol diffusion through membranes for water recovery by forward (direct) osmosis processes', *Journal of Membrane Science*, vol. 325, no. 1, pp. 467-78.

McCutcheon & Elimelech 2006a, 'Influence of concentrative and dilutive internal concentration polarization on flux behavior in forward osmosis', *Journal of Membrane Science*, vol. 284, no. 1-2, pp. 237-47.

McCutcheon & Elimelech, M. 2008a, 'Influence of membrane support layer hydrophobicity on water flux in osmotically driven membrane processes', *Journal of Membrane Science*, vol. 318, no. 1, pp. 458-66.

McCutcheon, McGinnis, R.L. & Elimelech, M. 2006, 'Desalination by ammonia–carbon dioxide forward osmosis: Influence of draw and feed solution concentrations on process performance', *Journal of Membrane Science*, vol. 278, no. 1–2, pp. 114-23.

McCutcheon, J.R. & Elimelech, M. 2006b, 'Influence of concentrative and dilutive internal concentration polarization on flux behavior in forward osmosis', *Journal of Membrane Science*, vol. 284, no. 1–2, pp. 237-47.

McCutcheon, J.R. & Elimelech, M. 2006c, 'Influence of concentrative and dilutive internal concentration polarization on flux behavior in forward osmosis', *Journal of Membrane Science*, vol. 284, no. 1, pp. 237-47.

Mccutcheon, J.R. & Elimelech, M. 2007, 'Modeling water flux in forward osmosis: implications for improved membrane design', *AIChE Journal*, vol. 53, no. 7, pp. 1736-44.

McCutcheon, J.R. & Elimelech, M. 2008b, 'Influence of membrane support layer hydrophobicity on water flux in osmotically driven membrane processes', *Journal of Membrane Science*, vol. 318, no. 1–2, pp. 458-66.

McCutcheon, J.R., McGinnis, R.L. & Elimelech, M. 2005, 'A novel ammonia—carbon dioxide forward (direct) osmosis desalination process', *Desalination*, vol. 174, no. 1, pp. 1-11.

McCutcheon. & Elimelech. 2007, 'Modeling water flux in forward osmosis: Implications for improved membrane design', *AIChE Journal*, vol. 53, no. 7, pp. 1736-44.

McCutcheon., McGinnis, R.L. & Elimelech, M. 2005, 'A novel ammonia—carbon dioxide forward (direct) osmosis desalination process', *Desalination*, vol. 174, no. 1, pp. 1-11.

McGinnis & Elimelech, M. 2008, 'Global challenges in energy and water supply: the promise of engineered osmosis', *Environmental science & technology*, vol. 42, no. 23, pp. 8625-9.

McGinnis, R. & McGurgan, G. 2013, 'Forward osmosis membranes', Google Patents, <https://www.google.com/patents/US8460554>.

McGinnis, R.L. 2002, 'Osmotic desalinization process', Google Patents, <https://www.google.com/patents/US6391205>.

Mi, B. & Elimelech, M. 2008, 'Chemical and physical aspects of organic fouling of forward osmosis membranes', *Journal of Membrane Science*, vol. 320, no. 1–2, pp. 292-302.

Mi, B. & Elimelech, M. 2010, 'Organic fouling of forward osmosis membranes: fouling reversibility and cleaning without chemical reagents', *Journal of Membrane Science*, vol. 348, no. 1, pp. 337-45.

Miller, R., Mark, H. & Gaylord, N. 1966, 'Encyclopedia of Polymer Science and Technology', *Vol. 4Wiley, New York, USA*, p. 451.

Mitragotri, S., Anissimov, Y.G., Bunge, A.L., Frasch, H.F., Guy, R.H., Hadgraft, J., Kasting, G.B., Lane, M.E. & Roberts, M.S. 2011, 'Mathematical models of skin permeability: An overview', *International journal of pharmaceutics*, vol. 418, no. 1, pp. 115-29.

Ng, H.Y., Tang, W. & Wong, W.S. 2006, 'Performance of forward (direct) osmosis process: membrane structure and transport phenomenon', *Environmental science & technology*, vol. 40, no. 7, pp. 2408-13.

Nunes, S.P. & Peinemann, K.-V. 2001, *Membrane technology*, Wiley Online Library.

Oh, Y., Lee, S., Elimelech, M., Lee, S. & Hong, S. 2014, 'Effect of hydraulic pressure and membrane orientation on water flux and reverse solute flux in pressure assisted osmosis', *Journal of Membrane Science*, vol. 465, no. 0, pp. 159-66.

Pearce, G.K. 2008, 'UF/MF pre-treatment to RO in seawater and wastewater reuse applications: a comparison of energy costs', *Desalination*, vol. 222, no. 1–3, pp. 66-73.

Peinemann, K.-V., Gerstandt, K., Skilhagen, S.E., Thorsen, T. & Holt, T. 2008, 'Membranes for Power Generation by Pressure Retarded Osmosis', *Membranes for Energy Conversion*, Wiley-VCH Verlag GmbH & Co. KGaA, pp. 263-73.

Pendergast, M.T.M., Nygaard, J.M., Ghosh, A.K. & Hoek, E. 2010, 'Using nanocomposite materials technology to understand and control reverse osmosis membrane compaction', *Desalination*, vol. 261, no. 3, pp. 255-63.

Perreault, F., Tousley, M.E. & Elimelech, M. 2013, 'Thin-Film Composite Polyamide Membranes Functionalized with Biocidal Graphene Oxide Nanosheets', *Environmental Science & Technology Letters*, vol. 1, no. 1, pp. 71-6.

Petersen, R.J. 1993, 'Composite reverse osmosis and nanofiltration membranes', *Journal of Membrane Science*, vol. 83, no. 1, pp. 81-150.

Phillip, W.A., Yong, J.S. & Elimelech, M. 2010, 'Reverse Draw Solute Permeation in Forward Osmosis: Modeling and Experiments', *Environmental Science & Technology*, vol. 44, no. 13, pp. 5170-6.

Phuntsho, S., HoKyong, S., Seungkwan, H., Sangyoup, L., Saravanamuthu, V. & Jaya, K. 2012, 'Fertiliser drawn forward osmosis desalination: the concept, performance and limitations for fertigation', *Reviews in Environmental Science and Bio/Technology*, vol. 11, no. 2, pp. 147-68.

Phuntsho, S., Seung-kwan, H., Menachem, E. & Kyong, S.H. 2013, 'Forward osmosis desalination of brackish groundwater: Meeting water quality requirements for fertigation by integrating nanofiltration', *Journal of Membrane Science*, vol. 436, no. 0, pp. 1-15.

Phuntsho, S., Shon, H.K., Hong, S., Lee, S. & Vigneswaran, S. 2011, 'A novel low energy fertilizer driven forward osmosis desalination for direct fertigation: evaluating the performance of fertilizer draw solutions', *Journal of Membrane Science*, vol. 375, no. 1, pp. 172-81.

Phuntsho, S., Shon , H.K., Majeed, T., El Saliby, I., Vigneswaran, S., Kandasamy, J., Hong, S. & Lee, S. 2012, 'Blended fertilizers as draw solutions for fertilizer-drawn forward osmosis desalination', *Environmental science & technology*, vol. 46, no. 8, pp. 4567-75.

Phuntsho., Hong, S., Elimelech, M. & Shon, H.K. 2014, 'Osmotic equilibrium in the forward osmosis process: Modelling, experiments and implications for process performance', *Journal of Membrane Science*, vol. 453, pp. 240-52.

Phuntsho., Shon, H.K., Majeed, T., El Salibya, I., Vigneswarana, S., Kandasamy, J., Hong, S. & Leeb, S. 2012, 'Blended fertilisers as draw solutions for fertiliser drawn forward osmosis desalination', *Environmental science & technology*, vol. 46, no. 8, p. 4567−75.

Phuntsho., S., Soleyman, S., Tahir, M., Fezeh, L., Eun, K.J. & Kyong, S.H. 2013, 'Assessing the major factors affecting the performances of forward osmosis and its implications on the desalination process', *Chemical Engineering Journal*, vol. 231, no. 0, pp. 484-96.

Picorel, R., Chumanov, G., Torrado, E., Cotton, T.M. & Seibert, M. 1998, 'Surface-Enhanced Resonance Raman Scattering Spectroscopy of Plant Photosystem II

Reaction Centers Excited on the Red-Edge of the Q y Band', *The Journal of Physical Chemistry B*, vol. 102, no. 15, pp. 2609-13.

Qadir, M., Sharma, B., Bruggeman, A., Choukr-Allah, R. & Karajeh, F. 2007, 'Non-conventional water resources and opportunities for water augmentation to achieve food security in water scarce countries', *Agricultural water management*, vol. 87, no. 1, pp. 2-22.

Qiu, C., Qi, S. & Tang, C.Y. 2011, 'Synthesis of high flux forward osmosis membranes by chemically crosslinked layer-by-layer polyelectrolytes', *Journal of Membrane Science*, vol. 381, no. 1, pp. 74-80.

Qiu, C., Setiawan, L., Wang, R., Tang, C.Y. & Fane, A.G. 2012a, 'High performance flat sheet forward osmosis membrane with an NF-like selective layer on a woven fabric embedded substrate', *Desalination*, vol. 287, pp. 266-70.

Qiu, C., Setiawan, L., Wang, R., Tang, C.Y. & Fane, A.G. 2012b, 'High performance flat sheet forward osmosis membrane with an NF-like selective layer on a woven fabric embedded substrate', *Desalination*, vol. 287, no. 0, pp. 266-70.

Rahardianto, A., Gao, J., Gabelich, C.J., Williams, M.D. & Cohen, Y. 2007, 'High recovery membrane desalting of low-salinity brackish water: Integration of accelerated precipitation softening with membrane RO', *Journal of Membrane Science*, vol. 289, no. 1, pp. 123-37.

Ramakrishna, S., Fujihara, K., Teo, W.-E., Lim, T.-C. & Ma, Z. 2005, *An introduction to electrospinning and nanofibers*, vol. 90, World Scientific.

Ramakrishna, S., Fujihara, K., Teo, W.-E., Yong, T., Ma, Z. & Ramaseshan, R. 2006, 'Electrospun nanofibers: solving global issues', *Materials Today*, vol. 9, no. 3, pp. 40-50.

Rigaud, J.-L., Pitard, B. & Levy, D. 1995, 'Reconstitution of membrane proteins into liposomes: application to energy-transducing membrane proteins', *Biochimica et Biophysica Acta (BBA)-Bioenergetics*, vol. 1231, no. 3, pp. 223-46.

Rong, W., Lei, S., Chuyang, T., Shuren, C., Changquan, Q. & Anthony, F. 2010, 'Characterization of novel forward osmosis hollow fiber membranes', *Journal of Membrane Science*, vol. 355, no. 1–2, pp. 158-67.

S., L., Y.B, Y. & Seo, S.K. 2012, 'Forward osmosis membranes and method for fabricating the same', Google Patents, <https://www.google.com/patents/US20120012520>.

Sagle, A. & Freeman, B. 2004, 'Fundamentals of membranes for water treatment', *the future of desalination in Texas*, vol. 2, pp. 137-54.

Sahebi, Phuntsho, S., Eun Kim, J., Hong, S. & Kyong Shon, H., 'Pressure assisted fertiliser drawn osmosis process to enhance final dilution of the fertiliser draw solution beyond osmotic equilibrium', *Journal of Membrane Science*, no. 0.

Sahebi, s., Phuntsho, S., Jung, E.K., Seungkwan, H. & Shon, K. 2015, 'Pressure assisted fertiliser drawn osmosis process to enhance final dilution of the fertiliser draw solution beyond osmotic equilibrium', *Journal of Membrane Science*, vol. 481, no. 0, pp. 63-72.

Saren, Q., Qiu, C.Q. & Tang, C.Y. 2011, 'Synthesis and characterization of novel forward osmosis membranes based on layer-by-layer assembly', *Environmental science & technology*, vol. 45, no. 12, pp. 5201-8.

Schwinge, J., Neal, P., Wiley, D., Fletcher, D. & Fane, A. 2004, 'Spiral wound modules and spacers: review and analysis', *Journal of Membrane Science*, vol. 242, no. 1, pp. 129-53.

Setiawan, L., Wang, R., Li, K. & Fane, A.G. 2011, 'Fabrication of novel poly (amide–imide) forward osmosis hollow fiber membranes with a positively charged nanofiltration-like selective layer', *Journal of Membrane Science*, vol. 369, no. 1, pp. 196-205.

Shaffer, D.L., Arias Chavez, L.H., Ben-Sasson, M., Romero-Vargas Castrillón, S., Yip, N.Y. & Elimelech, M. 2013, 'Desalination and reuse of high-salinity shale gas produced water: drivers, technologies, and future directions', *Environmental science & technology*, vol. 47, no. 17, pp. 9569-83.

She, Q., Jin, X., Li, Q. & Tang, C.Y. 2012, 'Relating reverse and forward solute diffusion to membrane fouling in osmotically driven membrane processes', *Water research*, vol. 46, no. 7, pp. 2478-86.

She, Q., Jin, X. & Tang, C.Y. 2012, 'Osmotic power production from salinity gradient resource by pressure retarded osmosis: Effects of operating conditions and reverse solute diffusion', *Journal of Membrane Science*, vol. 401–402, no. 0, pp. 262-73.

Shuaifei, Z., Linda, Z., Y, T.C. & Dennis, M. 2012, 'Recent developments in forward osmosis: opportunities and challenges', *Journal of Membrane Science*, vol. 396, pp. 1-21.

Sincero, A.P. & Sincero, G.A. 2002, *Physical-chemical treatment of water and wastewater*, CRC press.

Singh, P.S., Joshi, S.V., Trivedi, J.J., Devmurari, C.V., Rao, A.P. & Ghosh, P.K. 2006, 'Probing the structural variations of thin film composite RO membranes obtained by coating polyamide over polysulfone membranes of different pore dimensions', *Journal of Membrane Science*, vol. 278, no. 1–2, pp. 19-25.

Smitha, B., Sridhar, S. & Khan, A. 2003, 'Synthesis and characterization of proton conducting polymer membranes for fuel cells', *Journal of Membrane Science*, vol. 225, no. 1, pp. 63-76.

Song, X., Liu, Z. & Sun, D.D. 2011, 'Nano gives the answer: breaking the bottleneck of internal concentration polarization with a nanofiber composite forward osmosis membrane for a high water production rate', *Advanced Materials*, vol. 23, no. 29, pp. 3256-60.

Stache, K. 1989, 'Apparatus for transforming sea water, brackish water, polluted water or the like into a nutrious drink by means of osmosis', Google Patents.

Stephenson, T., Judd, S., Jefferson, B., Brindle, K. & Association, I.W. 2000, 'Membrane bioreactors for wastewater treatment'.

Su, J., Yang, Q., Teo, J.F. & Chung, T.-S. 2010, 'Cellulose acetate nanofiltration hollow fiber membranes for forward osmosis processes', *Journal of Membrane Science*, vol. 355, no. 1, pp. 36-44.

Sukitpaneenit, P. & Chung, T.-S. 2009, 'Molecular elucidation of morphology and mechanical properties of PVDF hollow fiber membranes from aspects of phase inversion, crystallization and rheology', *Journal of Membrane Science*, vol. 340, no. 1–2, pp. 192-205.

Sukitpaneenit, P. & Chung, T.-S. 2012, 'High performance thin-film composite forward osmosis hollow fiber membranes with macrovoid-free and highly porous structure for sustainable water production', *Environmental science & technology*, vol. 46, no. 13, pp. 7358-65.

Sun, G., Chung, T.-S., Jeyaseelan, K. & Armugam, A. 2013, 'A layer-by-layer self-assembly approach to developing an aquaporin-embedded mixed matrix membrane', *RSC Advances*, vol. 3, no. 2, pp. 473-81.

Tan, C.H. & Ng, H.Y. 2008, 'Modified models to predict flux behavior in forward osmosis in consideration of external and internal concentration polarizations', *Journal of Membrane Science*, vol. 324, no. 1, pp. 209-19.

Tan, C.H. & Ng, H.Y. 2010, 'A novel hybrid forward osmosis – nanofiltration (FO-NF) process for seawater desalination: Draw solution selection and system configuration', *Desalination and Water Treatment*, vol. 13, no. 2010, pp. 356–61.

Tang, C., QIU, C., Wei, J., Wang, R. & Fane, A.G. 2014, 'Forward osmosis membrane and method of forming a forward osmosis membrane', Google Patents, <http://www.google.com/patents/US20140008291>.

Tang, C., Zhao, Y., Wang, R., Hélix-Nielsen, C. & Fane, A. 2013, 'Desalination by biomimetic aquaporin membranes: Review of status and prospects', *Desalination*, vol. 308, pp. 34-40.

Tang, C.Y., Kwon, Y.-N. & Leckie, J.O. 2009, 'Effect of membrane chemistry and coating layer on physiochemical properties of thin film composite polyamide RO and NF membranes: I. FTIR and XPS characterization of polyamide and coating layer chemistry', *Desalination*, vol. 242, no. 1–3, pp. 149-67.

Tang, C.Y., She, Q., Lay, W.C., Wang, R. & Fane, A.G. 2010, 'Coupled effects of internal concentration polarization and fouling on flux behavior of forward osmosis membranes during humic acid filtration', *Journal of Membrane Science*, vol. 354, no. 1, pp. 123-33.

Tang., Kwon, Y.-N. & Leckie, J.O. 2009, 'Effect of membrane chemistry and coating layer on physiochemical properties of thin film composite polyamide RO and NF membranes: I. FTIR and XPS characterization of polyamide and coating layer chemistry', *Desalination*, vol. 242, no. 1, pp. 149-67.

Tang., She, Q., Lay, W.C.L., Wang, R. & Fane, A.G. 2010, 'Coupled effects of internal concentration polarization and fouling on flux behavior of forward osmosis membranes during humic acid filtration', *Journal of Membrane Science*, vol. 354, no. 1-2, pp. 123-33.

Tavolaro, A. & Drioli, E. 1999, 'Zeolite membranes', *Advanced Materials*, vol. 11, no. 12, pp. 975-96.

Tijing, L.D., Choi, J.-S., Lee, S., Kim, S.-H. & Shon, H.K. 2014, 'Recent progress of membrane distillation using electrospun nanofibrous membrane', *Journal of Membrane Science*, vol. 453, pp. 435-62.

Tiraferri, A., Yip, N.Y., Phillip, W.A., Schiffman, J.D. & Elimelech, M. 2011a, 'Relating performance of thin-film composite forward osmosis membranes to support layer formation and structure', *Journal of Membrane Science*, vol. 367, no. 1, pp. 340-52.

Tiraferri, A., Yip, N.Y., Phillip, W.A., Schiffman, J.D. & Elimelech, M. 2011b, 'Relating performance of thin-film composite forward osmosis membranes to support layer formation and structure', *Journal of Membrane Science*, vol. 367, no. 1–2, pp. 340-52.

Tsay, C. & McHugh, A. 1990, 'Mass transfer modeling of asymmetric membrane formation by phase inversion', *Journal of Polymer Science Part B: Polymer Physics*, vol. 28, no. 8, pp. 1327-65.

Vörösmarty, C.J., McIntyre, P., Gessner, M.O., Dudgeon, D., Prusevich, A., Green, P., Glidden, S., Bunn, S.E., Sullivan, C.A. & Liermann, C.R. 2010, 'Global threats to human water security and river biodiversity', *Nature*, vol. 467, no. 7315, pp. 555-61.

Wang, H., Xiang, Z., Hu, C.-F., Pant, A., Fang, W., Alonso, S., Pastorin, G. & Lee, C. 2013, 'Development of Stretchable Membrane Based Nanofilters Using Patterned Array of Vertically Grown Carbon Nanotubes', *Nanoscale*.

Wang, K.Y., Chung, T.-S. & Amy, G. 2012a, 'Developing thin-film-composite forward osmosis membranes on the PES/SPSf substrate through interfacial polymerization', *AIChE Journal*, vol. 58, no. 3, pp. 770-81.

Wang, K.Y., Chung, T.S. & Amy, G. 2012b, 'Developing thin-film-composite forward osmosis membranes on the PES/SPSf substrate through interfacial polymerization', *AIChE Journal*, vol. 58, no. 3, pp. 770-81.

Wang, K.Y., Ong, R.C. & Chung, T.-S. 2010, 'Double-skinned forward osmosis membranes for reducing internal concentration polarization within the porous sublayer', *Industrial & Engineering Chemistry Research*, vol. 49, no. 10, pp. 4824-31.

Wang, K.Y., Teoh, M.M., Nugroho, A. & Chung, T.-S. 2011, 'Integrated forward osmosis–membrane distillation (FO–MD) hybrid system for the concentration of protein solutions', *Chemical Engineering Science*, vol. 66, no. 11, pp. 2421-30.

Wang, K.Y., Yang, Q., Chung, T.-S. & Rajagopalan, R. 2009, 'Enhanced forward osmosis from chemically modified polybenzimidazole (PBI) nanofiltration hollow fiber membranes with a thin wall', *Chemical Engineering Science*, vol. 64, no. 7, pp. 1577-84.

Wei, J., Qiu, C., Tang, C.Y., Wang, R. & Fane, A.G. 2011a, 'Synthesis and characterization of flat-sheet thin film composite forward osmosis membranes', *Journal of Membrane Science*, vol. 372, no. 1, pp. 292-302.

Wei, J., Qiu, C., Tang, C.Y., Wang, R. & Fane, A.G. 2011b, 'Synthesis and characterization of flat-sheet thin film composite forward osmosis membranes', *Journal of Membrane Science*, vol. 372, no. 1–2, pp. 292-302.

Wen, S., Gong, C., Tsen, W.-C., Shu, Y.-C. & Tsai, F.-C. 2009, 'Sulfonated poly (ether sulfone)(SPES)/boron phosphate (BPO 4) composite membranes for high-temperature proton-exchange membrane fuel cells', *International journal of hydrogen energy*, vol. 34, no. 21, pp. 8982-91.

Widjojo, N., Chung, T.-S., Weber, M., Maletzko, C. & Warzelhan, V. 2011, 'The role of sulphonated polymer and macrovoid-free structure in the support layer for thin-film composite (TFC) forward osmosis (FO) membranes', *Journal of Membrane Science*, vol. 383, no. 1, pp. 214-23.

Widjojo, N., Chung, T.-S., Weber, M., Maletzko, C. & Warzelhan, V. 2013, 'A sulfonated polyphenylenesulfone (sPPSU) as the supporting substrate in thin film composite (TFC) membranes with enhanced performance for forward osmosis (FO)', *Chemical Engineering Journal*, vol. 220, pp. 15-23.

Wijmans, J., Baaij, J. & Smolders, C. 1983, 'The mechanism of formation of microporous or skinned membranes produced by immersion precipitation', *Journal of Membrane Science*, vol. 14, no. 3, pp. 263-74.

Wijmans, J., Kant, J., Mulder, M. & Smolders, C. 1985a, 'Phase separation phenomena in solutions of polysulfone in mixtures of a solvent and a nonsolvent: relationship with membrane formation', *Polymer*, vol. 26, no. 10, pp. 1539-45.

Wijmans, J.G., Kant, J., Mulder, M.H.V. & Smolders, C.A. 1985b, 'Phase separation phenomena in solutions of polysulfone in mixtures of a solvent and a nonsolvent: relationship with membrane formation', *Polymer*, vol. 26, no. 10, pp. 1539-45.

Williams, M.E. 2003, 'A brief review of reverse osmosis membrane technology', *EET Corporation and Williams Engineering Services Company*, p. 2.

Xiao, D., Tang, C.Y., Zhang, J., Lay, W.C.L., Wang, R. & Fane, A.G. 2011, 'Modeling salt accumulation in osmotic membrane bioreactors: Implications

for FO membrane selection and system operation', *Journal of Membrane Science*, vol. 366, no. 1–2, pp. 314-24.

Xiao, Y., Chng, M.L., Chung, T.-S., Toriida, M., Tamai, S., Chen, H. & Jean, Y.J. 2010, 'Asymmetric structure and enhanced gas separation performance induced by in situ growth of silver nanoparticles in carbon membranes', *Carbon*, vol. 48, no. 2, pp. 408-16.

Xie, M., Nghiem, L.D., Price, W.E. & Elimelech, M. 2013, 'A Forward Osmosis–Membrane Distillation Hybrid Process for Direct Sewer Mining: System Performance and Limitations', *Environmental science & technology*, vol. 47, no. 23, pp. 13486-93.

Xie, W., He, F., Wang, B., Chung, T.-S., Jeyaseelan, K., Armugam, A. & Tong, Y.W. 2013, 'An aquaporin-based vesicle-embedded polymeric membrane for low energy water filtration', *Journal of Materials Chemistry A*, vol. 1, no. 26, pp. 7592-600.

Xie, W. & Tong, Y., 'Aquaporin Z embedded membrane for water purification'.

Xu, Y., Peng, X., Tang, C.Y., Fu, Q.S. & Nie, S. 2010, 'Effect of draw solution concentration and operating conditions on forward osmosis and pressure retarded osmosis performance in a spiral wound module', *Journal of Membrane Science*, vol. 348, no. 1, pp. 298-309.

Yang, Q., Wang, K.Y. & Chung, T.-S. 2009, 'A novel dual-layer forward osmosis membrane for protein enrichment and concentration', *Separation and Purification Technology*, vol. 69, no. 3, pp. 269-74.

Yangali-Quintanilla, V., Li, Z., Valladares, R., Li, Q. & Amy, G. 2011, 'Indirect desalination of Red Sea water with forward osmosis and low pressure reverse osmosis for water reuse', *Desalination*, vol. 280, no. 1–3, pp. 160-6.

Yip, N.Y. & Elimelech, M. 2011, 'Performance limiting effects in power generation from salinity gradients by pressure retarded osmosis', *Environmental science & technology*, vol. 45, no. 23, pp. 10273-82.

Yip, N.Y., Tiraferri, A., Phillip, W.A., Schiffman, J.D. & Elimelech, M. 2010, 'High performance thin-film composite forward osmosis membrane', *Environmental Science & Technology*, vol. 44, no. 10, pp. 3812-8.

You, S., Tang, C., Yu, C., Wang, X., Zhang, J., Han, J., Gan, Y. & Ren, N. 2013, 'Forward osmosis with a novel thin-film inorganic membrane', *Environmental science & technology*, vol. 47, no. 15, pp. 8733-42.

Yu, Y., Seo, S., Kim, I.-C. & Lee, S. 2011, 'Nanoporous polyethersulfone (PES) membrane with enhanced flux applied in forward osmosis process', *Journal of Membrane Science*, vol. 375, no. 1–2, pp. 63-8.

Yun, T., Kim, Y.-J., Lee, S., Hong, S. & Kim, G.I. 2013a, 'Flux behavior and membrane fouling in pressure-assisted forward osmosis', *Desalination and Water Treatment*, vol. 52, no. 4-6, pp. 564-9.

Yun, T., Kim, Y.-J., Lee, S., Hong, S. & Kim, G.I. 2013b, 'Flux behavior and membrane fouling in pressure-assisted forward osmosis', *Desalination and Water Treatment*, pp. 1-6.

Zhang, Pinoy, L., Meesschaert, B. & Van der Bruggen, B. 2013, 'A natural driven membrane process for brackish and wastewater treatment: Photovoltaic powered ED and FO hybrid system', *Environmental science & technology*, vol. 47, no. 18, pp. 10548-55.

Zhang, Wang, K.Y., Chung, T.-S., Chen, H., Jean, Y. & Amy, G. 2010, 'Well-constructed cellulose acetate membranes for forward osmosis: minimized internal concentration polarization with an ultra-thin selective layer', *Journal of Membrane Science*, vol. 360, no. 1, pp. 522-35.

Zhao & Zou, L. 2011, 'Relating solution physicochemical properties to internal concentration polarization in forward osmosis', *Journal of Membrane Science*, vol. 379, no. 1, pp. 459-67.

Zhao, Zou, L. & Mulcahy, D. 2011, 'Effects of membrane orientation on process performance in forward osmosis applications', *Journal of Membrane Science*, vol. 382, no. 1-2, pp. 308-15.

Zhao, S., Zou, L., Tang, C.Y. & Mulcahy, D. 2012, 'Recent developments in forward osmosis: Opportunities and challenges', *Journal of Membrane Science*, vol. 396, no. 0, pp. 1-21.

Zhao., Zou, L., Tang. & Mulcahy. 2012, 'Recent developments in forward osmosis: opportunities and challenges', *Journal of Membrane Science*, vol. 396, pp. 1-21.

Zhou., Lee, J.Y. & Chung, T.-S. 2014, 'Thin film composite forward-osmosis membranes with enhanced internal osmotic pressure for internal concentration polarization reduction', *Chemical Engineering Journal*, vol. 249, no. 0, pp. 236-45.

Zhou., Yu, S., Gao, C. & Feng, X. 2009, 'Surface modification of thin film composite polyamide membranes by electrostatic self deposition of polycations for improved fouling resistance', *Separation and Purification Technology*, vol. 66, no. 2, pp. 287-94.